

University of Memphis

## University of Memphis Digital Commons

---

Electronic Theses and Dissertations

---

2021

# IDENTIFICATION OF EPIGENETIC MARKERS FOR ALLERGIC DISEASES VIA GENOME-SCALE ASSOCIATION STUDIES

Aniruddha Rathod

Follow this and additional works at: <https://digitalcommons.memphis.edu/etd>

---

### Recommended Citation

Rathod, Aniruddha, "IDENTIFICATION OF EPIGENETIC MARKERS FOR ALLERGIC DISEASES VIA GENOME-SCALE ASSOCIATION STUDIES" (2021). *Electronic Theses and Dissertations*. 2729.  
<https://digitalcommons.memphis.edu/etd/2729>

This Dissertation is brought to you for free and open access by University of Memphis Digital Commons. It has been accepted for inclusion in Electronic Theses and Dissertations by an authorized administrator of University of Memphis Digital Commons. For more information, please contact [khggerty@memphis.edu](mailto:khggerty@memphis.edu).

IDENTIFICATION OF EPIGENETIC MARKERS FOR ALLERGIC DISEASES VIA  
GENOME-SCALE ASSOCIATION STUDIES

by

Aniruddha Bhadresh Rathod

A Dissertation

Submitted in Partial Fulfillment of the  
Requirements for the Degree of  
Doctor of Philosophy

Major: Epidemiology

The University of Memphis

December 2021

Copyright© Aniruddha Bhadresh Rathod  
All rights reserved

## **Dedication**

I dedicate this dissertation to my loving and caring wife, Rutu Rathod. Her love, support and care have been invaluable to my success, and it is my honor to share this accomplishment with her. I thank my parents, Dr. Bhadresh Rathod and Poorvaxi Rathod for instilling the value of education and hard work in me, and for their constant love, support, and encouragement. I also thank my sister Mrunande and her husband Michael III, for their support throughout this journey. I also dedicate this achievement to our son, Shivansh Rathod. He has given us the most beautiful moments by coming in our lives. I am forever indebted for the unconditional love and support of my family.

## **Acknowledgements**

I gratefully acknowledge the guidance and support of my dissertation committee members - Hongmei Zhang (Dissertation Chair), Wilfried Karmaus, Fawaz Mzayek, Syed Hasan Arshad, and John W. Holloway. I am extremely grateful to my advisor, Dr. Hongmei Zhang for her instrumental support, patience, and encouragement. I would like to thank her for her time to teach me and her invaluable guidance throughout these studies. I extend my sincerest gratitude to Dr. Wilfried Karmaus for giving me opportunities to explore the field of epigenetics through the eye of epidemiology in the context of public health. I would like to particularly thank, Dr. John Holloway for his guidance and support to answer difficult questions throughout these studies. I highly acknowledge, Dr. Fawaz Mzayek and Dr. Hasan Arshad for their support and continuous feedback throughout these studies. I am truly appreciative of my entire committee for their mentorship, guidance, and their patience throughout this dissertation.

I am thankful to the School of Public Health (SPH) for providing all the support and building wonderful memories over the years. It was my privilege to be your student and I will forever be grateful to all the professors. I also extend my deepest gratitude to Dr. Rajesh Miranda from Texas A&M University for opening the doors of his laboratory to me and introducing me to the field of research. He has been the most influential person in the field of science that I have come across. You continue to inspire me every day. A special thank you to a wonderful friend, mentor and colleague, Dr. Amanda Mahnke for her support both socially and professionally. I thank my SPH friends- Ashley Lauren Robison, Liang Li, Emily San Diego, Kristen Howell and Parnian Kheirkhah for being an extraordinary support system.

The studies conveyed in this publication was supported by the National Institute of Allergy and Infectious Diseases under Award Number R01 AI121226, R01 AI091905 and National Heart,

Lung, and Blood Institute under Award Number R01 HL132321. The UK Medical Research Council (MRC) and Wellcome (Grant's ref: 102215/2/13/2) and the University of Bristol provide core support for ALSPAC. A comprehensive list of grants funding is available on the ALSPAC website (<http://www.bristol.ac.uk/alspac/external/documents/grant-acknowledgements.pdf>). The author gratefully acknowledges the cooperation of the children and parents who participated in this study and appreciate the hard work of the Isle of Wight and ALSPAC research team in collecting data. We thank the High-Throughput Genomics Group at the Wellcome Trust Centre for Human Genetics (funded by Wellcome Trust grant reference 090532/Z/09/Z and MRC Hub grant G0900747 91070) for the generation of the methylation data. I am thankful to the High-Performance Computing facility at the University of Memphis.

## **Abstract**

Asthma is a global public health concern with limited preventive strategies. Recently, DNA methylation (DNAm) has been studied to understand the underlying pathogenesis of asthma. The role of DNAm in asthma acquisition from pre- to post- adolescence is unclear, and how its role changes from adolescence to adulthood is also unknown. The studies in this dissertation were carried out using data in two birth cohorts with one as a discovery cohort and the other as replication cohort. Longitudinal assessments in both cohorts revealed that the associations of DNAm at 62 Cytosine-Guanine sites (CpG sites) with asthma acquired during adolescence were different from those with asthma acquired in young adulthood since post-adolescence. Asthma can be atopic and non-atopic, and their underlying mechanisms are likely to be different in terms of DNAm markers. To this end, I further examined the mediating role of atopy in childhood on the association of DNAm in newborns with childhood asthma acquisition. I identified 30 CpGs that showed only indirect effects, i.e., DNAm in newborns at these CpGs might play a role in the development of atopic asthma with atopy being a mediator. Also, I found 103 CpGs showing only direct effects, which may contribute to the occurrence of non-atopic asthma. Asthma and rhinitis commonly coexist and share common biomarkers. I examined CpGs in newborns for their association in DNAm with these two allergic conditions during pre-adolescence. I detected 133 CpGs at birth that were associated with preadolescent asthma and/or rhinitis in both cohorts. Further, for all the studies, pathway enrichment analyses were conducted to understand the biological functionality of the identified CpGs. Additionally, biological relevance of the CpGs showing consistent findings between the two cohorts was evaluated using gene expressions. Findings from this dissertation will help identify epigenetic biomarkers for asthma acquisition and coexisting asthma and/or rhinitis as well as understand the underlying pathogenesis of these

conditions. More importantly, it will benefit our future efforts in allergic disease prediction and consequently prevention of these common allergic conditions.

## Table of Contents

|   |     |
|---|-----|
| List of Tables .....                        | vii |
| List of Figures .....                       | ix  |
| Abstract.....                               | x   |
| Chapter 1: Introduction .....               | 1   |
| Chapter 2: Aims and Research question ..... | 5   |
| Chapter 3                                   |     |
| Background .....                            | 8   |
| Methods.....                                | 9   |
| Results.....                                | 16  |
| Discussion.....                             | 31  |
| Chapter 4                                   |     |
| Background .....                            | 36  |
| Methods.....                                | 38  |
| Results.....                                | 43  |
| Discussion.....                             | 49  |
| Chapter 5                                   |     |
| Background .....                            | 54  |
| Methods.....                                | 55  |
| Results.....                                | 59  |
| Discussion.....                             | 65  |
| Chapter 6: Summary .....                    | 68  |
| References.....                             | 71  |
| Appendix.....                               | 81  |

## List of Tables

| <b>Table</b> |   | <b>Page</b> |
|--------------|---|-------------|
| Table 1(A)   | Asthma acquisition and never asthma subjects included in the current study compared to subjects in the complete cohort for 10-18 period (IOWBC).  | 16          |
| Table 1(B)   | Asthma acquisition and never asthma subjects included in the current study compared to subjects in the complete cohort for 18-26 period (IOWBC).  | 17          |
| Table 2(A)   | Top 10 most statistically significant GO terms and its biological processes from pathway enrichment analysis along with the number of genes in each pathway for males, for the identified CpGs.   | 27          |
| Table 2(B)   | Top 10 most statistically significant GO terms and its biological processes from pathway enrichment analysis along with the number of genes in each pathway for females, for the identified CpGs. | 28          |
| Table 3      | Differentially methylated regions (DMRs) for asthma acquisition identified by <i>DMRcate</i> package for males and females.   | 29          |
| Table 4      | Top 5 most significant associations of DNAm with expression of neighboring mapped genes.  | 30          |
| Table 5      | Comparison of analytical subsample with complete cohort   | 43          |
| Table 6(A)   | Top 10 most statistically significant GO terms and its biological processes from pathway enrichment analysis in each pathway for males, for the identified CpGs.                                  | 45          |
| Table 6(B)   | Top 10 most statistically significant GO terms and its biological processes from pathway enrichment analysis in each pathway for females, for the identified CpGs.                                | 45          |
| Table 7      | Top 5 most significant associations of DNAm with expression of neighboring mapped genes in each sex.  | 47          |
| Table 8      | Comparison of analytical subsample with complete cohort   | 60          |
| Table 9(A)   | Top 10 most statistically significant GO terms and its biological processes from pathway enrichment analysis in each pathway for males, for the CpGs that passed screening                        | 61          |
| Table 9(B)   | Top 10 most statistically significant GO terms and its biological processes from pathway enrichment analysis in each pathway for females, for the CpGs that passed screening.                     | 62          |
| Table 10     | Top 5 most significant associations of DNAm with expression of neighboring mapped genes in each sex.  | 64          |

## List of Figures

| Figure       |   | Page      |
|--------------|---|-----------|
| Figure 1     | Overview of epigenetic mechanisms. Epigenetic processes contribute to sustaining patterns of gene expression that define a cell's function.   | <b>2</b>  |
| Figure 2 (A) | Bar graph showing the direction of DNAm effect at each of the 17 identified CpGs in IOWBC from pre- to post-adolescence asthma acquisition in males. Gene names corresponding to each CpG site are also labeled on the X-axis.  | <b>19</b> |
| Figure 2(B)  | Bar graph showing the direction of effect at each of the 17 identified CpGs in IOWBC from post-adolescence to adulthood asthma acquisition in males. Gene names corresponding to each CpG site are also labeled on the X-axis.  | <b>20</b> |
| Figure 3(A): | Bar graph showing the direction of effect at each of the 98 identified CpGs in IOWBC from pre- to post-adolescence asthma acquisition in females. Gene names corresponding to each CpG site are also labeled on the X-axis.     | <b>21</b> |
| Figure 3(B)  | Bar graph showing the direction of effect at each of the 17 identified CpGs in IOWBC from post-adolescence to adulthood asthma acquisition in females. Gene names corresponding to each CpG site are also labeled on the X-axis | <b>22</b> |
| Figure 4(A)  | Bar graph showing the main effects of DNAm on asthma acquisition at each of the 38 identified CpGs in IOWBC in males. Gene names corresponding to each CpG site are also labeled on the X-axis.                                 | <b>23</b> |
| Figure 4(B)  | Bar graph showing the main effects of DNAm on asthma acquisition at each of the 52 identified CpGs in IOWBC in females. Gene names corresponding to each CpG site are also labeled on the X-axis.                               | <b>24</b> |
| Figure 5     | Flowchart of the study design and brief summaries of findings in each step.   | <b>26</b> |
| Figure       | Structural equation analyses model with atopy at 10 years as the mediator in the association of DNAm in newborns with asthma acquisition at young adulthood   | <b>41</b> |

## **Chapter 1. Introduction**

Epigenetics represents mitotically heritable and reversible changes in gene expression without changes to the DNA sequence [1, 2]. It was first coined as the ‘study of the interactions between genes and their products that bring the phenotype into being’ by Conrad Hal Waddington in 1942 [3]. It plays an important role in transcription, nuclear organization, genome stability and imprinting [1]. Environmental exposures and genetics only partly explain the pathogenesis of a disease, and recent epidemiologic research have demonstrated epigenetics as an important missing link in the etiological puzzle between genes and phenotypes/exposures [1, 2, 4].

Epigenetic epidemiology has the potential to help explain underlying biological mechanisms for diseases. It may play a mechanistic etiologic role by serving as a biomarker of exposure or disease [1]. Altered epigenetics has been shown to be associated with several exposures and diseases [5]. The clinical utility of epigenetic data may include its use as a biomarker for diagnosis, prognosis, treatment or as a performance metric in clinical trials [1]. DNA methylation, histone modifications, microRNA and prions are different types of epigenetic mechanisms (Figure 1). Most epigenetic studies focus on DNA methylation (DNAm) because of its long-term stable nature and availability of several analytical platforms [2, 6].

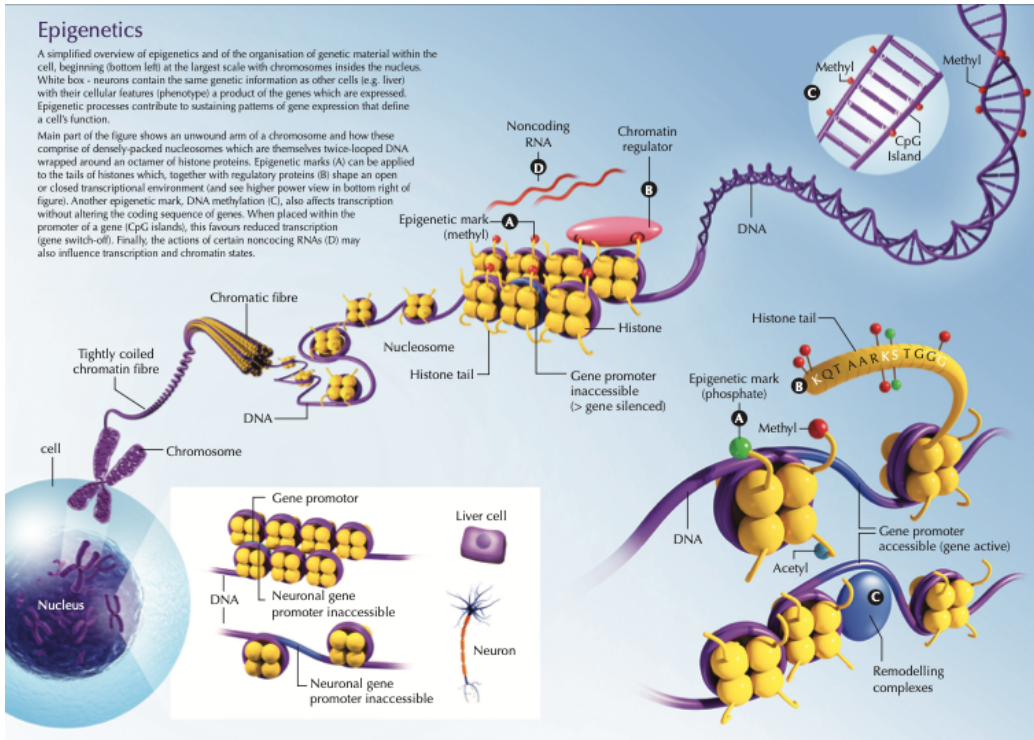


Figure 1. Overview of epigenetic mechanisms. Epigenetic processes contribute to sustaining patterns of gene expression that define a cell's function. DNA methylation (labeled C in the figure) affects transcription without altering the coding sequence of genes. When placed within the promoter of a gene (CpG islands), it favors reduced transcription (gene switch-off) [7].

DNA methylation (labeled C in the figure) is an addition of a methyl group ( $\text{CH}_3$ ) to the DNA strand. DNA methylation is mitotically heritable, highly stable and plays an important role in gene expression regulation [6]. As DNA methylation can be influenced by both genetic and environmental factors, it can be an exposure (risk factor), mediator or consequence of a disease. Therefore, DNA methylation can serve as biomarker of exposure or risk factor, and disease. Several epigenome-wide association studies (EWAS) have demonstrated the association between DNA methylation and exposures such as smoking [8-12], body mass index [13-16], air pollution [17-19], breastfeeding [20-23], alcohol [24-26], drugs [27, 28]. Similarly, studies have shown association of DNA methylation with several diseases such as cancers [29, 30], autoimmune [31-34], allergic [35-37], metabolic [38-41],

neurological [42, 43], cardiovascular [44-46] diseases. My dissertation focuses on allergic diseases including asthma and rhinitis.

The prevalence of allergic diseases is increasing globally with children and young adults bearing a large burden. According to World Allergy Organization and World Health Organization, more than 300 million people worldwide suffer from asthma and 400 million from rhinitis [47].

Asthma is responsible for 250,000 deaths annually worldwide [47]. The prevalence of allergic diseases is steadily increasing in the United States and 23 million people have asthma, of which 7 million are children [47]. Allergic diseases are a global public health concern and preventive efforts are needed to reduce its prevalence, death, and economic costs [47]. Several epidemiologic studies have identified prenatal and early-life environmental exposures such as tobacco smoke [47-49], air pollution [47, 48, 50, 51], allergen exposure [48, 52] that contribute towards the increasing burden of asthma and allergic diseases. Control measures for these exposures will prevent the incidence of asthma and allergic diseases. Apart from these exposures, genetics also play an important role in the susceptibility and development of asthma and allergic diseases. Studies have identified several loci related to asthma [53-56] and allergic rhinitis [57]; however, these explain only a fraction of variation in the disease risk and its replication in other populations have largely failed [58]. Because of these limitations, recently there has been an increased focus towards epigenetic studies to understand the pathogenesis of asthma and allergic rhinitis.

Several EWAS studies have demonstrated association of DNAm with the status of asthma [59-62] and rhinitis [35, 63, 64], and identified biomarkers for the same. However, the role of DNAm in asthma acquisition, especially during the critical transition period from pre- to post-adolescence, and how its role changes over time, e.g., from adolescence to adulthood, is

unknown. Atopy is a risk factor for asthma acquisition [65], but asthma can also be non-atopic. The underlying mechanisms of different types of asthma may be explainable by DNAm at earlier ages. Additionally, co-existence of asthma and rhinitis is common and have been known to share common genetic variants [57]. However, it is unclear whether these two conditions share common epigenetic factors, and if so, whether they are consistent with findings in genetic studies. These “unknowns” motivated the projects of this dissertation, as findings in these areas will improve our understanding of allergic disease development from the angle of epigenetics and benefit allergic disease prediction at a much earlier age. In the next chapter, I will outline the projects and related study questions.

## **Chapter 2. Aims and Research Questions**

The proposed dissertation is comprised of three aims with an emphasis on identification of epigenetic markers that has the potential to explain the underlying pathogenesis of allergic diseases in childhood and early adulthood. In aim 1, using an epigenome-wide approach, I will identify novel epigenetic loci during pre- and post- adolescence that are associated with asthma acquisition during adolescence and in later adulthood in males and females separately. In aim 2, using a longitudinal epigenome-wide approach, the direct and indirect effects of DNA methylation (DNAm) in newborns on asthma acquisition across adolescence via pre-adolescence atopy will be evaluated in both sexes separately. In aim 3, I will examine sex-specific associations of DNAm in newborns and pre-adolescence asthma and rhinitis in an epigenome-wide study. Pathway enrichment analysis and association of gene expression with DNAm will be assessed for all the aims to gain better understanding elucidating the biological significance of the identified CpGs.

### **Aim 1**

**To examine the association of pre- and post-adolescence DNAm with asthma acquisition during adolescence and in later adulthood.**

**Research question 1.1:** Are pre- and post-adolescence (age 10 and 18 years) DNAm associated with asthma acquisition during adolescence (age 10 to 18 years) and in later adulthood (age 18 to 26 years) for each gender in discovery cohort, Isle of Wight Birth Cohort (IOWBC)?

**Research question 1.2:** Does replication analysis in an independent cohort, ALSPAC support the findings from the IOWBC?

**Research question 1.3:** Are there any differentially methylated regions (DMRs) at preadolescent DNAm associated with asthma acquisition from pre- to post-adolescence.

**Research question 1.4:** What are the biological pathways of genes corresponding to the identified CpGs in IOWBC?

**Research question 1.5:** Is there an association between DNAm at ages 10 and 18 years and gene expression of nearby genes i.e., within 250kb upstream and downstream region of the identified CpGs at 26 years?

## **Aim 2**

**To examine whether atopy in childhood mediates the association of DNAm in newborns with asthma acquisition across adolescence.**

**Research question 2.1:** Does pre-adolescence atopy mediate the association of DNAm in newborns with asthma acquisition across adolescence in IOWBC?

**Research question 2.2:** Can the findings of research question 2.1 be replicated in ALSPAC?

**Research question 2.3:** What are the biological pathways of genes corresponding to the identified CpGs in IOWBC?

**Research question 2.4:** Is there an association between DNAm at age 26 years and gene expression of nearby genes i.e., within 250kb upstream and downstream region of the identified CpGs at 26 years?

## **Aim 3**

**To examine sex-specific associations of DNAm in newborns with pre-adolescence asthma and/or rhinitis**

**Research question 3.1:** Is the association of DNAm in newborns with pre-adolescence asthma and/or rhinitis sex-specific?

**Research question 3.2:** What are the biological pathways of genes corresponding to the identified CpGs in IOWBC?

**Research question 3.3:** Is there a genetic influence on the identified CpGs, i.e., are they methQTLs?

**Research question 3.4:** Is there an association between DNAm at age 26 years and gene expression of nearby genes i.e., within 250kb upstream and downstream region of the identified CpGs at 26 years?

**Research question 3.5:** Is there a genetic influence on DNAm at the replicated CpGs, i.e., are there any methQTLs?

## **Chapter 3**

**Aim 1: To examine the association of pre- and post-adolescence DNAm with asthma acquisition during adolescence and in later adulthood.**

### **Background**

Asthma is the most prevalent chronic respiratory condition[66] affecting 1-18% of population in several countries[67]. Over recent decades, childhood asthma has become a major public health issue[68] with an increasing prevalence worldwide[69]. Environmental factors such as air pollution, infectious agents, and tobacco smoke have been shown to be associated with the development of asthma[70].

DNA methylation (DNAm), a robust and stable epigenetic mark, represents a potential mechanism mediating environmental impacts on human diseases[71]. Recent studies suggest that DNAm signatures of cytosine-phosphate-guanines (CpG) sites are associated with asthma[58, 61, 72]. Since peripheral blood is readily obtainable and easy to handle in laboratory processing, and information of immune cells in blood is relevant to asthma pathogenesis[73], DNAm in peripheral blood cells has been commonly examined in epigenome-wide studies of asthma[62, 74, 75].

While the development of asthma clearly reflects the combination of inherited susceptibility and environmental exposures, the pathogenesis and underlying biological mechanisms involved in the onset of asthma later in life are not well understood. Asthma most commonly develops during early childhood[76], and the prevalence of asthma depends on gender and age. Asthma is more prevalent among pre-adolescent boys, while it becomes more prevalent among females after puberty with prevalence in males and females being approximately equal in adulthood[77-79].

79]. However, the pathogenesis of these sex differences in asthma across adolescence and adulthood remains unclear.

Although previous studies have demonstrated association between DNAm and asthma, the role that DNAm plays in asthma acquisition, especially during the critical transition period from pre- to post-adolescence, and how its role changes over time, e.g., from adolescence to adulthood, are unknown. Findings from this type of studies will not only identify important markers for asthma acquisition, and more importantly, benefit our future efforts in asthma prediction and consequently asthma prevention. To this end, in this study, for each gender, we examined the association between DNAm at pre-adolescence and asthma acquisition from pre- to post-adolescence (10 to 18 years), and between DNAm at post-adolescence and asthma acquisition from post-adolescence to adulthood (18 – 26 years), utilizing genome-wide DNA methylation data. We hypothesized that DNAm at specific CpG sites measured before disease onset, either in pre- or post-adolescence would be associated with asthma acquisition both during adolescence and in later adulthood and that there would be differences in such DNA methylation patterns by time window (adolescence or post-adolescence) and by gender. Additionally, differentially methylated regions (DMRs) were identified to incorporate CpGs located close to one another which may be associated with asthma acquisition as a group or cluster of CpGs. These CpGs might have been missed when looking at the associations using individual CpG sites.

## Methods

### ***IOWBC study population***

The study population comprised of children born between January 1, 1989 and February 28, 1990 on the Isle of Wight (IoW), UK (IOWBC)[80]. Out of the 1,536 children born and recruited, 1,456 in IOWBC were available for further follow-up at ages 1, 2, 4, 10, 18 and 26

years. Ethics approval was obtained by the local research ethics committee (NRES Committee South Central – Hampshire B) (06/Q1701/34)[81]. The details on study design, enrollment, and follow-up procedures for the IoW birth cohort (IOWBC) are described elsewhere [80, 82].

### ***Asthma acquisition***

Questionnaires that included the questions of the International Study of Asthma and Allergy in Childhood (ISAAC) was filled by parents/participants at ages 4, 10, 18 and 26 years[61, 83-85]. Asthma was defined as “physician diagnosed asthma” and “wheezing or whistling in the chest in the last 12 months” or “current treatment for asthma.” Subjects with asthma at age four years were excluded. The outcome used in this study, asthma acquisition, was defined as individuals who were asthma free at age 10 years and recorded as having asthma at age 18 years (no→yes). The same definition was applied for asthma acquisition from 18 to 26 years (no→yes). Subjects who did not have asthma at both the transition periods were taken as reference (no→no).

### ***Covariates***

Atopic status was evaluated at ages 10 and 18 years based on results from skin prick test (SPT) on 11 common allergens (house dust mite, cat dander, dog dander, grass pollen mix, tree pollen mix, *Alternaria alternate*, *Cladosporium herbarium*, cow’s milk, hen’s egg, peanut, and cod). Being SPT positive to one or more of the 11 allergens was treated as being atopic. Active smoking status at 18 and 26 years was recorded as ‘yes’ if the participant was a current smoker at that respective age. Second-hand smoke exposure was coded at age 18- and 26-years using information obtained from smoking status of parents and other smokers in the household. To evaluate the contribution of transition periods, 10-18 and 18-26 years, to the association of DNAm with asthma transition, transition periods will be included in the analyses as adjusting factors.

## **DNA methylation**

Using a standardized salting procedure, DNA was extracted from peripheral whole blood samples collected at ages 10 and 18 years[86]. Fluorometric quantitation was used to estimate DNA concentration. Methylation levels at each CpG site was measured using Illumina Infinium HumanMethylation450 or MethylationEPIC BeadChips (Illumina, Inc., San Diego, ca, USA). Probes that did not reach a p-value of  $10^{-16}$  in at least 95% of samples were exclude. The same criterion was applied to exclude samples, i.e., samples with p-value  $>10^{-16}$  in at least 95% of the CpGs. CpGs on sex chromosome were excluded. Probes that contained single nucleotide polymorphisms (SNPs) within 10 base pairs of a targeted CpG site with a minor allele in at least 0.7% subjects (corresponding to at least 10 subjects in IoW with n = 1,456) were excluded due to their influence on the measures of DNAm.

Using CPACOR pipeline, DNA methylation (DNAm) was pre-processed for the data from both HumanMethylation450 and MethylationEPIC. DNAm intensities were quantile normalized using the *minfi* R computing package [87]. The quantile normalized intensities at autosomal probes were then converted to beta values.  $\beta$  values is a ratio of methylated (M) over the sum of methylated and unmethylated (U) probes ( $\beta=M/[c+M+U]$ ), where c is a constant to prevent from zero in the denominator. Often  $\beta$  values suffer from severe heteroscedasticity, so in statistical analyses, logit transformed DNAm levels, i.e., M values, were used. Principal components (PCs) inferred based on control probes were used to represent latent chip to chip and technical variation. We determined PCs based on DNAm at shared control probes of the two DNAm platforms HumanMethylation450 and MethylationEPIC. In total, 195 shared control probes were used to calculate the control probe PCs with top 15 PCs included in our study to represent latent batch factors [88]. In this study, CpG sites common between Illumina 450k platform and EPIC

platform will be examined. In additions, CpG sites were excluded if the minor allele frequency of a probe SNP at that site is > 0.7% (i.e., ~ ≥ 10 out of 1456 subjects expected to have the minor allele in the cohort) and the probe SNP was within 10 base pairs of the targeted CpG site. After quality control and pre-processing, 442,475 CpG sites will be included in subsequent analysis. Since whole blood is a mixture of distinct cell types[89], there is a need to adjust for cell type composition to account for their potentially confounding effects[90]. Cell type proportions were estimated using the Bioconductor *minfi* package[91] [92]. The estimated cell type proportions of CD4+ T cells, natural killer cells, neutrophil, B cells, monocytes, and eosinophil cells will be included in the analyses as confounders.

#### ***Genome-wide RNA-seq gene expression data generation***

Gene expression levels from peripheral blood samples collected at 26 years from the IOWBC was determined using paired-end (2×75 bp) RNA sequencing with the Illumina Tru-Seq Stranded mRNA Library Preparation Kit with IDT for Illumina Unique Dual Index (UDI) barcode primers following the manufacturer's recommendations. All samples were sequenced twice using the identical protocol and for each sample the output from both runs were combined. FASTQC were run to assess the quality of the FASTQ files (<https://www.bioinformatics.babraham.ac.uk/projects/fastqc/>). Reads were mapped against Human Genome (GRch37 version 75) using HISAT2 (v2.1.0) aligner [93]. The alignment files, produced in the Sequence Alignment Map (SAM) format, were converted into the Binary Alignment Map (BAM) format using SAMtools (v1.3.1) [94]. HTseq (v0.11.1) was used to count the number of reads mapped to each gene in the same reference genome used for alignment [95]. Normalized read count FPKM (Fragments Per Kilobase of transcript per Million

mapped reads) were calculated using the countToFPKM package (<https://github.com/AAlhendi1707/countToFPKM>) and their log-transformed values were used for data analysis.

### ***Statistical analyses***

**Research question 1.1:** Are pre- and post-adolescence DNAm associated with asthma acquisition during adolescence and in later adulthood for each gender in discovery cohort, Isle of Wight Birth Cohort (IOWBC)?

By regressing the M-values (base-2 logit transformed beta values of DNAm) at each CpG site on the aforementioned 15 PCs and 6 cell type proportions, we obtained cell-type and batch-adjusted DNAm (residuals) at each of the 442,475 CpG sites for each gender in IOWBC. Screening of CpG sites was done to obtain DNAm potentially associated with asthma acquisition from pre- to post-adolescence using simple linear regressions. Here, asthma acquisition from 10 to 18 years of age was the independent variable and DNAm at age 10 years was the dependent variable. The analysis was stratified by gender. For the screening purpose, multiple testing was adjusted by controlling false discovery rate (FDR) at a higher rate of 0.2. CpG sites that pass screening were included in subsequent analyses.

Logistic regressions with repeated measurements were applied to the CpGs that pass screening to evaluate the association of asthma acquisitions (no→yes) at two transition periods (10-18 years and 18-26 years) with DNAm at earlier ages (10 and 18 years, respectively). Adolescence is a period accompanied by significant physical and mental development and such changes gradually stabilize as children enter post-adolescence [96, 97]. The unique phenomenon in each transition period motivated a study question, i.e., are the associations between asthma acquisition and DNAm different at different transition periods, in addition to the main effects of DNAm? To

answer this question, I included an interaction term in the final model to test interaction effects between DNAm and transition period. For both situations (the models with main effects only, and the models that included interaction effects) multiple testing was adjusted by controlling FDR of 0.05.

**Research question 1.2:** Does replication analysis in an independent cohort, ALSPAC support the findings from the IOWBC?

CpGs showing significant interaction effects with transition periods in IOWBC were further tested in the Avon Longitudinal study of Parents and Children (ALSPAC) cohort [98-100].

Pregnant women residing in the Southwest of England and expecting to deliver between April 1, 1991 and December 31, 1992 were eligible to be recruited. Of the 14,541 pregnant women eligible for recruitment, 13,761 were included in the study with 10,321 participants having their DNA sampled. DNAm in the ALSPAC cohort was assessed using the Infinium HumanMethylation450 BeadChip. DNAm data on 604 children in the ALSPAC cohort are available at ages 7 and 17 years [101]. DNAm pre-processing was performed by correcting for batch effects using the *minfi* package [87] and removing CpGs with detection p-value  $\geq 0.01$ . Samples were flagged that contained sex-mismatch based on X-chromosome methylation.

Estimated cell type proportions of CD4+ T cells, natural killer cells, neutrophil, B cells, monocytes, and granulocytes cells were used in the analyses to adjust for cell heterogeneity.

Asthma acquisition status from 7 to 17 years, and 17 to 22 years was included in the analysis. It was defined as having no asthma at age 7 years and having asthma at age 17 years. The same definition was applied for asthma acquisition from 17 to 22 years. Logistic regression with repeated measurements were used with similar covariates (as those in IOWBC) available in ALSPAC, i.e., atopy status at age 7 years and second-hand smoke exposure status at age 17 and

24 years. Please note that the study website contains details of all the data that is available through a fully searchable data dictionary and variable search tool (<http://www.bristol.ac.uk/alspac/researchers/our-data/>).

**Research question 1.3:** Are there any differentially methylated regions (DMRs) at preadolescent DNAm associated with asthma acquisition from pre- to post-adolescence?

Differentially methylated regions (DMRs) were identified using the *DMRcate* package in R[102]. To secure enough CpGs for DMR enrichment analysis and to avoid missing important DMRs, CpGs with DNAm (in M values) associated with asthma acquisition via logistic regression at FDR of 0.4 were included in the analysis.

**Research question 1.4:** What are the biological pathways of genes corresponding to the identified CpGs in IOWBC?

For CpGs showing associations of DNAm with asthma acquisition status, the genes annotated to the CpGs will be summarized along with information such as gene location, chromosome number based on Illumina's manifest file and USCS genome browser (<https://genome.ucsc.edu>). Pathway enrichment analysis of the identified CpGs were conducted using the *gomech* function [103] in the R package to better understand their biological functionality.

**Research question 1.5:** Is there an association between DNAm at ages 10 and 18 years and gene expression of nearby genes i.e., within 250kb upstream and downstream region of the identified CpGs at 26 years?

Genes annotated to the replicated CpGs associated with asthma acquisition were extracted along with information such as gene location, chromosome number from the Illumina's manifest file or UCSC genome browser (<https://genome.ucsc.edu>). To assess the biological relevance of these CpGs, linear regressions were applied to test the association of DNAm (in M-values;

independent variable) at ages 10 and 18 years separately at each CpG site with expression of its neighboring genes (250k base pairs [bps] upstream and 250k bps downstream of the CpG site) in blood at 26 years of age. Paired DNAm and expression data of n=140 subjects were included in the analyses. As we previously have found the association between gene expression and DNAm to be different in both males and females, the analysis was stratified by sex [61, 104].

## Results

Since our study focused on asthma acquisition starting from age 10 years in IOWBC, subjects with asthma at four years were excluded. Participants in IOWBC with both asthma transition and DNAm data available at ages 10 and 18 years were included in the study. The subsamples represented the complete IOWBC (such that no asthma at age 4 years) with respect to asthma acquisition, active and second-hand smoking, and atopy status, (Table 1 A & B). The flow chart of samples included in the study is in Supplement Figure S3

**Table 1(A): Asthma acquisition and never asthma subjects included in the current study compared to subjects in the complete cohort for 10-18 period (IOWBC).**

| Variables N (%)     | Females                      |                                       |             | Males                        |                                       |             |
|---------------------|------------------------------|---------------------------------------|-------------|------------------------------|---------------------------------------|-------------|
|                     | Subsample<br>N=102;<br>n (%) | Complete<br>cohort<br>N=431;<br>n (%) | p-value     | Subsample<br>N=133;<br>n (%) | Complete<br>cohort<br>N=402;<br>n (%) | p-value     |
| Asthma transition   | Acquisition                  | 7 (6.86)                              | 41 (9.51)   | 0.40                         | 11 (8.27)                             | 26 (6.47)   |
|                     | Never Asthma                 | 95 (93.14)                            | 390 (90.49) |                              | 122 (91.73)                           | 376 (93.53) |
| Active smoking      | Yes                          | 25 (23.36)                            | 120 (25.86) | 0.59                         | 33 (21.85)                            | 105 (22.98) |
|                     | No                           | 82 (76.64)                            | 344 (74.14) |                              | 118 (78.15)                           | 352 (77.02) |
| Second-hand smoking | Yes                          | 54 (50)                               | 212 (44.92) | 0.34                         | 66 (43.42)                            | 204 (43.59) |
|                     | No                           | 54 (50)                               | 260 (55.08) |                              | 86 (56.58)                            | 264 (56.41) |

Table 1(A): Continue

| Variables N (%) |     | Females    |            |      | Males       |             |      |
|-----------------|-----|------------|------------|------|-------------|-------------|------|
| Atopy           | Yes | 14 (12.96) | 76 (19.1)  | 0.14 | 42 (27.81)  | 108 (27.91) | 0.97 |
|                 | No  | 94 (87.04) | 322 (80.9) |      | 109 (72.19) | 279 (72.09) |      |

Table 1(B): Asthma acquisition and never asthma subjects included in the current study compared to subjects in the complete cohort for 18-26 period (IOWBC).

| Variables N (%)            |                 | Females                      |                                       |         | Males                        |                                       |         |
|----------------------------|-----------------|------------------------------|---------------------------------------|---------|------------------------------|---------------------------------------|---------|
|                            |                 | Subsample<br>N=156;<br>n (%) | Complete<br>cohort<br>N=330;<br>n (%) | p-value | Subsample<br>N=121;<br>n (%) | Complete<br>cohort<br>n=286;<br>n (%) | p-value |
| Asthma<br>transition       | Acquisition     | 5 (3.21)                     | 12 (3.64)                             | 0.81    | 3 (2.48)                     | 10 (3.5)                              | 0.59    |
|                            | Never<br>Asthma | 151 (96.79)                  | 318 (96.36)                           |         | 118 (97.52)                  | 276 (96.5)                            |         |
| Active<br>smoking          | Yes             | 46 (27.54)                   | 107 (26.95)                           | 0.89    | 46 (31.94)                   | 99 (28.95)                            | 0.51    |
|                            | No              | 121 (72.46)                  | 290 (73.05)                           |         | 98 (68.06)                   | 243 (71.05)                           |         |
| Second-<br>hand<br>smoking | Yes             | 35 (20.96)                   | 98 (24.75)                            | 0.33    | 27 (18.75)                   | 80 (23.39)                            | 0.26    |
|                            | No              | 132 (79.04)                  | 298 (75.25)                           |         | 117 (81.25)                  | 262 (76.61)                           |         |
| Atopy                      | Yes             | 55 (29.73)                   | 115 (32.63)                           | 0.36    | 73 (42.2)                    | 146 (46.65)                           | 0.35    |
|                            | No              | 130 (70.27)                  | 227 (66.37)                           |         | 100 (57.8)                   | 167 (53.35)                           |         |

In total, 55 CpGs for males and 183 CpGs for females in IOWBC passed screening based on their potential associations with asthma acquisition from 10 to 18 years of age. These CpGs were included in subsequent analyses for their longitudinal associations of DNA methylation with asthma acquisition from pre- to post-adolescence and from post-adolescence to young adulthood and for

interaction effects between DNAm and transition periods, using logistic regressions with repeated measurements.

After adjusting for multiple testing by controlling FDR of 0.05, statistically significant interaction effects of DNAm and transition period were observed at 17 CpGs in males and 98 CpGs in females (no common CpGs identified between males and females), controlling for atopy status, active and second-hand smoking (Figures 2 and 3, Supplemental Table S1). Of the 17 identified CpGs in males, 4 CpGs (23.5%) were located in the promoter region, while for the 98 CpGs identified in females, a much larger portion of CpGs (54 CpGs, 55.1%) were in the promoter region. For 7 of the 17 CpGs in males, an increase in DNAm is associated with an increased odds of asthma acquisition in the 10-18 transition period but decreased odds in the 18-26 period (Figures 2A and 2B, Supplemental Table S1a). For 47 of the 98 CpGs in females, an increase in DNAm is associated with a decreased odds of asthma acquisition in the 10-18 transition period, but increased odds in the 18-26 period (Figures 3A and 3B, Supplemental Table S1b). In addition, the overall effect sizes at the first transition period were larger than the effect sizes in the second transition period.

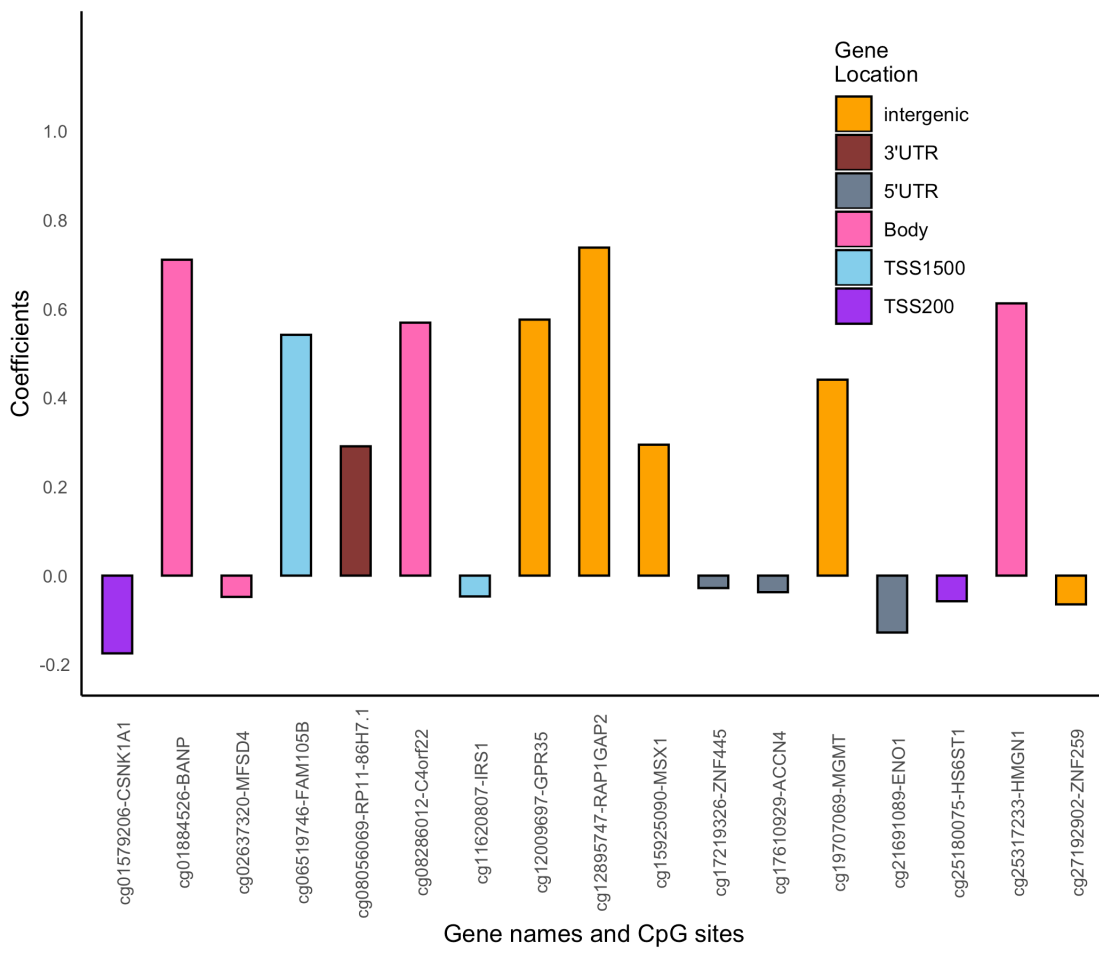


Figure 2 (A): Bar graph showing the direction of DNAm effect at each of the 17 identified CpGs in IOWBC from pre- to post-adolescence asthma acquisition in males. Gene names corresponding to each CpG site are also labeled on the X-axis.

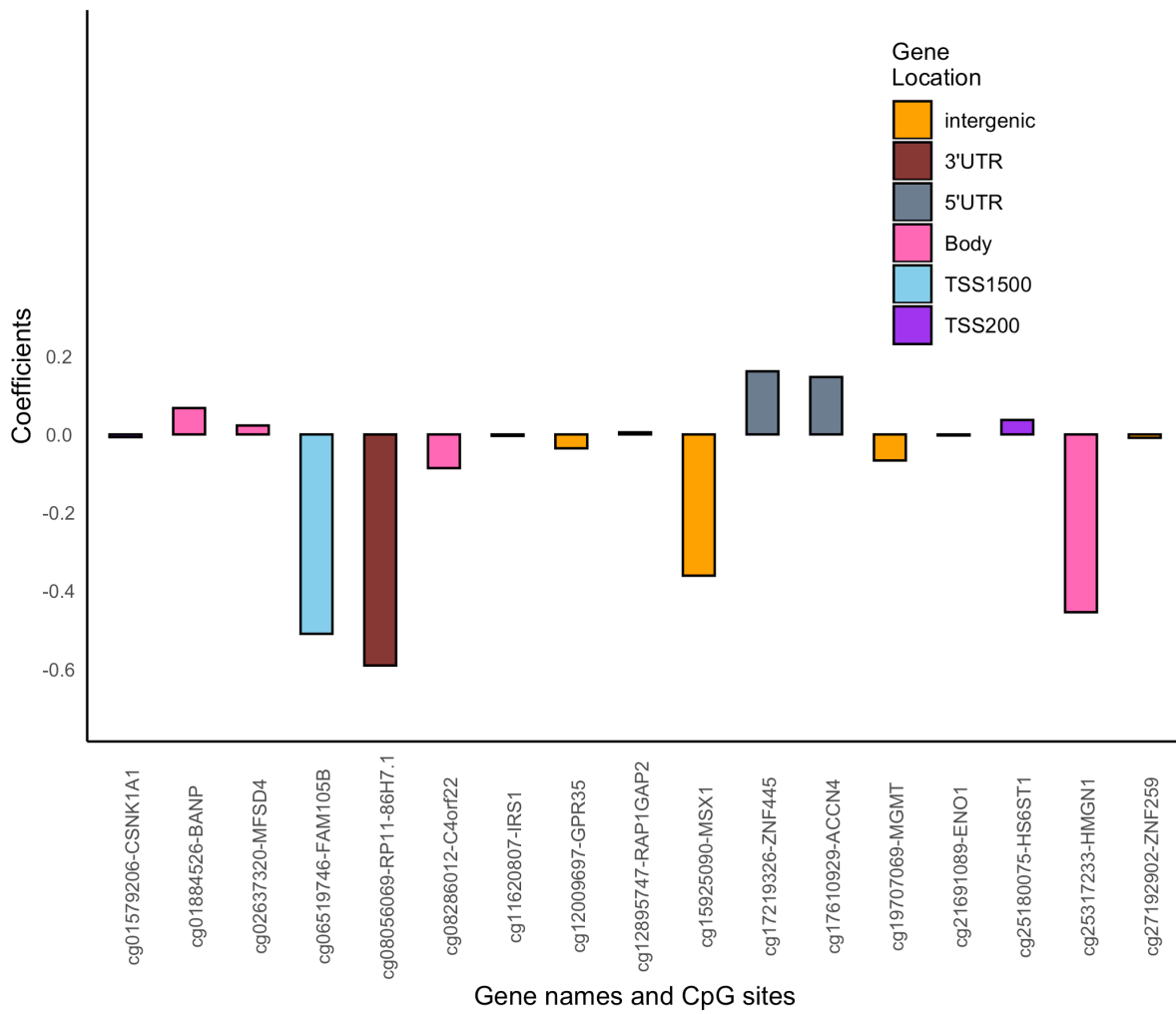


Figure 2(B): Bar graph showing the direction of effect at each of the 17 identified CpGs in IOWBC from post-adolescence to adulthood asthma acquisition in males. Gene names corresponding to each CpG site are also labeled on the X-axis.

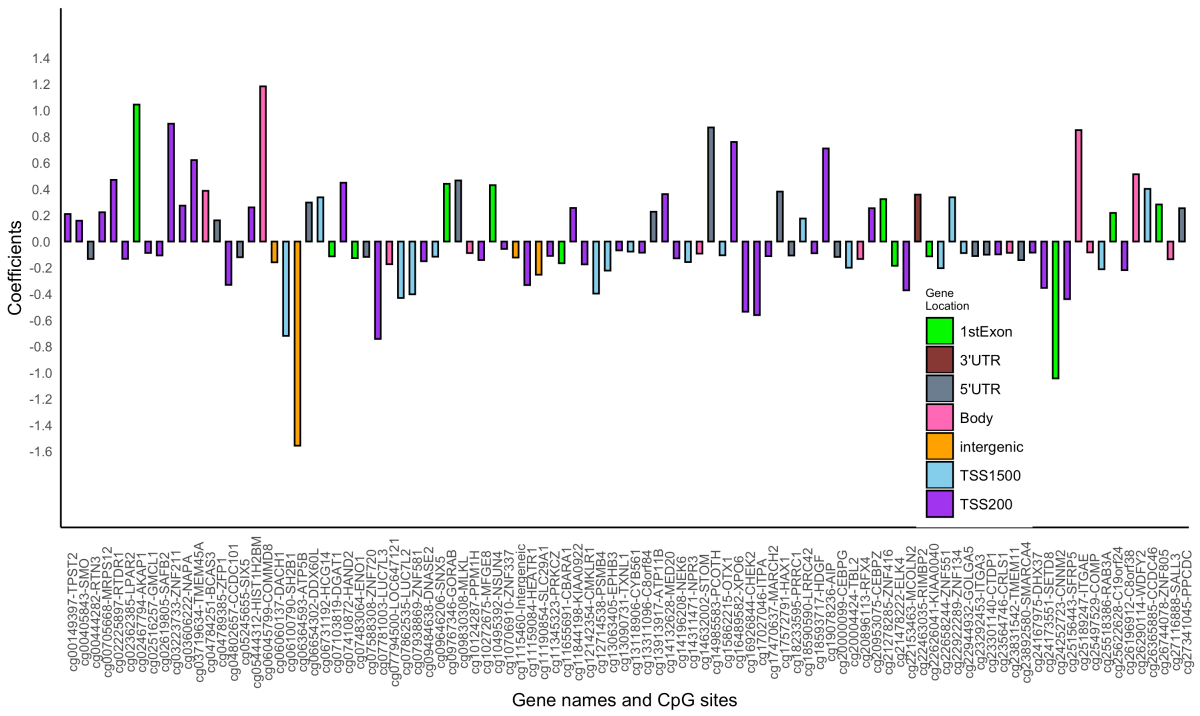


Figure 3(A): Bar graph showing the direction of effect at each of the 98 identified CpGs in IOWBC from pre- to post-adolescence asthma acquisition in females. Gene names corresponding to each CpG site are also labeled on the X-axis.

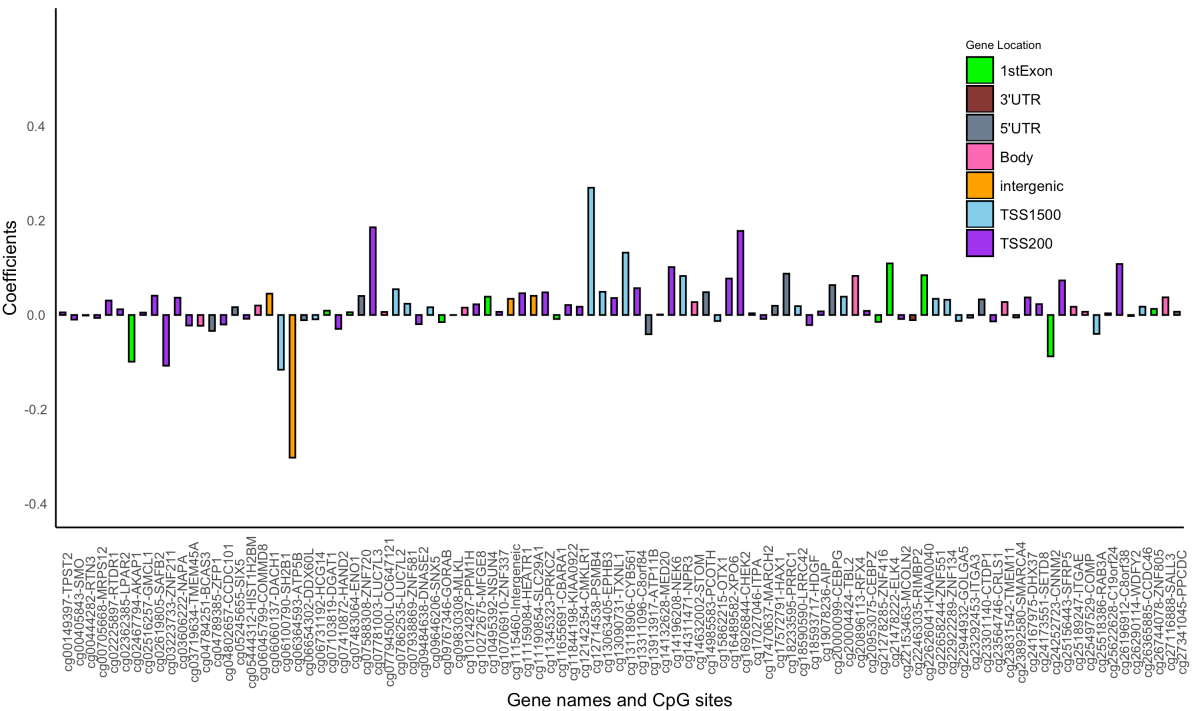


Figure 3(B): Bar graph showing the direction of effect at each of the 17 identified CpGs in IOWBC from post-adolescence to adulthood asthma acquisition in females. Gene names corresponding to each CpG site are also labeled on the X-axis.

For CpGs not showing significant interaction effects between DNAm and transition period, we assessed the main effects of DNAm on asthma acquisition via logistic regression models with repeated measures. After adjusting for multiple testing at FDR=0.05, we identified 38 CpGs in males and 52 CpGs in females (Figure 4, Supplemental Table 3S.2) showing association of DNAm with asthma acquisition status (no common CpGs between males and females). Of the 38 CpGs in males, 13 CpGs (34.2%) were in the promoter region, while for the 52 CpGs identified in females, a much larger portion of CpGs (25 CpGs, 48.1%) were in the promoter region. At 25 of the 38 CpGs in males, an increase in DNAm is associated with a decreased odds of asthma acquisition (Supplemental Table S2a). At 45 of the 52 CpGs in females, an increase in DNAm is associated with a decreased odds of asthma acquisition (Supplemental Table S2b). Overall, the

effect sizes of DNAm on asthma acquisition were larger in males than in females.

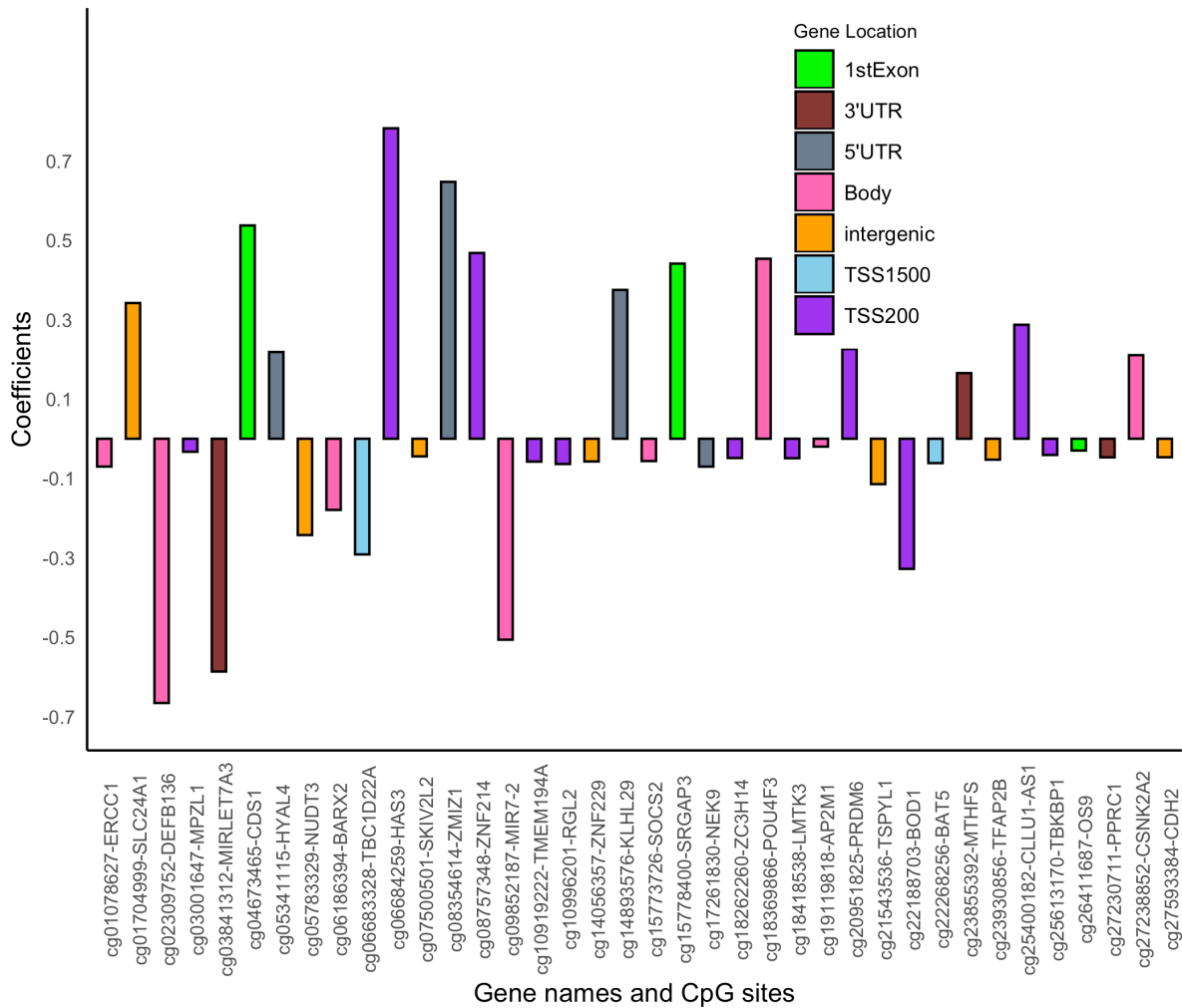


Figure 4(A): Bar graph showing the main effects of DNAm on asthma acquisition at each of the 38 identified CpGs in IOWBC in males. Gene names corresponding to each CpG site are also labeled on the X-axis.

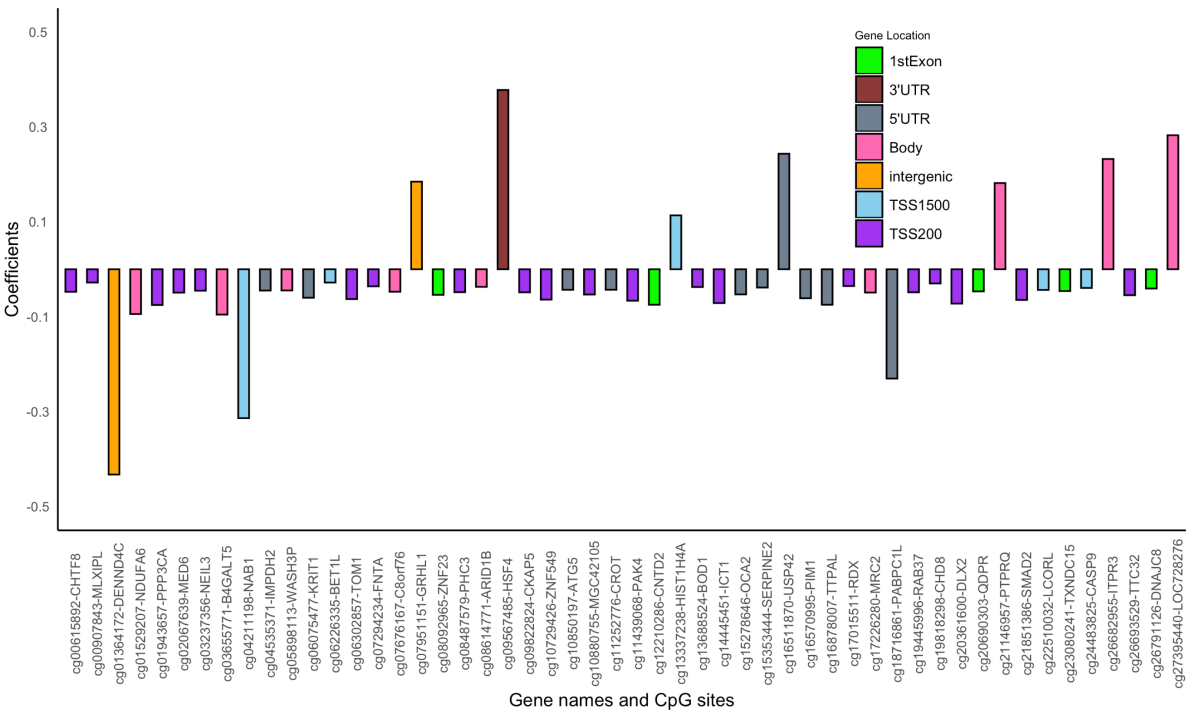


Figure 4(B): Bar graph showing the main effects of DNAm on asthma acquisition at each of the 52 identified CpGs in IOWBC in females. Gene names corresponding to each CpG site are also labeled on the X-axis.

Altogether, we identified 115 CpGs (17 in males) showing interactions with transition period and 90 CpGs (38 in males) showing main effects (excluded CpGs with interaction effects), leading to a total of 205 identified CpGs. We further tested these CpGs in the ALSPAC cohort. For the 115 CpGs (17 in males) showing interaction effects in IOWBC, consistent directions of interaction effects were observed at 9 CpGs in males, with 1 CpG being statistically significant, and 53 CpGs in females, with 3 CpGs being statistically significant, compared to the directions of associations identified in the IOWBC (Supplemental Tables S1a and S1b). Of the 9 CpGs showing consistent interactions in males, 2 CpGs (22.2%) were in the body region of gene, while of the 53 such CpGs in females, 34 (64.2%) were in the promoter region. For the 90 CpGs (38 in males) showing main effects on asthma acquisition, 13 CpGs in males (3 CpGs [23.1%] in the

promoter region) and 37 CpGs in females (19 CpGs [51.4%] in the promoter region) showed consistent directions of main effects (Supplemental Table S2a and S2b) between the two cohorts. The flowchart of the study along with brief summaries of results is in Figure 5.

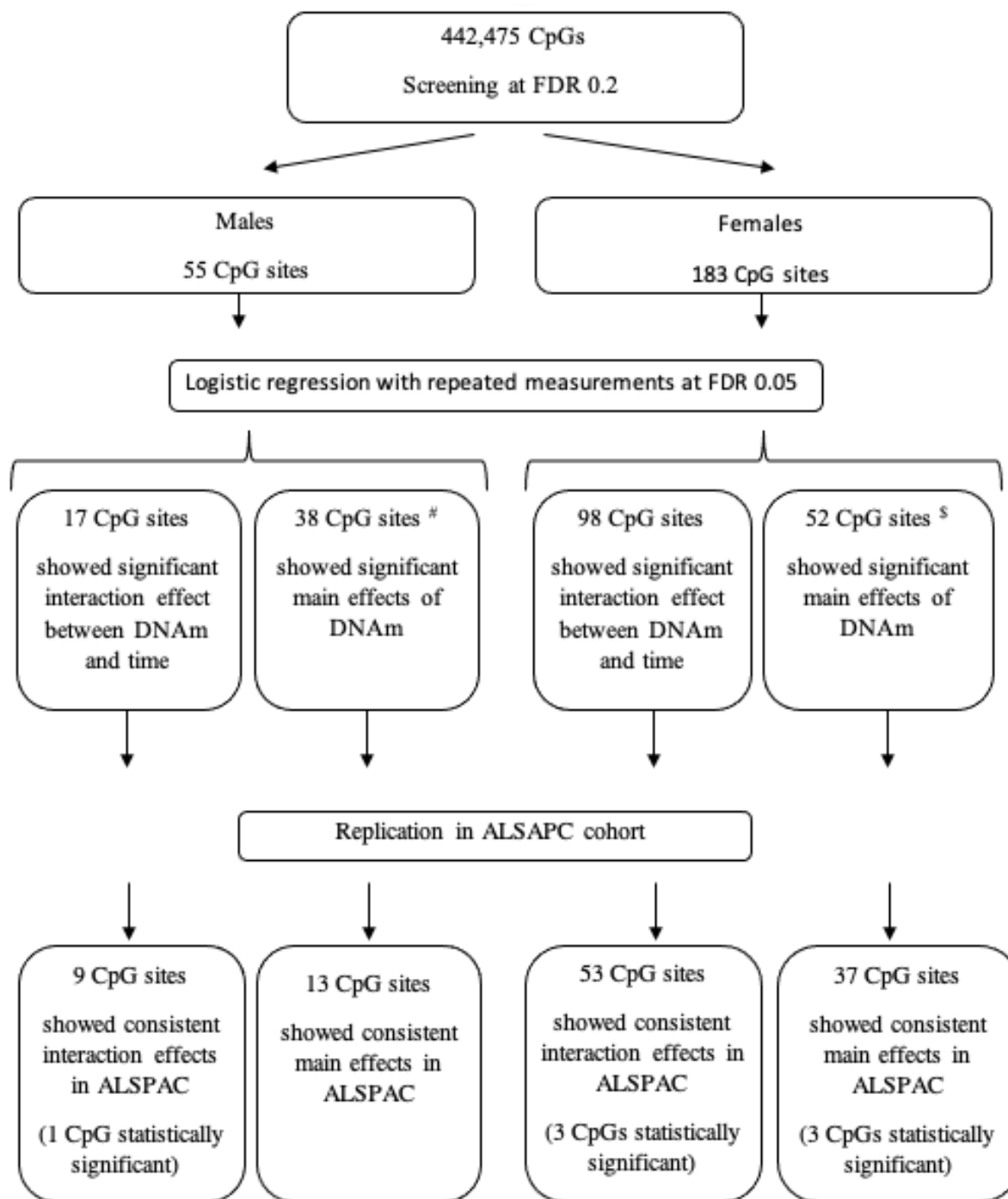


Figure 5. Flowchart of the study design and brief summaries of findings in each step.

# - Out of 38 CpGs after excluding significant interaction  
 \$ = Out of 85 CpGs after excluding significant interaction

Pathway enrichment analyses was conducted based on CpGs identified for each sex (55 in males and 150 in females with 205 CpGs in total) to better understand their biological functionality. These CpGs were mapped to 54 and 149 genes in males and females respectively. Using these CpGs in the *gopath* function in R, we identified 212 biological processes in males and 228 in females that were enriched at p-value of 0.05. Although none of the biological processes survived multiple testing at FDR of 0.05, genes involved in the top processes for each sex based on statistical significance (top 10 processes in Table 2) were potentially important and may deserve a further assessment. For males, multiple biological processes among the top 10 for males focus on catabolic processes (breakdown glucose for energy), while for females they are biosynthetic processes (synthesizing glucose from food). Among these top processes identified for males, 13 genes corresponding to the identified CpGs were involved in those processes, and for females, 60 genes were involved (Supplemental Table S3).

Table 2(A): Top 10 most statistically significant GO terms and its biological processes from pathway enrichment analysis along with the number of genes in each pathway for males, for the identified CpGs.

| <b>GO term</b> | <b>Biological processes</b>                       | <b>P-value</b> | <b>No. of Genes</b> |
|----------------|---|----------------|---------------------|
| GO:1901575     | organic substance catabolic process               | 0.0005         | 12                  |
| GO:0046657     | folic acid catabolic process                      | 0.001          | 1                   |
| GO:0042219     | cellular modified amino acid catabolic process    | 0.002          | 1                   |
| GO:0038111     | interleukin-7-mediated signaling pathway          | 0.002          | 2                   |
| GO:1990261     | pre-mRNA catabolic process                        | 0.002          | 1                   |
| GO:0071544     | diphosphoinositol polyphosphate catabolic process | 0.002          | 1                   |
| GO:0042365     | water-soluble vitamin catabolic process           | 0.003          | 1                   |
| GO:0009056     | catabolic process                                 | 0.003          | 13                  |
| GO:0098760     | response to interleukin-7                         | 0.003          | 2                   |

**Table 2 (A): continue**

| <b>GO term</b> | <b>Biological processes</b>        | <b>P-value</b> | <b>No. of Genes</b> |
|----------------|------------------------------------|----------------|---------------------|
| GO:0098761     | cellular response to interleukin-7 | 0.003          | 2                   |

Table 2(B): Top 10 most statistically significant GO terms and its biological processes from pathway enrichment analysis along with the number of genes in each pathway for females, for the identified CpGs.

| <b>GO term</b> | <b>Biological processes</b>                         | <b>P-value</b> | <b>No. of Genes</b> |
|----------------|---|----------------|---------------------|
| GO:0019438     | aromatic compound biosynthetic process              | 0.0004         | 57                  |
| GO:0032774     | RNA biosynthetic process                            | 0.0007         | 49                  |
| GO:0008589     | regulation of smoothened signaling pathway          | 0.0007         | 5                   |
| GO:0018130     | heterocycle biosynthetic process                    | 0.0008         | 56                  |
| GO:1903506     | regulation of nucleic acid-templated transcription  | 0.0008         | 49                  |
| GO:2001141     | regulation of RNA biosynthetic process              | 0.0008         | 49                  |
| GO:1901362     | organic cyclic compound biosynthetic process        | 0.001          | 57                  |
| GO:0034654     | nucleobase-containing compound biosynthetic process | 0.001          | 55                  |
| GO:0006355     | regulation of transcription, DNA-templated          | 0.001          | 48                  |
| GO:0009757     | hexose mediated signaling                           | 0.001          | 2                   |

For DMR enrichment analysis, we used CpGs in the screening process that were statistically significant at FDR of 0.4 to cover epigenetic information comprehensively on asthma acquisition. In total, 427 CpGs in males and 372 CpGs in females were included in the DMR analysis. We identified three DMRs in males and three DMRs in females after adjusting for multiple testing at FDR=0.05 level based on the Stouffer test statistics. (Table 3).

Table 3: Differentially methylated regions (DMRs) for asthma acquisition identified by *DMRcate* package for males and females.

| Sex | Chr. <sup>\$</sup> | Start <sup>#</sup> | End <sup>&amp;</sup> | Gene <sup>£</sup>                  | CpGs <sup>¥</sup>          | P-value                 |
|-----|--------------------|--------------------|----------------------|------------------------------------|----------------------------|-------------------------|
| M   | 3                  | 196065106          | 196065569            | <i>TM4SF19</i>                     | cg05556202,<br>cg05445326  | 4.89*10 <sup>-206</sup> |
|     | 12                 | 57472396           | 57472611             | <i>TMEM194A</i>                    | cg10919222,<br>cg09934365  | 3.03*10 <sup>-150</sup> |
|     | 17                 | 27899874           | 27899966             | <i>TP53I13</i>                     | cg05877788,<br>cg04498198  | 2.69*10 <sup>-53</sup>  |
| F   | 2                  | 224903369          | 224903487            | <i>SERPINE2</i>                    | cg15353444,<br>cg11719885  | 5.84*10 <sup>-177</sup> |
|     | 1                  | 156721844          | 156722068            | <i>HDGF</i>                        | cg04402095,<br>cg18593717  | 5.35*10 <sup>-162</sup> |
|     | 17                 | 79633496           | 79633565             | <i>CCDC137,</i><br><i>C17orf90</i> | cg199963747,<br>cg11820993 | 1.70*10 <sup>-160</sup> |

<sup>\$</sup>Chr.: Chromosome

<sup>#</sup>Start: Start position of the region

<sup>&</sup>End: End position of the region

<sup>£</sup>Gene: Genes corresponding to the CpGs in the region

<sup>¥</sup>CpGs: CpGs in the region

To assess the biological relevance of CpGs showing consistent association with asthma acquisition in both cohorts, we evaluated the association of DNAm at the identified 113 CpGs (22 in males) with the expression of genes that the CpGs were mapped to. Nearby genes were also examined defined as genes in a window of 500k base pairs (bps) of each identified CpG site (250k bps up and down stream). In this analysis, DNAm was measured at 10 and 18 years and gene expression levels were assessed at age 26 years. Significant effects of DNAm at 10 years were observed at 14 CpGs on their association with expression of 29 genes in males, and at 73 CpGs with expression of 321 genes in females. Similarly, for DNAm at 18 years, significant associations were found at 10 and 51 CpGs with expression of 29 and 117 genes in males and

females, respectively (Table 4 and Supplemental Table S4). Of the 350 genes' expression (29 in males) associated with DNAm at 10 years, increased DNAm was associated with increased expression of 310 genes (18 in males). Similarly, of the 146 gene expressions associated with DNAm at 18 years, increased DNAm was associated with increased expression of 91 genes (24 in males). Of the CpGs showing associations with expression of their neighbouring genes, 8 genes in males and 39 in females were commonly identified at both ages (10 and 18 years). Among the top 5 most significant associations for each age and sex, 4 genes associated with 3 CpGs in males were found to be common at both ages, i.e., they may represent stable biological relevance of the CpGs during adolescence.

Table 4: Top 5 most significant associations of DNAm with expression of neighboring mapped genes.

| CpG site   | DNAm age<br>in years | Gene name    | Estimate | P-value               | Sex   |
|------------|----------------------|--------------|----------|-----------------------|-------|
| cg06684259 | 10                   | <i>ACAA2</i> | 0.57     | 0.0006                | Males |
|            | 18                   |              | 0.84     | $3.40 \times 10^{-5}$ | Males |
|            | 10                   | <i>ACP2</i>  | 0.67     | 0.001                 | Males |
| cg09852187 | 18                   | <i>ABCD3</i> | 0.60     | $2.08 \times 10^{-5}$ | Males |
|            | 10                   |              | 0.53     | 0.0006                | Males |
|            | 18                   |              | 0.48     | $3.40 \times 10^{-5}$ | Males |
| cg08354614 | 10                   | <i>CPM</i>   | 0.42     | 0.003                 | Males |
| cg12009697 | 10                   | <i>ABAT</i>  | 0.27     | 0.004                 | Males |
|            | 18                   |              | 0.40     | 0.0003                | Males |

Table 4: Continue

| CpG site        | DNAm age | Gene name     | Estimate | P-value                 | Sex     |
|-----------------|----------|---------------|----------|-------------------------|---------|
| <b>in years</b> |          |               |          |                         |         |
| cg25518386      | 10       | <i>AKAP10</i> | 0.89     | 1.24x10 <sup>-10</sup>  | Females |
| cg26791126      | 10       | <i>AIM1</i>   | 0.30     | 5.14 x10 <sup>-10</sup> | Females |
| cg24173551      | 10       | <i>ALKBH5</i> | 0.75     | 5.64 x10 <sup>-10</sup> | Females |
| cg06060137      | 10       | <i>ACE</i>    | 0.84     | 1.31 x10 <sup>-9</sup>  | Females |
| cg25156443      | 10       | <i>ACVRL1</i> | 0.87     | 2.27 x10 <sup>-9</sup>  | Females |
|                 |          |               |          |                         |         |
| 18              |          |               |          |                         |         |
| cg14056357      |          | <i>ACSF3</i>  | 0.45     | 0.0002                  | Males   |
| cg13063405      | 18       | <i>C5</i>     | -0.11    | 0.0002                  | Females |
|                 |          |               |          |                         |         |
| <i>MRC2</i>     |          |               |          |                         |         |
| cg02516257      | 18       | <i>ZHX3</i>   | 0.73     | 0.0003                  | Females |
| cg00907843      | 18       | <i>SOS1</i>   | 0.67     | 0.0007                  | Females |
| cg04535371      | 18       | <i>AKR7A3</i> | -0.75    | 0.002                   | Females |

Note: Top 5 most statistically significant associations for each sex and age are shown here.

## Discussion

### Strengths and limitations

The strength of this study exists in its focus on longitudinal assessment of asthma acquisition at two important transition periods, pre- to post-adolescence and to later adulthood, along with DNAm at two critical time points, pre- and post-adolescence. Although for the CpGs discovered in IOWBC, more than 50% showed consistent findings in ALSPAC, statistical significance was observed at a small number of CpG sites. One reason for this lack of significance might be the age differences between the two cohorts. In addition, there is a potential concern of data double dipping. However, we do not see this as a significant concern in that the statistical model applied

in the screening process (linear regression without covariates such as atopic and smoking status) was different from the model in the final analyses (logistic regression with potential covariates). Another potential limitation is in the design of data analyses, which focused on each individual CpG site. However, CpG sites might be correlated and work jointly to impact the risk of asthma acquisition, which certainly deserves future investigations accompanied by carefully designed analytical plans. Finally, both cohorts, although independent, are mainly Caucasians. Thus, our findings are likely limited to only this population.

### **Innovation**

To our knowledge, this is the first study to examine the epigenetics of asthma acquisition from pre- to post- adolescence, and post-adolescence to young adulthood with respect to gender and transition period specificity.

### **Conclusion**

We assessed the longitudinal association of DNAm measured at earlier ages with asthma acquisition at later ages for each sex based on data in two independent cohorts with IOWBC as the discovery cohort and ALSPAC as the replication cohort. In the IOWBC, at 205 CpGs, pre-adolescence DNAm was shown to be associated with the odds of asthma acquisition from pre- to post-adolescence, and post-adolescence DNAm was associated with asthma acquisition from post-adolescence to adulthood. At 112 of these 205 CpGs, (54.6%), consistent associations were observed in the ALSPAC cohort, including statistically significant findings at 7 CpGs. These 112 CpGs included 62 CpGs (9 in males) showing transition-specific associations with asthma acquisition in that the association of DNAm with asthma acquisition at these 62 CpGs was different between the pre- to post-adolescence transition period and the post- to adulthood transition period. The identified CpGs based on two independent cohorts have a potential to

guide future studies in asthma acquisition prediction at different transition periods. Assessment of biological relevance of the identified CpGs indicated a potential epigenetic regulatory functionality of these CpGs on expression of their mapped and neighboring genes using a window size of 500 kbps.

Our findings also indicated significant differences between males and females. For the 62 CpGs showing consistent transition-specific effects between the two cohorts, at most of the CpGs in males, we found that an increase in DNAm was associated with an increased odds of asthma acquisition during the period from pre- to post-adolescence transition, while for the next transition period, at most of the CpGs, increased DNAm was associated with decreased odds. However, in females, at most of the CpGs, the associations were opposite compared to those in males; in females, an increase in DNAm was shown to be associated with a decreased odds of asthma acquisition from pre- to post-adolescence at most CpGs, but with increased odds at most of the CpGs in the transition period from post-adolescence to adulthood. Among the 50 CpGs (13 in males) showing main effects on asthma acquisition, although at most of the CpGs, an increase in DNAm was associated with a decreased odds of asthma acquisition for both males and females, the proportion of such CpGs was larger in females than in males. Furthermore, the effect sizes were overall weaker in females than in males. Before adolescence, asthma is more prevalent in males but during adolescence, more females acquire asthma and the prevalence of asthma in females surpasses that of males. The unique CpGs identified for each sex without any overlap and the inconsistent associations of DNAm with asthma acquisition between males and females seemed to be related to the gender-reversal phenomenon of asthma prevalence from pre- to post-adolescence.

In order to make sure that the identified CpGs are unique to each sex, the CpGs that were replicated in both cohorts were re-analyzed in opposite sex. For this, CpGs identified in males were evaluated for their association with asthma acquisition in females, and vice-versa. But I did not identify significant associations in either sex through this re-analysis. This ensures that the identified CpGs are unique to each sex.

Although we did not identify statistically significant biological processes after adjusting for multiple testing, biological processes involved in host immune function related to IL7 (i.e., interleukin-7-mediated signaling pathway, response to interleukin-7, cellular response to interleukin-7) were among the top processes determined based on statistical significance. IL7 signaling has been suggested to promote immunopathogenesis of asthma [105, 106], indicating the potentially informativity of the identified CpGs on asthma acquisition. In addition, the *TMEM194A* gene identified based on DMR analyses in males has been previously shown to be associated with asthma in GWAS catalog [107]. For females, gene *SERPINE2* in one of the identified DMRs has been connected with asthma based on genetic studies [108].

The gene *AKAP1*, mapped to the CpG showing consistent and statistically significant interaction effects in both cohorts in females, has been showed to be associated with asthma in the Agricultural Lung Health Study[109]. Although there was no overlap in identified CpGs between males and females, the gene *ENO1* was among the mapped genes of the associated CpGs in both sexes. The detection of IgG autoantibodies to alpha-enolase has been shown to be the most significant indicator for distinguishing severe asthma from mild-to-moderate asthma (OR= 5.2, 95% CI= 2.1-12.9, p-value < .001). It has been shown that alpha-enolase, an autoantigen, was associated with severe asthma[110]. The connection of gene *ENO1* with asthma acquisition

shown in our study is consistent with its differentiation between severe and mild-to-moderate asthma.

## **Chapter 4**

**Aim 2: To examine whether atopy in childhood mediates the association of DNAm in newborns with asthma acquisition across adolescence.**

### **Background**

Asthma is a common chronic respiratory condition and a major public health concern. Globally, it is ranked 16th among the leading causes of years lived with disability and 28th among the leading causes of burden of disease, as measured by disability-adjusted life years [111]. Atopy is defined as tendency to produce immunoglobulin E (IgE) antibodies in response to small amounts of common environmental exposures. It is a risk factor of asthma incidence [112] and affects 10-30% of general population in developed countries [113]. A number of studies have shown atopic diseases in early childhood are associated with asthma development later in life [114-116].

Carroll et.al. have shown a dose-response relationship in the association of atopic sensitization and asthma among children, i.e., the severity of asthma increases with increase in atopic sensitization to allergens [117].

For childhood asthma, a gender reversal in asthma prevalence from pre- to post-adolescence has been observed; more boys remit asthma than girls during adolescence whereas more girls acquire asthma than boys [118-121]. The underlying mechanisms involved in these sex differences of asthma across adolescence are unclear. The pathogenesis of asthma reflects a combination of genetic and epigenetic components; however, genetics explain only a fraction of variation in asthma risk. In addition to the effect of genetic factors, their interaction with changing environmental factors may also be responsible for atopy susceptibility and consequently contribute to the increase in prevalence of atopy-related disorders [122]. Several studies have explained the role of epigenetics in response to environmental factors in the development of

asthma [123-125]. One of the widely studied epigenetic mechanism is DNA methylation (DNAm) [71, 126]. DNAm or longitudinal changes in DNAm at specific cytosine-phosphate-guanine (CpG) sites have been shown to be associated with both atopy [127-130] and asthma or asthma acquisition [58, 59, 61, 75, 129, 130] in children and young adults. Among these studies, most utilized cross-sectional design to assess the associations of DNAm with atopy or asthma, except for the studies of Danielewicz, et al. and Reese, et al. Danielewicz, et al., via an epigenome-wide association study of 96 mother-child pairs, identified 83 CpG sites in cord blood of newborns that were associated with maternal atopy [127]. Reese et.al. demonstrated using 8 cohort studies that 9 CpGs in newborns were differentially methylated in relation to asthma [59]. However, no studies have focused on identification of methylation sites in newborns that are associated with these chronic conditions at later age.

DNAm in embryonic and pluripotent stem cell is close to zero [131] and it changes extensively from fertilization to implantation [132]. DNAm in newborns has been shown to be influenced by several maternal factors, such as smoking during pregnancy, pre-pregnancy BMI and gestational weight gain [133-136], potentially increase their offspring's risk of atopy and asthma. DNAm in newborns, as a memory of accumulated prenatal exposure, may serve as effective markers and be applied to predict the risk of later age atopy and asthma at a much earlier age.

However, as a risk factor of asthma, the role of atopy on the association of DNAm in newborns with asthma at a later age is unknown. Asthma can be atopic and non-atopic, and the underlying mechanisms is likely to be different in terms of DNAm markers. That is, at certain CpGs, it is possible that effects of DNAm at these CpGs in newborns on asthma at a later age are not mediated by atopy, and these CpGs might play a role in the development of non-atopic rather than atopic asthma. All these motivated the current study. In particular via path analyses, we

examine whether atopy in childhood mediates the association of DNAm in newborns with asthma acquisition at a later age. In addition to using SPT to determine atopic status, specific IgE have been used to assess the status of allergic sensitization against a specific allergen. The agreement between these two methods has been demonstrated in the literature [137]. Furthermore, one of our earlier studies showed that specific IgE-based and SPT-based assessment of atopic status were consistent in terms of their association with DNAm [138]. Such an agreement further supported the use of atopic status determined based on SPT in this study. We specifically focus on asthma acquisition from pre- to post-adolescence to identify epigenetic markers in newborns to facilitate our understanding of the phenomenon on gender reversal of asthma prevalence during this period. Direct and indirect effects (via pre-adolescence atopy status) of DNAm in newborns on asthma acquisition are evaluated using path analyses, based on which we identify potential epigenetic markers for asthma acquisition and at least some of the markers are associated with asthma acquisition via atopy.

## Methods

IOWBC Study Population, asthma acquisition and gene expression at 26 years were explained previously in Chapter 3.

### ***Covariates***

Information regarding sex, breastfeeding duration in weeks and age at specific pubertal events, i.e., age at onset of voice deepening in males and age at onset of menarche in females, was extracted from questionnaire data. Socio-economic status (SES) was defined based on household income, number of rooms and maternal education. Active smoking status at 18 years was recorded as ‘yes’ if the participant was a current smoker. Second-hand smoke exposure at 18 years was determined using information obtained for tobacco smoke exposure from mother,

father, others, or outside home. Smoke exposure at 18 years was defined by combining active and second-hand smoke exposure at 18 years.

### **DNA methylation**

DNA was extracted from Guthrie cards (blood collected within 5 days of birth) using standard procedures. One microgram of DNA was bisulfite-treated for cytosine to thymine conversion using the EZ 96-DNA methylation kit (Zymo Research, Irvine, CA, USA) for each sample, following the manufacturer's standard protocol. Genome-wide DNAm for each CpG was assessed using the Infinium MethylationEPIC BeadChip (Illumina, Inc, San Diego, CA, USA), which interrogate >850,000 CpG sites. Arrays were processed using a standard protocol as described elsewhere [139], with multiple identical control samples assigned to each bisulfite conversion batch to assess assay variability.

Preprocessing and quantile-normalization of DNAm intensity data was done similarly as explained previously for ages 10 and 18 years. The R package *ComBat* [140] was then applied to the M-values to adjust for batch effects. Cell type compositions were adjusted similarly as explained for ages 10 and 18 years.

### **Statistical analysis**

Chi-square tests for categorical variables and one-sample t-tests for continuous variables were applied, stratified by sex to examine whether the analytic sample (n= 796) reasonably represents the complete cohort (n=1456). Considering the observed phenomenon of gender reversal in asthma prevalence from pre-adolescence to post-adolescence, we performed the analyses separately for each sex.

**Research question 2.1:** Does pre-adolescence atopy mediate the association of DNAm in newborns with asthma acquisition across adolescence in IOWBC?

Screening for CpGs related to atopy status at 10 years and asthma acquisition at 18 years

Regression of M-values of DNAm at each CpG site on the 6 cell type proportions [92] was done to obtain cell-type-adjusted DNAm (residuals) for each sex, and residuals were used in the subsequent analyses. Genome-wide screening of CpGs in newborns for their potential association with atopic status at 10 years and asthma acquisition from 10 to 18 years was done separately using an R package, *ttScreening* [141]. The screenings were performed on 551,710 CpGs separately for each sex.

In addition, via epigenome-wide DNAm data, we identified candidate CpGs based on detection of differentially methylated regions (DMRs) for their association with asthma acquisition from 10 to 18 years using *DMRff* package in R [142]. *DMRff* overcomes the shortcomings of *DMRcate* by consistently controlling for false positive rates, and more importantly, considers the uneven distribution of CpGs on the arrays. CpGs in DMRs that were statistically significant, after adjusting for multiple testing by controlling false discovery rate (FDR) of 0.2, along with CpGs that passed *ttScreening*, were included in subsequent analysis as candidate CpGs.

Structural equation analyses

We evaluated the mediating effects of atopy at 10 years in the association of DNAm in newborns and asthma acquisition from 10 to 18 years using structural equation analyses (Figure 6), with potential confounders included in each path. The path coefficients (direct and indirect estimates) represent a partial correlation between the independent and dependent variables after adjusting for confounders and covariates in the model [143]. An R package, *MplusAutomation*, was

implemented to iteratively call *MPlus* from R to perform structural equation analyses with each CpGs as an independent variable (Figure 6) [144]. Goodness of fit was determined using Chi-square test p-value  $>0.05$ , RMSEA  $\leq 0.06$ , TLI  $\geq 0.95$ , and CFI  $\geq 0.95$  [145].

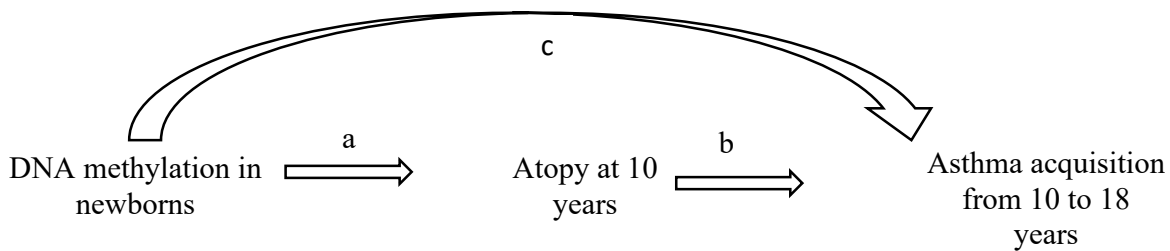


Figure 6: Structural equation analyses\_model with atopy at 10 years as the mediator in the association of DNAm in newborns with asthma acquisition at young adulthood

a=effects of DNAm in newborns on atopic status at 10 years, controlled for socio-economic status (SES) and breastfeeding duration

b= effects of atopy at 10 years on asthma acquisition from 10 to 18 years, controlled for breastfeeding duration, socio-economic status (SES), smoke exposure at 18 years, pubertal events (age at onset of voice deepening in males and age at onset of menarche in females)

c= direct effects of DNAm in newborns on asthma acquisition from 10 to 18 years

#### **Research question 2.2:** Can the findings of research question 2.1 be replicated in ALSPAC?

CpGs in newborns showing association with asthma acquisition from 10 to 18 years via atopy at 10 years were further tested in an independent cohort, the Avon Longitudinal Study of Children and Parents (ALSPAC) [98-100]. DNAm from cord blood in the ALSPAC cohort was assessed using the Infinium HumanMethylation450 BeadChip. The pre-processing of DNAm was performed using the *minfi* package [87] and CpGs with detection p-value  $\geq 0.01$  were excluded. Samples that contained sex-mismatch based on X-chromosome methylation were also excluded. In total, 420,399 probes are available for analysis after excluding probes that failed quality control. Estimated cell type proportions of CD4+ T cells, natural killer cells, B cells, monocytes, and granulocytes cells were adjusted to control for cell heterogeneity in the analysis. DNAm in

newborns was included in our study and its residuals were calculated by regression of M-values on cell type proportions (cell-type adjusted DNAm).

Asthma acquisition was assessed from 7 to 17 years, i.e., not having asthma at 7 years and having asthma at 17 years (no→yes). Identical structural equation analyses\_models with comparable covariates available in ALSPAC, including SES, breastfeeding duration, smoke exposure at 15 and 17 years and pubertal events were used.

**Research question 2.3:** What are the biological pathways of genes corresponding to the identified CpGs in IOWBC?

Using the screened CpGs in newborns showing potential association with atopy and/or asthma acquisition, the genes annotated to the CpGs were summarized based on Illumina's manifest file. Pathway enrichment analysis of the genes were conducted using *gometh* package [146] in R software [147] using statistical significance level of 0.05.

**Research question 2.4:** Is there an association between DNAm at age 26 years and gene expression of nearby genes i.e., within 250kb upstream and downstream region of the identified CpGs at 26 years?

Genes annotated to the replicated CpGs showing indirect and direct effects on asthma acquisition were extracted along with information such as gene location, chromosome number from the Illumina's manifest file or UCSC genome browser (<https://genome.ucsc.edu/>). To assess the biological relevance of these CpGs, linear regressions were applied to test the association of DNAm (in M- values; independent variable) at age 26 years at each CpG site with expression of its neighboring genes (250k base pairs [bps] upstream and 250k bps downstream of the CpG site) in blood at 26 years of age. Paired DNAm and expression data of n=140 subjects were included

in the analyses. As we previously have found the association between gene expression and DNAm to be different in both males and females, the analysis was stratified by sex [61, 104].

## Results

We included 401 male and 395 female participants in our study. Our subsample represented the complete cohort in terms of variables included in our study, shown by p-value > 0.05 in Table 5.

The flow chart of sample selection for the present study is in Supplement Figure S4.

Table 5: Comparison of analytical subsample with complete cohort

| Variables                 |              | Males                          |                                      |         | Females                        |                                      |         |
|---------------------------|--------------|--------------------------------|--------------------------------------|---------|--------------------------------|--------------------------------------|---------|
| Categorical variables     |              | Subsample<br>(n=285);<br>n (%) | Complete cohort<br>(n=401);<br>n (%) | P-value | Subsample<br>(n=323);<br>n (%) | Complete cohort<br>(n=395);<br>n (%) | P-value |
|                           |              |                                |                                      |         |                                |                                      |         |
| Asthma transition         | Acquisition  | 27 (9.47)                      | 36 (5.87)                            | 0.23    | 43 (13.31)                     | 59 (9.50)                            | 0.28    |
|                           | Never asthma | 258 (90.53)                    | 473 (77.16)                          |         | 280 (86.69)                    | 485 (78.10)                          |         |
| Atopy at 10 years         | Yes          | 111 (31.18)                    | 160 (31.01)                          | 0.96    | 87 (24.37)                     | 119 (22.88)                          | 0.61    |
|                           | No           | 245 (68.82)                    | 356 (68.99)                          |         | 270 (75.63)                    | 401 (77.12)                          |         |
| Socio-economic status     | Low          | 61 (15.52)                     | 106 (15.5)                           | 0.68    | 48 (12.37)                     | 103 (15.30)                          | 0.38    |
|                           | Mid          | 303 (77.1)                     | 517 (75.58)                          |         | 307 (79.12)                    | 520 (77.27)                          |         |
|                           | High         | 29 (7.38)                      | 61 (8.92)                            |         | 33 (8.51)                      | 50 (7.43)                            |         |
| Smoke exposure (18 years) | Yes          | 241 (65.85)                    | 428 (65.64)                          | 0.95    | 250 (66.31)                    | 451 (68.33)                          | 0.51    |
|                           | No           | 125 (34.15)                    | 224 (34.36)                          |         | 127 (33.69)                    | 209 (31.67)                          |         |
| Continuous variables      |              | Mean ± SD                      | Mean ± SD                            |         | Mean ± SD                      | Mean ± SD                            |         |
| Age at puberty            |              | 14.21 ± 1.23                   | 14.24 ± 1.24                         | 0.67    | 12.74 ± 1.39                   | 12.72 ± 1.42                         | 0.69    |
| Duration of breastfeeding |              | 14.95 ± 14.18                  | 14.55 ± 14.62                        | 0.65    | 14.37 ± 15.05                  | 13.99 ± 14.99                        | 0.62    |

The *ttScreening* package in R was applied to 551,710 CpGs to identify candidate CpGs potentially associated with atopy at 10 years or asthma acquisition from 10 to 18 years, stratified by sex. In males, 126 CpGs were potentially associated with atopy at 10 years of age and 93 CpG with asthma acquisition from 10 to 18 years. In females, 196 CpGs were potentially associated with atopy and 182 CpG with asthma acquisition. No common CpGs were found between atopy and asthma in both sexes, and there were no overlapping CpGs between males and females.

Thus, in total 597 CpGs passed screening by use of the *ttScreening* package in R. To incorporate CpG sites located in differentially methylated regions into the analyses, we further analyzed DNA methylation at the genome-scale to identify DMRs with respect to asthma acquisition as an additional screening process. At FDR=0.2, in males, we identified one DMR located on chromosome 6. The region starts at nucleotide position 33255784 and covers 432 base pairs. Four CpGs, cg17131579, cg19048360 and cg27355501 on gene *PFDN6* and cg02272258 on *WDR46*, are in this region. For females, no DMRs were identified. Altogether, 223 CpGs in males and 378 CpGs in females (in total, 601 CpGs) were analyzed for their enrichment in pathways or biological processes and tested via path analysis to assess their effects on asthma acquisition in adolescence via childhood atopy.

To better understand the biological function of the screened CpGs showing potential association with atopy and asthma acquisition (223 CpGs in males and 378 CpGs in females), pathway enrichment analyses was conducted for. The 223 CpGs in males were mapped to 192 genes and 378 CpGs in females to 324 genes. Using these CpGs in *gometh* package in R, we identified 152 biological processes in males and 215 in females that were enriched at p-value <0.05. Among the total 192 and 324 genes in males and females respectively, 45 genes in males and 82 in females

were involved in the identified pathways (Table 6 and Supplemental Table S5). No common biological processes were identified between males and females.

**Table 6(A):** Top 10 most statistically significant GO terms and its biological processes from pathway enrichment analysis in each pathway for males, for the identified CpGs.

| <b>GO term</b> | <b>Biological processes</b>  | <b>P-value</b> |
|----------------|--|----------------|
| GO:0046380     | N-acetylneuraminate biosynthetic process                               | 0.005          |
| GO:0035459     | vesicle cargo loading  | 0.006          |
| GO:0042700     | luteinizing hormone signaling pathway                                  | 0.007          |
| GO:0033140     | negative regulation of peptidyl-serine phosphorylation of STAT protein | 0.007          |
| GO:0032462     | regulation of protein homooligomerization                              | 0.008          |
| GO:0006045     | N-acetylglucosamine biosynthetic process                               | 0.008          |
| GO:1901073     | glucosamine-containing compound biosynthetic process                   | 0.008          |
| GO:0072665     | protein localization to vacuole  | 0.009          |
| GO:0044727     | DNA demethylation of male pronucleus                                   | 0.009          |
| GO:1903895     | negative regulation of IRE1-mediated unfolded protein response         | 0.009          |

**Table 6(B):** Top 10 most statistically significant GO terms and its biological processes from pathway enrichment analysis in each pathway for females, for the identified CpGs.

| <b>GO term</b> | <b>Biological processes</b>                          | <b>P-value</b> |
|----------------|--|----------------|
| GO:1901985     | positive regulation of protein acetylation           | 0.0009         |
| GO:0033144     | negative regulation of intracellular steroid hormone | 0.001          |
| GO:0051582     | positive regulation of neurotransmitter uptake       | 0.002          |
| GO:0045214     | sarcomere organization                               | 0.003          |
| GO:0021853     | cerebral cortex GABAergic interneuron migration      | 0.003          |
| GO:1904936     | interneuron migration                                | 0.003          |
| GO:0001188     | RNA polymerase I preinitiation complex assembly      | 0.004          |
| GO:0043438     | acetoacetic acid metabolic process                   | 0.004          |

---

Table 6(B): continue

---

| <b>GO term</b> | <b>Biological processes</b>                       | <b>P-value</b> |
|----------------|---|----------------|
| GO:0035066     | positive regulation of histone acetylation        | 0.004          |
| GO:0021894     | cerebral cortex GABAergic interneuron development | 0.004          |

---

After controlling for confounders, DNAm in newborns at 68 CpGs in males and 41 CpGs in females were found to be indirectly associated with asthma acquisition via atopy. It is worth noting that at 60 of the 68 and 37 of the 41 CpGs, only indirect effects were statistically significant. Of these, at 21 CpGs in males and 18 CpGs in females, a higher DNAm was indirectly associated with an increased risk of asthma acquisition via an increased risk of atopy. Whereas, at the remaining CpGs (39 CpGs in males and 19 CpGs in females), an increase in DNAm was indirectly associated with decreased risk of asthma acquisition via decreased risk of atopy (Supplemental Table S6). DNAm at certain number of CpGs only showed direct effects on asthma acquisition; in particular, DNAm in newborns at 99 CpGs in males and 192 CpGs in females were directly associated with asthma acquisition from 10 to 18 years age. Of these, for 50 (51%) CpGs in males and 72 (38%) CpGs in females, an increase in DNAm was directly associated with an increase in the risk of asthma acquisition (Supplemental Table S7).

CpGs showing indirect associations in IOWBC were further tested in the ALSPAC cohort to assess their potential of reproducibility. In ALSPAC cohort, DNAm data in newborns was available for 41 CpGs (of the 68 in IOWBC) in males and 18 CpGs (of the 41 in IOWBC) in females. Of these, the direction of indirect effects was consistent with those in IOWBC at 20 (49%) CpGs in males and 10 (56%) CpGs in females, although none of these CpGs were statistically significant. It is worth mentioning that of the 20 and 10 CpGs in males and females, all CpGs showed only indirect effects (Supplement Table S6). For CpGs showing only direct

effects in IOWBC (99 in males and 192 in females), DNAm in ALSPAC was available for 54 and 113 CpGs in males and females respectively. Of these, at 25 CpGs in males and 78 CpGs in females were in the same direction with one CpG (cg12938020) in males and 11 in females as being statistically significant (Supplemental Table S7).

The biological relevance of CpGs showing consistent direct and indirect effects on asthma acquisition between the two cohorts were further assessed. We evaluated the association of DNAm at the identified 133 CpGs (45 in males) with the expression of nearby genes (measure at age 26 years) that the CpGs were mapped to. To identify nearby genes, we used a range of 500k base pairs (bps) (i.e., 250k bps up and down stream) of the CpG site were also included in the assessment. In this analysis, DNAm and gene expression levels were assessed at age 26 years. Significant effects of DNAm were observed at 35 CpGs on their association with expression of 213 genes in males, and at 61 CpGs with expression of 357 genes in females (Table 7 and Supplement Table S8). Of the 570 genes' expression (213 in males) associated with DNAm, increased DNAm was associated with increased expression of 289 genes (130 in males).

Table 7: Top 5 most significant associations of DNAm with expression of neighboring mapped genes in each sex.

| CpG site   | Gene name    | Estimate | P-value                 | Sex     |
|------------|--------------|----------|-------------------------|---------|
| cg25121621 | <i>COPRS</i> | 1        | 5.14x10 <sup>-11</sup>  | Males   |
|            | <i>PAGRI</i> | 1.34     | 1.48 x10 <sup>-9</sup>  |         |
|            | <i>GDPD3</i> | 0.79     | 7.66 x10 <sup>-9</sup>  |         |
|            | <i>TBX6</i>  | 0.52     | 1.16 x10 <sup>-8</sup>  |         |
|            | <i>LTI</i>   | 0.65     | 1.85 x10 <sup>-8</sup>  |         |
| cg04720635 | <i>CCDC7</i> | -1.84    | 3.01 x10 <sup>-26</sup> | Females |

Table 7: Continue

| CpG site | Gene name       | Estimate | P-value                 | Sex     |
|----------|-----------------|----------|-------------------------|---------|
|          | <i>TP53INP2</i> | -0.93    | 5.38 x10 <sup>-10</sup> | Females |
|          | <i>MAK16</i>    | -0.69    | 2.16 x10 <sup>-9</sup>  |         |
|          | <i>AQP3</i>     | -1.36    | 3.74 x10 <sup>-9</sup>  |         |
|          | <i>N4BP2L2</i>  | -0.40    | 3.79 x10 <sup>-8</sup>  |         |

Note: Top 5 most statistically significant associations for each sex are shown here.

***Connections with findings in Chapter 3.*** There was no overlap in the CpGs identified in this study (indirect or direct) and those identified in aim 1 for both sexes. DNAm in aim 1 was measured at 10 and 18 years while in aim 2 was at birth. The different sets of identified CpGs at this two time points may reflect potential dynamicity of epigenetic markers of asthma acquisition. Denser DNAm assessment between birth and age 10 years may help reveal the drifting effects of DNAm at birth as markers for asthma acquisition during adolescence. Atopic status at 10 years of age was included as a mediator in the assessment on the association of DNAm in newborns with asthma acquisition in aim 2. While in aim 1, atopic status at 10 years was used as a confounder. It is possible that atopic status in aim 1 may have played a role as a mediator as well. However, since atopic status determination and DNAm assessment both happened at the same age (10 years), the role of atopic status as a mediator conceptually may not hold under this specific design, but rather a potential confounder as done in aim 1. Nevertheless, it will be of interest to examine the role of atopy as a mediator at different time points.

## **Discussion**

### **Strengths and limitations**

The availability of asthma status at two key time points, pre- and post-adolescence, offered the possibility to examine asthma acquisition during adolescence. Identification of DNAm markers in newborns provides epigenetic insights in fetal life that potentially offered us an opportunity to predict the risk of later-life allergic and respiratory morbidity much earlier before disease manifestation. This study design with a clear time order (birth, pre-adolescence, and post-adolescence) allowed dissection of the total effects of DNAm in newborns on the risk of childhood asthma and whether and how atopy played a role in between.

Although the direction of mediating effects was consistent between the two cohorts at 16 and 7 CpG sites in males and females, respectively, none of them were statistically significant in the ALSPAC cohort. A possible reason for the statistical insignificance in the ALSPAC cohort might be due to the differences in the ages of assessment. In the ALSPAC cohort, atopy at age 7 years and asthma acquisition from 7 to 17 years was included, while in IOWBC, atopy was at age 10 years and asthma acquisition from 10 to 18 years. It is possible that the effect of DNAm in newborns on atopy was not strong enough to be detected at age 7 years. In addition, DNAm in IOWBC was measured in Guthrie cards while DNAm in ALSPAC was measured in cord blood. A recent study noted that when outcome or exposure are binary, agreement in findings between these two sources is expected to be at 70% of all CpGs under investigation [148]. This discrepancy between these two different sources of DNA might also have affected the statistical power in the replication analyses in the ALSPAC cohort.

In addition, our study evaluated the contributions of each individual CpG site. These CpGs may be correlated and jointly impact asthma acquisition, which could not be addressed by the present

study. Nevertheless, the consistency in the results between the two cohorts indicate that the identified CpGs in newborns are likely to play a role in the underlying mechanisms of asthma acquisition across adolescence. The recognized CpGs have a potential to improve our understanding of different underlying pathways (through atopy or not) from DNAm in newborns to asthma acquisition during adolescence.

### **Innovation**

To our knowledge, this is the first study to examine the direct and indirect effects of DNAm in newborns on asthma acquisition from pre- to post-adolescence via pre-adolescence atopy status.

### **Conclusion**

We examined the direct and indirect effects of DNAm in newborns on asthma acquisition from pre- to post-adolescence via pre-adolescence atopy status in two independent cohorts. In the IOWBC discovery cohort, DNAm in newborns at 68 CpGs in males and 41 CpGs in females were found to be indirectly associated with asthma acquisition from 10 to 18 years via atopy. Of these discovered CpGs that were available in the ALSPAC replication cohort (41 CpGs in males and 18 in females), 20 (49%) CpGs in males and 10 (56%) in females showed consistent direction of mediation effects in the ALSPAC, although not statistically significant. All these 30 CpGs showed only indirect effects. Of these 30 CpGs, at six CpGs in males and two CpGs in females, an increase in DNAm was indirectly associated with an increase in asthma acquisition risk via an increase in risk of atopy. For the remaining 22 of the 30 CpGs, an increase in DNAm was indirectly associated with decreased risk of asthma acquisition via decreased risk of atopy at 14 CpGs in males and eight CpGs in females.

In addition to these CpGs showing an effect on asthma acquisition via atopy, we discovered in total 291 CpGs (99 in males) that only had direct effects on asthma acquisition. Among these

291 CpGs, 103 showed consistent direction of effects in the ALSPAC cohort (25 in males) with one CpG site (cg12938020) in males and 11 in females showing statistical significance at 0.05, and at about half of these CpGs, a higher DNAm was associated with a higher odds of asthma acquisition.

Re-analysis of the DNAm sites (direct and indirect) replicated in both cohorts were evaluated in opposite sex. For this, CpGs identified in males were analyzed in females for their association with asthma acquisition, and vice versa. At 4 CpGs in males and 4 in females, statistically significant direct effects of DNAm on asthma acquisition were detected. Of these 8 CpGs (4 in males), 4 CpGs (3 in males) had same direction of effects. These 4 CpGs (cg18694780, cg16622920, cg06365057 in males and cg13331559 in females) may represent common underlying mechanisms for non-atopic asthma development during adolescence in both sexes. No such CpGs were identified for atopic asthma.

Assessment of biological relevance of the replicated CpGs indicated a potential epigenetic regulatory functionality of these CpGs on expression of their neighboring genes using a window size of 500 kbps. DNAm at 35 CpGs were associated with expression of 213 genes in males, and at 61 CpGs with expression of 357 genes in females. At 130 of the 213 genes in males and at 159 of the 357 genes in females, an increase in DNAm was associated with increased gene expression levels.

Allergic asthma can be atopic or non-atopic asthma. Atopic asthma is IgE mediated while non-atopic asthma is non-IgE mediated, i.e., eosinophilic or Th2 (T-helper 2) asthma. We postulate that the 30 CpGs showing only indirect effects might play a role in the development of atopic asthma due to the involvement of atopy as a mediator. On the other hand, the 103 CpGs showing direct effects only may contribute to the occurrence of non-atopic asthma

since whether an individual was atopic or non-atopic did not influence the association of DNAm in newborns with asthma acquisition. CpG site cg12938020 showing significant direct effects in both cohorts is mapped to *HOXD3* gene, and Wang et.al. have shown rs10954213, located in *HOXD3* gene, influences *IRF5* gene expression, which is further linked to asthma [149].

In the top biological pathways detected through enrichment analysis based on CpGs that passed screening, several pathways and biological processes drew our attention and have been suggested to play an important role in the pathogenesis of asthma and allergy. In relation to the luteinizing hormone signaling pathway identified based on CpGs that passed screening for males, studies have shown lower levels of luteinizing hormone in patients with bronchial asthma [150, 151].

Annotated genes of the CpGs that passed screening were possibly also enriched in two biological processes related to biosynthesis of glucosamine, N-acetylglucosamine biosynthetic process and glucosamine-containing compound biosynthetic process, and glucosamine has been linked to atopy and respiratory tract secretions of asthmatic patients [152]. For the identified pathways of positive regulation of protein acetylation and histone acetylation, they are likely to be involved in the development of allergic diseases and asthma [153, 154]. The airway epithelium from asthmatic subjects displayed increased histone acetylation levels compared to non-asthmatic subjects [155]. These previous studies support the findings from our enrichment analyses and strengthen the possible connection between those CpGs with atopy and/or asthma. *PEX14* gene was involved in the top biological processes in males and also showed only indirect effects in both the cohorts. It has been found to be associated with asthma [156-158] as well as atopy [159]. *TMED10*, *BFAR* in males and *OBSL1* in females were among the top 10 biological processes and showed only direct effects in both cohorts. Previous studies have shown *TMED10* to be differentially- expressed in severe asthma [160], and *OBSL1* is overexpressed in asthma

cases compared to controls (foldchange= 1.305937, FDR p-value= 0.00217526) [161]. These findings may support the role of *PEX14* gene in atopic asthma while *TMED10* and *OBSL1* gene in non-atopic asthma. The identified CpGs from both cohorts may serve as biomarkers of atopic and non-atopic asthma. Future studies are encouraged to investigate the role of DNAm at these CpGs as mediator in the association of exposures during fetal development with asthma.

## **Chapter 5**

**Aim 3: To examine sex-specific associations of DNAm in Guthrie cards of newborns with pre-adolescence asthma and/or rhinitis**

### **Background**

Asthma affects more than 300 million people worldwide [162], and is ranked 16<sup>th</sup> among the leading causes of years lived with disability. Asthma most often originates in childhood and so higher incidence and prevalence is found among children. Asthma incidence and prevalence is different between males and females. A higher incidence, prevalence and hospitalization is seen in pre-pubertal boys than girls of same age, while a reverse trend is observed during adolescence [61, 163]. Another closely related airway disease, rhinitis, has been treated as a risk factor of asthma [164]. Among different types of rhinitis, allergic rhinitis affects 10-40% of world population with a prevalence of 8.4% in children and 14.9% in adolescents. It is the most common allergic disease among children [165] leading to long-term consequences in adulthood. Asthma and rhinitis are common chronic conditions that occur as comorbidities. About 40% of patients with allergic rhinitis have asthma, and 94% of patients with allergic asthma have allergic rhinitis [166-169]. Another study found allergic rhinitis patients have three times increased risk of developing asthma. Also, relief of rhinitis symptoms over time had a correlation with improvement in asthma symptoms, and subjects with severe and persistent rhinitis are at increased risk of developing asthma [170]. It has been found that the prevalence of coexisting asthma and allergic rhinitis in pre-adolescence is predominant in males[171]. Both these conditions have complex etiologies involving both genetic and epigenetic mechanisms. The heritability estimates representing genetic contribution vary substantially, 35-95% for asthma and 33-91% for allergic rhinitis [172]. Studies have found genetic similarities

between asthma and rhinitis as shared phenotypes [57, 173] explained by concept of united airway disease, IgE and non-IgE sensitizations [174]. Recent studies further incorporated epigenetics to explain the pathogenesis of asthma [58] and allergic conditions due to its ability to mediate environmental effects. DNA methylation (DNAm) at 5'-C-phosphate-G-3' (CpG) sites is one of the most studied epigenetic mechanisms. Several studies have shown an association of DNAm in blood with the status of asthma [13, 58, 61] and allergic diseases [175-177]. A recent meta-analysis demonstrated that DNAm in newborns was associated with asthma in school-aged children in 8 cohorts [59]. However, literature on the connection between DNAm and rhinitis is limited. A study of allergic rhinitis (AR) participants identified 42 CpG sites showing correlations of AR symptoms with DNAm [64].

In this study, we focused on subjects with asthma and/or rhinitis (Ast\_Rh) and aim to identify CpG sites with DNAm in newborns associated with these two allergic diseases, asthma, and rhinitis, among pre-adolescent children. Genome-scale DNAm data and clinical data collected in the Isle of Wight birth cohort (IOWBC) were included in the study. Previously, a cross-sectional study with focus on Ast\_Rh was conducted among children aged 16 years based on DNAm in nasal epithelium [63]. Our study, on the other hand, is longitudinal with DNAm in blood on Guthrie cards of newborns. Findings from this study has a potential to identify individuals with higher risk of Ast\_Rh at a much earlier age.

## Methods

IOWBC Study Population and gene expression data at 26 years was explained in Chapter 3. DNAm at birth is explained in Chapter 4.

### ***Asthma and/or Rhinitis (Ast\_Rh)***

Asthma at 10 years was defined using ISAAC questionnaire as “ever had asthma” and “wheezing or whistling in the chest in the last 12 months” and/or “current treatment for asthma”. Based on responses to these questions, a participant was determined to have asthma if she/he had experienced recurrent wheezing in the last 12 months and been given a clinical diagnosis of asthma by the physician with or without being treated with asthma medications. Rhinitis at 10 years was defined as ‘In the past 12 months have you had a problem with sneezing or a runny or a blocked nose when you did not have a cold or the flu?’ [180]. The outcome of the study was asthma and/or rhinitis (Ast\_Rh) at 10 years, i.e., subjects with asthma only, rhinitis only, or both asthma and rhinitis were included in the study. Participants who did not have asthma nor rhinitis at 10 years were included in our study as a reference group.

### ***Covariates***

Atopic status at 10 years and SES are explained in Chapter 4. Second-hand smoke exposure at 10 years was determined using information obtained from tobacco smoke exposure from mother, father, others, or outside home at 1, 2, 4 and 10 years.

### ***Statistical analysis***

Chi-square tests for categorical variables and one-sample t-tests for continuous variables were applied, stratified by sex to examine whether the analytic sample (n=796) reasonably represents the complete cohort (n=1456).

**Research question 3.1:** Is the association of DNAm in newborns with pre-adolescence asthma and/or rhinitis sex-specific?

### **Screening for CpGs in newborns related to asthma and/or rhinitis at 10 years**

Regression of M-values of DNAm at each CpG site on the 6 cell type proportions [92] was done to obtain cell-type-adjusted DNAm (residuals) for each sex, and residuals were used in the subsequent analyses.

Screening of genome-scale CpGs potentially associated with Ast\_Rh was performed from two directions, separately for each sex, with the first direction focusing on individual CpGs and the second on CpGs in regions. To screen individual CpGs with DNAm in newborns possibly associated with Ast\_Rh at 10 years, an R package, *ttScreening* [141], was implemented. The method implemented in *ttScreening* can control both type I and type II errors.

In the second approach of screening, we identified candidate CpGs based on detection of differentially methylated regions (DMRs) for their association with Ast\_Rh at 10 years using the *DMRff* package in R [142]. CpGs in DMRs that were statistically significant at the level of false discovery rate (FDR) of 0.2 along with CpGs that passed *ttScreening* were included in subsequent analysis as candidate CpGs.

#### Association of DNAm in newborns with Ast\_Rh at 10 years

Multivariable logistic regression analysis was conducted to evaluate the association of DNAm in newborns (independent variable) at CpGs that passed screening with Ast\_Rh at 10 years (dependent variable). Sex, SES, duration of breastfeeding, atopy, and second-hand smoke at 10 years were included in the model as potential confounders. An interaction term of DNAm and sex was included in the model as an attempt to address sex difference in childhood asthma or rhinitis prevalence. For CpGs not showing significant interaction effects, their main effects were evaluated. In both situations (the models with main effects only, and the models that included interaction effects) multiple testing was adjusted by controlling FDR of 0.05.

**Research question 3.2:** What are the biological pathways of genes corresponding to the identified CpGs in IOWBC?

For candidate CpGs showing associations of DNAm with Ast\_Rh, genes annotated to the CpGs were summarized along with information including gene location and chromosome number extracted from the Illumina's manifest file and USCS genome browser (<https://genome.ucsc.edu>).

Pathway enrichment analysis of the identified candidate CpGs was conducted using the R function *gometh* [103] to gain insight of their biological functionality.

**Research question 3.3:** Can the findings of research question 3.1 be replicated in ALSPAC?

CpGs in newborns showing association with Ast\_Rh at 10 were further tested in an independent cohort, the Avon Longitudinal Study of Children and Parents (ALSPAC) [98-100]. DNAm measurement from cord blood has been explained previously in Chapter 4 (Research question 2.2).

Ast\_Rh was assessed at 7 years, i.e., subjects with asthma only, rhinitis only, or both asthma and rhinitis. Logistic regressions with comparable covariates available in ALSPAC, including SES, sex, atopy at 7 years and second-hand smoke at 7 years were used.

**Research question 3.4:** Is there an association between DNAm at age 26 years and gene expression of nearby genes i.e., within 250kb upstream and downstream region of the identified CpGs at 26 years?

Genes annotated to the replicated CpGs showing association with Ast\_Rh were extracted along with information such as gene location, chromosome number from the Illumina's manifest file or UCSC genome browser (<https://genome.ucsc.edu/>). To assess the biological relevance of these CpGs, linear regressions were applied to test the association of DNAm (in M- values; independent variable) at age 26 years at each CpG site with expression of its neighboring genes

(250k base pairs [bps] upstream and 250k bps downstream of the CpG site) in blood at 26 years of age. Paired DNAm and expression data of n=140 subjects were included in the analyses. As we previously have found the association between gene expression and DNAm to be different in both males and females, the analysis was stratified by sex [61, 104].

**Research question 3.5:** Is there a genetic influence on DNAm at the replicated CpGs, i.e., are there any methQTLs?

Single nucleotide polymorphisms (SNPs) associated with methylation levels of CpGs are known as methQTLs [179]. SNPs to be included in the analyses for methQTL assessment were the ones located on the CpGs' mapping genes using the Illumina manifestation file. Linear regression was used to evaluate this association where DNAm at birth was the dependent variables and SNPs was independent variables. CpGs with p-value <0.05 indicated its statistical significance on its association with SNPs (as methQTLs).

## Results

Descriptive statistics on the status of Ast\_Rh and variables potentially associated with the childhood asthma and rhinitis indicated that the subsamples represented the complete IOWBC (Table 8). The consort diagram for the study on samples included in the analyses is in Supplement Figure S5. Additionally, I looked at atopic status to make sure not all participants in Ast\_Rh are atopic (Supplement Figure S6).

Table 8: Comparison of analytical subsample with complete cohort

| Variables                         | Males                          |   |                | Females                        |   |                |
|-----------------------------------|--------------------------------|---|----------------|--------------------------------|---|----------------|
|                                   | Subsample<br>(n=392);<br>n (%) | Complete<br>cohort<br>(n=401);<br>n (%) | P-<br>value    | Subsample<br>(n=387);<br>n (%) | Complete<br>cohort<br>(n=395);<br>n (%) | P-<br>value    |
| Ast_Rh                            | Yes                            | 144 (36.7)                              | 222 (31.9)     | 0.1                            | 119 (30.8)                              | 192 (28.4)     |
|                                   | No                             | 248 (63.3)                              | 475 (68.1)     |                                | 268 (69.2)                              | 484 (71.6)     |
| Atopy at 10 years                 | Yes                            | 111 (31.2)                              | 160<br>(31.01) | 0.9                            | 87 (24.4)                               | 119<br>(22.88) |
|                                   | No                             | 245 (68.8)                              | 356<br>(68.99) |                                | 270 (75.6)                              | 401<br>(77.12) |
| Socio-economic status             | Low                            | 61 (15.5)                               | 106 (15.5)     | 0.68                           | 48 (12.4)                               | 103<br>(15.30) |
|                                   | Mid                            | 303 (77.1)                              | 517<br>(75.58) |                                | 307 (79.1)                              | 520<br>(77.27) |
|                                   | High                           | 29 (7.4)                                | 61 (8.92)      |                                | 33 (8.5)                                | 50 (7.43)      |
| Second-hand smoke at age 10 years | Yes                            | 266 (66.8)                              | 489 (64.3)     | 0.38                           | 246 (62.3)                              | 445 (68.4)     |
|                                   | No                             | 132 (33.2)                              | 272 (35.7)     |                                | 149 (37.7)                              | 280 (31.6)     |
| Continuous variables              | Mean ±<br>SD                   | Mean ±<br>SD                            |                | Mean ±<br>SD                   | Mean ±<br>SD                            |                |
| Duration of breastfeeding         | 14.95 ±<br>14.81               | 14.55 ±<br>14.62                        | 0.6            | 14.37 ±<br>15.05               | 13.99 ±<br>14.99                        | 0.63           |

To identify candidate CpGs potentially associated with Ast\_Rh at 10 years of age, *tScreening* stratified by sex was applied to 551,710 CpGs using residuals (cell-type adjusted DNAm) in newborns. In total, 154 CpGs in males and 339 in females in IOWBC passed screening. There were no overlapping CpGs between males and females, and union of these CpGs, i.e., 493 CpGs, were included in subsequent analyses. Additionally, using the R package *DMRff*, at FDR 0.2 level, we identified one DMR with 2 CpGs (cg00701456, cg08196106) in females on chromosome 12. As these 2 CpGs were in one DMR, they may work together. We treated these two CpGs as one CpG unit and used the mean of their cell-type-adjusted DNAm levels to represent DNAm of the CpG unit. No DMRs were identified in males. One CpG (cg08196106)

was common between the CpGs identified via *ttScreening* and those by *DMRff*. Thus, in total,

492 CpGs plus one CpG unit were included in further analyses.

Pathway enrichment analysis was conducted to better understand the biological functionality of the 154 screened CpGs in males and 340 CpGs (=339 CpGs from *ttScreening* + 1 CpG from *DMRff*) in females. The 154 CpGs in males were mapped to 123 genes, and 340 CpGs were mapped to 266 genes. Using these CpGs in *gometh* package in R, we identified 110 biological processes in males and 278 in females that were enriched at p-value <0.05. Among the mapped 123 and 266 genes in males and females respectively, 10 genes in males and 29 in females were involved in the identified pathways (Table 9 and Supplemental Table S9). No common biological processes were identified between males and females.

**Table 9(A): Top 10 most statistically significant GO terms and its biological processes from pathway enrichment analysis in each pathway for males, for the CpGs that passed screening.**

| <b>GO term</b> | <b>Biological processes</b>                                | <b>P-value</b> |
|----------------|--|----------------|
| GO:0045116     | protein neddylation  | 0.001          |
| GO:0033622     | integrin activation  | 0.004          |
| GO:0045956     | positive regulation of calcium ion-dependent exocytosis    | 0.004          |
| GO:1905078     | positive regulation of interleukin-17 secretion            | 0.004          |
| GO:0008049     | male courtship behavior                                    | 0.004          |
| GO:0042407     | cristae formation  | 0.005          |
| GO:0006393     | termination of mitochondrial transcription                 | 0.006          |
|                | regulation of substrate-dependent cell migration, cell     |                |
| GO:1904235     | attachment to substrate                                    | 0.006          |
|                | positive regulation of substrate-dependent cell migration, |                |
| GO:1904237     | cell attachment to substrate                               | 0.006          |
| GO:0002636     | positive regulation of germinal center formation           | 0.007          |

Table 9(B): Top 10 most statistically significant GO terms and its biological processes from pathway enrichment analysis in each pathway for females, for the CpGs that passed screening.

| <b>GO term</b> | <b>Biological processes</b>   | <b>P-value</b> |
|----------------|---|----------------|
| GO:0014834     | skeletal muscle satellite cell maintenance involved in skeletal muscle regeneration | 0.0007         |
| GO:0035264     | multicellular organism growth   | 0.001          |
| GO:0001678     | cellular glucose homeostasis  | 0.002          |
| GO:0089718     | amino acid import across plasma membrane  | 0.002          |
| GO:0071499     | cellular response to laminar fluid shear stress                                     | 0.003          |
| GO:0035902     | response to immobilization stress   | 0.003          |
| GO:0043090     | amino acid import   | 0.003          |
| GO:1904491     | protein localization to ciliary transition zone                                     | 0.003          |
| GO:0060563     | neuroepithelial cell differentiation  | 0.003          |
| GO:0046324     | regulation of glucose import  | 0.003          |

Via logistic regressions, we examined the interaction effects of DNAm and sex on the odds of Ast\_Rh at the 492 CpGs and one CpG unit, controlling for second-hand smoke exposure at 10 years, SES, duration of breastfeeding and atopy. After adjusting for multiple testing by controlling FDR at 0.05 level, 404 CpGs and one CpG unit showed significant interaction with sex. Of these, opposite effects of DNAm were observed at 330 CpGs in males and females, i.e., at 130 CpGs, an increase in DNAm was associated with a decreased odds of Ast\_Rh in males but increased odds in females. And at 199 CpGs and one CpG unit, an increase in DNAm was associated with an increased odds of Ast\_Rh in males but decreased odds in females. (Supplemental Table S10a). For CpGs not showing interaction effects between DNAm and sex, main effects of DNAm were assessed at 88 CpGs. After adjusting for FDR at 0.05 level, we identified 70 CpGs showing association of DNAm with Ast\_Rh controlling for sex and

previously mentioned covariates. At 32 of the 70 CpGs, an increase in DNAm was associated with an increased odds of Ast\_Rh while at the remaining 38 CpGs, the association was in the opposite direction (Supplemental Table S10b).

Altogether, we identified 475 (=405+70) CpGs in newborns with DNAm associated with Ast\_Rh at 10 years. We further tested these CpGs in the ALSPAC cohort. For the 405 CpGs showing interaction effects in IOWBC, consistent directions of interaction effects were observed at 116 CpGs of the available 242 CpGs, with 3 CpGs being statistically significant in ALSPAC. For the 70 CpGs showing main effects in IOWBC, 17 CpGs of the available 37 CpGs in ALSPAC showed same directions of associations identified in the IOWBC.

To assess the biological relevance of replicated CpGs showing association with Ast\_Rh, we evaluated the association of DNAm at the identified 129 CpGs with the expression of genes that the CpGs were mapped to as well as their nearby genes by considering a window of 500k base pairs (bps) of the CpG site (250k bps up and down stream). In this analysis, DNAm and gene expression levels were assessed at age 26 years. Significant effects of DNAm were observed at 86 CpGs on their association with expression of 396 genes in males, and at 96 CpGs with expression of 589 genes in females (Table 10 and Supplemental Table S11). Of the genes' expression associated with DNAm, increased DNAm was associated with increased expression of 208 genes in males and 345 genes in females.

Table 10: Top 5 most significant associations of DNAm with expression of neighboring mapped genes in each sex.

| CpG site   | Gene name     | Estimate | P-value                 | Sex     |
|------------|---------------|----------|-------------------------|---------|
| cg01662869 | <i>DPYSL4</i> | 0.92     | 4.30x10 <sup>-7</sup>   | Males   |
|            | <i>QRFP</i>   | 0.83     | 6.55 x10 <sup>-7</sup>  |         |
| cg19248893 | <i>RGS6</i>   | -1.8     | 8.53 x10 <sup>-7</sup>  | Males   |
| cg01662869 | <i>JADE2</i>  | 1.05     | 1.56 x10 <sup>-6</sup>  | Males   |
|            | <i>JAM3</i>   | 1.92     | 2.18 x10 <sup>-6</sup>  |         |
|            | <i>JADE2</i>  | 0.93     | 1.72 x10 <sup>-11</sup> | Females |
|            | <i>DPYSL4</i> | 0.83     | 2.99 x10 <sup>-10</sup> |         |
|            | <i>MOSPD1</i> | 0.56     | 8.41 x10 <sup>-8</sup>  |         |
|            | <i>GLB1L2</i> | 0.62     | 1.66 x10 <sup>-7</sup>  |         |
|            | <i>LAMC3</i>  | 0.68     | 1.67 x10 <sup>-7</sup>  |         |

Note: Top 5 most statistically significant associations for each sex are shown here.

For replicated 133 CpGs, their genetic influence was further assessed by evaluating if those CpGs had methQTLs. SNPs were extracted using the Illumina manifestation file and SNPs on the mapping genes of these CpGs were included in the analyses. In total, 791 SNPs for 47 CpGs were included in the analyses to assess methQTL. The analysis was sex stratified. We identified 29 CpGs in males and 31 CpGs in females (25 CpGs in common) showing association with SNPs i.e., methQTLs existed at those CpGs (Supplement Table S12).

## **Discussion**

### **Strengths and limitations**

The strength of this study exists in its focus on a longitudinal assessment of DNAm at a critical time point, less than a week after birth, with pre-adolescent asthma and/or rhinitis. In addition to assess contribution of individual CpG sites, we examined joint effects of CpGs identified via DMR analyses and some of those CpGs were otherwise excluded from analyses based on individual CpGs. Several limitations of the study exist. First, the study population was mainly Caucasians. This may be a limiting factor in the external validity of findings, and hence generalization of these findings should be implemented with caution. Second, the focus of the study was on associations rather than causality, and this analytical approach does not allow predictions or inferring causality. Third, DNA was extracted from blood cells while asthma and rhinitis primarily affect cells of the respiratory tract. Although DNAm of the blood cells has concordance with that of the respiratory system cells [181], some differences exist between the two. Hence, DNAm in blood may not fully reflect the DNAm in respiratory tract cells.

### **Innovation**

To our knowledge, this is the first longitudinal study to examine the association of epigenetics in newborns with pre-adolescent asthma and/or rhinitis in blood with respect to gender specificity.

### **Conclusion**

We assessed the longitudinal association of DNAm in newborns with pre-adolescent asthma and/or rhinitis. At 404 CpGs and a CpG unit of cg00701456 and cg08196106, we identified significant interaction effects of DNAm and sex in the association with Ast\_Rh at FDR 0.05 level. Of these, an increase in DNAm at 199 CpGs and one CpG unit was associated with an increased odds of Ast\_Rh in males but a decreased odds in females. Of the CpGs not showing

interaction effects, 70 CpGs were found to be associated with Ast\_Rh adjusting for sex, of which an increase in DNAm at 32 CpGs was associated with an increased odds of Ast\_Rh. Of the 404 CpGs and a CpG unit showing significant interaction effects in IOWBC, at 116 of the available 242 CpGs, (48%), consistent associations were observed in the ALSPAC cohort, including statistically significant findings at 3 CpGs. Of the 70 CpGs showing main effects in IOWBC, 17 of the available 37 CpGs (46%) showed same direction of association in ALSPAC.

Assessment of biological relevance of the replicated CpGs indicated a potential epigenetic regulatory functionality of these CpGs on expression of their neighboring genes using a window size of 500 kbps. DNAm at 86 CpGs were associated with expression of 396 genes in males, and at 96 CpGs with expression of 589 genes in females. At 208 of the 396 genes in males and at 345 of the 589 genes in females, an increase in DNAm was associated with increased gene expression levels. Of the replicated 133 CpGs, 29 CpGs in males and 31 CpGs in females were linked to genetic variants (methQTLs) indicating potential contribution of genetic factors on the identified CpGs. It is worth noting that between these 29 and 31 CpGs, 25 were in common, strengthening the existence of methQTLs. That is, the observed epigenetic effects at these CpG sites were likely due to the contribution of genetic factors, supporting the findings on the genetic connection between asthma and rhinitis [57, 173]. On the other hand, CpGs with DNAm not associated with SNPs may represent epigenetic effects only without significant genetic contribution.

Although we did not identify statistically significant biological processes after adjusting for multiple testing, biological processes such as integrin activation and interleukin-17 secretion were among the top processes determined based on statistical significance. Activation of integrins have been shown to be correlated with eosinophil recruitment and pulmonary

function in asthma [182]. Eosinophil arrest and recruitment to the airway in asthma are mediated, at least in part, by integrins [182-184]. Therefore, antagonists targeting integrins may potentially be involved in asthma treatment [184]. Expression of IL-17A in nasal mucosa is associated with pathophysiology of allergic rhinitis including its severity and nasal eosinophilia [185]. Neutralization of IL-17 has been found to improve symptoms of allergic rhinitis [186].

## **Chapter 6. Summary**

Epigenetic investigations of asthma will help us better understand its etiology and help direct preventive measures. The summary of main findings of this dissertation from two independent cohorts are:

- I identified DNAm at 62 CpGs (9 in males) showing transition-specific associations with asthma acquisition (AA) such that the associations were different between the pre- to post-adolescence transition period and the post- to adulthood transition period. I also found significant differences between males and females at these CpGs i.e., at most of the CpGs in males, an increase in DNAm was associated with an increased odds of AA from pre- to post-adolescence transition, while from post-adolescence to adulthood, increased DNAm at most of the CpGs was associated with decreased odds. The associations in females for both transition periods were opposite compared to those in males. Among the 50 CpGs (13 in males) showing main effects on AA, at most of the CpGs, an increase in DNAm was associated with a decreased odds of AA for both males and females, although the proportion of such CpGs was larger in females than in males. Furthermore, the effect sizes were weaker in females than in males.
- I identified 30 CpGs (20 in males) in newborns that are associated with AA via atopy. Of these, an increase in DNAm at 22 CpGs (14 in males) was indirectly associated with decreased risk of AA via decreased risk of atopy. These CpGs might play a role in atopic asthma. At 103 CpGs, only direct effects of DNAm in newborns on AA during adolescence were observed which might contribute towards non-atopic asthma.
- Sex-specific effects of DNAm in newborns on preadolescent Ast\_Rh were observed at 116 CpGs, and at most CpGs opposite effects in males and females were detected.

For each aim, it will be informative to examine DNAm trajectories at the identified CpGs and the longitudinal associations between DNAm and the endpoint (asthma acquisition or asthma/rhinitis status). Such an investigation will allow us to assess the potential of dynamicity of DNAm along with its potentially changing effect, if any.

Within each aim, it was noticed that a small number of CpGs in IOWBC were replicated in ALSPAC showing the same direction of effects with statistical significance. There is a possibility of false-positive findings. Other factors such as age and sources of DNAm might have also caused the discrepancy in the findings between the two cohorts. Further assessment of the identified CpGs is desired in large scale cohort studies.

In addition, none of the identified CpGs showed overlap in these 3 studies, which was expected. The DNAm was assessed at 10 and 18 years for aim 1, while in newborns for aim 2 and 3. Reflected in my analyses was that CpGs identified in newborns are likely not to continue their association at ages 10 or 18 years with AA at later ages. This may be the result of changes in environmental exposures over time, from birth to adolescence. Also, the outcomes for the three studies are different. Aim 1 and 2 focused on AA, i.e., transition during adolescence (while the DNAm ages were different) and aim 3 focused on the status of preadolescent Ast\_Rh rather than changes in asthma status. The CpGs identified in aim 1 and 2 may represent involvement in the development of asthma during a critical period of adolescent, while those in aim 3 are related to the status of asthma and/or rhinitis before adolescence (i.e., conditions are already developed, and some may have persistent asthma).

The unique CpGs identified for each sex without any overlap in these findings and the inconsistent associations of DNAm with AA between males and females might be related to the gender-reversal phenomenon of asthma prevalence from pre- to post-adolescence. It is worth

noting that for most of the associations of DNAm with AA, a greater number of CpGs were identified in females compared to males. The reason for this observation is unknown and remains to be biologically determined through future investigations. I speculate that X chromosome inactivation due to genetic mechanism may be related to such a difference in number of identified CpGs in each sex [187]. These identified CpGs can guide future studies in AA prediction at different transition periods in both sexes, whether atopic or non-atopic asthma. The biological functionality of the identified CpGs will strengthen their potential as causal factors in addition to epigenetic markers. The CpGs identified in this dissertation have a potential to serve as epigenetic biomarkers due to the strength of associations assessed based on statistical significance.

## References

1. Ladd-Acosta, C. and M.D. Fallin, *The role of epigenetics in genetic and environmental epidemiology*. Epigenomics, 2016. **8**(2): p. 271-83.
2. Bakulski, K.M. and M.D. Fallin, *Epigenetic epidemiology: promises for public health research*. Environ Mol Mutagen, 2014. **55**(3): p. 171-83.
3. Waddington, C.H., *CANALIZATION OF DEVELOPMENT AND THE INHERITANCE OF ACQUIRED CHARACTERS*. Nature, 1942. **150**(3811): p. 563-565.
4. Mill, J. and B.T. Heijmans, *From promises to practical strategies in epigenetic epidemiology*. Nat Rev Genet, 2013. **14**(8): p. 585-94.
5. Relton, C.L. and G. Davey Smith, *Epigenetic Epidemiology of Common Complex Disease: Prospects for Prediction, Prevention, and Treatment*. PLOS Medicine, 2010. **7**(10): p. e1000356.
6. Gunasekara, C.J. and R.A. Waterland, *A new era for epigenetic epidemiology*. Epigenomics, 2019. **11**(15): p. 1647-1649.
7. Kobow, K., et al., *Epigenetics explained: a topic “primer” for the epilepsy community by the ILAE Genetics/Epigenetics Task Force*. Epileptic Disorders, 2020. **22**(2): p. 127-141.
8. Kheirkhah Rahimabad, P., et al., *Nicotine and Its Downstream Metabolites in Maternal and Cord Sera: Biomarkers of Prenatal Smoking Exposure Associated with Offspring DNA Methylation*. Int J Environ Res Public Health, 2020. **17**(24).
9. Kheirkhah Rahimabad, P., et al., *Nicotine and Its Downstream Metabolites in Maternal and Cord Sera: Biomarkers of Prenatal Smoking Exposure Associated with Offspring DNA Methylation*. International journal of environmental research and public health, 2020. **17**(24): p. 9552.
10. Christiansen, C., et al., *Novel DNA methylation signatures of tobacco smoking with trans-ethnic effects*. Clinical Epigenetics, 2021. **13**(1): p. 36.
11. Philibert, R.A., S.R.H. Beach, and G.H. Brody, *The DNA methylation signature of smoking: an archetype for the identification of biomarkers for behavioral illness*. Nebraska Symposium on Motivation. Nebraska Symposium on Motivation, 2014. **61**: p. 109-127.
12. Tsai, P.-C., et al., *Smoking induces coordinated DNA methylation and gene expression changes in adipose tissue with consequences for metabolic health*. Clinical Epigenetics, 2018. **10**(1): p. 126.
13. Rathod, R., et al., *BMI trajectory in childhood is associated with asthma incidence at young adulthood mediated by DNA methylation*. Allergy, Asthma & Clinical Immunology, 2021. **17**(1): p. 77.
14. Wahl, S., et al., *Epigenome-wide association study of body mass index, and the adverse outcomes of adiposity*. Nature, 2017. **541**(7635): p. 81-86.
15. Do, W.L., et al., *Examining the association between adiposity and DNA methylation: A systematic review and meta-analysis*. Obes Rev, 2021: p. e13319.
16. Vehmeijer, F.O.L., et al., *DNA methylation and body mass index from birth to adolescence: meta-analyses of epigenome-wide association studies*. Genome Medicine, 2020. **12**(1): p. 105.
17. Ferrari, L., M. Carugno, and V. Bollati, *Particulate matter exposure shapes DNA methylation through the lifespan*. Clin Epigenetics, 2019. **11**(1): p. 129.

18. Plusquin, M., et al., *DNA methylation and exposure to ambient air pollution in two prospective cohorts*. Environ Int, 2017. **108**: p. 127-136.
19. Rider, C.F. and C. Carlsten, *Air pollution and DNA methylation: effects of exposure in humans*. Clinical Epigenetics, 2019. **11**(1): p. 131.
20. Hartwig, F.P., et al., *Breastfeeding effects on DNA methylation in the offspring: A systematic literature review*. PloS one, 2017. **12**(3): p. e0173070-e0173070.
21. Ozkan, H., et al., *Epigenetic Programming Through Breast Milk and Its Impact on Milk-Siblings Mating*. Frontiers in Genetics, 2020. **11**(1141).
22. Mallisetty, Y., et al., *Epigenome-Wide Association of Infant Feeding and Changes in DNA Methylation from Birth to 10 Years*. Nutrients, 2020. **13**(1).
23. Verduci, E., et al., *Epigenetic effects of human breast milk*. Nutrients, 2014. **6**(4): p. 1711-1724.
24. Liu, C., et al., *A DNA methylation biomarker of alcohol consumption*. Molecular Psychiatry, 2018. **23**(2): p. 422-433.
25. Wilson, L.E., et al., *Alcohol and DNA Methylation: An Epigenome-Wide Association Study in Blood and Normal Breast Tissue*. American Journal of Epidemiology, 2019. **188**(6): p. 1055-1065.
26. Zakhari, S., *Alcohol metabolism and epigenetics changes*. Alcohol Res, 2013. **35**(1): p. 6-16.
27. Fragou, D. and L. Kovatsi, *Chapter 14 - Drugs of Abuse and DNA Methylation in the Brain: Ethanol, Cocaine, Amphetamine-Methamphetamine, Heroin, Antidepressants, and Antipsychotics*, in *Neuropathology of Drug Addictions and Substance Misuse*, V.R. Preedy, Editor. 2016, Academic Press: San Diego. p. 137-143.
28. Lax, E. and M. Szyf, *The Role of DNA Methylation in Drug Addiction: Implications for Diagnostic and Therapeutics*. Prog Mol Biol Transl Sci, 2018. **157**: p. 93-104.
29. Ulaner, G.A., et al., *Loss of imprinting of IGF2 and H19 in osteosarcoma is accompanied by reciprocal methylation changes of a CTCF-binding site*. Hum Mol Genet, 2003. **12**(5): p. 535-49.
30. Leick, M.B., et al., *Loss of imprinting of IGF2 and the epigenetic progenitor model of cancer*. American journal of stem cells, 2011. **1**(1): p. 59-74.
31. Sukapan, P., et al., *Types of DNA methylation status of the interspersed repetitive sequences for LINE-1, Alu, HERV-E and HERV-K in the neutrophils from systemic lupus erythematosus patients and healthy controls*. J Hum Genet, 2014. **59**(4): p. 178-88.
32. Cai, X.Y., et al., *[Effect of interleukin-6 promoter DNA methylation on the pathogenesis of systemic lupus erythematosus]*. Zhonghua Yi Xue Za Zhi, 2017. **97**(19): p. 1491-1495.
33. Meng, W., et al., *DNA methylation mediates genotype and smoking interaction in the development of anti-citrullinated peptide antibody-positive rheumatoid arthritis*. Arthritis Research & Therapy, 2017. **19**(1): p. 71.
34. Marabita, F., et al., *Smoking induces DNA methylation changes in Multiple Sclerosis patients with exposure-response relationship*. Scientific Reports, 2017. **7**(1): p. 14589.
35. Xu, C.J., et al., *Shared DNA methylation signatures in childhood allergy: The MeDALL study*. J Allergy Clin Immunol, 2021. **147**(3): p. 1031-1040.
36. DeVries, A. and D. Vercelli, *Epigenetics in allergic diseases*. Curr Opin Pediatr, 2015. **27**(6): p. 719-23.

37. Lockett, G.A., et al., *Epigenomics and allergic disease*. Epigenomics, 2013. **5**(6): p. 685-699.
38. Braun, K.V.E., et al., *Epigenome-wide association study (EWAS) on lipids: the Rotterdam Study*. Clinical Epigenetics, 2017. **9**(1): p. 15.
39. de Toro-Martín, J., et al., *A CpG-SNP Located within the ARPC3 Gene Promoter Is Associated with Hypertriglyceridemia in Severely Obese Patients*. Ann Nutr Metab, 2016. **68**(3): p. 203-12.
40. Dick, K.J., et al., *DNA methylation and body-mass index: a genome-wide analysis*. Lancet, 2014. **383**(9933): p. 1990-8.
41. Guay, S.P., et al., *Epigenome-wide analysis in familial hypercholesterolemia identified new loci associated with high-density lipoprotein cholesterol concentration*. Epigenomics, 2012. **4**(6): p. 623-39.
42. Andrews, S.V., et al., *Cross-tissue integration of genetic and epigenetic data offers insight into autism spectrum disorder*. Nat Commun, 2017. **8**(1): p. 1011.
43. Nour El Huda, A.R., et al., *DNA methylation of membrane-bound catechol-O-methyltransferase in Malaysian schizophrenia patients*. Psychiatry Clin Neurosci, 2018. **72**(4): p. 266-279.
44. Zhong, J., G. Agha, and A.A. Baccarelli, *The Role of DNA Methylation in Cardiovascular Risk and Disease*. Circulation Research, 2016. **118**(1): p. 119-131.
45. Westerman, K., et al., *DNA methylation modules associate with incident cardiovascular disease and cumulative risk factor exposure*. Clinical Epigenetics, 2019. **11**(1): p. 142.
46. Soler-Botija, C., C. Gálvez-Montón, and A. Bayés-Genís, *Epigenetic Biomarkers in Cardiovascular Diseases*. Frontiers in Genetics, 2019. **10**(950).
47. Pawankar, R., *Allergic diseases and asthma: a global public health concern and a call to action*. The World Allergy Organization journal, 2014. **7**(1): p. 12-12.
48. Burbank, A.J., et al., *Environmental determinants of allergy and asthma in early life*. The Journal of allergy and clinical immunology, 2017. **140**(1): p. 1-12.
49. Wittig, H.J., et al., *Risk factors for the development of allergic disease: analysis of 2,190 patient records*. Ann Allergy, 1978. **41**(2): p. 84-8.
50. To, T., et al., *Early life exposure to air pollution and incidence of childhood asthma, allergic rhinitis and eczema*. Eur Respir J, 2020. **55**(2).
51. Kozyrskyj, A.L., S. Bahreinian, and M.B. Azad, *Early life exposures: impact on asthma and allergic disease*. Curr Opin Allergy Clin Immunol, 2011. **11**(5): p. 400-6.
52. Ly, N.P. and J.C. Celedón, *Family history, environmental exposures in early life, and childhood asthma*. J Allergy Clin Immunol, 2007. **120**(2): p. 271-2.
53. Pividori, M., et al., *Shared and distinct genetic risk factors for childhood-onset and adult-onset asthma: genome-wide and transcriptome-wide studies*. Lancet Respir Med, 2019. **7**(6): p. 509-522.
54. Wijst, M., M. Sargurupremraj, and M. Arnold, *Genome-wide association studies in asthma: what they really told us about pathogenesis*. Curr Opin Allergy Clin Immunol, 2013. **13**(1): p. 112-8.
55. Demenais, F., et al., *Multiancestry association study identifies new asthma risk loci that colocalize with immune-cell enhancer marks*. Nat Genet, 2018. **50**(1): p. 42-53.

56. Galanter, J.M., et al., *Genome-wide association study and admixture mapping identify different asthma-associated loci in Latinos: the Genes-environments & Admixture in Latino Americans study*. The Journal of allergy and clinical immunology, 2014. **134**(2): p. 295-305.
57. Ferreira, M.A., et al., *Shared genetic origin of asthma, hay fever and eczema elucidates allergic disease biology*. Nat Genet, 2017. **49**(12): p. 1752-1757.
58. Rathod, A., et al., *Interweaving Between Genetic and Epigenetic Studies on Childhood Asthma*. Epigenet Insights, 2020. **13**: p. 2516865720923395.
59. Reese, S.E., et al., *Epigenome-wide meta-analysis of DNA methylation and childhood asthma*. J Allergy Clin Immunol, 2018.
60. den Dekker, H.T., et al., *Newborn DNA-methylation, childhood lung function, and the risks of asthma and COPD across the life course*. Eur Respir J, 2019. **53**(4).
61. Patel, R., et al., *Sex-specific associations of asthma acquisition with changes in DNA methylation during adolescence*. Clin Exp Allergy, 2020.
62. Xu, C.J., et al., *DNA methylation in childhood asthma: an epigenome-wide meta-analysis*. Lancet Respir Med, 2018. **6**(5): p. 379-388.
63. Qi, C., et al., *Nasal DNA methylation profiling of asthma and rhinitis*. J Allergy Clin Immunol, 2020. **145**(6): p. 1655-1663.
64. North, M.L., et al., *Blood and nasal epigenetics correlate with allergic rhinitis symptom development in the environmental exposure unit*. Allergy, 2018. **73**(1): p. 196-205.
65. Holt, P.G., et al., *The role of allergy in the development of asthma*. Nature, 1999. **402**(6760): p. 12-17.
66. Fuchs, O., et al., *Asthma transition from childhood into adulthood*. Lancet Respir Med, 2017. **5**(3): p. 224-234.
67. Asthma, G.I.f., *Global Strategy for Asthma management and prevention*. 2020.
68. Castro-Rodriguez, J.A., et al., *Risk and Protective Factors for Childhood Asthma: What Is the Evidence?* J Allergy Clin Immunol Pract, 2016. **4**(6): p. 1111-1122.
69. Loftus, P.A. and S.K. Wise, *Epidemiology of asthma*. Curr Opin Otolaryngol Head Neck Surg, 2016. **24**(3): p. 245-9.
70. Murrison, L.B., et al., *Environmental exposures and mechanisms in allergy and asthma development*. The Journal of Clinical Investigation, 2019. **129**(4): p. 1504-1515.
71. Joubert, B.R., et al., *DNA Methylation in Newborns and Maternal Smoking in Pregnancy: Genome-wide Consortium Meta-analysis*. Am J Hum Genet, 2016. **98**(4): p. 680-96.
72. DeVries, A. and D. Vercelli, *Early predictors of asthma and allergy in children: the role of epigenetics*. Curr Opin Allergy Clin Immunol, 2015. **15**(5): p. 435-9.
73. Vercelli, D., *Does epigenetics play a role in human asthma?* Allergol Int, 2016. **65**(2): p. 123-126.
74. Reese, S.E., et al., *Epigenome-wide meta-analysis of DNA methylation and childhood asthma*. J Allergy Clin Immunol, 2019. **143**(6): p. 2062-2074.
75. Arathimos, R., et al., *Epigenome-wide association study of asthma and wheeze in childhood and adolescence*. Clin Epigenetics, 2017. **9**: p. 112.
76. Martinez, F.D., et al., *Asthma and wheezing in the first six years of life. The Group Health Medical Associates*. N Engl J Med, 1995. **332**(3): p. 133-8.

77. Koper, I., K. Hufnagl, and R. Ehmann, *Gender aspects and influence of hormones on bronchial asthma - Secondary publication and update*. World Allergy Organ J, 2017. **10**(1): p. 46.
78. Pignataro, F.S., et al., *Asthma and gender: The female lung*. Pharmacol Res, 2017. **119**: p. 384-390.
79. Osman, M., et al., *Gender-specific presentations for asthma, allergic rhinitis and eczema in primary care*. Prim Care Respir J, 2007. **16**(1): p. 28-35.
80. Arshad, S.H., et al., *Cohort Profile: The Isle Of Wight Whole Population Birth Cohort (IOWBC)*. Int J Epidemiol, 2018. **47**(4): p. 1043-1044i.
81. Zhang, H., et al., *DNA methylation and allergic sensitizations: A genome-scale longitudinal study during adolescence*. Allergy, 2019. **74**(6): p. 1166-1175.
82. Arshad, S.H., et al., *Multigenerational cohorts in patients with asthma and allergy*. J Allergy Clin Immunol, 2017. **139**(2): p. 415-421.
83. Soto-Ramirez, N., et al., *The interaction of genetic variants and DNA methylation of the interleukin-4 receptor gene increase the risk of asthma at age 18 years*. Clin Epigenetics, 2013. **5**(1): p. 1.
84. Zhang, H., et al., *Acquisition, remission, and persistence of eczema, asthma, and rhinitis in children*. Clin Exp Allergy, 2018. **48**(5): p. 568-576.
85. Ziyab, A.H., et al., *Association of filaggrin variants with asthma and rhinitis: is eczema or allergic sensitization status an effect modifier?* Int Arch Allergy Immunol, 2014. **164**(4): p. 308-18.
86. Zhang, H., et al., *The interplay of DNA methylation over time with Th2 pathway genetic variants on asthma risk and temporal asthma transition*. Clin Epigenetics, 2014. **6**(1): p. 8.
87. Aryee, M.J., et al., *Minfi: a flexible and comprehensive Bioconductor package for the analysis of Infinium DNA methylation microarrays*. Bioinformatics, 2014. **30**(10): p. 1363-9.
88. Lehne, B., et al., *A coherent approach for analysis of the Illumina HumanMethylation450 BeadChip improves data quality and performance in epigenome-wide association studies*. Genome Biol, 2015. **16**: p. 37.
89. Reinius, L.E., et al., *Differential DNA methylation in purified human blood cells: implications for cell lineage and studies on disease susceptibility*. PLoS One, 2012. **7**(7): p. e41361.
90. Koestler, D.C., et al., *Blood-based profiles of DNA methylation predict the underlying distribution of cell types: a validation analysis*. Epigenetics, 2013. **8**(8): p. 816-26.
91. Jaffe, A.E. and R.A. Irizarry, *Accounting for cellular heterogeneity is critical in epigenome-wide association studies*. Genome Biol, 2014. **15**(2): p. R31.
92. Houseman, E.A., et al., *DNA methylation arrays as surrogate measures of cell mixture distribution*. BMC Bioinformatics, 2012. **13**: p. 86.
93. Kim, D., B. Langmead, and S.L. Salzberg, *HISAT: a fast spliced aligner with low memory requirements*. Nat Methods, 2015. **12**(4): p. 357-60.
94. Li, H., et al., *The Sequence Alignment/Map format and SAMtools*. Bioinformatics, 2009. **25**(16): p. 2078-9.

95. Anders, S., P.T. Pyl, and W. Huber, *HTSeq--a Python framework to work with high-throughput sequencing data*. Bioinformatics, 2015. **31**(2): p. 166-9.
96. Council, N.R. and I.o. Medicine, *Challenges in Adolescent Health Care: Workshop Report*. 2007, Washington, DC: The National Academies Press. 90.
97. Blakemore, S.J., *Adolescence and mental health*. Lancet, 2019. **393**(10185): p. 2030-2031.
98. Boyd, A., et al., *Cohort Profile: the 'children of the 90s'--the index offspring of the Avon Longitudinal Study of Parents and Children*. Int J Epidemiol, 2013. **42**(1): p. 111-27.
99. Fraser, A., et al., *Cohort Profile: the Avon Longitudinal Study of Parents and Children: ALSPAC mothers cohort*. Int J Epidemiol, 2013. **42**(1): p. 97-110.
100. Northstone, K., et al., *The Avon Longitudinal Study of Parents and Children (ALSPAC): an update on the enrolled sample of index children in 2019*. Wellcome Open Res, 2019. **4**: p. 51.
101. Relton, C.L., et al., *Data Resource Profile: Accessible Resource for Integrated Epigenomic Studies (ARIES)*. Int J Epidemiol, 2015. **44**(4): p. 1181-90.
102. Peters, T.J., et al., *De novo identification of differentially methylated regions in the human genome*. Epigenetics Chromatin, 2015. **8**: p. 6.
103. Geeleher, P., et al., *Gene-set analysis is severely biased when applied to genome-wide methylation data*. Bioinformatics (Oxford, England), 2013. **29**(15): p. 1851-1857.
104. Rathod, R., et al., *Methylation of Host Genes Associated with Coronavirus Infection from Birth to 26 Years*. Genes, 2021. **12**(8): p. 1198.
105. Reeder, K.M., et al., *The common γ-chain cytokine IL-7 promotes immunopathogenesis during fungal asthma*. Mucosal Immunol, 2018. **11**(5): p. 1352-1362.
106. Kelly, E.A., et al., *Potential contribution of IL-7 to allergen-induced eosinophilic airway inflammation in asthma*. J Immunol, 2009. **182**(3): p. 1404-10.
107. Hoang, T.T., et al., *Epigenome-wide association study of DNA methylation and adult asthma in the Agricultural Lung Health Study*. Eur Respir J, 2020. **56**(3).
108. Himes, B.E., et al., *Association of SERPINE2 with asthma*. Chest, 2011. **140**(3): p. 667-674.
109. Hoang, T.T., et al., *Epigenome-Wide Association Study of DNA Methylation and Adult Asthma in the Agricultural Lung Health Study*. European Respiratory Journal, 2020: p. 2000217.
110. Nahm, D.H., et al., *Identification of alpha-enolase as an autoantigen associated with severe asthma*. J Allergy Clin Immunol, 2006. **118**(2): p. 376-81.
111. Dharmage, S.C., J.L. Perret, and A. Custovic, *Epidemiology of Asthma in Children and Adults*. Front Pediatr, 2019. **7**: p. 246.
112. Thomsen, S.F., *Epidemiology and natural history of atopic diseases*. Eur Clin Respir J, 2015. **2**.
113. Justiz Vaillant, A.A., P. Modi, and A. Jan, *Atopy*, in *StatPearls*. 2021, StatPearls Publishing Copyright © 2021, StatPearls Publishing LLC.: Treasure Island (FL).
114. Simpson, A., et al., *Beyond atopy: multiple patterns of sensitization in relation to asthma in a birth cohort study*. Am J Respir Crit Care Med, 2010. **181**(11): p. 1200-6.
115. Lowe, A.J., et al., *Do boys do the atopic march while girls dawdle?* J Allergy Clin Immunol, 2008. **121**(5): p. 1190-5.

116. Schroeder, A., et al., *Food allergy is associated with an increased risk of asthma*. Clin Exp Allergy, 2009. **39**(2): p. 261-70.
117. Carroll, W.D., et al., *Asthma severity and atopy: how clear is the relationship?* Arch Dis Child, 2006. **91**(5): p. 405-9.
118. Arathimos, R., et al., *Sex discordance in asthma and wheeze prevalence in two longitudinal cohorts*. PLoS One, 2017. **12**(4): p. e0176293.
119. Patel, R., et al., *Sex-specific associations of asthma acquisition with changes in DNA methylation during adolescence*. Clin Exp Allergy, 2021. **51**(2): p. 318-328.
120. Vink, N.M., et al., *Gender differences in asthma development and remission during transition through puberty: the TRacking Adolescents' Individual Lives Survey (TRAILS) study*. J Allergy Clin Immunol, 2010. **126**(3): p. 498-504.e1-6.
121. Hohmann, C., et al., *Sex-specific incidence of asthma, rhinitis and respiratory multimorbidity before and after puberty onset: individual participant meta-analysis of five birth cohorts collaborating in MeDALL*. BMJ Open Respir Res, 2019. **6**(1): p. e000460.
122. Sengler, C., et al., *Interactions between genes and environmental factors in asthma and atopy: new developments*. Respiratory Research, 2001. **3**(1): p. 7.
123. Begin, P. and K.C. Nadeau, *Epigenetic regulation of asthma and allergic disease*. Allergy Asthma Clin Immunol, 2014. **10**(1): p. 27.
124. Durham, A.L., C. Wiegman, and I.M. Adcock, *Epigenetics of asthma*. Biochim Biophys Acta, 2011. **1810**(11): p. 1103-9.
125. Yang, I.V. and D.A. Schwartz, *Epigenetic mechanisms and the development of asthma*. J Allergy Clin Immunol, 2012. **130**(6): p. 1243-55.
126. Joubert, B.R., et al., *450K epigenome-wide scan identifies differential DNA methylation in newborns related to maternal smoking during pregnancy*. Environ Health Perspect, 2012. **120**(10): p. 1425-31.
127. Danielewicz, H., et al., *Maternal atopy and offspring epigenome-wide methylation signature*. Epigenetics, 2020: p. 1-13.
128. Everson, T.M., et al., *DNA methylation loci associated with atopy and high serum IgE: a genome-wide application of recursive Random Forest feature selection*. Genome Med, 2015. **7**(1): p. 89.
129. Yang, I.V., *DNA methylation signatures of atopy and asthma*. Lancet Respir Med, 2019. **7**(4): p. 289-290.
130. Forno, E., et al., *DNA methylation in nasal epithelium, atopy, and atopic asthma in children: a genome-wide study*. The Lancet Respiratory Medicine, 2019. **7**(4): p. 336-346.
131. Horvath, S., *DNA methylation age of human tissues and cell types*. Genome Biol, 2013. **14**(10): p. R115.
132. Kawai, K., et al., *Parental age and gene expression profiles in individual human blastocysts*. Sci Rep, 2018. **8**(1): p. 2380.
133. Markunas, C.A., et al., *Identification of DNA methylation changes in newborns related to maternal smoking during pregnancy*. Environ Health Perspect, 2014. **122**(10): p. 1147-53.
134. Sharp, G.C., et al., *Maternal pre-pregnancy BMI and gestational weight gain, offspring DNA methylation and later offspring adiposity: findings from the Avon Longitudinal Study of Parents and Children*. Int J Epidemiol, 2015. **44**(4): p. 1288-304.

135. Joubert, B.R., et al., *Maternal plasma folate impacts differential DNA methylation in an epigenome-wide meta-analysis of newborns*. Nat Commun, 2016. **7**: p. 10577.
136. Joubert, B.R., et al., *DNA Methylation in Newborns and Maternal Smoking in Pregnancy: Genome-wide Consortium Meta-analysis*. Am J Hum Genet, 2016. **98**(4): p. 680-96.
137. Bignardi, D., et al., *Allergen-specific IgE: comparison between skin prick test and serum assay in real life*. Allergologie select, 2019. **3**(1): p. 9-14.
138. Zhang, H., et al., *DNA methylation and allergic sensitizations: A genome-scale longitudinal study during adolescence*. Allergy, 2019. **74**(6): p. 1166-1175.
139. Bibikova, M. and J.B. Fan, *GoldenGate assay for DNA methylation profiling*. Methods Mol Biol, 2009. **507**: p. 149-63.
140. Johnson, W.E., C. Li, and A. Rabinovic, *Adjusting batch effects in microarray expression data using empirical Bayes methods*. Biostatistics, 2007. **8**(1): p. 118-27.
141. Ray, M.A., et al., *An Efficient Approach to Screening Epigenome-Wide Data*. Biomed Res Int, 2016. **2016**: p. 2615348.
142. Suderman, M., et al., *dmrff: identifying differentially methylated regions efficiently with power and control*. bioRxiv, 2018: p. 508556.
143. Rathod, R., et al., *BMI trajectory in childhood is associated with asthma incidence at young adulthood mediated by DNA methylation*. Allergy, asthma, and clinical immunology : official journal of the Canadian Society of Allergy and Clinical Immunology, 2021. **17**(1): p. 77-77.
144. Hallquist, M.N. and J.F. Wiley, *MplusAutomation: An R Package for Facilitating Large-Scale Latent Variable Analyses in Mplus*. Struct Equ Modeling, 2018. **25**(4): p. 621-638.
145. Hu, L.t. and P.M. Bentler, *Cutoff criteria for fit indexes in covariance structure analysis: Conventional criteria versus new alternatives*. Structural Equation Modeling: A Multidisciplinary Journal, 1999. **6**(1): p. 1-55.
146. Geeleher, P., et al., *Gene-set analysis is severely biased when applied to genome-wide methylation data*. Bioinformatics, 2013. **29**(15): p. 1851-7.
147. Team, R.C., *R: A language and environment for statistical computing*. 2013, Vienna, Austria.
148. Jiang, Y., et al., *Epigenome wide comparison of DNA methylation profile between paired umbilical cord blood and neonatal blood on Guthrie cards*. Epigenetics, 2020. **15**(5): p. 454-461.
149. Wang, C., et al., *Evidence of association between interferon regulatory factor 5 gene polymorphisms and asthma*. Gene, 2012. **504**(2): p. 220-225.
150. Farina, F., et al., [Study of hypophyseal and gonadal hormones and cases of postmenopausal occurrence of bronchial asthma]. Minerva Med, 1986. **77**(7-8): p. 243-7.
151. Balzano, G., et al., *Asthma and sex hormones*. Allergy, 2001. **56**(1): p. 13-20.
152. Tallia, A.F. and D.A. Cardone, *Asthma exacerbation associated with glucosamine-chondroitin supplement*. J Am Board Fam Pract, 2002. **15**(6): p. 481-4.
153. Alaskhar Alhamwe, B., et al., *Histone modifications and their role in epigenetics of atopy and allergic diseases*. Allergy, Asthma & Clinical Immunology, 2018. **14**(1): p. 39.
154. Bhavsar, P., T. Ahmad, and I.M. Adcock, *The role of histone deacetylases in asthma and allergic diseases*. J Allergy Clin Immunol, 2008. **121**(3): p. 580-4.

155. Stefanowicz, D., et al., *Elevated H3K18 acetylation in airway epithelial cells of asthmatic subjects*. Respiratory Research, 2015. **16**(1): p. 95.
156. Morales, E. and D. Duffy, *Genetics and Gene-Environment Interactions in Childhood and Adult Onset Asthma*. Frontiers in pediatrics, 2019. **7**: p. 499-499.
157. Shrine, N., et al., *Moderate-to-severe asthma in individuals of European ancestry: a genome-wide association study*. Lancet Respir Med, 2019. **7**(1): p. 20-34.
158. Ziani, M., A.P. Henry, and I.P. Hall, *Association study between asthma and single nucleotide polymorphisms of ORMDL3, GSDMB, and IL1RL1 genes in an Algerian population*. Egyptian Journal of Medical Human Genetics, 2021. **22**(1): p. 40.
159. Hinds, D.A., et al., *A genome-wide association meta-analysis of self-reported allergy identifies shared and allergy-specific susceptibility loci*. Nature genetics, 2013. **45**(8): p. 907-911.
160. Takahashi, K., et al., *Sputum proteomics and airway cell transcripts of current and ex-smokers with severe asthma in U-BIOPRED: an exploratory analysis*. Eur Respir J, 2018. **51**(5).
161. Supinda Bunyavanich, G.P., *Nasal Biomarkers of Asthma*, I.B.o.W.I.P. Organization, Editor. 2017.
162. Dharmage, S.C., J.L. Perret, and A. Custovic, *Epidemiology of Asthma in Children and Adults*. Frontiers in pediatrics, 2019. **7**: p. 246-246.
163. Fuhlbrigge, A.L., B. Jackson, and R.J. Wright, *Gender and asthma*. Immunology and Allergy Clinics of North America, 2002. **22**(4): p. 753-789.
164. Bergeron, C. and Q. Hamid, *Relationship between Asthma and Rhinitis: Epidemiologic, Pathophysiologic, and Therapeutic Aspects*. Allergy, Asthma & Clinical Immunology, 2005. **1**(2): p. 81.
165. García-Almaraz, R., et al., *Prevalence and risk factors associated with allergic rhinitis in Mexican school children: Global Asthma Network Phase I*. World Allergy Organization Journal, 2021. **14**(1): p. 100492.
166. Yawn, B.P., et al., *Allergic rhinitis in Rochester, Minnesota residents with asthma: frequency and impact on health care charges*. J Allergy Clin Immunol, 1999. **103**(1 Pt 1): p. 54-9.
167. Togias, A.G., *Systemic immunologic and inflammatory aspects of allergic rhinitis*. J Allergy Clin Immunol, 2000. **106**(5 Suppl): p. S247-50.
168. Vinuya, R.Z., *Upper airway disorders and asthma: a syndrome of airway inflammation*. Ann Allergy Asthma Immunol, 2002. **88**(4 Suppl 1): p. 8-15.
169. Leynaert, B., et al., *Epidemiologic evidence for asthma and rhinitis comorbidity*. J Allergy Clin Immunol, 2000. **106**(5 Suppl): p. S201-5.
170. Guerra, S., et al., *Rhinitis as an independent risk factor for adult-onset asthma*. J Allergy Clin Immunol, 2002. **109**(3): p. 419-25.
171. Fröhlich, M., et al., *Is there a sex-shift in prevalence of allergic rhinitis and comorbid asthma from childhood to adulthood? A meta-analysis*. Clinical and translational allergy, 2017. **7**: p. 44-44.
172. Ober, C. and T.-C. Yao, *The genetics of asthma and allergic disease: a 21st century perspective*. Immunological reviews, 2011. **242**(1): p. 10-30.

173. Laulajainen-Hongisto, A., et al., *Genomics of asthma, allergy and chronic rhinosinusitis: novel concepts and relevance in airway mucosa*. Clinical and Translational Allergy, 2020. **10**(1): p. 45.
174. Pinart, M., et al., *Comorbidity of eczema, rhinitis, and asthma in IgE-sensitised and non-IgE-sensitised children in MeDALL: a population-based cohort study*. Lancet Respir Med, 2014. **2**(2): p. 131-40.
175. DeVries, A. and D. Vercelli, *Epigenetics in allergic diseases*. Current opinion in pediatrics, 2015. **27**(6): p. 719-723.
176. Xu, C.-J., et al., *Shared DNA methylation signatures in childhood allergy: The MeDALL study*. Journal of Allergy and Clinical Immunology, 2021. **147**(3): p. 1031-1040.
177. Potaczek, D.P., et al., *Epigenetics and allergy: from basic mechanisms to clinical applications*. Epigenomics, 2017. **9**(4): p. 539-571.
178. Gao, X., et al., *The impact of methylation quantitative trait loci (mQTLs) on active smoking-related DNA methylation changes*. Clinical Epigenetics, 2017. **9**(1): p. 87.
179. Bell, J.T., et al., *DNA methylation patterns associate with genetic and gene expression variation in HapMap cell lines*. Genome Biology, 2011. **12**(1): p. R10.
180. Ziyab, A.H., et al., *Association of filaggrin variants with asthma and rhinitis: is eczema or allergic sensitization status an effect modifier?* International archives of allergy and immunology, 2014. **164**(4): p. 308-318.
181. Stueve, T.R., et al., *Epigenome-wide analysis of DNA methylation in lung tissue shows concordance with blood studies and identifies tobacco smoke-inducible enhancers*. Hum Mol Genet, 2017. **26**(15): p. 3014-3027.
182. Johansson, M.W. and D.F. Mosher, *Integrin activation States and eosinophil recruitment in asthma*. Frontiers in pharmacology, 2013. **4**: p. 33-33.
183. Johansson, M.W., et al., *Up-regulation and activation of eosinophil integrins in blood and airway after segmental lung antigen challenge*. Journal of immunology (Baltimore, Md. : 1950), 2008. **180**(11): p. 7622-7635.
184. Barthel, S.R., et al., *Roles of integrin activation in eosinophil function and the eosinophilic inflammation of asthma*. J Leukoc Biol, 2008. **83**(1): p. 1-12.
185. Makihara, S., et al., *Local expression of interleukin-17a is correlated with nasal eosinophilia and clinical severity in allergic rhinitis*. Allergy Rhinol (Providence), 2014. **5**(1): p. 22-7.
186. Gu, Z.W., Y.X. Wang, and Z.W. Cao, *Neutralization of interleukin-17 suppresses allergic rhinitis symptoms by downregulating Th2 and Th17 responses and upregulating the Treg response*. Oncotarget, 2017. **8**(14): p. 22361-22369.
187. Nino, C.L., et al., *Characterization of Sex-Based Dna Methylation Signatures in the Airways During Early Life*. Scientific Reports, 2018. **8**(1): p. 5526.

## Appendix

Supplement Table S1 (A): Association of DNAm with asthma acquisition from pre- to post-adolescence, and post-adolescence to young adulthood at 17 CpGs in males that are transition period specific. Significant interaction between DNAm and transition period on asthma acquisition identified in the IoW(a) cohort were further tested in the ALSPAC(b) cohort. 10-18transition period is the reference group.

| IoW Main<br>estimates<br>(10-18<br>years) | IoW<br>Interaction<br>Estimates | Raw p<br>value Int | FDR p<br>value Int | Gene  | CpG<br>islands     | Gene<br>location | Chromosome |    |
|---|---------------------------------|--------------------|--------------------|-------|--------------------|------------------|------------|----|
| cg01579206                                | -0.17                           | 0.17               | 0.002              | 0.019 | <i>CSNK1AI</i>     | Island           | TSS200     | 5  |
| <b>cg01884526</b>                         | 0.71                            | -0.64              | 0.015              | 0.048 | <i>BANP</i>        | Body             |            | 16 |
| cg02637320                                | -0.05                           | 0.07               | 0.009              | 0.048 | <i>MFSD4</i>       | Island           | Body       | 1  |
| cg06519746                                | 0.54                            | -1.05              | 0.002              | 0.019 | <i>FAM105B</i>     | Island           | TSS1500    | 5  |
| <b>cg08056069</b>                         | 0.29                            | -0.88              | 0.002              | 0.020 | <i>RPL1-86H7.1</i> |                  | 3UTR       | 1  |
| cg08286012                                | 0.57                            | -0.66              | 0.000              | 0.008 | <i>C4orf22</i>     | Island           | Body       | 4  |
| <b>cg11620807</b>                         | -0.05                           | 0.04               | 0.012              | 0.048 | <i>IRSI</i>        | Island           | TSS1500    | 2  |
| <b>cg12009697</b>                         | 0.58                            | -0.61              | 0.014              | 0.048 | <i>GPR35</i>       | N_Shore          |            | 2  |
| cg12895747                                | 0.74                            | -0.73              | 0.004              | 0.030 | <i>RAPIGAP2</i>    | Island           |            | 17 |
| cg15925090                                | 0.29                            | -0.66              | 0.001              | 0.015 | <i>MSXI</i>        | Island           |            | 4  |
| <b>cg17219326</b>                         | -0.03                           | 0.19               | 0.011              | 0.048 | <i>ZNF445</i>      | N_Shore          | 5'UTR      | 3  |
| cg17610929                                | -0.04                           | 0.18               | 0.006              | 0.039 | <i>ACCN4</i>       | S_Shore          | 5'UTR      | 2  |
| <b>cg19707069</b>                         | 0.44                            | -0.51              | 0.013              | 0.048 | <i>MGMT</i>        |                  |            | 10 |
| <b>cg21691089</b>                         | -0.13                           | 0.13               | 0.010              | 0.048 | <i>ENOL</i>        | Island           | 1stExon    | 1  |
| cg25180075                                | -0.06                           | 0.09               | 0.011              | 0.048 | <i>HS6ST1</i>      | Island           | TSS200     | 2  |
| cg25317233                                | 0.61                            | -1.07              | 0.000              | 0.000 | <i>HMGNI</i>       | N_Shelf          | Body       | 21 |
| <b>cg27192902</b>                         | -0.06                           | 0.06               | 0.015              | 0.048 | <i>ZNF259</i>      | Island           |            | 11 |

| CpG sites         | Gene            | ALSPAC                         |                       | ALSPAC                            |                |
|-------------------|-----------------|--------------------------------|-----------------------|-----------------------------------|----------------|
|                   |                 | Main Estimates<br>(7-17 years) | Interaction Estimates | ALSPAC estimates<br>(17-22 years) | ALSPAC p value |
| cg01579206        | <i>CSNK1A1</i>  | 0.07                           | -0.11                 | -0.04                             | 0.644          |
| <b>cg01884526</b> | <i>BANP</i>     | 0.00                           | -0.24                 | -0.25                             | 0.217          |
| cg02637320        | <i>MFSD4</i>    | 0.01                           | -0.13                 | -0.12                             | 0.682          |
| cg06519746        | <i>FAM105B</i>  | -0.02                          | 0.43                  | 0.42                              | 0.071          |
|                   | <i>RPL1-</i>    |                                |                       |                                   |                |
| <b>cg08056069</b> | <i>86H7.1</i>   | 0.07                           | -0.28                 | -0.21                             | 0.079          |
| cg08286012        | <i>C4orf22</i>  | 0.04                           | 0.46                  | 0.50                              | 0.167          |
| <b>cg11620807</b> | <i>IRSI</i>     | 0.01                           | 0.11                  | 0.13                              | 0.829          |
| <b>cg12009697</b> | <i>GPR35</i>    | 0.00                           | -0.29                 | -0.29                             | 0.065          |
| cg12895747        | <i>RAPIGAP2</i> | 0.02                           | 0.16                  | 0.18                              | 0.389          |
| cg15925090        | <i>MSXI</i>     | 0.06                           | 0.26                  | 0.33                              | 0.213          |
| <b>cg17219326</b> | <i>ZNF445</i>   | 0.03                           | 0.02                  | 0.05                              | 0.887          |
| cg17610929        | <i>ACCM4</i>    | 0.09                           | -0.05                 | 0.04                              | 0.836          |
| <b>cg19707069</b> | <i>MGMT</i>     | 0.02                           | -0.82                 | -0.80                             | 0.043          |
| <b>cg21691089</b> | <i>ENOI</i>     | -0.01                          | 0.27                  | 0.27                              | 0.521          |
| cg25180075        | <i>HS6ST1</i>   | 0.07                           | -0.25                 | -0.18                             | 0.402          |
| <b>cg25317233</b> | <i>HMGNI</i>    | -0.02                          | -0.04                 | -0.06                             | 0.808          |
| <b>cg27192902</b> | <i>ZNF259</i>   | 0.00                           | 0.30                  | 0.30                              | 0.311          |

Note: (a) For the analysis in IoW, logistic regression with repeated measurements were adjusted for atopic status at ages 10 and 18 years, active smoking, and secondhand smoke exposure at age 18 and 26 years, transition period 10-18 and 18-26 years.

(b) Analysis of ALSPAC used similar available covariates: atopic status at age 7 years, secondhand smoke exposure at age 17 and 24 years.

Interaction effects consistent between the two cohorts are with bold fonts of CpG.

Supplement Table S1 (B): Association of DNAm with asthma acquisition from pre- to post-adolescence, and post-adolescence to young adulthood at 98 CpGs in females that are transition period specific. Significant interaction between DNAm and transition period on asthma acquisition identified in the IoW(a) cohort were further tested in the ALSPAC(b) cohort. 10-18transition period is the reference group.

| CpG sites         | IoW Main estimates<br>(10-18 years) | IoW                   |           |        |                  | CpG islands | Gene location | Chromosome |
|-------------------|-------------------------------------|-----------------------|-----------|--------|------------------|-------------|---------------|------------|
|                   |                                     | Interaction Estimates | Raw value | p Int  | FDR p value      |             |               |            |
| cg00149397        | 0.21                                | -0.20                 | 8E-06     | 0.0004 | <i>TPST2</i>     | Island      | TSS200        | 22         |
| cg00405843        | 0.16                                | -0.17                 | 2E-03     | 0.0111 | <i>SMO</i>       | Island      | TSS200        | 7          |
| cg00444282        | -0.13                               | 0.13                  | 1E-02     | 0.0284 | <i>RTN3</i>      | Island      | 5UTR          | 11         |
| <b>cg00705668</b> | 0.22                                | -0.23                 | 2E-03     | 0.0111 | <i>MRPS12</i>    | Island      | TSS200        | 19         |
| cg02225897        | 0.47                                | -0.44                 | 5E-03     | 0.0182 | <i>RTDR1</i>     | S_Shore     | TSS200        | 22         |
| cg02362385        | -0.13                               | 0.14                  | 2E-02     | 0.0414 | <i>LPAR2</i>     | Island      | TSS200        | 19         |
| <b>cg02467794</b> | 1.04                                | -1.14                 | 1E-02     | 0.0338 | <i>AKAP1</i>     | Island      | 1stExon       | 17         |
| cg02516257        | -0.09                               | 0.09                  | 2E-02     | 0.0424 | <i>GMCLI</i>     | Island      | TSS200        | 2          |
| <b>cg02619805</b> | -0.11                               | 0.15                  | 4E-04     | 0.0037 | <i>S4FB2</i>     | Island      | TSS200        | 19         |
| cg03223733        | 0.90                                | -1.01                 | 6E-04     | 0.0052 | <i>ZNF211</i>    | Island      | TSS200        | 19         |
| cg03606222        | 0.27                                | -0.24                 | 6E-04     | 0.0052 | <i>NAPA</i>      | Island      | TSS200        | 19         |
| <b>cg03719634</b> | 0.62                                | -0.64                 | 5E-04     | 0.0045 | <i>TMEM45A</i>   | Island      | TSS200        | 3          |
| <b>cg04784251</b> | 0.39                                | -0.41                 | 1E-02     | 0.0371 | <i>BCAS3</i>     | Body        | 17            |            |
| cg04789385        | 0.16                                | -0.20                 | 2E-04     | 0.0029 | <i>ZFPI</i>      | Island      | 5UTR          | 16         |
| cg04802657        | -0.33                               | 0.31                  | 4E-03     | 0.0158 | <i>CCDC101</i>   | Island      | TSS200        | 16         |
| <b>cg05245655</b> | -0.12                               | 0.14                  | 9E-03     | 0.0271 | <i>SIX5</i>      | Island      | 5UTR          | 19         |
| cg05444312        | 0.26                                | -0.27                 | 1E-02     | 0.0342 | <i>HIST1H2BM</i> | S_Shore     | TSS200        | 6          |
| cg06045799        | 1.18                                | -1.16                 | 1E-03     | 0.0065 | <i>COMM8D</i>    | Island      | Body          | 4          |
| <b>cg06060137</b> | -0.16                               | 0.20                  | 1E-02     | 0.0336 | <i>DACHI</i>     |             |               | 13         |
| cg06100790        | -0.72                               | 0.60                  | 5E-03     | 0.0187 | <i>SH2B1</i>     | Island      | TSS1500       | 16         |
| cg06364593        | -1.56                               | 1.25                  | 2E-02     | 0.0424 | <i>ATP5B</i>     |             |               | 12         |
| cg06654302        | 0.30                                | -0.31                 | 4E-08     | 0.0000 | <i>DDX60L</i>    | Island      | 5UTR          | 4          |
| <b>cg06731192</b> | 0.34                                | -0.35                 | 2E-03     | 0.0111 | <i>HCG14</i>     | S_Shore     | TSS1500       | 6          |

|                   |       |       |       |        |                   |         |         |    |
|-------------------|-------|-------|-------|--------|-------------------|---------|---------|----|
| <b>cg07103819</b> | -0.11 | 0.12  | 1E-02 | 0.0359 | <i>DGAT1</i>      | Island  | 1stExon | 8  |
| cg07410872        | 0.45  | -0.48 | 2E-04 | 0.0030 | <i>HAND2</i>      | Island  | TSS200  | 4  |
| cg07483064        | -0.13 | 0.13  | 2E-02 | 0.0383 | <i>ENO1</i>       | Island  | 1stExon | 1  |
| <b>cg07588308</b> | -0.12 | 0.16  | 2E-02 | 0.0456 | <i>ZNF720</i>     | N_Shore | 5UTR    | 16 |
| cg07781003        | -0.74 | 0.93  | 2E-02 | 0.0474 | <i>LUC7L3</i>     | Island  | TSS200  | 17 |
| cg07794500        | -0.17 | 0.18  | 1E-02 | 0.0342 | <i>LOC647121</i>  | Island  | Body    | 1  |
| <b>cg07862535</b> | -0.43 | 0.48  | 1E-02 | 0.0342 | <i>LUC7L2</i>     | N_Shore | TSS1500 | 7  |
| <b>cg07938869</b> | -0.40 | 0.43  | 2E-04 | 0.0030 | <i>ZNF581</i>     | Island  | TSS1500 | 19 |
| <b>cg09484638</b> | -0.15 | 0.13  | 3E-02 | 0.0478 | <i>DNASE2</i>     | Island  | TSS200  | 19 |
| <b>cg09646206</b> | -0.12 | 0.13  | 2E-02 | 0.0470 | <i>SNX5</i>       | Island  | TSS1500 | 20 |
| <b>cg09767346</b> | 0.44  | -0.46 | 1E-03 | 0.0064 | <i>GORAB</i>      | 1stExon | 1       | 1  |
| cg09830308        | 0.47  | -0.47 | 5E-05 | 0.0014 | <i>MLKL</i>       | Island  | 5UTR    | 16 |
| cg10124287        | -0.09 | 0.10  | 5E-03 | 0.0174 | <i>PPMIH</i>      | Island  | Body    | 12 |
| cg10272675        | -0.14 | 0.16  | 2E-03 | 0.0111 | <i>MFGE8</i>      | Island  | TSS200  | 15 |
| cg10495392        | 0.43  | -0.39 | 2E-02 | 0.0474 | <i>NSUM4</i>      | Island  | 1stExon | 1  |
| <b>cg10706910</b> | -0.06 | 0.06  | 2E-02 | 0.0462 | <i>ZNF337</i>     | Island  | TSS200  | 20 |
| cg1115460         | -0.12 | 0.16  | 2E-02 | 0.0385 | <i>Intergenic</i> |         |         |    |
| cg11159084        | -0.33 | 0.38  | 2E-03 | 0.0105 | <i>HEATTRI</i>    | Island  | TSS200  | 1  |
| <b>cg11190854</b> | -0.25 | 0.29  | 2E-02 | 0.0456 | <i>SLC29A1</i>    |         |         | 6  |
| <b>cg11345323</b> | -0.11 | 0.16  | 2E-03 | 0.0111 | <i>PRKCCZ</i>     | Island  | TSS200  | 1  |
| cg11655691        | -0.17 | 0.16  | 2E-02 | 0.0383 | <i>CBARA1</i>     | Island  | 1stExon | 10 |
| <b>cg11844198</b> | 0.26  | -0.24 | 4E-03 | 0.0168 | <i>KIAA0922</i>   | Island  | TSS200  | 4  |
| <b>cg12142354</b> | -0.17 | 0.19  | 1E-02 | 0.0359 | <i>CMKLR1</i>     |         | TSS200  | 12 |
| cg12714538        | -0.40 | 0.67  | 1E-05 | 0.0004 | <i>PSMB4</i>      | Island  | TSS1500 | 1  |
| <b>cg13063405</b> | -0.22 | 0.27  | 7E-04 | 0.0052 | <i>EPHB3</i>      | Island  | TSS1500 | 3  |
| <b>cg13090731</b> | -0.07 | 0.10  | 2E-02 | 0.0373 | <i>TXNL1</i>      | Island  | TSS200  | 18 |
| <b>cg13118906</b> | -0.08 | 0.21  | 6E-05 | 0.0014 | <i>CYB56I</i>     | Island  | TSS1500 | 17 |
| cg13311096        | -0.08 | 0.14  | 1E-04 | 0.0026 | <i>C8orf84</i>    | Island  | TSS200  | 8  |
| <b>cg13913917</b> | 0.23  | -0.27 | 1E-06 | 0.0001 | <i>ATPL1B</i>     | Island  | 5UTR    | 3  |

|                    |       |       |       |        |                 |         |         |    |
|--------------------|-------|-------|-------|--------|-----------------|---------|---------|----|
| <b>cg14132628</b>  | 0.36  | -0.36 | 1E-02 | 0.0284 | <i>MED20</i>    | Island  | TSS200  | 6  |
| <b>cg14196208</b>  | -0.13 | 0.23  | 9E-04 | 0.0060 | <i>NEK6</i>     | N_Shore | TSS200  | 9  |
| <b>cg14311471</b>  | -0.16 | 0.24  | 2E-03 | 0.0111 | <i>NPR3</i>     | Island  | TSS1500 | 5  |
| <b>cg14632002</b>  | -0.09 | 0.12  | 9E-03 | 0.0271 | <i>STOM</i>     | Island  | Body    | 9  |
| <b>cg14985583</b>  | 0.87  | -0.82 | 5E-03 | 0.0185 | <i>PCOTH</i>    | Island  | 5UTR    | 13 |
| <b>cg15862215</b>  | -0.10 | 0.09  | 2E-02 | 0.0474 | <i>OTXI</i>     | Island  | TSS1500 | 2  |
| <b>cg16489582</b>  | 0.76  | -0.68 | 3E-03 | 0.0135 | <i>XPO6</i>     | Island  | TSS200  | 16 |
| <b>cg16926844</b>  | -0.53 | 0.71  | 4E-04 | 0.0037 | <i>CHEK2</i>    | Island  | TSS200  | 22 |
| <b>cg17027046</b>  | -0.56 | 0.56  | 1E-02 | 0.0339 | <i>ITPA</i>     | Island  | TSS200  | 20 |
| <b>cg17470637</b>  | -0.11 | 0.10  | 2E-02 | 0.0456 | <i>MARCH2</i>   | Island  | TSS200  | 19 |
| <b>cg17572791</b>  | 0.38  | -0.36 | 6E-05 | 0.0014 | <i>HAX1</i>     | Island  | 5UTR    | 1  |
| <b>cg18233595</b>  | -0.11 | 0.19  | 2E-04 | 0.0030 | <i>PRRC1</i>    | Island  | 5UTR    | 5  |
| <b>cg18590590</b>  | 0.18  | -0.16 | 5E-03 | 0.0188 | <i>LRRC42</i>   | Island  | TSS1500 | 1  |
| <b>cg18593717</b>  | -0.09 | 0.07  | 1E-02 | 0.0359 | <i>HDGF</i>     | Island  | TSS200  | 1  |
| <b>cg19078236</b>  | 0.71  | -0.70 | 8E-03 | 0.0255 | <i>AIP</i>      | N_Shore | TSS200  | 11 |
| <b>cg200000099</b> | -0.12 | 0.18  | 8E-04 | 0.0056 | <i>CEBPG</i>    | Island  | 5UTR    | 19 |
| <b>cg20004424</b>  | -0.20 | 0.24  | 2E-04 | 0.0030 | <i>TBL2</i>     | S_Shore | TSS1500 | 7  |
| <b>cg20896113</b>  | -0.13 | 0.22  | 5E-03 | 0.0174 | <i>RFX4</i>     | Body    | 12      |    |
| <b>cg20953075</b>  | 0.25  | -0.25 | 2E-04 | 0.0029 | <i>CEBPZ</i>    | Island  | TSS200  | 2  |
| <b>cg21278285</b>  | 0.32  | -0.34 | 1E-03 | 0.0075 | <i>ZNF416</i>   | Island  | 1stExon | 19 |
| <b>cg21478222</b>  | -0.18 | 0.29  | 2E-02 | 0.0456 | <i>ELK4</i>     | S_Shore | 1stExon | 1  |
| <b>cg22153463</b>  | -0.37 | 0.36  | 7E-03 | 0.0235 | <i>MCOLN2</i>   | Island  | TSS200  | 1  |
| <b>cg22463035</b>  | 0.36  | -0.37 | 9E-03 | 0.0271 | <i>RJMP2</i>    | Island  | 3UTR    | 12 |
| <b>cg22626041</b>  | -0.11 | 0.20  | 4E-03 | 0.0171 | <i>KIAA0040</i> | Island  | 1stExon | 1  |
| <b>cg22658244</b>  | -0.20 | 0.24  | 2E-02 | 0.0456 | <i>ZNF551</i>   | N_Shore | TSS1500 | 19 |
| <b>cg22922289</b>  | 0.34  | -0.31 | 6E-03 | 0.0216 | <i>ZNF134</i>   | Island  | TSS1500 | 19 |
| <b>cg22944932</b>  | -0.09 | 0.08  | 3E-02 | 0.0478 | <i>GOLG45</i>   | Island  | TSS1500 | 14 |
| <b>cg23292453</b>  | -0.11 | 0.10  | 1E-02 | 0.0284 | <i>ITGA3</i>    | Island  | 5UTR    | 17 |
| <b>cg23301140</b>  | -0.10 | 0.13  | 8E-04 | 0.0056 | <i>CTDPI</i>    | Island  | 5UTR    | 18 |

|                   |       |       |       |        |                 |                |         |    |
|-------------------|-------|-------|-------|--------|-----------------|----------------|---------|----|
| <b>cg23564746</b> | -0.10 | 0.08  | 2E-02 | 0.0383 | <i>CRLS1</i>    | Island         | TSS200  | 20 |
| <b>cg23831542</b> | -0.09 | 0.11  | 5E-04 | 0.0045 | <i>TMEM11</i>   | Island         | Body    | 17 |
| <b>cg23892580</b> | -0.14 | 0.14  | 9E-03 | 0.0284 | <i>SMARCA4</i>  | Island         | 5UTR    | 19 |
| <b>cg24167975</b> | -0.08 | 0.12  | 2E-02 | 0.0393 | <i>DHX37</i>    | Island         | TSS200  | 12 |
| <b>cg24173551</b> | -0.35 | 0.38  | 2E-02 | 0.0385 | <i>SETD8</i>    | Island         | TSS200  | 12 |
| <b>cg24252723</b> | -1.04 | 0.96  | 3E-03 | 0.0114 | <i>CNMM2</i>    | Island         | 1stExon | 10 |
| <b>cg25156443</b> | -0.44 | 0.51  | 3E-04 | 0.0037 | <i>SFRP5</i>    | Island         | TSS200  | 10 |
| <b>cg25189247</b> | 0.85  | -0.83 | 2E-03 | 0.0111 | <i>ITGAE</i>    | Body           | Body    | 17 |
| <b>cg25497529</b> | -0.08 | 0.09  | 1E-02 | 0.0335 | <i>COMP</i>     | Island         | Body    | 19 |
| <b>cg25518386</b> | -0.21 | 0.17  | 2E-02 | 0.0474 | <i>RAB34</i>    | <u>S_Shore</u> | TSSI500 | 19 |
| <b>cg25622628</b> | 0.22  | -0.21 | 2E-02 | 0.0456 | <i>C19orf24</i> | Island         | 1stExon | 19 |
| <b>cg26196912</b> | -0.22 | 0.33  | 3E-03 | 0.0114 | <i>C8orf38</i>  | Island         | TSS200  | 8  |
| <b>cg26290114</b> | 0.51  | -0.52 | 8E-04 | 0.0056 | <i>WDFY2</i>    | <u>S_Shore</u> | Body    | 13 |
| <b>cg26365885</b> | 0.40  | -0.38 | 5E-06 | 0.0003 | <i>CCDC46</i>   | TSS1500        | Island  | 17 |
| <b>cg26744078</b> | 0.28  | -0.27 | 2E-03 | 0.0105 | <i>ZNF805</i>   | Island         | 1stExon | 19 |
| <b>cg27116888</b> | -0.13 | 0.17  | 8E-03 | 0.0254 | <i>SALL3</i>    | Body           | Body    | 18 |
| <b>cg27341045</b> | 0.25  | -0.25 | 1E-03 | 0.0062 | <i>PPCDC</i>    | Island         | 5UTR    | 15 |

| CpG sites         | Gene          | ALSPAC                      |  |                          | ALSPAC P value |
|-------------------|---------------|-----------------------------|--|--------------------------|----------------|
|                   |               | Main Estimates (7-17 years) | ALSPAC Interaction Estimates (17-22 years) | ALSPAC estimates (years) |                |
| cg00149397        | <i>TPST2</i>  | 0.01                        | 0.31                                       | 0.31                     | 0.093          |
| cg00405843        | <i>SMO</i>    | -0.25                       | 0.13                                       | -0.12                    | 0.676          |
| cg00444282        | <i>RTN3</i>   | -0.02                       | 0.00                                       | -0.02                    | 0.979          |
| <b>cg00705668</b> | <i>MRPS12</i> | -0.04                       | -0.09                                      | -0.14                    | 0.707          |
| <b>cg02225897</b> | <i>RTDR1</i>  | -0.01                       | -0.16                                      | -0.17                    | 0.142          |

|                   |                  |       |       |       |       |
|-------------------|------------------|-------|-------|-------|-------|
| <b>cg02362385</b> | <i>LPAR2</i>     | -0.04 | 0.44  | 0.40  | 0.147 |
| <b>cg02467794</b> | <i>AKAP1</i>     | 0.03  | -0.37 | -0.33 | 0.026 |
| <b>cg02516257</b> | <i>GMCLI</i>     | -0.08 | 0.39  | 0.31  | 0.116 |
| <b>cg02619805</b> | <i>SAFB2</i>     | -0.09 | 0.16  | 0.07  | 0.601 |
| <b>cg03223733</b> | <i>ZNF21I</i>    | -0.01 | -0.18 | -0.19 | 0.307 |
| <b>cg03606222</b> | <i>NAPA</i>      | -0.07 | 0.61  | 0.54  | 0.072 |
| <b>cg03719634</b> | <i>TMEM45A</i>   | -0.09 | -0.16 | -0.25 | 0.343 |
| <b>cg04784251</b> | <i>BCAS3</i>     | -0.01 | -0.08 | -0.09 | 0.476 |
| <b>cg04789385</b> | <i>ZFPI</i>      | -0.09 | 0.24  | 0.15  | 0.407 |
| <b>cg04802657</b> | <i>CCDC101</i>   | -0.03 | -0.03 | -0.05 | 0.934 |
| <b>cg05245655</b> | <i>SLX5</i>      | -0.29 | 0.12  | -0.16 | 0.665 |
| <b>cg05444312</b> | <i>HSTTH2BM</i>  | 0.03  | 0.05  | 0.07  | 0.552 |
| <b>cg06045799</b> | <i>COMMD8</i>    | -0.05 | 0.23  | 0.18  | 0.392 |
| <b>cg06060137</b> | <i>DACH1</i>     | 0.00  | 0.02  | 0.02  | 0.893 |
| <b>cg06100790</b> | <i>SH2BI</i>     | 0.06  | -0.10 | -0.04 | 0.646 |
| <b>cg06364593</b> | <i>ATP5B</i>     | 0.10  | -0.02 | 0.09  | 0.888 |
| <b>cg06654302</b> | <i>DDX60L</i>    | -0.15 | 0.31  | 0.17  | 0.151 |
| <b>cg06731192</b> | <i>HCG14</i>     | -0.02 | -0.06 | -0.08 | 0.719 |
| <b>cg07103819</b> | <i>DGAT1</i>     | -0.12 | 0.11  | -0.01 | 0.693 |
| <b>cg07410872</b> | <i>HAND2</i>     | -0.01 | 0.29  | 0.28  | 0.220 |
| <b>cg07483064</b> | <i>ENOL</i>      | -0.12 | -0.22 | -0.35 | 0.335 |
| <b>cg07588308</b> | <i>ZNFX20</i>    | -0.04 | 0.22  | 0.19  | 0.408 |
| <b>cg07781003</b> | <i>LUC7L3</i>    | 0.01  | -0.13 | -0.13 | 0.447 |
| <b>cg07794500</b> | <i>LOC647121</i> | 0.07  | -0.21 | -0.14 | 0.337 |
| <b>cg07862535</b> | <i>LUC7L2</i>    | 0.01  | -0.29 | -0.28 | 0.103 |
| <b>cg07938869</b> | <i>ZNF581</i>    | -0.23 | 0.23  | 0.00  | 0.377 |
| <b>cg09484638</b> | <i>DNASE2</i>    | -0.11 | 0.17  | 0.06  | 0.598 |
| <b>cg09646206</b> | <i>SMX5</i>      | -0.05 | 0.09  | 0.04  | 0.773 |
| <b>cg09767346</b> | <i>GORAB</i>     | 0.01  | -0.03 | -0.02 | 0.885 |

|                   |                        |       |       |       |       |
|-------------------|------------------------|-------|-------|-------|-------|
| cg09830308        | <i>MLKL</i>            | -0.07 | 0.05  | -0.02 | 0.853 |
| cg10124287        | <i>PPMIH</i>           | -0.01 | -0.07 | -0.08 | 0.833 |
| cg10272675        | <i>MFGE8</i>           | -0.03 | -0.02 | -0.05 | 0.875 |
| cg10495392        | <i>NSUN4</i>           | -0.02 | 0.21  | 0.19  | 0.099 |
| <b>cg10706910</b> | <b><i>ZNF337</i></b>   | -0.06 | 0.11  | 0.05  | 0.601 |
| cg1115460         | <i>Intergeneic</i>     | 0.02  | -0.04 | -0.02 | 0.780 |
| cg11159084        | <i>HEATR1</i>          | 0.06  | -0.18 | -0.12 | 0.548 |
| <b>cg11190854</b> | <b><i>SLC29A1</i></b>  | -0.16 | 0.28  | 0.12  | 0.184 |
| <b>cg11345323</b> | <b><i>PRKCZ</i></b>    | -0.06 | 0.11  | 0.06  | 0.623 |
| cg11655691        | <i>CBARAI</i>          | 0.08  | -0.21 | -0.14 | 0.303 |
| <b>cg11844198</b> | <b><i>KIAA0922</i></b> | -0.01 | -0.38 | -0.40 | 0.174 |
| <b>cg12142354</b> | <b><i>CMKLR1</i></b>   | 0.03  | 0.00  | 0.03  | 0.999 |
| cg12714538        | <i>PSMB4</i>           | 0.03  | -0.09 | -0.06 | 0.634 |
| <b>cg13063405</b> | <b><i>EPHB3</i></b>    | -0.08 | 0.24  | 0.16  | 0.419 |
| <b>cg13090731</b> | <b><i>TXNL1</i></b>    | -0.13 | 0.29  | 0.16  | 0.228 |
| <b>cg13118906</b> | <b><i>CYB56I</i></b>   | 0.02  | 0.25  | 0.27  | 0.238 |
| cg13311096        | <i>C8orf84</i>         | -0.03 | -0.09 | -0.12 | 0.723 |
| <b>cg13913917</b> | <b><i>ATP1IB</i></b>   | -0.17 | -0.02 | -0.19 | 0.955 |
| cg14132628        | <i>MED20</i>           | 0.10  | 0.00  | 0.11  | 0.983 |
| <b>cg14196208</b> | <b><i>NEK6</i></b>     | -0.47 | 0.40  | -0.07 | 0.092 |
| <b>cg14311471</b> | <b><i>NPR3</i></b>     | 0.04  | 0.08  | 0.12  | 0.521 |
| <b>cg14632002</b> | <b><i>STOM</i></b>     | -0.06 | 0.27  | 0.21  | 0.303 |
| cg14985583        | <i>PCOTH</i>           | -0.09 | 0.07  | -0.02 | 0.731 |
| <b>cg15862215</b> | <b><i>OTXI</i></b>     | -0.02 | 0.02  | 0.00  | 0.817 |
| cg16489582        | <i>XPO6</i>            | 0.01  | 0.11  | 0.12  | 0.319 |
| <b>cg16926844</b> | <b><i>CHEK2</i></b>    | -0.02 | 0.12  | 0.10  | 0.438 |
| <b>cg17027046</b> | <b><i>ITPA</i></b>     | -0.08 | 0.22  | 0.15  | 0.207 |
| <b>cg17470637</b> | <b><i>MARCH2</i></b>   | -0.20 | 0.40  | 0.20  | 0.019 |
| <b>cg17572791</b> | <b><i>HAX1</i></b>     | -0.04 | -0.08 | 0.595 |       |

|                   |                 |       |       |       |       |
|-------------------|-----------------|-------|-------|-------|-------|
| <b>cg18233595</b> | <i>PRRCI</i>    | -0.08 | 0.10  | 0.02  | 0.652 |
| <b>cg18590590</b> | <i>LRRK42</i>   | -0.07 | 0.16  | 0.09  | 0.285 |
| <b>cg18593717</b> | <i>HDGF</i>     | -0.10 | 0.05  | -0.05 | 0.826 |
| <b>cg19078236</b> | <i>AIP</i>      | -0.04 | -0.11 | -0.14 | 0.510 |
| <b>cg20000099</b> | <i>CEBPG</i>    | -0.13 | 0.10  | -0.03 | 0.741 |
| <b>cg20004424</b> | <i>TBL2</i>     | 0.02  | 0.02  | 0.04  | 0.850 |
| <b>cg20896113</b> | <i>RFX4</i>     | 0.08  | -0.13 | -0.06 | 0.044 |
| <b>cg20953075</b> | <i>CEBPZ</i>    | -0.11 | 0.40  | 0.29  | 0.091 |
| <b>cg21278285</b> | <i>ZNF416</i>   | -0.03 | -0.22 | -0.25 | 0.387 |
| <b>cg21478222</b> | <i>ELK4</i>     | -0.06 | -0.47 | -0.53 | 0.060 |
| <b>cg22153463</b> | <i>MCOLN2</i>   | 0.00  | 0.16  | 0.16  | 0.034 |
| <b>cg22463035</b> | <i>RIMBP2</i>   | 0.03  | 0.24  | 0.27  | 0.190 |
| <b>cg22626041</b> | <i>KIAA0040</i> | -0.09 | 0.20  | 0.11  | 0.537 |
| <b>cg22658244</b> | <i>ZNF551</i>   | 0.06  | -0.06 | 0.00  | 0.766 |
| <b>cg22922289</b> | <i>ZNF134</i>   | -0.21 | 0.50  | 0.29  | 0.136 |
| <b>cg22944932</b> | <i>GOLG45</i>   | -0.20 | 0.05  | -0.15 | 0.855 |
| <b>cg23292453</b> | <i>ITGA3</i>    | -0.05 | 0.26  | 0.21  | 0.239 |
| <b>cg23301140</b> | <i>CTDPI</i>    | -0.09 | 0.15  | 0.06  | 0.616 |
| <b>cg23564746</b> | <i>CRLSI</i>    | -0.02 | -0.09 | -0.11 | 0.733 |
| <b>cg23831542</b> | <i>TMEM11</i>   | -0.02 | -0.12 | -0.15 | 0.656 |
| <b>cg23892580</b> | <i>SMARCA4</i>  | -0.15 | 0.32  | 0.17  | 0.238 |
| <b>cg24167975</b> | <i>DHX37</i>    | 0.05  | 0.12  | 0.17  | 0.670 |
| <b>cg24173551</b> | <i>SETD8</i>    | -0.07 | 0.27  | 0.19  | 0.394 |
| <b>cg24252723</b> | <i>CNNM2</i>    | -0.02 | -0.18 | -0.20 | 0.309 |
| <b>cg25156443</b> | <i>SFRP5</i>    | -0.17 | 0.26  | 0.09  | 0.072 |
| <b>cg25189247</b> | <i>ITGAE</i>    | -0.05 | 0.10  | 0.06  | 0.404 |
| <b>cg25497529</b> | <i>COMP</i>     | -0.07 | -0.15 | -0.22 | 0.398 |
| <b>cg25518386</b> | <i>RAB3A</i>    | 0.00  | 0.24  | 0.24  | 0.124 |
| <b>cg25622628</b> | <i>C19orf24</i> | -0.13 | 0.24  | 0.11  | 0.450 |

|                   |                |       |       |       |       |
|-------------------|----------------|-------|-------|-------|-------|
| <b>cg26196912</b> | <i>C8orf38</i> | -0.05 | -0.32 | -0.37 | 0.349 |
| <b>cg26290114</b> | <i>WDFY2</i>   | 0.04  | 0.00  | 0.04  | 0.992 |
| <b>cg26365885</b> | <i>CCDC46</i>  | -0.03 | 0.00  | -0.03 | 0.995 |
| <b>cg26744078</b> | <i>ZNF805</i>  | -0.23 | 0.33  | 0.11  | 0.166 |
| <b>cg27116888</b> | <i>SALL3</i>   | 0.03  | 0.01  | 0.04  | 0.956 |
| <b>cg27341045</b> | <i>PPCDC</i>   | -0.22 | 0.37  | 0.15  | 0.195 |

Note: (a) For the analysis in IoW, logistic regression with repeated measurements were adjusted for atopic status at ages 10 and 18 years, active smoking, and secondhand smoke exposure at age 18 and 26 years, transition period 10-18 and 18-26 years.

(b) Analysis of ALSPAC used similar available covariates: atopic status at age 7 years, secondhand smoke exposure at age 17 and 24 years. Interaction effects consistent between the two cohorts are with bold fonts of CpG.

Supplement Table S2 (A): Association of DNAm with asthma acquisition from pre- to post-adolescence, and post-adolescence to young adulthood at 38 CpGs in males that are transition period non-specific. Significant effects of DNAm on asthma acquisition identified in the IoW(a) cohort were further tested in the ALSPAC(b) cohort.

| CpG sites         | IoW<br>Estimates | Raw p value | FDR p<br>value | Gene             | CpG islands | Gene<br>location | ALSPAC |                      |
|-------------------|------------------|-------------|----------------|------------------|-------------|------------------|--------|----------------------|
|                   |                  |             |                |                  |             |                  | Chr.   | Estimates<br>P value |
| <b>cg01078627</b> | -0.07            | 2E-06       | 3E-05          | <i>ERCC1</i>     | Island      | Body             | 19     | 0.07<br>0.52         |
| <b>cg01704999</b> | 0.34             | 1E-02       | 1E-02          | <i>SLC24A1</i>   |             |                  | 15     | -0.03<br>0.54        |
| <b>cg02309752</b> | -0.67            | 5E-04       | 1E-03          | <i>DEFB136</i>   |             | Body             | 8      | 0.03<br>0.59         |
| <b>cg03001647</b> | -0.03            | 5E-03       | 7E-03          | <i>MPZL1</i>     | S_Shore     | TSS200           | 1      | 0.00<br>0.98         |
| <b>cg03841312</b> | -0.59            | 6E-06       | 5E-05          | <i>MIRLET7A3</i> |             | 3'UTR            | 22     | 0.02<br>0.62         |
| <b>cg04673465</b> | 0.54             | 1E-03       | 2E-03          | <i>CDS1</i>      |             | 1stExon          | 4      | -0.03<br>0.60        |
| <b>cg05341115</b> | 0.22             | 1E-03       | 2E-03          | <i>HVAL4</i>     |             | 5'UTR            | 7      | 0.06<br>0.28         |
| <b>cg05783329</b> | -0.24            | 1E-03       | 2E-03          | <i>NUDT3</i>     | Island      |                  | 6      | 0.03<br>0.42         |
| <b>cg06186394</b> | -0.18            | 7E-03       | 8E-03          | <i>BAXX2</i>     | S_Shore     | Body             | 11     | -0.04<br>0.22        |
| <b>cg06683328</b> | -0.29            | 1E-03       | 2E-03          | <i>TBC1D22A</i>  | S_Shelf     | TSS1500          | 22     | -0.06<br>0.27        |
| <b>cg06684259</b> | 0.78             | 3E-07       | 1E-05          | <i>HAS3</i>      | N_Shore     | TSS200           | 16     | 0.01<br>0.90         |
| <b>cg07500501</b> | -0.04            | 5E-04       | 1E-03          | <i>SKIV2L2</i>   | Island      |                  | 5      | 0.02<br>0.89         |
| <b>cg08354614</b> | 0.65             | 2E-05       | 1E-04          | <i>ZMZ1</i>      |             | 5'UTR            | 10     | 0.00<br>0.95         |

|                   |       |       |       |                  |         |         |       |       |      |
|-------------------|-------|-------|-------|------------------|---------|---------|-------|-------|------|
| <b>cg08757348</b> | 0.47  | 6E-05 | 2E-04 | <i>ZNF214</i>    | Island  | TSS200  | 11    | -0.03 | 0.38 |
| <b>cg09852187</b> | -0.51 | 2E-05 | 1E-04 | <i>MIR7-2</i>    | Body;   | Body;   | 15    | -0.01 | 0.77 |
| cg10919222        | -0.06 | 8E-04 | 2E-03 | <i>TMEM194A</i>  | Island  | TSS200  | 12    | 0.03  | 0.70 |
| <b>cg10996201</b> | -0.06 | 1E-03 | 2E-03 | <i>RGL2</i>      | Island  | TSS200  | 6     | -0.06 | 0.61 |
| <b>cg14056357</b> | -0.06 | 4E-06 | 5E-05 | <i>ZNF229</i>    | Island  |         | 19    | -0.01 | 0.62 |
| <b>cg14893576</b> | 0.37  | 3E-04 | 8E-04 | <i>KLHL29</i>    | N_Shelf | 5'UTR   | 2     | 0.03  | 0.26 |
| cg15773726        | -0.06 | 2E-03 | 2E-03 | <i>SOCS2</i>     | Island  | Body    | 12    | 0.02  | 0.85 |
| <b>cg15778400</b> | 0.44  | 3E-04 | 8E-04 | <i>SRGAP3</i>    | 1stExon | 3       | 0.01  | 0.88  |      |
| cg17261830        | -0.07 | 2E-03 | 2E-03 | <i>NEK9</i>      | Island  | 5'UTR   | 14    | 0.03  | 0.50 |
| cg18262260        | -0.05 | 2E-05 | 9E-05 | <i>ZC3H14</i>    | Island  | TSS200  | 14    | 0.04  | 0.37 |
| cg18369866        | 0.45  | 1E-03 | 2E-03 | <i>POU4F3</i>    | Island  | Body    | 5     | -0.02 | 0.71 |
| cg18418538        | -0.05 | 9E-05 | 5E-05 | <i>LMTK3</i>     | Island  | TSS200  | 19    | 0.07  | 0.08 |
| cg19119818        | -0.02 | 9E-03 | 9E-03 | <i>AP2MI</i>     | Island  | Body    | 3     | 0.01  | 0.91 |
| cg20951825        | 0.23  | 7E-03 | 8E-03 | <i>PRDM6</i>     | TSS200  | 5       | -0.02 | 0.75  |      |
| cg21543536        | -0.11 | 8E-03 | 9E-03 | <i>TSPYLI</i>    | S_Shore | 6       | 0.00  | 0.92  |      |
| cg22188703        | -0.33 | 9E-05 | 3E-04 | <i>BODI</i>      | S_Shelf | TSS200  | 5     | 0.02  | 0.69 |
| cg22268256        | -0.06 | 2E-04 | 5E-04 | <i>BAT5</i>      | Island  | TSS1500 | 6     | 0.01  | 0.86 |
| cg23855392        | 0.17  | 3E-03 | 5E-03 | <i>MTHFS</i>     | S_Shore | 3'UTR   | 15    | -0.02 | 0.62 |
| cg23930856        | -0.05 | 8E-06 | 5E-05 | <i>TFAP2B</i>    | N_Shore |         | 6     | 0.09  | 0.23 |
| cg25400182        | 0.29  | 2E-02 | 2E-02 | <i>CLLUI-ASI</i> |         | TSS200  | 12    | -0.04 | 0.35 |
| cg25613170        | -0.04 | 2E-03 | 2E-03 | <i>TBKBP1</i>    | Island  | TSS200  | 17    | 0.05  | 0.20 |
| <b>cg26411687</b> | -0.03 | 3E-02 | 3E-02 | <i>OS9</i>       | Island  | 1stExon | 12    | -0.06 | 0.08 |
| <b>cg27230711</b> | -0.05 | 4E-03 | 5E-03 | <i>PPRC1</i>     | Island  | 3'UTR   | 10    | -0.02 | 0.82 |
| cg27238852        | 0.21  | 1E-03 | 2E-03 | <i>CSNK2A2</i>   | Body    |         | 16    | -0.04 | 0.22 |
| <b>cg27593384</b> | -0.05 | 3E-05 | 1E-04 | <i>CDH2</i>      | Island  |         | 18    | -0.01 | 0.82 |

Note: (a) For the analysis in IoW, logistic regression with repeated measurements were adjusted for atopic status at ages 10 and 18 years, active smoking and second-hand smoke exposure at age 18 and 26 years, transition period 10-18 and 18-26 years.

(b) Analysis of ALSPAC used similar available covariates: atopic status at age 7 years, second-hand smoke exposure at age 17 and 24 years. Interaction effects consistent between the two cohorts are with bold fonts of CpG.

Supplement Table S2 (B): Association of DNAm with asthma acquisition from pre- to post-adolescence, and post-adolescence to young adulthood at 53 CpGs in females that are transition period non-specific. Significant effects of DNAm on asthma acquisition identified in the IoW(a) cohort were further tested in the ALSPAC(b) cohort.

| CpG sites         | IoW<br>Estimates | Raw p value | FDR p<br>value | Gene           | CpG islands | Gene<br>location | ALSPAC |                     |
|-------------------|------------------|-------------|----------------|----------------|-------------|------------------|--------|---------------------|
|                   |                  |             |                |                |             |                  | Chr.   | ALSPAC<br>Estimates |
| cg00615892        | -0.05            | 0.0030      | 0.0126         | <i>CHTF8</i>   | Island      | TSS200           | 16     | 0.01                |
| <b>cg00907843</b> | -0.03            | 0.0163      | 0.0342         | <i>MLXIP</i>   | Island      | TSS200           | 7      | 0.00                |
| <b>cg01364172</b> | -0.43            | 0.0110      | 0.0274         | <i>DENND4C</i> | N_Shore     |                  | 9      | -0.02               |
| cg01529207        | -0.09            | 0.0225      | 0.0407         | <i>NDUF46</i>  | N_Shore     | Body             | 22     | 0.04                |
| <b>cg01943657</b> | -0.08            | 0.0001      | 0.0020         | <i>PPP3CA</i>  | Island      | TSS200           | 4      | -0.08               |
| <b>cg02067639</b> | -0.05            | 0.0131      | 0.0293         | <i>MED6</i>    |             | TSS200           | 14     | -0.14               |
| cg03237356        | -0.05            | 0.0054      | 0.0165         | <i>NEIL3</i>   | Island      | TSS200           | 4      | 0.03                |
| <b>cg03655771</b> | -0.10            | 0.0122      | 0.0289         | <i>B4GALT5</i> | Island      | Body             | 20     | -0.03               |
| <b>cg04211198</b> | -0.31            | 0.0001      | 0.0019         | <i>NABI</i>    | Island      | TSS1500          | 2      | -0.15               |
| <b>cg04535371</b> | -0.04            | 0.0052      | 0.0162         | <i>IMPDH2</i>  | Island      | 5UTR             | 3      | -0.10               |
| <b>cg05898113</b> | -0.04            | 0.0175      | 0.0346         | <i>WASH3P</i>  | Island      | Body             | 15     | -0.01               |
| <b>cg06075477</b> | -0.06            | 0.0001      | 0.0019         | <i>KRT11</i>   | Island      | 5UTR             | 7      | -0.06               |
| <b>cg06226335</b> | -0.03            | 0.0264      | 0.0449         | <i>BETIL</i>   | Island      | TSS1500          | 11     | -0.06               |
| <b>cg06302857</b> | -0.06            | 0.0011      | 0.0079         | <i>TOMI</i>    | Island      | TSS200           | 22     | -0.18               |
| cg07294234        | -0.04            | 0.0169      | 0.0342         | <i>FNT4</i>    | Island      | TSS200           | 8      | 0.06                |
| cg07676167        | -0.05            | 0.0014      | 0.0084         | <i>C8orf76</i> | Island      | Body             | 8      | 0.05                |
| cg07951151        | 0.18             | 0.0289      | 0.0482         | <i>GRHL1</i>   |             |                  | 2      | -0.04               |
| <b>cg08092965</b> | -0.05            | 0.0001      | 0.0019         | <i>ZNF23</i>   | Island      | 1stExon          | 16     | -0.06               |
| <b>cg08487579</b> | -0.05            | 0.0007      | 0.0069         | <i>PHC3</i>    | Island      | TSS200           | 3      | -0.09               |
| <b>cg08614771</b> | -0.04            | 0.0199      | 0.0376         | <i>ARD1B</i>   |             | Body             | 6      | -0.04               |
| cg09567485        | 0.38             | 0.0041      | 0.0150         | <i>HSF4</i>    | N_Shore     | 3UTR             | 16     | -0.19               |
| <b>cg09822824</b> | -0.05            | 0.0208      | 0.0385         | <i>CKAP5</i>   | Island      | TSS200           | 11     | -0.01               |
| <b>cg10729426</b> | -0.06            | 0.0009      | 0.0074         | <i>ZNF549</i>  | Island      | TSS200           | 19     | 0.00                |
| <b>cg10850197</b> | -0.04            | 0.0155      | 0.0337         | <i>ATG5</i>    | Island      | 5UTR             | 6      | -0.01               |

|                   |       |        |        |                  |                |         |       |       |      |
|-------------------|-------|--------|--------|------------------|----------------|---------|-------|-------|------|
| <b>cg10880755</b> | -0.05 | 0.0029 | 0.0126 | <i>MGC42105</i>  | Island         | TSS200  | 5     | -0.09 | 0.27 |
| <b>cg11252776</b> | -0.04 | 0.0166 | 0.0342 | <i>CROT</i>      | Island         | 5UTR    | 7     | -0.05 | 0.57 |
| <b>cg11439068</b> | -0.07 | 0.0002 | 0.0021 | <i>PAK4</i>      | Island         | TSS200  | 19    | -0.11 | 0.20 |
| <b>cg12210286</b> | -0.07 | 0.0010 | 0.0074 | <i>CNTD2</i>     | Island         | 1stExon | 19    | -0.18 | 0.02 |
| <b>cg13337238</b> | 0.11  | 0.0033 | 0.0128 | <i>HIST1H4A</i>  | Island         | TSS1500 | 6     | 0.04  | 0.19 |
| <b>cg13688524</b> | -0.04 | 0.0072 | 0.0211 | <i>BODI</i>      | Island         | TSS200  | 5     | 0.02  | 0.80 |
| <b>cg14445451</b> | -0.07 | 0.0000 | 0.0019 | <i>ICT1</i>      | Island         | TSS200  | 17    | -0.14 | 0.11 |
| <b>cg15278646</b> | -0.05 | 0.0076 | 0.0211 | <i>OCA2</i>      | Island         | 5UTR    | 15    | -0.04 | 0.58 |
| <b>cg15353444</b> | -0.04 | 0.0091 | 0.0241 | <i>SERPINE2</i>  | Island         | 5'UTR   | 2     | 0.01  | 0.89 |
| <b>cg16511870</b> | 0.24  | 0.0016 | 0.0091 | <i>USP42</i>     | Island         | 5UTR    | 7     | -0.02 | 0.79 |
| <b>cg16570995</b> | -0.06 | 0.0002 | 0.0020 | <i>PIM1</i>      | Island         | 5UTR    | 6     | -0.04 | 0.56 |
| <b>cg16878007</b> | -0.07 | 0.0033 | 0.0128 | <i>TTPAL</i>     | Island         | 5UTR    | 20    | -0.06 | 0.45 |
| <b>cg17015511</b> | -0.04 | 0.0261 | 0.0449 | <i>RDX</i>       | Island         | TSS200  | 11    | -0.11 | 0.19 |
| <b>cg17226280</b> | -0.05 | 0.0049 | 0.0161 | <i>MRC2</i>      | Island         | Body    | 17    | -0.02 | 0.75 |
| <b>cg18716861</b> | -0.23 | 0.0095 | 0.0244 | <i>PABPC1L</i>   | Island         | 5UTR    | 20    | -0.09 | 0.21 |
| <b>cg19445996</b> | -0.05 | 0.0014 | 0.0084 | <i>RAB37</i>     | Island         | TSS200  | 17    | -0.12 | 0.22 |
| <b>cg19818298</b> | -0.03 | 0.0077 | 0.0211 | <i>CHD8</i>      |                | TSS200  | 14    | 0.16  | 0.01 |
| <b>cg20361600</b> | -0.07 | 0.0192 | 0.0371 | <i>DLX2</i>      | Island         | TSS200  | 2     | -0.10 | 0.29 |
| <b>cg20690303</b> | -0.05 | 0.0305 | 0.0498 | <i>QDPR</i>      | Island         | 1stExon | 4     | -0.04 | 0.58 |
| <b>cg21146957</b> | 0.18  | 0.0026 | 0.0126 | <i>PTPRQ</i>     | Body           | 12      | -0.02 | 0.43  |      |
| <b>cg21851386</b> | -0.06 | 0.0128 | 0.0293 | <i>SMAD2</i>     | Island         | TSS200  | 18    | -0.11 | 0.25 |
| <b>cg22510032</b> | -0.04 | 0.0234 | 0.0415 | <i>LCORL</i>     | <u>S_Shore</u> | TSS1500 | 4     | 0.02  | 0.44 |
| <b>cg23080241</b> | -0.05 | 0.0023 | 0.0122 | <i>TXNDC15</i>   | Island         | 1stExon | 5     | -0.10 | 0.25 |
| <b>cg24483825</b> | -0.04 | 0.0049 | 0.0161 | <i>CASP9</i>     | Island         | TSS1500 | 1     | -0.01 | 0.78 |
| <b>cg26682955</b> | 0.23  | 0.0115 | 0.0280 | <i>ITPR3</i>     | <u>S_Shelf</u> | Body    | 6     | -0.05 | 0.33 |
| <b>cg26693529</b> | -0.05 | 0.0000 | 0.0019 | <i>ITC32</i>     | Island         | TSS200  | 2     | -0.01 | 0.93 |
| <b>cg26791126</b> | -0.04 | 0.0029 | 0.0126 | <i>DNAJC8</i>    | Island         | 1stExon | 1     | -0.01 | 0.76 |
| <b>cg27395440</b> | 0.28  | 0.0047 | 0.0161 | <i>LOC728276</i> | Body           | 16      | -0.04 | 0.32  |      |

Note: (a) For the analysis in IoW, logistic regression with repeated measurements were adjusted for atopic status at ages 10 and 18 years, active smoking and second hand smoke exposure at age 18 and 26 years, transition period 10-18 and 18-26 years.

(b) Analysis of ALSPAC used similar available covariates: atopic status at age 7 years, second hand smoke exposure at age 17 and 24 years. Interaction effects consistent between the two cohorts are with bold fonts of CpG.

Supplement Table S3 (A): Top 10 most statistically significant GO terms and its biological processes from pathway enrichment analysis along with their genes names in each pathway for males, for the identified CpGs.

| GO term    | Biological processes                              | P-value  | Genes  |
|------------|---|----------|--|
|            |   |          |  |
| GO:0009056 | catabolic process                                 | 0.003682 | <b><i>IRSI</i></b> , <b><i>ENOL1</i></b> , <b><i>IRSI</i></b> , <b><i>MTHFS</i></b> , <b><i>OS9</i></b> , <b><i>NUDT3</i></b> , <b><i>HYAL4</i></b> , <b><i>BANP</i></b> , <b><i>ZC3H14</i></b> , <b><i>MIRLET7A3</i></b>  |
| GO:0038111 | interleukin-7-mediated signaling pathway          | 0.002124 | <b><i>SOC32</i></b>  |
| GO:0042219 | cellular modified amino acid catabolic process    | 0.002071 | <b><i>MTHFS</i></b>  |
| GO:0042365 | water-soluble vitamin catabolic process           | 0.003378 | <b><i>MTHFS</i></b>  |
| GO:0046657 | folic acid catabolic process                      | 0.001542 | <b><i>MTHFS</i></b>  |
| GO:0071544 | diphosphoinositol polyphosphate catabolic process | 0.002544 | <b><i>NUDT3</i></b>  |
| GO:0098760 | response to interleukin-7                         | 0.003907 | <b><i>IRSI</i></b> , <b><i>SOC32</i></b>   |
| GO:0098761 | cellular response to interleukin-7                | 0.003907 | <b><i>IRSI</i></b> , <b><i>SOC32</i></b>   |
| GO:1901575 | organic substance catabolic process               | 0.000585 | <b><i>AP2M1</i></b> , <b><i>CSNK1A1</i></b> , <b><i>CSNK2A2</i></b> , <b><i>ENOL1</i></b> , <b><i>IRSI</i></b> , <b><i>MTHFS</i></b> , <b><i>OS9</i></b> , <b><i>NUDT3</i></b> , <b><i>HYAL4</i></b> , <b><i>BANP</i></b> , <b><i>ZC3H14</i></b> , <b><i>MIRLET7A3</i></b> |

Note: CpGs mapped to genes in bold font showed consistent associations (interaction or main effects) between two cohorts.

Supplement STable 3 (B): Top 10 most statistically significant GO terms and its biological processes from pathway enrichment analysis along with their genes names in each pathway for females, for the identified CpGs.

| GO term    | Biological processes                     | P-value  | Genes   |
|------------|--|----------|---|
| GO:0019438 | aromatic compound biosynthetic process   | 0.00045  | <i>ATP5F1B, CEBPG, CMKLRI, DACHI, DLX2, ELK4, ENOL, HDGF, HSF4, IMPDH2, ITPA, SMAD2, NABI, OCA2, OTXI, PIM1, PPP3CA, PRKCZ, PSMB4, QDPR, TRIM27, RFX4, SFRP5, SMARCA4, SMO, ZNF23, ZNF41, ZNF134, AIP, CTDPL, HAND2, MED20, SAFB2, MED6, CEBPZ, HAX1, ZNF21L, CHEK2, SH2B1, ZNF337, SALL3, GRHL1, MLXIPL, ZNF58L, BCAS3, CHTF8, HEATR1, ARID1B, CHD8, PPCDC, PABPC1L, ZNF551, ZNF720, ZFP1, LCORL, ZNF549, ZNF805, CEBPG, CMKLRI, DACHI, DLX2, ELK4, ENOL, HDGF, HSF4, SMAD2, NABI, OTXI, PIM1, PPP3CA, PRKCZ, PSMB4, TRIM27, RFX4, SFRP5, SMARCA4, SMO, ZNF23, ZNF41, ZNF134, AIP, CTDPL, HAND2, MED20, SAFB2, MED6, CEBPZ, HAX1, ZNF21L, CHEK2, ZNF337, SALL3, GRHL1, MLXIPL, ZNF58L, BCAS3, HEATR1, ARID1B, CHD8, PABPC1L, ZNF551, ZNF720, ZFP1, LCORL, ZNF549, ZNF805</i> |
| GO:0032774 | RNA biosynthetic process                 | 0.000704 |   |
| GO:0008589 | regulation of smoothed signaling pathway | 0.000747 | <i>SERpine, RFX4, SMO, SALL3, GORAB, ATP5F1B, CEBPG, CMKLRI, DACHI, DLX2, ELK4, ENOL, HDGF, HSF4, IMPDH2, ITPA, SMAD2, NABI, OCA2, OTXI, PIM1, PPP3CA, PRKCZ, PSMB4, QDPR, TRIM27, RFX4, SFRP5, SMARCA4, SMO, ZNF23, ZNF41, ZNF134, AIP, CTDPL, HAND2, MED20, SAFB2, MED6, CEBPZ, HAX1, ZNF21L, CHEK2, SH2B1, ZNF337, SALL3, GRHL1, MLXIPL, ZNF58L, BCAS3, CHTF8, HEATR1, ARID1B, CHD8, PPCDC, PABPC1L, ZNF551, ZNF720, ZFP1, LCORL, ZNF549, ZNF805</i>   |
| GO:0018130 | heterocycle biosynthetic process         | 0.000804 |   |

|            |   |   |
|------------|---|---|
|            |   | <i>CEBPG, CMKLR1, DACH1, DLX2, ELK4, ENOL, HDGF, HSF4, SMAD2, NABI, OTXI, PIM1, PPP3CA, PRKCZ, PSMB4, TRIM27, RFX4, SFRP5, SMARCA4, SMO, ZNF23, ZNF41, ZNF134, AIP, CTDPI, HAND2, MED20, SAFB2, MED6, CEBPZ, HAX1, ZNF211, CHEK2, ZNF337, SALL3, GRHL1, MLXIPL, ZNF581, BCAS3, HEATRL, ARID1B, CHD8, PABPC1L, ZNF551, ZNF720, ZFP1, LCORL, ZNF549, ZNF805</i> |
| GO:1903506 | regulation of nucleic acid-templated transcription  | 0.00087   |
| GO:2001141 | regulation of RNA biosynthetic process              | 0.000893  |
| GO:1901362 | organic cyclic compound biosynthetic process        | 0.00101   |
| GO:0034654 | nucleobase-containing compound biosynthetic process | 0.001032  |

|            |  |  |
|------------|--|--|
|            |  | <i>HAND2, MED20, SAFB2, MED6, CEBPZ, HAXI, ZNF21I, CHEK2, SH2B1, ZNF337, SALL3, GRHL1, MLXIPL, ZNF58I, BCAS3, CHTF8, HEATR1, ARID1B, CHD8, PPCDC, PABPC1L, ZNF551, ZNF720, ZFP1, LCORL, ZNF549, ZNF805</i>   |
| GO:0006355 | regulation of transcription, DNA-templated |  |
| GO term    | Biological processes                       |  |
|            | P-value                                    |  |
|            | Genes                                      |  |
| 0.001117   | ZNF805                                     | <i>ATP5FB, CEBPG, CMKLRI, DACHI, DLX2, ELK4, ENOL, HDGF, HSF4, SMAD2, NABI, OTXI, PIM1, PPP3CA, PRKCZ, PSMB4, QDPR, TRIM27, RFX4, SFRP5, SMARCA4, SMO, ZNF23, ZNF41, ZNF134, AIP, CTDP1, HAND2, MED20, SAFB2, MED6, CEBPZ, HAXI, ZNF21I, CHEK2, SH2B1, ZNF337, SALL3, GRHL1, MLXIPL, ZNF58I, BCAS3, CHTF8, HEATR1, ARID1B, CHD8, PPCDC, PABPC1L, ZNF551, ZNF720, ZFP1, LCORL, ZNF806</i> |
| GO:0019438 | aromatic compound biosynthetic process     |  |
|            | P-value                                    |  |
| 0.001203   |  | <i>CEBPG, CMKLRI, DACHI, DLX2, ELK4, ENOL, HDGF, HSF4, SMAD2, NABI, OTXI, PIM1, PPP3CA, PRKCZ, PSMB4, TRIM27, RFX4, SFRP5, SMARCA4, SMO, ZNF23, ZNF41, ZNF134, AIP, CTDP1, HAND2, MED20, SAFB2, MED6, CEBPZ, HAXI, ZNF21I, CHEK2, SH2B1, ZNF337, SALL3, GRHL1, MLXIPL, ZNF58I, BCAS3, CHTF8, HEATR1, ARID1B, CHD8, PPCDC, PABPC1L, ZNF551, ZNF720, ZFP1, LCORL, ZNF806</i>               |
| GO:0032774 | RNA biosynthetic process                   |  |

*ZNF551*, *ZNF720*, *ZFPI*, *LCORL*, *ZNF549*,  
*ZNF806*

|            |  |          |  |
|------------|--|----------|--|
| GO:0008589 | regulation of smoothened signaling pathway         | 0.001345 | SERPINE, RFX4, SMO, <i>SALL3</i> , <i>GORAB</i> , <i>ATP5F1B</i> , <i>CEBPG</i> , <i>CMLK1</i> , <i>DACHI</i> , <i>DLX2</i> , <i>ELK4</i> , <i>ENOL</i> , <i>HDGF</i> , <i>HSF4</i> , <i>IMPDH2</i> , <i>ITPA</i> , <i>SMAD2</i> , <i>NABI</i> , <i>OCA2</i> , <i>OTXI</i> , <i>PIM1</i> , <i>PPP3CA</i> , <i>PRKCZ</i> , <i>PSMB4</i> , <i>QDPR</i> , <i>TRIM27</i> , <i>RFX4</i> , <i>SFRP5</i> , <i>SMARCA4</i> , <i>SMO</i> , <i>ZNF23</i> , <i>ZNF41</i> , <i>ZNF134</i> , <i>AIP</i> , <i>CTDPI</i> , <i>HAND2</i> , <i>MED20</i> , <i>SAFB2</i> , <i>MED6</i> , <i>CEBPZ</i> , <i>HAX1</i> , <i>ZNF211</i> , <i>CHEK2</i> , <i>SH2B1</i> , <i>ZNF337</i> , <i>SALL3</i> , <i>GRHL1</i> , <i>MLXIPL</i> , <i>ZNF581</i> , <i>BCAS3</i> , <i>CHTF8</i> , <i>HEATR1</i> , <i>ARID1B</i> , <i>CHD8</i> , <i>PPCDC</i> , <i>PABPC1L</i> , <i>ZNF551</i> , <i>ZNF720</i> , <i>ZFPI</i> , <i>LCORL</i> , <i>ZNF549</i> , <i>ZNF806</i> |
| GO:0018130 | heterocycle biosynthetic process                   | 0.001416 | <i>CEBPG</i> , <i>CMKL1</i> , <i>DACHI</i> , <i>DLX2</i> , <i>ELK4</i> , <i>ENOL</i> , <i>HDGF</i> , <i>HSF4</i> , <i>SMAD2</i> , <i>NABI</i> , <i>OTXI</i> , <i>PIM1</i> , <i>PPP3CA</i> , <i>PRKCZ</i> , <i>PSMB4</i> , <i>TRIM27</i> , <i>RFX4</i> , <i>SFRP5</i> , <i>SMARCA4</i> , <i>SMO</i> , <i>ZNF23</i> , <i>ZNF41</i> , <i>ZNF134</i> , <i>AIP</i> , <i>CTDPI</i> , <i>HAND2</i> , <i>MED20</i> , <i>SAFB2</i> , <i>MED6</i> , <i>CEBPZ</i> , <i>HAX1</i> , <i>ZNF211</i> , <i>CHEK2</i> , <i>ZNF337</i> , <i>SALL3</i> , <i>GRHL1</i> , <i>MLXIPL</i> , <i>ZNF581</i> , <i>BCAS3</i> , <i>HEATR1</i> , <i>ARID1B</i> , <i>CHD8</i> , <i>PABPC1L</i> , <i>ZNF551</i> , <i>ZNF720</i> , <i>ZFPI</i> , <i>LCORL</i> , <i>ZNF549</i> , <i>ZNF805</i>   |
| GO:1903506 | regulation of nucleic acid-templated transcription | 0.001487 | <i>ZNF805</i>  |

|            |  |          |   |
|------------|--|----------|---|
|            |  |          | <i>CEBPG, CMKLRI, DACH1, DLX2, ELK4, ENOL, HDGF, HSF4, SMAD2, NABL, OTXI, PIMI, PPP3CA, PRKCZ, PSMB4, TRIM27, RFX4, SFRP5, SMARCA4, SMO, ZNF23, ZNF41, ZNF134, AIP, CTDPI, HAND2, MED20, SAFB2, MED6, CEBPZ, HAX1, ZNF211, CHEK2, ZNF337, SALL3, GRHL1, MLXIPL, ZNF581, BCAS3, HEATRL, ARID1B, CHD8, PABPC1L, ZNF551, ZNF720, ZFPI, LCORL, ZNF549, ZNF805</i>   |
| GO:0001141 | regulation of RNA biosynthetic process   | 0.001558 | Genes   |
| GO term    | Biological processes                     | P-value  |   |
|            |  |          | <i>ATP5F1B, CEBPG, CMKLRI, DACH1, DLX2, ELK4, ENOL, HDGF, HSF4, IMPDH2, ITPA, SMAD2, NABI, OCA2, OTXI, PIMI, PPP3CA, PRKCZ, PSMB4, QDPR, TRIM27, RFX4, SFRP5, SMARCA4, SMO, ZNF23, ZNF41, ZNF134, AIP, CTDPI, HAND2, MED20, SAFB2, MED6, CEBPZ, HAX1, ZNF211, CHEK2, SH2B1, ZNF337, SALL3, GRHL1, MLXIPL, ZNF581, BCAS3, CHTF8, HEATRL, ARID1B, CHD8, PPCDC, PABPC1L, ZNF551, ZNF720, ZFPI, LCORL, ZNF549, ZNF806</i> |
| GO:0019438 | aromatic compound biosynthetic process   | 0.001203 |   |
|            |  |          | <i>CEBPG, CMKLRI, DACH1, DLX2, ELK4, ENOL, HDGF, HSF4, SMAD2, NABL, OTXI, PIMI, PPP3CA, PRKCZ, PSMB4, TRIM27, RFX4, SFRP5, SMARCA4, SMO, ZNF23, ZNF41, ZNF134, AIP, CTDPI, HAND2, MED20, SAFB2, MED6, CEBPZ, HAX1, ZNF211, CHEK2, ZNF337, SALL3, GRHL1, MLXIPL, ZNF581, BCAS3, HEATRL, ARID1B, CHD8, PABPC1L, ZNF551, ZNF720, ZFPI, LCORL, ZNF549, ZNF806</i>   |
| GO:0032774 | RNA biosynthetic process                 | 0.001274 |   |
| GO:0008589 | regulation of smoothed signaling pathway | 0.001345 | <i>SERpine, RFX4, SMO, SALL3, GORAB</i>   |

*ATP5F1B, CEBPG, CMKLR1, DACH1, DLX2, ELK4, ENO1, HDGF, HSF4, IMPDH2, ITPA, SMAD2, NABI, OCA2, OTX1, PIM1, PPP3CA, PRKCCZ, PSMB4, QDPR, TRM27, RFX4, SFRP5, SMARCA4, SIMO, ZNF23, ZNF41, ZNF134, AIP, CTDP1, HAND2, MED20, SAFB2, MED6, CEBPZ, HAX1, ZNF211, CHEK2, SH2B1, ZNF337, SALL3, GRHL1, MLXIPL, ZNF581, BCAS3, CHTF8, HEATR1, ARID1B, CHD8, PPCDC, PABPC1L, ZNF551, ZNF720, ZFPI, LCORL, ZNF549, ZNF806*

GO:0018130 heterocycle biosynthetic process

Note: CpGs mapped to genes in bold font showed consistent associations (interaction or main effects) between two cohorts.

Supplement Table S4 (A): Association of DNAM at 10 years in males with neighboring gene expression at 26 years (n=55)

| coefficient | Pvalue   | CpGs       | Genes         |
|-------------|----------|------------|---------------|
| 1           | 0        | cg01884526 | <i>A2M</i>    |
| 0.574357    | 0.000603 | cg06684259 | <i>ACAA2</i>  |
| 0.52864     | 0.000603 | cg09852187 | <i>ABCD3</i>  |
| 0.673389    | 0.001496 | cg06684259 | <i>ACP2</i>   |
| 0.417462    | 0.002771 | cg08354614 | <i>CPM</i>    |
| 0.266446    | 0.00353  | cg12009697 | <i>ABAT</i>   |
| 0.533883    | 0.00372  | cg08056069 | <i>ACOT8</i>  |
| 0.266522    | 0.0069   | cg14056357 | <i>ABCG2</i>  |
| 0.397577    | 0.007577 | cg14056357 | <i>ISG20</i>  |
| -0.58998    | 0.012191 | cg10996201 | <i>ELOVL4</i> |
| 0.248885    | 0.012797 | cg14056357 | <i>AEN</i>    |
| 0.697283    | 0.012797 | cg14893576 | <i>ACSS2</i>  |
| 0.117351    | 0.012923 | cg21691089 | <i>TRPS1</i>  |
| -0.42789    | 0.01339  | cg19707069 | <i>VNIRI</i>  |
| -0.7264     | 0.016615 | cg19707069 | <i>ZNF776</i> |
| -0.59436    | 0.018257 | cg08354614 | <i>CORO2B</i> |
| 0.311837    | 0.020645 | cg14056357 | <i>ACSF3</i>  |
| -0.43218    | 0.026245 | cg19707069 | <i>MMP15</i>  |

|                 |                 |                   |              |
|-----------------|-----------------|-------------------|--------------|
| 0.795243        | 0.027506        | cg19707069        | ZNF552       |
| -0.63205        | 0.030349        | cg06684259        | CDK16        |
| 0.230713        | 0.030425        | cg27230711        | RAMP3        |
| -0.60773        | 0.030815        | cg06684259        | CELSRI       |
| -0.50637        | 0.032182        | cg15778400        | IRSI         |
| 0.203504        | 0.036249        | cg19707069        | AGAP2        |
| 0.450854        | 0.036863        | cg10996201        | ANTXR2       |
| -0.41133        | 0.040424        | cg27593384        | PPP1R3E      |
| 0.404555        | 0.043048        | cg06684259        | TTC7A        |
| -0.70604        | 0.044696        | cg19707069        | ZNF550       |
| <b>-0.55431</b> | <b>0.049689</b> | <b>cg06684259</b> | <b>USP11</b> |

Supplement Table S4 (B): Association of DNAM at 10 years in females with neighboring gene expression at 26 years (n=85)

coefficient Pvalue CpGs Genes

|          |          |            |                |
|----------|----------|------------|----------------|
| 1        | 0        | cg18593717 | <i>AGPAT3</i>  |
| 0.888376 | 1.24E-10 | cg25518386 | <i>AKAP10</i>  |
| 0.300261 | 5.14E-10 | cg26791126 | <i>AIM1</i>    |
| 0.751707 | 5.64E-10 | cg24173551 | <i>ALKBH5</i>  |
| 0.839157 | 1.31E-09 | cg06060137 | <i>ACE</i>     |
| 0.873602 | 2.27E-09 | cg25156443 | <i>ACVRLI</i>  |
| 1.13045  | 5.53E-09 | cg06302857 | <i>AGAP2</i>   |
| 2.361207 | 2.25E-08 | cg23892580 | <i>ABCC13</i>  |
| 0.413501 | 3.67E-08 | cg12210286 | <i>AHRR</i>    |
| 2.299555 | 4.43E-08 | cg23892580 | <i>AGMAT</i>   |
| 0.504819 | 1.78E-07 | cg27116888 | <i>ACER3</i>   |
| 0.241357 | 2.33E-07 | cg07938869 | <i>WBSCR27</i> |
| 0.201176 | 4.79E-07 | cg23292453 | <i>AACS</i>    |
| 0.798827 | 8.28E-07 | cg25156443 | <i>ABHD14A</i> |
| 0.471668 | 8.61E-07 | cg06075477 | <i>AARS</i>    |
| 0.541115 | 1.63E-06 | cg08092965 | <i>ACSF2</i>   |
| -0.46654 | 1.81E-06 | cg04535371 | <i>AKR7A2</i>  |

|          |          |            |                |
|----------|----------|------------|----------------|
| -0.72349 | 2.23E-06 | cg14632002 | <i>ABC49</i>   |
| 0.82532  | 7.86E-06 | cg21278285 | <i>AIF1L</i>   |
| 1.415142 | 8.13E-06 | cg21278285 | <i>AKRIBI</i>  |
| 0.236382 | 8.69E-06 | cg06060137 | <i>AHS42</i>   |
| 1.294485 | 1.15E-05 | cg01943657 | <i>ABHD3</i>   |
| 0.609914 | 1.23E-05 | cg11190854 | <i>ADA</i>     |
| 0.520721 | 2.69E-05 | cg10850197 | <i>ADA</i>     |
| 0.906162 | 2.99E-05 | cg07862535 | <i>AHCY</i>    |
| 0.859667 | 3.07E-05 | cg20690303 | <i>ALKBH5</i>  |
| 0.492038 | 3.64E-05 | cg11190854 | <i>ACKR2</i>   |
| 0.340205 | 5.01E-05 | cg10706910 | <i>ACTR5</i>   |
| 0.088196 | 7.88E-05 | cg11252776 | <i>GPRC5C</i>  |
| 0.25099  | 8.53E-05 | cg27116888 | <i>WDR41</i>   |
| -0.31279 | 9.27E-05 | cg24167975 | <i>AAED1</i>   |
| 0.370447 | 0.000116 | cg10850197 | <i>AMBRA1</i>  |
| 0.703841 | 0.00013  | cg14311471 | <i>ADAL</i>    |
| 0.376625 | 0.000162 | cg22153463 | <i>MSH6</i>    |
| 1.160843 | 0.000184 | cg19445996 | <i>ADAMI9</i>  |
| 2.072194 | 0.000218 | cg02619805 | <i>ADAR</i>    |
| 0.341148 | 0.000294 | cg11190854 | <i>ADAMI1</i>  |
| 0.884396 | 0.000328 | cg06226335 | <i>ACTB</i>    |
| 0.308443 | 0.000509 | cg07862535 | <i>HDAC1</i>   |
| 1.303444 | 0.000687 | cg14632002 | <i>ABCA10</i>  |
| 0.211341 | 0.000712 | cg11252776 | <i>NAPIL2</i>  |
| 0.693113 | 0.000804 | cg18233595 | <i>ABHD6</i>   |
| 0.047971 | 0.000943 | cg07938869 | <i>SFXN5</i>   |
| 0.648877 | 0.000953 | cg16570995 | <i>AIFI</i>    |
| 0.252745 | 0.001    | cg02516257 | <i>RINL</i>    |
| 0.208035 | 0.001025 | cg11345323 | <i>DUSP4</i>   |
| 0.286072 | 0.001072 | cg14311471 | <i>SLC24A1</i> |
| 0.90579  | 0.001279 | cg06302857 | <i>ABHD6</i>   |

|          |          |            |                |
|----------|----------|------------|----------------|
| 0.198105 | 0.001319 | cg22153463 | <i>TEC</i>     |
| 0.119485 | 0.001438 | cg11345323 | <i>GOLG48M</i> |
| 0.108483 | 0.00155  | cg07862535 | <i>FRY</i>     |
| 0.181572 | 0.001705 | cg11345323 | <i>SNX29P2</i> |
| 0.148416 | 0.001761 | cg23292453 | <i>CPXM2</i>   |
| 0.106252 | 0.001798 | cg02516257 | <i>IDO2</i>    |
| 0.157721 | 0.001809 | cg11252776 | <i>POMI2I</i>  |
| 0.335936 | 0.001906 | cg23892580 | <i>HACLI</i>   |
| 0.608771 | 0.001994 | cg14445451 | <i>NPIP8</i>   |
| 0.301212 | 0.002129 | cg22153463 | <i>TXK</i>     |
| 0.185306 | 0.002142 | cg02516257 | <i>SYNGR1</i>  |
| 0.464686 | 0.002169 | cg09822824 | <i>ADCY6</i>   |
| 0.28933  | 0.002182 | cg14445451 | <i>GOLG48M</i> |
| 0.217725 | 0.00232  | cg17015511 | <i>UBE2S</i>   |
| 1.113797 | 0.002549 | cg23892580 | <i>ADORA2B</i> |
| 1.009593 | 0.002617 | cg14632002 | <i>AAGAB</i>   |
| -0.304   | 0.002695 | cg23080241 | <i>MYLK3</i>   |
| 0.21046  | 0.003009 | cg22153463 | <i>FOXD2</i>   |
| 0.093079 | 0.00308  | cg11345323 | <i>FLT1</i>    |
| 0.097257 | 0.003171 | cg11190854 | <i>NIM1K</i>   |
| -0.461   | 0.003209 | cg04535371 | <i>AKR7A3</i>  |
| 0.982721 | 0.003293 | cg14632002 | <i>ADHFE1</i>  |
| 0.09392  | 0.003303 | cg18233595 | <i>CDK4</i>    |
| 0.118872 | 0.003399 | cg11345323 | <i>RABEP2</i>  |
| 0.511332 | 0.003584 | cg20000099 | <i>MRPS14</i>  |
| 0.491325 | 0.003712 | cg14632002 | <i>ABC45</i>   |
| 0.186914 | 0.003803 | cg07588308 | <i>ARF5</i>    |
| 0.117059 | 0.003885 | cg24483825 | <i>KSRI</i>    |
| -1.03374 | 0.003967 | cg04535371 | <i>AKAP10</i>  |
| 0.555959 | 0.003986 | cg09646206 | <i>ADAMTS1</i> |
| 0.139283 | 0.004017 | cg10850197 | <i>SIX5</i>    |

|          |          |            |                |
|----------|----------|------------|----------------|
| 0.406413 | 0.004197 | cg14445451 | <i>FOSL2</i>   |
| 1.384777 | 0.004331 | cg14632002 | <i>ALDH3B2</i> |
| 0.445959 | 0.004403 | cg14445451 | <i>CCDC91</i>  |
| 0.345893 | 0.004436 | cg14445451 | <i>TBC1D29</i> |
| 0.201845 | 0.004626 | cg07862535 | <i>TMEM39B</i> |
| 0.383383 | 0.004954 | cg23892580 | <i>C45BPI</i>  |
| 0.254905 | 0.004969 | cg08487579 | <i>MEPCE</i>   |
| 0.157746 | 0.005062 | cg07588308 | <i>FSCN3</i>   |
| 0.204396 | 0.005281 | cg10729426 | <i>PDE4D</i>   |
| 0.101371 | 0.005432 | cg11844198 | <i>TMEM232</i> |
| 0.359739 | 0.00562  | cg02516257 | <i>MGAT3</i>   |
| 0.144734 | 0.005636 | cg06226335 | <i>CD274</i>   |
| 0.064974 | 0.005768 | cg09822824 | <i>GRWDI</i>   |
| 0.174955 | 0.005776 | cg07862535 | <i>TOPORS</i>  |
| 0.309503 | 0.005987 | cg10729426 | <i>DACT1</i>   |
| 0.232715 | 0.006084 | cg11252776 | <i>ATG16L2</i> |
| 1.337492 | 0.006164 | cg23080241 | <i>ALS2CL</i>  |
| 0.275666 | 0.006423 | cg11345323 | <i>ADAP2</i>   |
| 0.65345  | 0.006622 | cg08487579 | <i>AGFG2</i>   |
| 0.211885 | 0.006667 | cg22944932 | <i>PDIA6</i>   |
| 0.16493  | 0.00701  | cg06060137 | <i>FADSI</i>   |
| 0.179453 | 0.007129 | cg11252776 | <i>FZD9</i>    |
| 0.153677 | 0.007242 | cg08092965 | <i>PTPRJ</i>   |
| 0.219345 | 0.007584 | cg07862535 | <i>PRRG4</i>   |
| 0.095669 | 0.007783 | cg11190854 | <i>DCAKD</i>   |
| 0.214516 | 0.007824 | cg22944932 | <i>TMEDI</i>   |
| 0.488059 | 0.007986 | cg14445451 | <i>CREB5</i>   |
| -0.33983 | 0.007992 | cg25518386 | <i>ZNF486</i>  |
| 0.075498 | 0.008149 | cg24483825 | <i>NINL</i>    |
| -0.11709 | 0.008162 | cg02467794 | <i>NPW</i>     |
| 0.1244   | 0.008215 | cg06060137 | <i>DIDO1</i>   |

|          |          |            |                |
|----------|----------|------------|----------------|
| 0.134268 | 0.008446 | cg07588308 | <i>NR5A1</i>   |
| 0.064015 | 0.008466 | cg26693529 | <i>CDK4</i>    |
| 0.200741 | 0.009018 | cg27116888 | <i>USP36</i>   |
| 0.17143  | 0.009109 | cg22153463 | <i>NFXL1</i>   |
| 0.120691 | 0.009175 | cg17226280 | <i>TSPAN15</i> |
| 0.138499 | 0.009215 | cg24483825 | <i>STXBP6</i>  |
| 0.19066  | 0.00943  | cg20361600 | <i>CAMKID</i>  |
| 0.118233 | 0.009512 | cg24483825 | <i>UBE3A</i>   |
| 0.127302 | 0.009838 | cg11252776 | <i>FCHSD2</i>  |
| 0.35321  | 0.009941 | cg22153463 | <i>ZNF589</i>  |
| 0.261091 | 0.01027  | cg23892580 | <i>CD38</i>    |
| 0.165408 | 0.010228 | cg09484638 | <i>C8orf76</i> |
| 0.432855 | 0.010269 | cg18233595 | <i>AGAP2</i>   |
| 0.562242 | 0.010276 | cg14445451 | <i>YTHDF2</i>  |
| 0.068661 | 0.010437 | cg06075477 | <i>MXD1</i>    |
| 0.348048 | 0.010508 | cg14445451 | <i>DSG2</i>    |
| -0.2666  | 0.010599 | cg14445451 | <i>CPD</i>     |
| 0.132616 | 0.010677 | cg13118906 | <i>UBAP2L</i>  |
| 0.261382 | 0.011236 | cg14445451 | <i>RABEP2</i>  |
| 0.081197 | 0.011259 | cg06060137 | <i>CHD7</i>    |
| 0.771824 | 0.011868 | cg01943657 | <i>ACER2</i>   |
| 0.167747 | 0.012137 | cg02516257 | <i>D4AM2</i>   |
| 0.172042 | 0.012161 | cg22153463 | <i>SAMD14</i>  |
| 0.230787 | 0.012285 | cg13063405 | <i>RORA</i>    |
| 0.255171 | 0.012446 | cg14311471 | <i>PSTPIP2</i> |
| 0.105338 | 0.012743 | cg24483825 | <i>SMM20</i>   |
| 0.414708 | 0.012748 | cg08487579 | <i>ADH5</i>    |
| 0.108698 | 0.012813 | cg15278646 | <i>DGAT1</i>   |
| 0.146354 | 0.012913 | cg11844198 | <i>SYPL2</i>   |
| 0.201808 | 0.012988 | cg11345323 | <i>CDI9</i>    |
| 1.415696 | 0.013211 | cg19078236 | <i>ALPK3</i>   |

|          |          |            |                |
|----------|----------|------------|----------------|
| 0.308108 | 0.013217 | cg10729426 | <i>TRIM28</i>  |
| 0.477289 | 0.013491 | cg16570995 | <i>AHSP</i>    |
| -0.07232 | 0.013606 | cg26693529 | <i>KATNB1</i>  |
| 0.306907 | 0.013813 | cg06060137 | <i>FADS2</i>   |
| 0.193982 | 0.013861 | cg17027046 | <i>UNC5B</i>   |
| 0.097766 | 0.013873 | cg11190854 | <i>PTCRA</i>   |
| 0.262559 | 0.013992 | cg14445451 | <i>SULT1A1</i> |
| 0.120031 | 0.014409 | cg20690303 | <i>TBC1D5</i>  |
| 0.1334   | 0.014485 | cg07588308 | <i>PRRC1</i>   |
| 0.090816 | 0.014543 | cg09484638 | <i>ATAD2</i>   |
| 0.146585 | 0.014627 | cg07862535 | <i>SUBLI</i>   |
| 0.091332 | 0.014653 | cg11439068 | <i>ANKIB1</i>  |
| 0.117631 | 0.014678 | cg02516257 | <i>SMM14</i>   |
| -0.30739 | 0.01486  | cg23080241 | <i>ARHGAP1</i> |
| 0.425008 | 0.015032 | cg14445451 | <i>TUFM</i>    |
| 0.238878 | 0.015329 | cg07862535 | <i>C14orf1</i> |
| 0.130402 | 0.016059 | cg16878007 | <i>CAMSAPI</i> |
| 0.127401 | 0.016448 | cg11345323 | <i>TRIM27</i>  |
| 0.181908 | 0.016487 | cg09484638 | <i>KALLRN</i>  |
| 0.261328 | 0.016539 | cg18593717 | <i>FAM118A</i> |
| -0.05506 | 0.016588 | cg22944932 | <i>TDH</i>     |
| 0.073876 | 0.01703  | cg09822824 | <i>KCND1</i>   |
| 0.055871 | 0.017189 | cg09822824 | <i>TFE3</i>    |
| -0.0944  | 0.017231 | cg03223733 | <i>SART3</i>   |
| 0.124885 | 0.017491 | cg09822824 | <i>TMEM143</i> |
| 0.405711 | 0.017501 | cg14632002 | <i>ABC46</i>   |
| 0.10987  | 0.01779  | cg22153463 | <i>HUS1</i>    |
| 0.609012 | 0.017815 | cg25156443 | <i>ACY1</i>    |
| 0.315088 | 0.018045 | cg14445451 | <i>TRM27</i>   |
| 0.166978 | 0.018069 | cg08487579 | <i>MOSPD3</i>  |
| 0.129654 | 0.019052 | cg06060137 | <i>DCAF7</i>   |

|          |          |            |                |
|----------|----------|------------|----------------|
| 0.078161 | 0.019151 | cg02516257 | <i>SEC23A</i>  |
| 0.117782 | 0.019189 | cg11345323 | <i>CHN2</i>    |
| 0.128839 | 0.019413 | cg11252776 | <i>STARD10</i> |
| 0.08526  | 0.019436 | cg20361600 | <i>IQSECI</i>  |
| 0.193252 | 0.019447 | cg22153463 | <i>PDK2</i>    |
| 0.13776  | 0.019525 | cg09484638 | <i>PLEKHA1</i> |
| 0.139026 | 0.019561 | cg11190854 | <i>AKAP11</i>  |
| 0.068892 | 0.019567 | cg16878007 | <i>MRPS22</i>  |
| 0.074482 | 0.019882 | cg07938869 | <i>FCHSD2</i>  |
| 0.07278  | 0.019962 | cg24483825 | <i>TOP2B</i>   |
| 0.148083 | 0.020036 | cg13063405 | <i>TAF4</i>    |
| 0.11141  | 0.020149 | cg02516257 | <i>LRFNI</i>   |
| 0.06483  | 0.020342 | cg09822824 | <i>PPP1R3F</i> |
| 0.082667 | 0.020355 | cg11252776 | <i>MSC</i>     |
| 0.370583 | 0.020575 | cg14445451 | <i>PAN3</i>    |
| 0.114661 | 0.020627 | cg02516257 | <i>PROSER1</i> |
| 0.162122 | 0.020746 | cg11252776 | <i>TRIM50</i>  |
| 0.164265 | 0.020758 | cg09484638 | <i>TMED2</i>   |
| 0.135721 | 0.021347 | cg13063405 | <i>PHLPPI</i>  |
| 0.332998 | 0.021397 | cg14445451 | <i>RRN3P2</i>  |
| -0.10097 | 0.021702 | cg17226280 | <i>ENAM</i>    |
| -0.08553 | 0.021756 | cg26791126 | <i>PRKAR2B</i> |
| 0.18429  | 0.02189  | cg11345323 | <i>WAC</i>     |
| -0.09223 | 0.021967 | cg08487579 | <i>TFR2</i>    |
| 0.12065  | 0.022173 | cg20361600 | <i>GPRC5D</i>  |
| 0.576207 | 0.022292 | cg16570995 | <i>H3F3C</i>   |
| 0.322268 | 0.022435 | cg22626041 | <i>PEAK1</i>   |
| 0.076311 | 0.022677 | cg11252776 | <i>RYBP</i>    |
| 0.127784 | 0.022684 | cg20690303 | <i>ARRDC2</i>  |
| 0.074269 | 0.022826 | cg15278646 | <i>CYHRI</i>   |
| 0.19467  | 0.023022 | cg22153463 | <i>PTPRJ</i>   |

|          |          |            |                |
|----------|----------|------------|----------------|
| 0.07395  | 0.023044 | cg11844198 | <i>AMIGO1</i>  |
| 0.000606 | 0.023493 | cg00705668 | <i>KIF18B</i>  |
| 0.319929 | 0.023997 | cg09646206 | <i>ZKSCAN3</i> |
| 0.099319 | 0.02406  | cg17015511 | <i>SHISA7</i>  |
| -0.87798 | 0.024061 | cg03655771 | <i>ADAM20</i>  |
| 0.311103 | 0.024225 | cg10729426 | <i>PPMID</i>   |
| 0.211358 | 0.024461 | cg08092965 | <i>ZNF589</i>  |
| -0.17288 | 0.02471  | cg05245655 | <i>HOXC4</i>   |
| 0.165381 | 0.024764 | cg22153463 | <i>TMEM92</i>  |
| 0.080166 | 0.024854 | cg10850197 | <i>EML2</i>    |
| 0.082313 | 0.02508  | cg09484638 | <i>RAB14</i>   |
| 0.071777 | 0.025104 | cg27116888 | <i>SDADI</i>   |
| 0.064434 | 0.025164 | cg27116888 | <i>CCDC146</i> |
| 0.404341 | 0.025482 | cg18593717 | <i>NKPD1</i>   |
| 0.365921 | 0.025759 | cg14445451 | <i>EIF3C</i>   |
| -0.06281 | 0.026099 | cg17572791 | <i>NUP153</i>  |
| 0.265815 | 0.026231 | cg26290114 | <i>ZKSCAN3</i> |
| 0.377603 | 0.026967 | cg14445451 | <i>BAMBI</i>   |
| 0.250816 | 0.027274 | cg22153463 | <i>SLC48A1</i> |
| 0.139707 | 0.027471 | cg07862535 | <i>AVL9</i>    |
| 0.075356 | 0.027557 | cg06060137 | <i>LIMD2</i>   |
| 0.264642 | 0.027658 | cg19078236 | <i>GSE1</i>    |
| -0.1367  | 0.027772 | cg13337238 | <i>NFKBIA</i>  |
| 0.062848 | 0.027969 | cg18233595 | <i>CSNK2A2</i> |
| 0.082893 | 0.02798  | cg16878007 | <i>QSOX2</i>   |
| 0.106878 | 0.02799  | cg11252776 | <i>TMEM104</i> |
| -0.17001 | 0.028384 | cg03719634 | <i>TNRC6B</i>  |
| 0.105043 | 0.028537 | cg22153463 | <i>PPP1R9B</i> |
| 0.082317 | 0.028628 | cg18233595 | <i>DABI</i>    |
| 0.154478 | 0.028823 | cg08487579 | <i>TSC22D4</i> |
| 0.518484 | 0.029029 | cg21278285 | <i>FAMI27C</i> |

|          |          |            |                |
|----------|----------|------------|----------------|
| 0.076066 | 0.029144 | cg13063405 | <i>METTL2A</i> |
| 0.147189 | 0.02959  | cg06060137 | <i>USP34</i>   |
| 0.086846 | 0.029817 | cg08092965 | <i>GDF10</i>   |
| 0.057646 | 0.030046 | cg06075477 | <i>PPFIA1</i>  |
| 0.088114 | 0.030109 | cg11439068 | <i>CKS2</i>    |
| 0.446086 | 0.03022  | cg18593717 | <i>ICOSLG</i>  |
| 0.231993 | 0.030388 | cg16570995 | <i>ZBTB12</i>  |
| 0.231612 | 0.030407 | cg20690303 | <i>CECRI</i>   |
| 0.055203 | 0.030417 | cg20361600 | <i>HEBPI</i>   |
| 0.114795 | 0.030751 | cg10850197 | <i>COG3</i>    |
| 0.141882 | 0.030824 | cg11844198 | <i>GPR61</i>   |
| 0.060141 | 0.031011 | cg09822824 | <i>EMP3</i>    |
| 0.154599 | 0.031172 | cg07862535 | <i>EIF3I</i>   |
| 0.213865 | 0.032142 | cg20690303 | <i>SAAL1</i>   |
| 0.197654 | 0.032843 | cg22153463 | <i>PKDILL</i>  |
| 0.276256 | 0.032889 | cg20690303 | <i>SERGEF</i>  |
| 0.078173 | 0.03292  | cg08092965 | <i>ELAC1</i>   |
| 0.286654 | 0.033156 | cg22626041 | <i>CLN5</i>    |
| -0.31037 | 0.03362  | cg23080241 | <i>PNMALL2</i> |
| 0.027641 | 0.033646 | cg20361600 | <i>GPRI9</i>   |
| 0.132506 | 0.033789 | cg10729426 | <i>MYSM1</i>   |
| 0.160547 | 0.033862 | cg22153463 | <i>CAMP</i>    |
| 0.06543  | 0.03394  | cg11190854 | <i>STARD9</i>  |
| 0.355703 | 0.034437 | cg10729426 | <i>ZNF324B</i> |
| 0.161221 | 0.034531 | cg11252776 | <i>NCF1B</i>   |
| 0.088712 | 0.034584 | cg06060137 | <i>FTH1</i>    |
| 0.278832 | 0.034593 | cg20690303 | <i>LLGL1</i>   |
| 0.053228 | 0.036078 | cg11190854 | <i>RRP7A</i>   |
| 0.067995 | 0.036689 | cg21851386 | <i>RPL22L1</i> |
| 0.205205 | 0.036813 | cg08487579 | <i>CSTF2</i>   |
| -0.05727 | 0.03702  | cg06731192 | <i>MTMR6</i>   |

|          |          |            |         |
|----------|----------|------------|---------|
| 0.115821 | 0.037107 | cg26693529 | ZNF549  |
| 0.174823 | 0.037446 | cg08092965 | WAS     |
| 0.127648 | 0.037691 | cg09822824 | WFIKKN2 |
| 0.153353 | 0.037816 | cg20690303 | DRG2    |
| 0.205641 | 0.03783  | cg07862535 | GOLG48O |
| 0.042465 | 0.038065 | cg18716861 | SPC25   |
| 0.094512 | 0.038495 | cg11252776 | HEXA    |
| 0.192174 | 0.039046 | cg25518386 | TXNRD2  |
| 0.057479 | 0.039057 | cg09822824 | LMTK3   |
| 0.100064 | 0.039366 | cg20361600 | NFIX    |
| 0.153814 | 0.039677 | cg11252776 | ANKR42  |
| 0.082017 | 0.039879 | cg18233595 | HEATR6  |
| 0.186668 | 0.040281 | cg26693529 | ZNF319  |
| 0.118191 | 0.040788 | cg13063405 | PPM1A   |
| 0.509216 | 0.041199 | cg26290114 | ADAMTS5 |
| 0.554445 | 0.041302 | cg07862535 | AKAP6   |
| 0.128896 | 0.041398 | cg20690303 | B3GNT3  |
| 0.096139 | 0.041537 | cg09646206 | APOBR   |
| 0.066683 | 0.041944 | cg24483825 | TMEM57  |
| -0.07588 | 0.042029 | cg03223733 | FICD    |
| 0.104908 | 0.042173 | cg13063405 | PTGDR2  |
| 0.044404 | 0.042294 | cg18233595 | PXK     |
| 0.140154 | 0.042447 | cg09484638 | DAB2IP  |
| 0.111836 | 0.042461 | cg11345323 | DSG2    |
| 0.125699 | 0.042981 | cg06075477 | SNXL2   |
| 0.052137 | 0.043438 | cg07938869 | JPX     |
| 0.090521 | 0.043624 | cg15278646 | NBPF10  |
| 0.269335 | 0.043688 | cg23892580 | EPS8    |
| 0.14122  | 0.043952 | cg07862535 | ITCH    |
| 0.325167 | 0.043979 | cg23892580 | SAMSNI  |
| 0.096451 | 0.044033 | cg16570995 | LY6G6F  |

|          |          |            |                |
|----------|----------|------------|----------------|
| 0.117322 | 0.04436  | cg06060137 | <i>CCDC6</i>   |
| 0.186628 | 0.044531 | cg13337238 | <i>ZMYM4</i>   |
| -0.05566 | 0.04457  | cg09822824 | <i>RPL18</i>   |
| 0.123775 | 0.044692 | cg02467794 | <i>MSRB1</i>   |
| -0.76633 | 0.044829 | cg02067639 | <i>GNPTAB</i>  |
| 0.087099 | 0.044965 | cg08092965 | <i>TEC</i>     |
| 0.279409 | 0.045238 | cg22626041 | <i>RSBN1L</i>  |
| 0.134111 | 0.0455   | cg10706910 | <i>TMEM217</i> |
| 0.0514   | 0.045512 | cg16878007 | <i>SPOPL</i>   |
| 0.00055  | 0.045689 | cg00705668 | <i>BMSI</i>    |
| 0.123414 | 0.046412 | cg24173551 | <i>FAM106A</i> |
| -0.20574 | 0.046787 | cg23080241 | <i>DYM</i>     |
| 0.113827 | 0.04719  | cg14196208 | <i>P42G4P4</i> |
| 0.076352 | 0.047236 | cg11190854 | <i>SLC14A2</i> |
| 0.050291 | 0.047507 | cg16878007 | <i>CLEC2L</i>  |
| -0.06419 | 0.047626 | cg27116888 | <i>CAPN5</i>   |
| 0.196048 | 0.048262 | cg20690303 | <i>BCL2L13</i> |
| 0.078915 | 0.048455 | cg11345323 | <i>TTC28</i>   |
| 0.772067 | 0.04857  | cg14632002 | <i>AIP</i>     |
| -0.04902 | 0.048673 | cg01364172 | <i>CLDN4</i>   |
| 0.049417 | 0.048706 | cg15278646 | <i>POLR3GL</i> |
| 0.119623 | 0.04916  | cg07862535 | <i>NPR3</i>    |
| 0.148547 | 0.049259 | cg20690303 | <i>TPHI</i>    |
| 0.211489 | 0.049323 | cg24167975 | <i>GJC3</i>    |
| 0.178124 | 0.049599 | cg11190854 | <i>ZNF37BP</i> |

Supplement Table S4 (C): Association of DNAM at 18 years in males with neighboring gene expression at 26 years (n=55)

---

| coefficient | Pvalue | CpGs | Genes |
|-------------|--------|------|-------|
|-------------|--------|------|-------|

---

|          |          |            |              |
|----------|----------|------------|--------------|
| 1        | 0        | cg01884526 | <i>A2M</i>   |
| 0.597933 | 2.08E-05 | cg06684259 | <i>ACP2</i>  |
| 0.839567 | 3.40E-05 | cg06684259 | <i>ACAA2</i> |

---

|          |          |            |                |
|----------|----------|------------|----------------|
| 0.477653 | 3.40E-05 | cg09852187 | <i>ABCD3</i>   |
| 0.449276 | 0.000163 | cg14056357 | <i>ACSF3</i>   |
| 0.404666 | 0.000291 | cg12009697 | <i>ABAT</i>    |
| 0.814954 | 0.001791 | cg09852187 | <i>PDK4</i>    |
| 0.392199 | 0.008617 | cg06683328 | <i>BCORL1</i>  |
| 0.475772 | 0.016425 | cg14893576 | <i>HPCA</i>    |
| -0.57357 | 0.017653 | cg06684259 | <i>CALM3</i>   |
| 0.352765 | 0.018762 | cg14893576 | <i>ANKRD27</i> |
| 0.410258 | 0.019077 | cg14893576 | <i>ITCH</i>    |
| 0.656904 | 0.02035  | cg14893576 | <i>AKAP6</i>   |
| -0.71635 | 0.026519 | cg19707069 | <i>ABHD6</i>   |
| -0.38708 | 0.027086 | cg06684259 | <i>GNG8</i>    |
| 1.243804 | 0.027646 | cg08056069 | <i>DNTTIP1</i> |
| -0.63999 | 0.029427 | cg12009697 | <i>ZNF558</i>  |
| 0.71897  | 0.029721 | cg08056069 | <i>ZNF221</i>  |
| 0.318524 | 0.030186 | cg08056069 | <i>ACOT8</i>   |
| 0.398119 | 0.031384 | cg14893576 | <i>RP9</i>     |
| 0.289631 | 0.031447 | cg14893576 | <i>TARS</i>    |
| 0.268749 | 0.031529 | cg08354614 | <i>CPM</i>     |
| 0.407187 | 0.032552 | cg14893576 | <i>NUDT19</i>  |
| 0.466572 | 0.032768 | cg09852187 | <i>IPPK</i>    |
| 0.381913 | 0.041659 | cg08354614 | <i>SLC35E3</i> |
| 0.33788  | 0.044371 | cg14893576 | <i>GSS</i>     |
| 0.217225 | 0.046485 | cg14893576 | <i>CCDC7</i>   |
| -0.44495 | 0.048569 | cg06683328 | <i>GLTID1</i>  |
| 0.208746 | 0.049541 | cg06683328 | <i>HS6ST1</i>  |

Supplement Table S4 (D): Association of DNAm at 18 years in females with neighboring gene expression at 26 years (n=85)

| coefficient | Pvalue   | CpGs       | Genes         |
|-------------|----------|------------|---------------|
| 1           | 0        | cg18593717 | <i>AGPAT3</i> |
| -0.1099     | 0.000225 | cg13063405 | <i>C5</i>     |

|          |          |            |         |
|----------|----------|------------|---------|
| 0.73038  | 0.000317 | cg02516257 | ZHX3    |
| 0.667995 | 0.000697 | cg00907843 | SOS1    |
| -0.10592 | 0.000787 | cg13063405 | MRC2    |
| -0.75004 | 0.001521 | cg04535371 | AKR7A3  |
| -0.35624 | 0.002559 | cg00907843 | MAP4K3  |
| -0.52457 | 0.002589 | cg00907843 | RFC1    |
| -0.06047 | 0.003588 | cg07103819 | ITGA4   |
| 0.297358 | 0.004464 | cg13090731 | CLEC4E  |
| 0.569328 | 0.00448  | cg00907843 | CCR8    |
| -0.4945  | 0.004484 | cg00907843 | DAB2    |
| 0.128192 | 0.00479  | cg06226335 | FBXL18  |
| -0.1207  | 0.005752 | cg01364172 | RELT    |
| 0.127063 | 0.005814 | cg13063405 | CCDC86  |
| 0.164471 | 0.006441 | cg22944932 | CITA    |
| -0.12918 | 0.006803 | cg18233595 | VNIRI   |
| -0.45974 | 0.006828 | cg00907843 | KCNK5   |
| 0.434352 | 0.00742  | cg00907843 | RRAGC   |
| 0.249222 | 0.007558 | cg10880755 | HSP90AA |
| 0.191974 | 0.008024 | cg13063405 | LSM14B  |
| -0.05146 | 0.008957 | cg14196208 | P42G4P4 |
| 0.141952 | 0.010234 | cg16926844 | PRSS3   |
| 0.161717 | 0.011979 | cg15278646 | LIXIL   |
| 0.064039 | 0.012347 | cg22944932 | KANK2   |
| 0.117817 | 0.012401 | cg13063405 | Clorf87 |
| 0.196124 | 0.012522 | cg16926844 | ZSCAN20 |
| 0.106745 | 0.012661 | cg02225897 | POLR2J4 |
| 0.317295 | 0.013324 | cg23292453 | ALG1L   |
| -0.07128 | 0.013947 | cg14632002 | DOC2GP  |
| -0.13769 | 0.01426  | cg20361600 | TMEM40  |
| -0.32867 | 0.014397 | cg00907843 | CBX7    |
| -0.15523 | 0.014576 | cg25156443 | FPR3    |

|           |          |            |                |
|-----------|----------|------------|----------------|
| 0.403932  | 0.014581 | cg03223733 | <i>VAV3</i>    |
| 0.103377  | 0.014662 | cg22153463 | <i>SLAIN2</i>  |
| -0.07573  | 0.014712 | cg26693529 | <i>MMP15</i>   |
| -0.63704  | 0.015586 | cg05898113 | <i>KIR3DL2</i> |
| -0.0474   | 0.015609 | cg14196208 | <i>C5</i>      |
| 0.0633729 | 0.016289 | cg13337238 | <i>ARPP21</i>  |
| 0.093769  | 0.016879 | cg06302857 | <i>CYP27B1</i> |
| 0.382421  | 0.017534 | cg18233595 | <i>ABHD6</i>   |
| 0.060404  | 0.018106 | cg11345323 | <i>DSG3</i>    |
| 0.348638  | 0.018425 | cg17015511 | <i>ALPK2</i>   |
| -0.10376  | 0.018481 | cg23292453 | <i>TMEM65</i>  |
| 0.159577  | 0.019116 | cg21278285 | <i>SLC35B4</i> |
| -0.06643  | 0.019191 | cg14632002 | <i>KCTD19</i>  |
| -0.04984  | 0.019338 | cg14632002 | <i>EXOC3L1</i> |
| -0.36763  | 0.0204   | cg00907843 | <i>KRT36</i>   |
| 0.141686  | 0.020467 | cg06226335 | <i>FARS2</i>   |
| -0.06427  | 0.021495 | cg14311471 | <i>PABPC1L</i> |
| 0.11876   | 0.022624 | cg13063405 | <i>PSMA7</i>   |
| -0.06758  | 0.022836 | cg20004424 | <i>PCGF5</i>   |
| -0.11063  | 0.023231 | cg20004424 | <i>FAM174B</i> |
| -0.12414  | 0.023473 | cg14632002 | <i>ZDHHC1</i>  |
| -0.25622  | 0.023678 | cg07862535 | <i>AHCY</i>    |
| 0.144148  | 0.024605 | cg06226335 | <i>TRM22</i>   |
| 0.079739  | 0.024788 | cg06731192 | <i>LRP5L</i>   |
| -0.07526  | 0.024861 | cg13063405 | <i>TMEM109</i> |
| 0.168992  | 0.025096 | cg14196208 | <i>ADAM19</i>  |
| 0.092431  | 0.0258   | cg09822824 | <i>LAMB2</i>   |
| 0.276644  | 0.026154 | cg02467794 | <i>GABRD</i>   |
| -0.04257  | 0.026649 | cg07862535 | <i>KBTBD2</i>  |
| 0.282605  | 0.026698 | cg10729426 | <i>ZSCAN22</i> |
| 0.265258  | 0.027627 | cg02467794 | <i>T4ACC3</i>  |

|          |          |            |         |
|----------|----------|------------|---------|
| -0.0957  | 0.027751 | cg14632002 | KBTBD8  |
| 0.05973  | 0.027917 | cg22944932 | SPC24   |
| 0.000579 | 0.028178 | cg0705668  | TMEM62  |
| -0.34917 | 0.028366 | cg0907843  | CX3CRI  |
| 0.173283 | 0.028434 | cg22626041 | CIPC    |
| 0.065801 | 0.02963  | cg22944932 | TVP23A  |
| -0.06997 | 0.029705 | cg11190854 | ADAM1   |
| 0.157376 | 0.030261 | cg10850197 | MYOP    |
| 0.059637 | 0.030444 | cg22944932 | TARDBP  |
| 0.237657 | 0.030861 | cg02225897 | ZNF487  |
| -0.24988 | 0.031075 | cg04784251 | MAGEFI  |
| 0.124215 | 0.031756 | cg09822824 | RBI     |
| -0.10846 | 0.031977 | cg18593717 | FKBP3   |
| -0.09946 | 0.032465 | cg26693529 | KIF5A   |
| 0.150788 | 0.033237 | cg16570995 | LY6G6F  |
| -0.07492 | 0.03382  | cg14311471 | C2CD2   |
| 0.146959 | 0.034355 | cg06226335 | EVC     |
| 0.337518 | 0.034435 | cg12210286 | VPS53   |
| 0.171688 | 0.034619 | cg03223733 | NXT2    |
| 0.131316 | 0.03579  | cg15278646 | ITGA10  |
| 0.107918 | 0.036703 | cg14311471 | ERMAP   |
| 0.149858 | 0.037092 | cg09822824 | KCNJ14  |
| -0.07324 | 0.037192 | cg20004424 | SMCO4   |
| -0.08503 | 0.037263 | cg20004424 | EEAI    |
| 0.443    | 0.037641 | cg02067639 | POLR2D  |
| -0.07059 | 0.038317 | cg14632002 | SLC9A5  |
| 0.198418 | 0.03907  | cg21278285 | SMM10   |
| 0.330601 | 0.039285 | cg10880755 | DYNC1HI |
| -0.04002 | 0.039504 | cg26693529 | MARS    |
| -0.08761 | 0.04063  | cg25156443 | MCM3    |
| 0.134894 | 0.041158 | cg18716861 | SEC62   |

|          |          |            |                |
|----------|----------|------------|----------------|
| -0.03786 | 0.04179  | cg26693529 | <i>TUBD1</i>   |
| 0.144014 | 0.041823 | cg10880755 | <i>MOK</i>     |
| 0.095629 | 0.042829 | cg22153463 | <i>LONP2</i>   |
| 0.100274 | 0.043656 | cg13063405 | <i>PHLPP1</i>  |
| 0.056722 | 0.043709 | cg26791126 | <i>CKAP4</i>   |
| 0.323744 | 0.044327 | cg19078236 | <i>ZNF592</i>  |
| 0.053681 | 0.044349 | cg06731192 | <i>BNIP3L</i>  |
| -0.07178 | 0.044603 | cg08092965 | <i>PLXNBI</i>  |
| -0.05759 | 0.044636 | cg18593717 | <i>BTBD19</i>  |
| -0.05312 | 0.044651 | cg26693529 | <i>TSPAN31</i> |
| 0.381758 | 0.045081 | cg02467794 | <i>LSP1</i>    |
| -0.17607 | 0.045187 | cg00907843 | <i>CAPN12</i>  |
| 0.072321 | 0.045349 | cg22944932 | <i>HRH1</i>    |
| 0.123413 | 0.045427 | cg25156443 | <i>TMOD3</i>   |
| 0.256165 | 0.045561 | cg09646206 | <i>XPO6</i>    |
| -0.0974  | 0.046444 | cg25518386 | <i>RTN4R</i>   |
| 0.075735 | 0.046596 | cg11844198 | <i>GPR61</i>   |
| 0.088734 | 0.046637 | cg06226335 | <i>TNRC18</i>  |
| -0.17589 | 0.047397 | cg14311471 | <i>ZNF691</i>  |
| -0.06952 | 0.04749  | cg26693529 | <i>CTDSP2</i>  |
| -0.11971 | 0.048049 | cg20361600 | <i>SPTLC3</i>  |
| 0.067785 | 0.0492   | cg22944932 | <i>STYK1</i>   |

Supplement Table S5(A): Statistically significant GO terms and its biological processes from pathway enrichment analysis in each pathway for males, for the identified CpGs.

| GO term    | Biological Processes                     | N# | Raw p value |
|------------|--|----|-------------|
| GO:0046380 | N-acetylneuraminate biosynthetic process | 1  | 0.0050      |
| GO:0035459 | vesicle cargo loading                    | 22 | 0.0059      |
| GO:0042700 | luteinizing hormone signaling pathway    | 2  | 0.0075      |

|            |   |     |        |
|------------|---|-----|--------|
| GO:0033140 | negative regulation of peptidyl-serine phosphorylation          | 2   | 0.0079 |
| GO:0032462 | regulation of protein homooligomerization                       | 20  | 0.0084 |
| GO:0072665 | protein localization to vacuole                                 | 63  | 0.0086 |
| GO:0006045 | N-acetylglucosamine biosynthetic process                        | 2   | 0.0089 |
| GO:1901073 | glucosamine-containing compound biosynthetic process            | 2   | 0.0089 |
| GO:0044727 | DNA demethylation of male pronucleus                            | 2   | 0.0094 |
| GO:1903895 | negative regulation of IRE1-mediated unfolded protein response  | 3   | 0.0098 |
| GO:0060749 | mammary gland alveolus development                              | 18  | 0.0102 |
| GO:0061377 | mammary gland lobule development                                | 18  | 0.0102 |
| GO:0014822 | detection of wounding   | 1   | 0.0117 |
| GO:0048567 | ectodermal digestive tract morphogenesis                        | 1   | 0.0117 |
| GO:0048613 | embryonic ectodermal digestive tract morphogenesis              | 1   | 0.0117 |
| GO:0060461 | right lung morphogenesis  | 1   | 0.0117 |
| GO:0071373 | cellular response to luteinizing hormone stimulus               | 3   | 0.0126 |
| GO:0015798 | myo-inositol transport  | 4   | 0.0129 |
| GO:0044725 | chromatin reprogramming in the zygote                           | 3   | 0.0134 |
| GO:0007034 | vacuolar transport  | 139 | 0.0137 |
| GO:0061736 | engulfment of target by autophagosome                           | 1   | 0.0139 |
| GO:0061753 | substrate localization to autophagosome                         | 1   | 0.0139 |
| GO:0036250 | peroxisome transport along microtubule                          | 1   | 0.0142 |
| GO:0044721 | protein import into peroxisome matrix, substrate related        | 1   | 0.0142 |
| GO:0046105 | thymidine biosynthetic process                                  | 2   | 0.0143 |
| GO:0046120 | deoxyribonucleoside biosynthetic process                        | 2   | 0.0143 |
| GO:0046126 | pyrimidine deoxyribonucleoside biosynthetic process             | 2   | 0.0143 |
| GO:0043126 | regulation of 1-phosphatidylinositol 4-kinase activity          | 1   | 0.0145 |
| GO:0043128 | positive regulation of 1-phosphatidylinositol 4-kinase activity | 1   | 0.0145 |
| GO:1905676 | positive regulation of adaptive immune memory response          | 1   | 0.0145 |
| GO:0006227 | dUDP biosynthetic process                                       | 2   | 0.0152 |
| GO:0006233 | dTDP biosynthetic process                                       | 2   | 0.0152 |

|            |  |     |        |
|------------|--|-----|--------|
| GO:0009139 | pyrimidine nucleoside diphosphate biosynthetic process                               | 2   | 0.0152 |
| GO:0009196 | pyrimidine deoxyribonucleoside diphosphate metabolic process                         | 2   | 0.0152 |
| GO:0009197 | pyrimidine deoxyribonucleoside diphosphate biosynthesis                              | 2   | 0.0152 |
| GO:0046072 | dTDP metabolic process   | 2   | 0.0152 |
| GO:0046077 | dUDP metabolic process   | 2   | 0.0152 |
| GO:0055094 | response to lipoprotein particle   | 32  | 0.0164 |
| GO:2000311 | regulation of AMPA receptor activity   | 24  | 0.0172 |
| GO:0097029 | mature conventional dendritic cell differentiation                                   | 4   | 0.0181 |
| GO:0035621 | ER to Golgi ceramide transport   | 5   | 0.0184 |
| GO:0006120 | mitochondrial electron transport, NADH to ubiquinone adaptive immune memory response | 47  | 0.0185 |
| GO:0090716 | adaptive immune memory response  | 2   | 0.0188 |
| GO:1905674 | regulation of adaptive immune memory response  | 2   | 0.0188 |
| GO:0071402 | cellular response to lipoprotein particle stimulus                                   | 34  | 0.0192 |
| GO:0016561 | protein import into peroxisome matrix, translocation                                 | 2   | 0.0192 |
| GO:0090461 | glutamate homeostasis  | 3   | 0.0199 |
| GO:0051966 | regulation of synaptic transmission, glutamatergic                                   | 70  | 0.0201 |
| GO:0043418 | homocysteine catabolic process   | 3   | 0.0207 |
| GO:0006352 | DNA-templated transcription, initiation  | 245 | 0.0209 |
| GO:0035783 | CD4-positive, alpha-beta T cell costimulation  | 3   | 0.0210 |
| GO:0046836 | glycolipid transport   | 5   | 0.0212 |
| GO:0006211 | 5-methylcytosine catabolic process   | 3   | 0.0227 |
| GO:0019857 | 5-methylcytosine metabolic process   | 3   | 0.0227 |
| GO:1901090 | regulation of protein tetramerization  | 2   | 0.0235 |
| GO:1901091 | negative regulation of protein tetramerization                                       | 2   | 0.0235 |
| GO:1901093 | regulation of protein homotetramerization  | 2   | 0.0235 |
| GO:1901094 | negative regulation of protein homotetramerization                                   | 2   | 0.0235 |
| GO:0009138 | pyrimidine nucleoside diphosphate metabolic process                                  | 3   | 0.0236 |
| GO:0060458 | right lung development   | 2   | 0.0242 |
| GO:0018023 | peptidyl-lysine trimethylation   | 43  | 0.0243 |

|            |   |     |        |
|------------|---|-----|--------|
| GO:0080144 | amino acid homeostasis                                | 4   | 0.0247 |
| GO:0002587 | negative regulation of antigen processing and presen  | 2   | 0.0248 |
| GO:1905224 | clathrin-coated pit assembly                          | 3   | 0.0253 |
| GO:0006235 | dTTP biosynthetic process                             | 4   | 0.0256 |
| GO:0009212 | pyrimidine deoxyribonucleoside triphosphate biosynth  | 4   | 0.0256 |
| GO:0046075 | dTTP metabolic process                                | 4   | 0.0256 |
| GO:0034699 | response to luteinizing hormone                       | 4   | 0.0258 |
| GO:0061030 | epithelial cell differentiation involved in mammary   | 4   | 0.0261 |
| GO:0010257 | NADH dehydrogenase complex assembly                   | 58  | 0.0264 |
| GO:0032981 | mitochondrial respiratory chain complex I assembly    | 58  | 0.0264 |
| GO:0046813 | receptor-mediated virion attachment to host cell      | 4   | 0.0266 |
| GO:0007439 | ectodermal digestive tract development                | 2   | 0.0269 |
| GO:0048611 | embryonic ectodermal digestive tract development      | 2   | 0.0269 |
| GO:0009249 | protein lipoylation                                   | 6   | 0.0271 |
| GO:0035964 | COP1-coated vesicle budding                           | 6   | 0.0273 |
| GO:0048200 | Golgi transport vesicle coating                       | 6   | 0.0273 |
| GO:0048205 | COP1 coating of Golgi vesicle                         | 6   | 0.0273 |
| GO:0048009 | insulin-like growth factor receptor signaling pathway | 38  | 0.0276 |
| GO:0045039 | protein insertion into mitochondrial inner membrane   | 8   | 0.0278 |
| GO:0032459 | regulation of protein oligomerization                 | 42  | 0.0279 |
| GO:0051389 | inactivation of MAPKK activity                        | 2   | 0.0289 |
| GO:0019418 | sulfide oxidation                                     | 5   | 0.0290 |
| GO:0070221 | sulfide oxidation, using sulfide:quinone oxidoreduct  | 5   | 0.0290 |
| GO:1902389 | ceramide 1-phosphate transport                        | 8   | 0.0291 |
| GO:0032963 | collagen metabolic process                            | 113 | 0.0293 |
| GO:0043305 | negative regulation of mast cell degranulation        | 7   | 0.0295 |
| GO:2001190 | positive regulation of T cell activation via T cell   | 3   | 0.0299 |
| GO:0120009 | intermembrane lipid transfer                          | 8   | 0.0300 |
| GO:0061462 | protein localization to lysosome                      | 40  | 0.0301 |

|            |  |     |        |
|------------|--|-----|--------|
| GO:0022602 | ovulation cycle process                              | 46  | 0.0302 |
| GO:0034238 | macrophage fusion                                    | 6   | 0.0306 |
| GO:0032417 | positive regulation of sodium:proton antiporter acti | 4   | 0.0306 |
| GO:0051668 | localization within membrane                         | 93  | 0.0307 |
| GO:0032365 | intracellular lipid transport                        | 45  | 0.0310 |
| GO:0046104 | thymidine metabolic process                          | 5   | 0.0317 |
| GO:0046125 | pyrimidine deoxyribonucleoside metabolic process     | 5   | 0.0317 |
| GO:0002584 | negative regulation of antigen processing and presen | 4   | 0.0318 |
| GO:0002586 | regulation of antigen processing and presentation of | 4   | 0.0325 |
| GO:0071211 | protein targeting to vacuole involved in autophagy   | 4   | 0.0336 |
| GO:0014905 | myoblast fusion involved in skeletal muscle regenera | 4   | 0.0339 |
| GO:0007041 | lysosomal transport                                  | 103 | 0.0342 |
| GO:0060750 | epithelial cell proliferation involved in mammary gl | 4   | 0.0350 |
| GO:0048371 | lateral mesodermal cell differentiation              | 3   | 0.0352 |
| GO:0015791 | polyol transport                                     | 11  | 0.0353 |
| GO:0071806 | protein transmembrane transport                      | 57  | 0.0353 |
| GO:0044273 | sulfur compound catabolic process                    | 53  | 0.0355 |
| GO:0009211 | pyrimidine deoxyribonucleoside triphosphate metaboli | 6   | 0.0356 |
| GO:0009189 | deoxyribonucleoside diphosphate biosynthetic process | 4   | 0.0357 |
| GO:0016560 | protein import into peroxisome matrix, docking       | 4   | 0.0358 |
| GO:2000563 | positive regulation of CD4-positive, alpha-beta T ce | 5   | 0.0359 |
| GO:0090131 | mesenchyme migration                                 | 5   | 0.0364 |
| GO:0006367 | transcription initiation from RNA polymerase II prom | 186 | 0.0364 |
| GO:0002581 | negative regulation of antigen processing and presen | 3   | 0.0366 |
| GO:0032962 | positive regulation of inositol trisphosphate biosyn | 6   | 0.0366 |
| GO:0048566 | embryonic digestive tract development                | 34  | 0.0374 |
| GO:0006383 | transcription by RNA polymerase III                  | 55  | 0.0377 |
| GO:0035329 | hippo signaling                                      | 38  | 0.0379 |
| GO:0070813 | hydrogen sulfide metabolic process                   | 7   | 0.0384 |

|             |  |     |        |
|-------------|--|-----|--------|
| GO:0032415  | regulation of sodium:proton antiporter activity      | 6   | 0.0393 |
| GO:0002583  | regulation of antigen processing and presentation of | 6   | 0.0394 |
| GO:0046462  | monoacylglycerol metabolic process                   | 5   | 0.0398 |
| GO:0052651  | monoacylglycerol catabolic process                   | 5   | 0.0398 |
| GO:2001188  | regulation of T cell activation via T cell receptor  | 6   | 0.0398 |
| GO:0033139  | regulation of peptidyl-serine phosphorylation of STA | 12  | 0.0400 |
| GO:0034773  | histone H4 K20 trimethylation                        | 6   | 0.0402 |
| GO:00333007 | negative regulation of mast cell activation involved | 9   | 0.0407 |
| GO:0070973  | protein localization to endoplasmic reticulum exit s | 7   | 0.0409 |
| GO:0060523  | prostate epithelial cord elongation                  | 3   | 0.0410 |
| GO:0035249  | synaptic transmission, glutamatergic                 | 93  | 0.0411 |
| GO:0048369  | lateral mesoderm morphogenesis                       | 4   | 0.0412 |
| GO:0048370  | lateral mesoderm formation                           | 4   | 0.0412 |
| GO:0016191  | synaptic vesicle uncoating                           | 5   | 0.0424 |
| GO:0030579  | ubiquitin-dependent SMAD protein catabolic process   | 6   | 0.0426 |
| GO:0060751  | branch elongation involved in mammary gland duct bra | 5   | 0.0432 |
| GO:0072666  | establishment of protein localization to vacuole     | 49  | 0.0433 |
| GO:0060426  | lung vasculature development                         | 6   | 0.0439 |
| GO:0002580  | regulation of antigen processing and presentation of | 5   | 0.0441 |
| GO:0009120  | deoxyribonucleoside metabolic process                | 8   | 0.0442 |
| GO:0009202  | deoxyribonucleoside triphosphate biosynthetic proces | 6   | 0.0446 |
| GO:0060075  | regulation of resting membrane potential             | 8   | 0.0453 |
| GO:0009186  | deoxyribonucleoside diphosphate metabolic process    | 6   | 0.0457 |
| GO:0032526  | response to retinoic acid                            | 108 | 0.0462 |
| GO:0061734  | parkin-mediated stimulation of mitophagy in response | 6   | 0.0464 |
| GO:0009221  | pyrimidine deoxyribonucleotide biosynthetic process  | 8   | 0.0466 |
| GO:0098943  | neurotransmitter receptor transport, postsynaptic en | 7   | 0.0466 |
| GO:0048806  | genitalia development                                | 47  | 0.0469 |
| GO:0072318  | clathrin coat disassembly                            | 6   | 0.0473 |

| GO term    | Biological Processes                                 | N# | Raw P-value |
|------------|--|----|-------------|
| GO:1901985 | positive regulation of protein acetylation           | 43 | 0.0010      |
| GO:0033144 | negative regulation of intracellular steroid hormone | 35 | 0.0011      |
| GO:0051582 | positive regulation of neurotransmitter uptake       | 6  | 0.0025      |
| GO:0045214 | sarcomere organization                               | 53 | 0.0033      |
| GO:0021853 | cerebral cortex GABAergic interneuron migration      | 6  | 0.0038      |
| GO:1904936 | interneuron migration                                | 6  | 0.0038      |
| GO:0001188 | RNA polymerase I preinitiation complex assembly      | 9  | 0.0040      |
| GO:0043438 | acetoacetic acid metabolic process                   | 1  | 0.0041      |
| GO:0035066 | positive regulation of histone acetylation           | 30 | 0.0043      |
| GO:0021894 | cerebral cortex GABAergic interneuron development    | 7  | 0.0043      |
| GO:0060415 | muscle tissue morphogenesis                          | 82 | 0.0043      |
| GO:2000758 | positive regulation of peptidyl-lysine acetylation   | 33 | 0.0054      |
| GO:0048644 | muscle organ morphogenesis                           | 88 | 0.0055      |
| GO:0006308 | DNA catabolic process                                | 40 | 0.0056      |
| GO:0150070 | regulation of arginase activity                      | 1  | 0.0065      |
| GO:0150072 | positive regulation of arginase activity             | 1  | 0.0065      |
| GO:0006507 | GPI anchor release                                   | 1  | 0.0071      |

Note: #N: Number of genes involved in the respective pathways

|            |  |     |        |
|------------|--|-----|--------|
| GO:0034014 | response to triglyceride                             | 1   | 0.0071 |
| GO:0071401 | cellular response to triglyceride                    | 1   | 0.0071 |
| GO:0097241 | hematopoietic stem cell migration to bone marrow     | 1   | 0.0071 |
| GO:0043630 | ncRNA polyadenylation involved in polyadenylation-de | 1   | 0.0076 |
| GO:1901983 | regulation of protein acetylation                    | 72  | 0.0082 |
| GO:0032651 | regulation of interleukin-1 beta production          | 89  | 0.0085 |
| GO:0006029 | proteoglycan metabolic process                       | 94  | 0.0090 |
| GO:0030241 | skeletal muscle myosin thick filament assembly       | 11  | 0.0090 |
| GO:0071688 | striated muscle myosin thick filament assembly       | 11  | 0.0090 |
| GO:0003139 | secondary heart field specification                  | 9   | 0.0092 |
| GO:0021826 | substrate-independent telencephalic tangential migra | 9   | 0.0095 |
| GO:0021830 | interneuron migration from the subpallium to the cor | 9   | 0.0095 |
| GO:0021843 | substrate-independent telencephalic tangential inter | 9   | 0.0095 |
| GO:0031034 | myosin filament assembly                             | 12  | 0.0100 |
| GO:0030239 | myofibril assembly                                   | 73  | 0.0102 |
| GO:0032675 | regulation of interleukin-6 production               | 149 | 0.0108 |
| GO:0046606 | negative regulation of centrosome cycle              | 14  | 0.0109 |
| GO:0050652 | dermatan sulfate proteoglycan biosynthetic process,  | 1   | 0.0113 |
| GO:0150073 | regulation of protein-glutamine gamma-glutamyltransf | 2   | 0.0113 |
| GO:0150074 | positive regulation of protein-glutamine gamma-gluta | 2   | 0.0113 |
| GO:0032611 | interleukin-1 beta production                        | 100 | 0.0115 |
| GO:0033147 | negative regulation of intracellular estrogen recept | 13  | 0.0117 |
| GO:0032652 | regulation of interleukin-1 production               | 100 | 0.0118 |
| GO:0055008 | cardiac muscle tissue morphogenesis                  | 69  | 0.0119 |
| GO:0021515 | cell differentiation in spinal cord                  | 54  | 0.0121 |
| GO:0021892 | cerebral cortex GABAergic interneuron differentiatio | 11  | 0.0122 |
| GO:0030240 | skeletal muscle thin filament assembly               | 14  | 0.0125 |
| GO:0031033 | myosin filament organization                         | 13  | 0.0125 |
| GO:0033143 | regulation of intracellular steroid hormone receptor | 75  | 0.0132 |

|            |   |     |        |
|------------|---|-----|--------|
| GO:0032635 | interleukin-6 production  | 158 | 0.0134 |
| GO:0002038 | positive regulation of L-glutamate import across plasma membrane              | 2   | 0.0137 |
| GO:0030166 | proteoglycan biosynthetic process   | 69  | 0.0140 |
| GO:0030204 | chondroitin sulfate metabolic process   | 39  | 0.0142 |
| GO:0007517 | muscle organ development  | 406 | 0.0144 |
| GO:0035020 | regulation of Rac protein signal transduction                                 | 14  | 0.0153 |
| GO:0019520 | aldonic acid metabolic process  | 2   | 0.0154 |
| GO:0019521 | D-gluconate metabolic process   | 2   | 0.0154 |
| GO:0046176 | aldonic acid catabolic process  | 2   | 0.0154 |
| GO:0046177 | D-gluconate catabolic process   | 2   | 0.0154 |
| GO:0030522 | intracellular receptor signaling pathway                                      | 278 | 0.0158 |
| GO:0032612 | interleukin-1 production  | 112 | 0.0160 |
| GO:1900134 | negative regulation of renin secretion into blood stream                      | 1   | 0.0164 |
| GO:1904975 | response to bleomycin   | 2   | 0.0170 |
| GO:1904976 | cellular response to bleomycin  | 2   | 0.0170 |
| GO:0034147 | regulation of toll-like receptor 5 signaling pathway                          | 1   | 0.0175 |
| GO:0034148 | negative regulation of toll-like receptor 5 signaling pathway                 | 1   | 0.0175 |
| GO:0070429 | negative regulation of nucleotide-binding oligomerization domain containing 1 | 1   | 0.0175 |
| GO:0072573 | tolerance induction to lipopolysaccharide                                     | 1   | 0.0175 |
| GO:0060766 | negative regulation of androgen receptor signaling pathway                    | 15  | 0.0186 |
| GO:0050654 | chondroitin sulfate proteoglycan metabolic process                            | 44  | 0.0190 |
| GO:0014866 | skeletal myofibril assembly   | 16  | 0.0192 |
| GO:0043652 | engulfment of apoptotic cell  | 15  | 0.0198 |
| GO:0030073 | insulin secretion   | 206 | 0.0199 |
| GO:2000772 | regulation of cellular senescence   | 52  | 0.0200 |
| GO:0097154 | GABAergic neuron differentiation  | 14  | 0.0201 |
| GO:1990918 | double-strand break repair involved in meiotic recombination                  | 3   | 0.0204 |
| GO:0035853 | chromosome passenger complex localization to spindle                          | 1   | 0.0205 |
| GO:0016333 | morphogenesis of follicular epithelium  | 1   | 0.0212 |

|            |  |     |        |
|------------|--|-----|--------|
| GO:0016334 | establishment or maintenance of polarity of follicul | 1   | 0.0212 |
| GO:0042247 | establishment of planar polarity of follicular epith | 1   | 0.0212 |
| GO:0048739 | cardiac muscle fiber development                     | 18  | 0.0213 |
| GO:0033233 | regulation of protein sumoylation                    | 21  | 0.0214 |
| GO:0044467 | glial cell-derived neurotrophic factor secretion     | 2   | 0.0218 |
| GO:1900166 | regulation of glial cell-derived neurotrophic factor | 2   | 0.0218 |
| GO:1900168 | positive regulation of glial cell-derived neurotroph | 2   | 0.0218 |
| GO:0070428 | regulation of nucleotide-binding oligomerization dom | 2   | 0.0219 |
| GO:0062029 | positive regulation of stress granule assembly       | 2   | 0.0227 |
| GO:0061061 | muscle structure development                         | 668 | 0.0227 |
| GO:0006535 | cysteine biosynthetic process from serine            | 1   | 0.0234 |
| GO:0046603 | negative regulation of mitotic centrosome separation | 1   | 0.0238 |
| GO:2000349 | negative regulation of CD40 signalling pathway       | 2   | 0.0241 |
| GO:0021527 | spinal cord association neuron differentiation       | 14  | 0.0242 |
| GO:0051580 | regulation of neurotransmitter uptake                | 20  | 0.0244 |
| GO:0021953 | central nervous system neuron differentiation        | 183 | 0.0244 |
| GO:0090291 | negative regulation of osteoclast proliferation      | 2   | 0.0244 |
| GO:1901741 | positive regulation of myoblast fusion               | 19  | 0.0245 |
| GO:0043401 | steroid hormone mediated signaling pathway           | 182 | 0.0247 |
| GO:1904464 | regulation of matrix metallopeptidase secretion      | 5   | 0.0250 |
| GO:1904465 | negative regulation of matrix metallopeptidase secr  | 5   | 0.0250 |
| GO:1990773 | matrix metallopeptidase secretion                    | 5   | 0.0250 |
| GO:0035065 | regulation of histone acetylation                    | 53  | 0.0252 |
| GO:0090251 | protein localization involved in establishment of pl | 1   | 0.0256 |
| GO:0009051 | pentose-phosphate shunt, oxidative branch            | 3   | 0.0259 |
| GO:0015798 | myo-inositol transport                               | 4   | 0.0259 |
| GO:0003128 | heart field specification                            | 15  | 0.0266 |
| GO:0007529 | establishment of synaptic specificity at neuromuscul | 2   | 0.0270 |
| GO:0071929 | alpha-tubulin acetylation                            | 2   | 0.0273 |

|            |   |     |        |
|------------|---|-----|--------|
| GO:0048936 | peripheral nervous system neuron axonogenesis   | 2   | 0.0280 |
| GO:0051151 | negative regulation of smooth muscle cell differentiation                             | 23  | 0.0281 |
| GO:0090667 | cell chemotaxis to vascular endothelial growth factor                                 | 4   | 0.0287 |
| GO:0090668 | endothelial cell chemotaxis to vascular endothelial                                   | 4   | 0.0287 |
| GO:1901739 | regulation of myoblast fusion   | 21  | 0.0297 |
| GO:0019343 | cysteine biosynthetic process via cystathionine                                       | 2   | 0.0301 |
| GO:0007538 | primary sex determination   | 3   | 0.0305 |
| GO:0090342 | regulation of cell aging  | 60  | 0.0305 |
| GO:0090277 | positive regulation of peptide hormone secretion                                      | 96  | 0.0306 |
| GO:2000111 | positive regulation of macrophage apoptotic process                                   | 3   | 0.0308 |
| GO:0043111 | replication fork arrest   | 4   | 0.0311 |
| GO:2000756 | regulation of peptidyl-lysine acetylation   | 59  | 0.0313 |
| GO:0050796 | regulation of insulin secretion   | 175 | 0.0313 |
| GO:0043629 | ncRNA polyadenylation   | 2   | 0.0316 |
| GO:0071050 | snoRNA polyadenylation  | 2   | 0.0316 |
| GO:0010983 | positive regulation of high-density lipoprotein part                                  | 6   | 0.0318 |
| GO:0000737 | DNA catabolic process, endonucleolytic  | 33  | 0.0322 |
| GO:0034140 | negative regulation of toll-like receptor 3 signaling                                 | 3   | 0.0328 |
| GO:0018335 | protein succinylation   | 4   | 0.0333 |
| GO:0106077 | histone succinylation   | 4   | 0.0333 |
| GO:0072719 | cellular response to cisplatin  | 5   | 0.0333 |
| GO:0000472 | endonucleolytic cleavage to generate mature 5'-end of                                 | 3   | 0.0343 |
| GO:0000967 | rRNA 5'-end processing  | 3   | 0.0343 |
| GO:0035442 | dipeptide transmembrane transport   | 5   | 0.0344 |
| GO:0042938 | dipeptide transport   | 5   | 0.0344 |
| GO:0070425 | negative regulation of nucleotide-binding oligomerization domain containing protein 2 | 3   | 0.0347 |
| GO:0070433 | negative regulation of nucleotide-binding oligomerization domain containing protein 3 | 3   | 0.0347 |
| GO:0034146 | toll-like receptor 5 signaling pathway  | 2   | 0.0354 |
| GO:0070427 | nucleotide-binding oligomerization domain containing protein 4                        | 4   | 0.0355 |

|             |  |     |        |
|-------------|--|-----|--------|
| GO:0019322  | pentose biosynthetic process                         | 4   | 0.0355 |
| GO:1902659  | regulation of glucose mediated signaling pathway     | 3   | 0.0356 |
| GO:1902661  | positive regulation of glucose mediated signaling pa | 3   | 0.0356 |
| GO:0006739  | NADP metabolic process                               | 31  | 0.0356 |
| GO:0071787  | endoplasmic reticulum tubular network formation      | 4   | 0.0357 |
| GO:0060212  | negative regulation of nuclear-transcribed mRNA poly | 3   | 0.0357 |
| GO:1900152  | negative regulation of nuclear-transcribed mRNA cata | 3   | 0.0357 |
| GO:0050653  | chondroitin sulfate proteoglycan biosynthetic proces | 2   | 0.0358 |
| GO:0044550  | secondary metabolite biosynthetic process            | 28  | 0.0363 |
| GO:0050708  | regulation of protein secretion                      | 465 | 0.0363 |
| GO:0043418  | homocysteine catabolic process                       | 3   | 0.0364 |
| GO:0060143  | positive regulation of syncytium formation by plasma | 27  | 0.0366 |
| GO:0002677  | negative regulation of chronic inflammatory response | 4   | 0.0367 |
| GO:1990168  | protein K33-linked deubiquitination                  | 4   | 0.0370 |
| GO:0060913  | cardiac cell fate determination                      | 3   | 0.0371 |
| GO:1990809  | endoplasmic reticulum tubular network membrane organ | 4   | 0.0378 |
| GO:0010982  | regulation of high-density lipoprotein particle clea | 7   | 0.0380 |
| GO:00000706 | metotic DNA double-strand break processing           | 4   | 0.0382 |
| GO:0035986  | senescence-associated heterochromatin focus assembly | 3   | 0.0385 |
| GO:0035054  | embryonic heart tube anterior/posterior pattern spec | 3   | 0.0389 |
| GO:0071657  | positive regulation of granulocyte colony-stimulatin | 3   | 0.0390 |
| GO:1901258  | positive regulation of macrophage colony-stimulating | 3   | 0.0390 |
| GO:0045589  | regulation of regulatory T cell differentiation      | 32  | 0.0396 |
| GO:1905319  | mesenchymal stem cell migration                      | 3   | 0.0399 |
| GO:1905320  | regulation of mesenchymal stem cell migration        | 3   | 0.0399 |
| GO:1905322  | positive regulation of mesenchymal stem cell migrati | 3   | 0.0399 |
| GO:0051586  | positive regulation of dopamine uptake involved in s | 3   | 0.0400 |
| GO:0051944  | positive regulation of catecholamine uptake involved | 3   | 0.0400 |
| GO:1900133  | regulation of renin secretion into blood stream      | 4   | 0.0401 |

|            |  |     |        |
|------------|--|-----|--------|
| GO:0150173 | positive regulation of phosphatidylcholine metabolic | 3   | 0.0404 |
| GO:2001247 | positive regulation of phosphatidylcholine biosynthe | 3   | 0.0404 |
| GO:0021526 | medial motor column neuron differentiation           | 2   | 0.0405 |
| GO:0030262 | apoptotic nuclear changes                            | 34  | 0.0407 |
| GO:2001025 | positive regulation of response to drug              | 33  | 0.0415 |
| GO:0009092 | homoserine metabolic process                         | 4   | 0.0415 |
| GO:0019346 | transsulfuration                                     | 4   | 0.0415 |
| GO:0045066 | regulatory T cell differentiation                    | 34  | 0.0418 |
| GO:0090289 | regulation of osteoclast proliferation               | 5   | 0.0418 |
| GO:0030072 | peptide hormone secretion                            | 249 | 0.0419 |
| GO:0060765 | regulation of androgen receptor signaling pathway    | 26  | 0.0420 |
| GO:1901491 | negative regulation of lymphangiogenesis             | 3   | 0.0421 |
| GO:0006741 | NADP biosynthetic process                            | 3   | 0.0421 |
| GO:0055003 | cardiac myofibril assembly                           | 26  | 0.0422 |
| GO:0060142 | regulation of syncytium formation by plasma membrane | 29  | 0.0426 |
| GO:0090074 | negative regulation of protein homodimerization acti | 4   | 0.0427 |
| GO:0097194 | execution phase of apoptosis                         | 74  | 0.0432 |
| GO:0071076 | RNA 3' uridylation                                   | 4   | 0.0433 |
| GO:0002036 | regulation of L-glutamate import across plasma membr | 5   | 0.0434 |
| GO:0071655 | regulation of granulocyte colony-stimulating factor  | 4   | 0.0437 |
| GO:0016925 | protein sumoylation                                  | 79  | 0.0438 |
| GO:0006361 | transcription initiation from RNA polymerase I prono | 35  | 0.0439 |
| GO:0009093 | cysteine catabolic process                           | 4   | 0.0442 |
| GO:0019448 | L-cysteine catabolic process                         | 4   | 0.0442 |
| GO:0046439 | L-cysteine metabolic process                         | 4   | 0.0442 |
| GO:0003215 | cardiac right ventricle morphogenesis                | 20  | 0.0442 |
| GO:0050707 | regulation of cytokine secretion                     | 204 | 0.0442 |
| GO:0042321 | negative regulation of circadian sleep/wake cycle, s | 5   | 0.0443 |
| GO:0030043 | actin filament fragmentation                         | 4   | 0.0450 |

|            |  |     |        |
|------------|--|-----|--------|
| GO:0048386 | positive regulation of retinoic acid receptor signal | 4   | 0.0451 |
| GO:0060488 | orthogonal dichotomous subdivision of terminal units | 2   | 0.0451 |
| GO:0060489 | planar dichotomous subdivision of terminal units inv | 2   | 0.0451 |
| GO:0060490 | lateral sprouting involved in lung morphogenesis     | 2   | 0.0451 |
| GO:2000620 | positive regulation of histone H4-K16 acetylation    | 2   | 0.0455 |
| GO:0042138 | meiotic DNA double-strand break formation            | 6   | 0.0458 |
| GO:0062028 | regulation of stress granule assembly                | 5   | 0.0461 |
| GO:0071947 | protein deubiquitination involved in ubiquitin-depen | 5   | 0.0464 |
| GO:1905868 | regulation of 3'-UTR-mediated mRNA stabilization     | 3   | 0.0466 |
| GO:1905870 | positive regulation of 3'-UTR-mediated mRNA stabiliz | 3   | 0.0466 |
| GO:0090325 | regulation of locomotion involved in locomotory beha | 5   | 0.0471 |
| GO:0010927 | cellular component assembly involved in morphogenesi | 115 | 0.0472 |
| GO:0006921 | cellular component disassembly involved in execution | 36  | 0.0474 |
| GO:0099552 | trans-synaptic signaling by lipid, modulating synapt | 3   | 0.0475 |
| GO:0099553 | trans-synaptic signaling by endocannabinoid, modulat | 3   | 0.0475 |
| GO:0043634 | Polyadenylation-dependent ncRNA catabolic process    | 7   | 0.0479 |
| GO:0006552 | leucine catabolic process                            | 6   | 0.0480 |
| GO:0071611 | granulocyte colony-stimulating factor production     | 5   | 0.0481 |
| GO:0030206 | chondroitin sulfate biosynthetic process             | 26  | 0.0483 |
| GO:0021895 | cerebral cortex neuron differentiation               | 24  | 0.0486 |
| GO:0060392 | negative regulation of SMAD protein signal transduct | 5   | 0.0487 |
| GO:0070814 | hydrogen sulfide biosynthetic process                | 5   | 0.0487 |
| GO:0060160 | negative regulation of dopamine receptor signaling p | 4   | 0.0495 |
| GO:0021516 | dorsal spinal cord development                       | 22  | 0.0498 |

Note: #N: Number of genes involved in the respective pathways

Supplement Table S6 (A): Indirect association of DNAm at birth at 68 CpG sites in males, with asthma acquisition from pre- to post-adolescence mediated by pre-adolescent Atopy.

| CpGs              | IOWBC<br>estimate | IOWBC<br>pvalue | ALSPAC<br>estimate | ALSPAC<br>pvalue | CHR       | Gene                 | Gene location | CpG Island |
|-------------------|-------------------|-----------------|--------------------|------------------|-----------|----------------------|---------------|------------|
| cg06028605        | -0.07             | 0.01            | 0.01               | 0.31             | 16        | <i>SLC5A11</i>       | 5'UTR         |            |
| cg00067274        | -0.06             | 0.01            | 0.00               | 0.70             | 4         | <i>DCHS2</i>         | TSS1500       |            |
| cg09760697        | 0.06              | 0.02            | -0.01              | 0.41             | 10        | <i>RPII-163F15.1</i> |               |            |
| <b>cg25165501</b> | <b>0.06</b>       | <b>0.02</b>     | <b>0.02</b>        | <b>0.11</b>      | <b>11</b> | <i>SLC22A11</i>      | Body          | Island     |
| <b>cg25693132</b> | <b>-0.06</b>      | <b>0.02</b>     | <b>-0.01</b>       | <b>0.41</b>      | <b>3</b>  | <i>GRM2</i>          | TSS1500       | Island     |
| cg22878693        | -0.06             | 0.02            | 0.01               | 0.41             | 17        | <i>RPTOR</i>         | Body          |            |
| <b>cg16010911</b> | <b>0.06</b>       | <b>0.02</b>     | <b>0.00</b>        | <b>0.81</b>      | <b>17</b> | <i>C17orf77</i>      | TSS200        |            |
| cg01804036        | -0.05             | 0.03            | 0.00               | 0.75             | 12        | <i>TESC</i>          | Body          |            |
| cg00892999        | 0.06              | 0.03            | 0.00               | 0.78             | 4         | <i>GAK</i>           | Body          | N_Shore    |
| cg26435502        | 0.06              | 0.03            | -0.01              | 0.49             | 3         | <i>NISCH</i>         | Body          | N_Shore    |
|                   |                   |                 |                    |                  |           | <i>THAP5,DNAJB</i>   |               |            |
| cg00459447        | 0.06              | 0.03            | -0.02              | 0.21             | 7         | <i>9</i>             | TSS200        | Island     |
| <b>cg22780731</b> | <b>-0.05</b>      | <b>0.03</b>     | <b>-0.01</b>       | <b>0.40</b>      | <b>19</b> | <i>EVIL5L</i>        | 5'UTR         |            |
| <b>cg16781287</b> | <b>-0.05</b>      | <b>0.03</b>     | <b>-0.01</b>       | <b>0.40</b>      | <b>11</b> | <i>UBE4A</i>         | Body          |            |
| <b>cg20250341</b> | <b>-0.06</b>      | <b>0.03</b>     | <b>0.00</b>        | <b>0.83</b>      | <b>17</b> | <i>C17orf44</i>      | Body          | Island     |
| cg24085655        | -0.05             | 0.03            | 0.01               | 0.49             | 6         | <i>RPL10A</i>        | 1stExon       | Island     |
| <b>cg26453588</b> | <b>-0.06</b>      | <b>0.03</b>     | <b>0.00</b>        | <b>0.83</b>      | <b>22</b> | <i>BIK</i>           | TSS1500       | Island     |
| cg09990169        | -0.05             | 0.03            | 0.01               | 0.33             | 2         | <i>C2orf54</i>       | TSS200        |            |
| <b>cg10475970</b> | <b>-0.05</b>      | <b>0.03</b>     | <b>0.00</b>        | <b>0.78</b>      | <b>5</b>  | <i>PCDHG44</i>       | Body          | Island     |
| <b>cg08991599</b> | <b>-0.05</b>      | <b>0.03</b>     | <b>-0.01</b>       | <b>0.50</b>      | <b>8</b>  | <i>FAM84B</i>        | TSS200        | Island     |
| <b>cg18073883</b> | <b>-0.05</b>      | <b>0.03</b>     | <b>0.00</b>        | <b>0.80</b>      | <b>6</b>  | <i>HLA-DOB</i>       | 3'UTR         |            |
|                   |                   |                 |                    |                  |           |                      |               |            |
| cg03488284        | 0.06              | 0.04            | 0.01               | 0.40             | 16        | <i>NDUFABI</i>       | TSS200        | Island     |
| cg17425144        | -0.05             | 0.04            | 0.01               | 0.38             | 1         | <i>PEX14</i>         | Body          |            |
| <b>cg02776315</b> | <b>-0.04</b>      | <b>0.04</b>     | <b>-0.01</b>       | <b>0.33</b>      | <b>2</b>  | <i>LHCGR</i>         | TSS1500       | S_Shore    |
| <b>cg19987540</b> | <b>-0.05</b>      | <b>0.04</b>     | <b>-0.01</b>       | <b>0.57</b>      | <b>12</b> | <i>RAB21</i>         |               | N_Shore    |
| cg14551279        | 0.05              | 0.04            | -0.02              | 0.24             | 8         | <i>SLC20A2</i>       | Body          | Island     |

|                   |       |      |       |      |    |                         |               |
|-------------------|-------|------|-------|------|----|-------------------------|---------------|
| <b>cg2264738</b>  | -0.06 | 0.04 | -0.02 | 0.20 | 17 | <i>CCL16</i>            | 3'UTR         |
| cg04956882        | -0.05 | 0.04 | 0.01  | 0.61 | 14 | <i>Cl4orf48</i>         | TSS1500       |
| <b>cg04432599</b> | -0.05 | 0.04 | -0.01 | 0.43 | 17 | <i>GPIBA</i>            | 1stExon;5'UTR |
| cg22571278        | -0.05 | 0.04 | 0.02  | 0.19 | 17 | <i>RPL1-159D12.11</i>   |               |
| cg02820040        | -0.05 | 0.04 | 0.00  | 0.82 | 2  | <i>C2orf54</i>          | TSS1500       |
| <b>cg04214710</b> | 0.05  | 0.04 | 0.00  | 0.83 | 7  | <i>PITRN2</i>           | Body          |
| <b>cg15909600</b> | 0.05  | 0.04 | 0.00  | 0.95 | 22 | <i>MAPK8IP2</i>         | TSS1500       |
| cg06207120        | -0.05 | 0.04 | 0.01  | 0.35 | 15 | <i>CTD-2306412.I</i>    |               |
| cg04940570        | 0.05  | 0.05 | -0.01 | 0.29 | 11 | <i>TEADI</i>            | 5'UTR         |
| cg063391046       | 0.05  | 0.05 | 0.00  | 0.88 | 16 | <i>CMP</i>              | TSS200        |
| cg02366519        | 0.05  | 0.05 | -0.01 | 0.34 | 4  | <i>ABLIM2</i>           | Body          |
| <b>cg02730843</b> | -0.05 | 0.05 | -0.01 | 0.35 | 10 | <i>MCM10</i>            | 3'UTR         |
| <b>cg16347828</b> | 0.04  | 0.05 | 0.00  | 0.75 | 14 | <i>FLJ10357</i>         | TSS1500       |
| cg12156887        | -0.04 | 0.05 | 0.01  | 0.36 | 17 | <i>AKAP10</i>           |               |
| cg00615241        | -0.04 | 0.05 | 0.01  | 0.45 | 19 | <i>PRTN3</i>            | TSS1500       |
| <b>cg13139542</b> | -0.05 | 0.05 | 0.00  | 0.94 | 2  | <i>LINC00298, LINC0</i> |               |
| cg00425661        | -0.05 | 0.03 |       |      | 14 |                         |               |
| cg00880959        | 0.05  | 0.02 |       |      | 5  | <i>PLEKHG4B</i>         | TSS200        |
| cg01265507        | -0.06 | 0.04 |       |      | 8  | <i>TRAPP C9</i>         | TSS1500       |
| cg02449147        | 0.05  | 0.04 |       |      | 22 | <i>NCF4</i>             | Body          |
| cg03308555        | -0.05 | 0.03 |       |      | 9  | <i>RORB</i>             | Body          |
| cg04216721        | -0.05 | 0.02 |       |      | 6  | <i>ARRHGA P18</i>       | Body          |
| cg05866778        | -0.06 | 0.02 |       |      | 7  | <i>DBNL</i>             | Body          |
| cg06795516        | 0.06  | 0.01 |       |      | 17 | <i>LRRC75A</i>          | Body,Body     |
| cg08805613        | 0.06  | 0.04 |       |      | 15 |                         |               |
| cg09940657        | 0.06  | 0.03 |       |      | 15 |                         |               |
| cg10727229        | 0.05  | 0.05 |       |      | 4  |                         |               |
| cg11367790        | -0.05 | 0.03 |       |      | 12 | <i>CACNA1C</i>          | 3'UTR;        |
| cg11934012        | -0.06 | 0.03 |       |      | 14 | <i>PNP</i>              | 3'UTR         |

S\_Shore

| CpGs              | IOWBC estimate | IOWBC pvalue | ALSPAC estimate | ALSPAC Cpvalue | CHR | Gene         | Gene location   | CpG Island |
|-------------------|----------------|--------------|-----------------|----------------|-----|--------------|-----------------|------------|
| cg06508623        | -0.04          | 0.04         | 0.02            | 0.09           | 13  | DNAJC15      |                 |            |
| cg02997605        | 0.04           | 0.04         | -0.01           | 0.32           | 16  | LINC02177    |                 |            |
| <b>cg06636625</b> | -0.04          | 0.04         | -0.01           | 0.41           | 19  | ZNF17        | Body            | S_Shore    |
| <b>cg05934125</b> | -0.04          | 0.04         | -0.01           | 0.31           | 1   | NID1         | Body            |            |
| <b>cg18844144</b> | -0.04          | 0.04         | -0.01           | 0.23           | 14  | ACIN1        | Body            | Island     |
| <b>cg04720635</b> | 0.04           | 0.04         | 0.01            | 0.50           | 5   | TNFAIP8      | 1stExon,5'UTR   | Island     |
| cg13849727        | -0.04          | 0.04         | 0.01            | 0.26           | 9   | C9orf93      | Body            |            |
| cg14803350        | 0.04           | 0.04         | -0.01           | 0.50           | 5   | PWWP2A       | 1stExon,1stExon | Island     |
| cg04888037        | -0.04          | 0.04         | 0.00            | 0.73           | 12  | RP4-809F18.I |                 | S_Shore    |

|                   |       |      |       |                |             |                 |           |         |
|-------------------|-------|------|-------|----------------|-------------|-----------------|-----------|---------|
| cg26647291        | -0.04 | 0.04 | 0.00  | 0.73           | 11          | <i>ESRRRA</i>   | Body      | N_Shelf |
| <b>cg04466022</b> | -0.04 | 0.05 | 0.00  | 0.79           | 6           | <i>MDGAI</i>    | Body      | Island  |
| cg07621385        | -0.04 | 0.05 | 0.00  | 0.86           | 3           | <i>MYLK</i>     | 5'UTR     | S_Shore |
| <b>cg15761799</b> | -0.04 | 0.05 | -0.01 | 0.14           | 17          | <i>AATK</i>     | Body      |         |
| <b>cg06589109</b> | -0.04 | 0.05 | 0.00  | 0.88           | 16          | <i>KIAA0182</i> | Body;Body |         |
| <b>cg08566044</b> | 0.04  | 0.05 | 0.01  | 0.37           | 6           | <i>SNORD48</i>  | 5'UTR;    |         |
| <b>cg11320144</b> | -0.04 | 0.05 | -0.01 | 0.50           | 20          | <i>PDYN</i>     | TSS1500   |         |
| cg13601799        | 0.04  | 0.05 | -0.01 | 0.19           | 9           | <i>CDKN2A</i>   | 1stExon   | Island  |
| <b>cg23796713</b> | -0.03 | 0.05 | -0.01 | 0.60           | 6           | <i>ZBTB22</i>   | TSS1500   | N_Shore |
| cg00141391        | -0.04 | 0.03 | 8     |                |             |                 |           |         |
| cg01329939        | -0.03 | 0.05 | 12    | <i>ANO2</i>    | Body        |                 |           |         |
| cg01426804        | 0.04  | 0.05 | 3     | <i>KLHL6</i>   | Body        |                 |           |         |
| cg02115490        | 0.04  | 0.05 | 20    |                |             |                 |           |         |
| cg02407116        | -0.05 | 0.02 | 1     | <i>DUSP12</i>  | TSS1500     |                 |           |         |
| cg03727227        | 0.05  | 0.04 | 6     | <i>SRF</i>     | Body;TSS200 | Island          |           |         |
| cg04878489        | 0.04  | 0.04 | 6     | <i>SRF</i>     | Body;TSS200 | Island          |           |         |
| cg08587654        | 0.04  | 0.05 | 9     | <i>KLHL9</i>   | TSS200      | Island          |           |         |
| cg09487370        | 0.04  | 0.05 | 1     |                |             |                 |           |         |
| cg11106136        | -0.04 | 0.04 | 18    | <i>CELF4</i>   | Body        |                 |           |         |
| cg11500743        | 0.05  | 0.04 | 14    | <i>WDR89</i>   | Body        |                 |           |         |
| cg12033528        | 0.04  | 0.05 | 6     |                |             |                 |           |         |
| cg12600901        | -0.04 | 0.04 | 1     | <i>MIRI90B</i> | TSS1500     |                 |           |         |
| cg12884325        | -0.04 | 0.04 | 10    |                |             |                 |           |         |
| cg13006926        | -0.04 | 0.05 | 7     | <i>CDK14</i>   | Body        |                 |           |         |
| cg13225210        | 0.05  | 0.02 | 1     | <i>TMEM39B</i> | Body        |                 |           |         |
| cg14325335        | 0.04  | 0.05 | 15    | <i>PARP6</i>   | TSS200      |                 |           |         |
| cg14975786        | 0.04  | 0.05 | 12    |                |             |                 |           |         |
| cg16716563        | 0.04  | 0.05 | 9     | <i>STXBPI</i>  | Body        |                 |           |         |
| cg20451039        | 0.04  | 0.04 | 15    | <i>ITGA11</i>  | Body        |                 |           |         |

|            |       |      |  |    |                |        |
|------------|-------|------|--|----|----------------|--------|
| cg22808375 | -0.04 | 0.04 |  | 1  |                |        |
| cg24099241 | 0.03  | 0.05 |  | 19 | <i>ITPKC</i>   | Body   |
| cg24206614 | -0.04 | 0.05 |  | 1  | <i>KLHDC8A</i> | TSS200 |

**Supplement Table S7 (A): Direct association of DNAm at birth at 98 CpG sites in males, with asthma acquisition from pre- to post-adolescence.**

| CpGs              | IOWBC estimate | IOWBC pvalue | ALSPAC estimate | ALSPA C pvalue | CHR | Gene                  | Gene location | CpG Island |
|-------------------|----------------|--------------|-----------------|----------------|-----|-----------------------|---------------|------------|
| cg03304017        | 0.23           | 0            | -0.125          | 0.07           | 8   | <i>DEFB4</i>          | 3UTR          |            |
| cg02582183        | -0.238         | 0            | 0.136           | 0.082          | 11  | <i>TMEM80</i>         | TSS200        | Island     |
| <b>cg00800038</b> | -0.235         | 0            | -0.094          | 0.161          | 16  | <i>TCF25</i>          | Body          | N_Shore    |
| cg08638939        | 0.314          | 0            | -0.073          | 0.275          | 17  | <i>TMM22</i>          | TSS200        | Island     |
| <b>cg14789960</b> | 0.26           | 0            | 0.056           | 0.349          | 17  | <i>MRPS23</i>         | Body          | N_Shelf    |
| <b>cg19558503</b> | -0.184         | 0            | -0.051          | 0.377          | 7   | <i>PLEKHA8</i>        | TSS1500       | Island     |
| cg06226384        | 0.221          | 0            | -0.028          | 0.67           | 17  | <i>CACNG5</i>         | TSS200        |            |
| <b>cg20215212</b> | 0.238          | 0            | 0.024           | 0.705          | 17  | <i>BLMH</i>           | Body          | N_Shore    |
| cg19780308        | 0.189          | 0            | -0.026          | 0.724          | 4   | <i>MAML3</i>          | Body          |            |
| <b>cg01024247</b> | 0.2            | 0            | 0.018           | 0.773          | 7   | <i>MIR589</i>         | TSS200;Body   | S_Shore    |
| <b>cg14093886</b> | 0.294          | 0            | 0.013           | 0.829          | 7   | <i>LOC285954</i>      | Body;Body     | Island     |
| cg16097124        | 0.254          | 0            | -0.011          | 0.86           | 14  | <i>TMED10</i>         | Body          | N_Shore    |
| cg03508095        | 0.276          | 0            | -0.006          | 0.92           | 4   | <i>C4orf39,TRIM61</i> | 3UTR          | S_Shore    |
| cg04355222        | -0.254         | 0            | 0.002           | 0.971          | 11  | <i>CD8I</i>           | Body          | N_Shore    |
| <b>cg16481969</b> | 0.172          | 0.001        | 0.072           | 0.252          | 16  | <i>CPPEDI</i>         | TSS1500       | S_Shore    |
| <b>cg17725477</b> | 0.207          | 0.001        | 0.08            | 0.289          | 15  | <i>SNAPC5</i>         | Body          | N_Shore    |
| cg24027263        | 0.265          | 0.001        | -0.049          | 0.482          | 3   | <i>ATXN7</i>          | Body          |            |
| cg15203632        | 0.186          | 0.001        | -0.041          | 0.557          | 1   | <i>KCNKL</i>          | Body          |            |
| <b>cg13331559</b> | 0.244          | 0.001        | 0.036           | 0.606          | 1   | <i>MCOLN3</i>         | TSS1500       | Island     |
| cg15391807        | -0.22          | 0.001        | 0.023           | 0.733          | 10  | <i>KCNK18</i>         | N_Shelf       |            |
| <b>cg07452560</b> | 0.216          | 0.001        | 0.008           | 0.9            | 8   | <i>KIAA1688</i>       | Body          |            |
| cg14080518        | 0.237          | 0.001        | 0.008           | 0.911          | 7   | <i>SMURF1</i>         | Body          | S_Shelf    |

|                   |        |       |        |       |    |                      |              |
|-------------------|--------|-------|--------|-------|----|----------------------|--------------|
| <b>cg12938020</b> | -0.176 | 0.002 | -0.15  | 0.027 | 2  | <i>HOXD3</i>         | N_Shore      |
| <b>cg13425962</b> | -0.191 | 0.002 | -0.079 | 0.205 | 9  | <i>EXD3</i>          | Island       |
| <b>cg18809973</b> | -0.207 | 0.002 | 0.03   | 0.686 | 17 | <i>LINC01987</i>     |              |
| <b>cg09760697</b> | -0.153 | 0.002 | 0.012  | 0.869 | 10 | <i>RPII-163F15.1</i> |              |
| <b>cg05541258</b> | 0.196  | 0.003 | 0.059  | 0.299 | 6  | <i>RNU7-26P</i>      |              |
| <b>cg07670736</b> | 0.206  | 0.003 | -0.041 | 0.535 | 1  | <i>ALG14</i>         | Body         |
| <b>cg22729438</b> | 0.233  | 0.003 | -0.041 | 0.561 | 15 | <i>TJPI</i>          |              |
| <b>cg10855395</b> | 0.159  | 0.003 | 0.01   | 0.885 | 12 | <i>UBC</i>           |              |
| <b>cg25121621</b> | 0.208  | 0.004 | 0.05   | 0.423 | 15 | <i>SQRDL</i>         |              |
| <b>cg19775582</b> | -0.199 | 0.004 | -0.028 | 0.66  | 5  | <i>ODZ2</i>          | Body         |
| <b>cg22106810</b> | 0.183  | 0.004 | -0.026 | 0.706 | 12 | <i>PLEKHA5</i>       | Body         |
| <b>cg17675639</b> | -0.219 | 0.004 | 0.012  | 0.845 | 13 | <i>EEF1DP3</i>       | TSS200       |
| <b>cg07056644</b> | 0.149  | 0.005 | -0.038 | 0.53  | 16 | <i>FOXF1</i>         | S_Shore      |
| <b>cg18306327</b> | -0.229 | 0.006 | 0.052  | 0.39  | 16 | <i>BFAF</i>          | TSS200       |
| <b>cg19288752</b> | -0.203 | 0.006 | -0.007 | 0.907 | 2  | <i>DTYMK</i>         | Island       |
| <b>cg11968414</b> | -0.211 | 0.007 | 0.09   | 0.191 | 6  | <i>MDCE1.00</i>      | 5UTR         |
| <b>cg05616472</b> | 0.195  | 0.007 | -0.054 | 0.42  | 9  | <i>EHMT1</i>         | Body         |
| <b>cg11170810</b> | 0.223  | 0.008 | 0.043  | 0.545 | 6  | <i>IGF2R</i>         | S_Shore      |
| <b>cg15886596</b> | 0.222  | 0.008 | -0.021 | 0.72  | 19 | <i>WASH5P</i>        | Island       |
| <b>cg03921529</b> | 0.139  | 0.009 | 0.061  | 0.335 | 13 | <i>LINC00327</i>     | N_Shore      |
| <b>cg25958857</b> | -0.218 | 0.009 | 0.037  | 0.562 | 12 | <i>TENCL</i>         | Island       |
| <b>cg20318748</b> | 0.146  | 0.011 | 0.081  | 0.254 | 20 | <i>NANP</i>          | TSS1500      |
| <b>cg17117277</b> | 0.196  | 0.015 | -0.042 | 0.517 | 19 | <i>ZFR2</i>          | Body         |
| <b>cg00067274</b> | 0.151  | 0.016 | 0.079  | 0.219 | 4  | <i>DCHS2</i>         | TSS1500;Body |
| <b>cg06028605</b> | 0.128  | 0.016 | -0.031 | 0.669 | 16 | <i>SLC5A11</i>       | 5UTR         |
| <b>cg01098234</b> | -0.193 | 0.018 | -0.123 | 0.077 | 11 | <i>FAM86GP</i>       | Island       |
| <b>cg11663481</b> | -0.159 | 0.019 | -0.076 | 0.195 | 3  | <i>TMEM41A</i>       | Island       |
| <b>cg22878693</b> | 0.138  | 0.033 | -0.09  | 0.207 | 17 | <i>RPTOR</i>         | Body         |
| <b>cg06698093</b> | 0.165  | 0.037 | -0.053 | 0.397 | 8  | <i>AC084082.3</i>    | S_Shore      |

|                   |        |       |        |       |    |                |           |         |
|-------------------|--------|-------|--------|-------|----|----------------|-----------|---------|
| cg04930211        | -0.17  | 0.037 | 0.008  | 0.9   | 22 | <i>FAM19A5</i> | Body      |         |
| <b>cg00892999</b> | -0.204 | 0.041 | -0.01  | 0.874 | 4  | <i>GAK</i>     | Body      | N_Shore |
| <b>cg13918948</b> | -0.151 | 0.043 | -0.084 | 0.198 | 10 | <i>DIP2C</i>   | Body      |         |
| cg00061313        | 0.251  | 0     |        |       | 10 |                |           |         |
| cg00241558        | -0.216 | 0     |        |       | 10 |                |           |         |
| cg01181929        | 0.125  | 0.013 |        |       | 12 | <i>PLEKHG6</i> | TSS1500   | Island  |
| cg01344289        | -0.223 | 0.002 |        |       | 15 | <i>GNB5</i>    | Body      |         |
| cg03137783        | -0.215 | 0     |        |       | 1  | <i>HIVEP3</i>  | 5UTR      |         |
| cg03251789        | -0.203 | 0.002 |        |       | 15 |                |           |         |
| cg04124763        | 0.213  | 0.008 |        |       | 19 |                |           |         |
| cg04400433        | -0.27  | 0.001 |        |       | 6  | <i>PKIB</i>    | 5UTR      |         |
| cg04591284        | 0.205  | 0.002 |        |       | 22 | <i>CRKL</i>    | TSS1500   |         |
| cg04854616        | -0.21  | 0.003 |        |       | 22 | <i>ZC3H7B</i>  | 5UTR      |         |
| cg04857808        | -0.244 | 0     |        |       | 1  | <i>APHL4</i>   | Body;     | N_Shore |
| cg05271437        | -0.18  | 0.042 |        |       | 8  | <i>NUDCDI</i>  | Body      |         |
| cg05747243        | 0.206  | 0.004 |        |       | 15 | <i>SQRDL</i>   | TSS1500   | N_Shelf |
| cg06672144        | 0.209  | 0     |        |       | 18 |                |           |         |
| cg06795516        | -0.186 | 0.025 |        |       | 17 | <i>LRRC75A</i> | Body;Body |         |
| cg06895337        | -0.251 | 0     |        |       | 19 | <i>GLTSCR1</i> | 5UTR      |         |
| cg09961998        | -0.155 | 0.005 |        |       | 7  | <i>TPK1</i>    | Body      |         |
| cg11747595        | -0.195 | 0.003 |        |       | 1  | <i>PODN</i>    | TSS1500   | N_Shore |
| cg11764125        | -0.155 | 0.014 |        |       | 1  | <i>GNGL2</i>   | 5UTR      |         |
| cg11984187        | -0.285 | 0     |        |       | 1  | <i>SH3D21</i>  | Body      |         |
| cg12154726        | -0.184 | 0.002 |        |       | 22 | <i>MYO18B</i>  | Body      |         |
| cg12524068        | -0.266 | 0     |        |       | 1  | <i>LRIG2</i>   | Body      |         |
| cg12558795        | -0.203 | 0.001 |        |       | 7  |                |           |         |
| cg12691745        | 0.238  | 0.002 |        |       | 13 | <i>COG6</i>    | Body      |         |
| cg12774854        | 0.236  | 0.002 |        |       | 17 | <i>ANKFV1</i>  | Body      |         |
| cg13246505        | -0.195 | 0     |        |       | 19 | <i>LRFNI</i>   | TSS200    | S_Shore |

|            |        |       |    |                 |         |         |
|------------|--------|-------|----|-----------------|---------|---------|
| cg13575045 | -0.236 | 0.002 | 22 | <i>PLA2G3</i>   | TSS1500 |         |
| cg13982174 | -0.218 | 0     | 2  |                 |         |         |
| cg14188354 | 0.187  | 0.024 | 3  | <i>EOMES</i>    | 5UTR    | Island  |
| cg14273507 | 0.197  | 0.002 | 18 |                 |         |         |
| cg14715653 | -0.203 | 0.001 | 17 |                 |         |         |
| cg14894593 | 0.214  | 0.001 | 1  |                 |         |         |
| cg15668843 | -0.221 | 0.001 | 2  |                 |         |         |
| cg15956957 | -0.165 | 0.004 | 12 | <i>ENO2</i>     | Body    | S_Shelf |
| cg17097187 | -0.271 | 0     | 1  |                 |         | S_Shore |
| cg17697043 | 0.19   | 0     | 20 |                 |         |         |
| cg18005079 | 0.21   | 0.001 | 15 |                 |         |         |
| cg18491851 | 0.202  | 0.014 | 1  | <i>Clorf106</i> | Body    | N_Shore |
| cg18925412 | 0.132  | 0.037 | 2  |                 |         |         |
| cg19727897 | -0.152 | 0.025 | 11 | <i>SMTNL1</i>   | TS200   |         |
| cg20587396 | -0.266 | 0     | 1  |                 |         |         |
| cg21463078 | -0.187 | 0.014 | 14 |                 |         |         |
| cg21981207 | 0.24   | 0     | 21 | <i>PDXK</i>     | Body    |         |
| cg23507180 | -0.24  | 0.001 | 1  | <i>PAX7</i>     | Body    |         |
| cg25561286 | -0.138 | 0.041 | 12 |                 |         |         |

Supplement Table S7 (B): Direct association of DNAm at birth at 193 CpG sites in females, with asthma acquisition from pre- to post-adolescence.

| CpGs       | LOWBC  | LOWBC | ALSpAC | ALSpAC | CHR | Gene   | Gene location | CpG Is'land |
|------------|--------|-------|--------|--------|-----|--------|---------------|-------------|
| cg07823273 | -0.249 | 0     | -0.176 | 0.002  | 19  | SYCN   | TSS200        | S_Shore     |
| cg04011711 | -0.226 | 0     | -0.137 | 0.015  | 8   | ANGPT2 | Body          |             |
| cg09890200 | -0.222 | 0     | -0.116 | 0.021  | 2   | PRKRA  | TSS1500       |             |
| cg14291650 | -0.217 | 0     | -0.124 | 0.022  | 15  | MTFMT  | Island        |             |
| cg04491367 | -0.232 | 0     | -0.113 | 0.023  | 16  | ZNF778 | S_Shelf       | Island      |

|            |        |   |        |       |    |                      |              |         |
|------------|--------|---|--------|-------|----|----------------------|--------------|---------|
| cg21330703 | -0.235 | 0 | -0.115 | 0.029 | 11 | <i>DRD2</i>          | TSS1500      | S_Shore |
| cg22103637 | -0.27  | 0 | -0.1   | 0.055 | 13 | <i>HS65T3</i>        | TSS1500      | N_Shore |
| cg26580576 | -0.224 | 0 | -0.099 | 0.068 | 4  | <i>LOC93622</i>      | TS200        | Island  |
| cg19807836 | 0.241  | 0 | 0.094  | 0.071 | 1  | <i>NEK7</i>          |              |         |
| cg02960777 | -0.183 | 0 | 0.1    | 0.082 | 7  | <i>PHTF2</i>         | Body         |         |
| cg07834476 | -0.201 | 0 | -0.085 | 0.091 | 10 | <i>ENKUR,THNSLI</i>  | TSS1500;5UTR | Island  |
| cg03016446 | -0.249 | 0 | -0.093 | 0.107 | 10 | <i>CBARAI</i>        | TSS1500      | S_Shore |
| cg18393722 | -0.218 | 0 | -0.086 | 0.123 | 15 | <i>UBE2QPI</i>       | Body         | Island  |
| cg02054358 | -0.233 | 0 | -0.076 | 0.126 | 17 | <i>LINC0051I</i>     |              |         |
| cg17339484 | -0.227 | 0 | -0.079 | 0.129 | 10 | <i>RHOBTBI</i>       | Body         | Island  |
| cg22085380 | 0.236  | 0 | 0.09   | 0.149 | 3  | <i>FSTLL</i>         |              | S_Shelf |
| cg04080041 | -0.207 | 0 | -0.073 | 0.174 | 5  | <i>PCDHG44</i>       | Body         | Island  |
| cg14714391 | -0.24  | 0 | -0.073 | 0.174 | 5  | <i>F2R</i>           | TSS1500      | N_Shore |
| cg22708914 | -0.209 | 0 | -0.072 | 0.175 | 8  | <i>SH2D4A</i>        | TS1500       | N_Shore |
| cg07199257 | -0.248 | 0 | -0.076 | 0.177 | 15 | <i>CRABPI</i>        | 3'UTR        |         |
| cg24739326 | -0.206 | 0 | -0.069 | 0.196 | 19 | <i>CHST8</i>         | 5'UTR        |         |
| cg11846905 | 0.207  | 0 | 0.073  | 0.208 | 12 | <i>NTS</i>           |              | Island  |
| cg08230105 | 0.208  | 0 | -0.071 | 0.215 | 17 | <i>RPL1-3920I.4</i>  |              |         |
| cg24736380 | 0.191  | 0 | 0.07   | 0.221 | 10 | <i>PFKP</i>          | Body         | N_Shore |
| cg05653887 | -0.226 | 0 | -0.058 | 0.273 | 22 | <i>CELSRI</i>        | Body         | N_Shelf |
| cg00740870 | -0.244 | 0 | -0.061 | 0.29  | 14 | <i>PLEKHHI</i>       | Body         |         |
| cg22329021 | -0.205 | 0 | -0.061 | 0.305 | 4  | <i>RPL1-1398P2.I</i> |              | S_Shelf |
| cg20730619 | 0.248  | 0 | 0.055  | 0.323 | 5  | <i>SLC12A7</i>       | Body         | S_Shore |
| cg14159342 | -0.235 | 0 | -0.055 | 0.331 | 1  | <i>TP73</i>          | Body         | S_Shore |
| cg14868994 | -0.236 | 0 | -0.052 | 0.334 | 2  | <i>LINC01833</i>     |              | Island  |
| cg11586330 | -0.199 | 0 | -0.054 | 0.345 | 12 | <i>LHX5</i>          | 3'UTR        | Island  |
| cg11414821 | -0.226 | 0 | -0.051 | 0.355 | 6  | <i>KIAA1949</i>      | Body;1stExon | N_Shore |
| cg16825643 | 0.261  | 0 | 0.048  | 0.367 | 16 | <i>FAM38A</i>        | Body         | N_Shore |
| cg01120851 | 0.222  | 0 | -0.056 | 0.368 | 1  | <i>KLHL2I</i>        | Body         | N_Shore |

|                    |        |   |        |       |    |                      |                 |         |
|--------------------|--------|---|--------|-------|----|----------------------|-----------------|---------|
| <b>cg00530448</b>  | -0.212 | 0 | -0.052 | 0.386 | 11 | <i>NELLI</i>         | Body            | Island  |
| <b>cg22824651</b>  | -0.212 | 0 | -0.045 | 0.39  | 12 | <i>RPS4P52</i>       | Island          | Island  |
| <b>cg03059112</b>  | -0.22  | 0 | 0.048  | 0.416 | 12 | <i>FKBP11</i>        | 1stExon         | Island  |
| <b>cg02122376</b>  | -0.223 | 0 | -0.041 | 0.423 | 5  | <i>G3BPI</i>         | TSS1500         | Island  |
| <b>cg11970192</b>  | -0.203 | 0 | -0.04  | 0.444 | 15 | <i>C15orf37,ST20</i> | Body;5UTR       | Island  |
| <b>cg06988995</b>  | -0.244 | 0 | -0.038 | 0.491 | 10 | <i>CSGALNACT2</i>    | TSS200          | Island  |
| <b>cg02838492</b>  | -0.211 | 0 | -0.038 | 0.498 | 9  | <i>KIF12</i>         | 1stExon;5UTR    | Island  |
| <b>cg01193064</b>  | -0.222 | 0 | -0.036 | 0.525 | 21 | <i>CBS</i>           | 5'UTR           | Island  |
| <b>cg13246264</b>  | -0.193 | 0 | -0.034 | 0.527 | 3  | <i>LRCH3</i>         | TSS1500         | N_Shore |
| <b>cg15161177</b>  | -0.197 | 0 | 0.034  | 0.554 | 12 | <i>TIMELESS</i>      | TSS1500         | S_Shore |
| <b>cg12527440</b>  | 0.237  | 0 | 0.03   | 0.555 | 19 | <i>ZSWIM4</i>        | Body            | S_Shore |
| <b>cg10777851</b>  | -0.277 | 0 | -0.037 | 0.563 | 3  | <i>CD200</i>         | TSS200          | N_Shore |
| <b>cg06513695</b>  | -0.222 | 0 | -0.034 | 0.574 | 22 | <i>RPLIS</i>         | Island          | Island  |
| <b>cg09457121</b>  | 0.199  | 0 | -0.031 | 0.576 | 2  | <i>OBSLI</i>         | Island          | Island  |
| <b>cg03827835</b>  | 0.217  | 0 | -0.027 | 0.593 | 5  | <i>C5orf66</i>       | S_Shore         | S_Shore |
| <b>cg10527525</b>  | -0.243 | 0 | -0.032 | 0.595 | 7  | <i>AUTS2</i>         | Body            | Island  |
| <b>cg04115418</b>  | -0.246 | 0 | -0.027 | 0.608 | 20 | <i>STMN3</i>         | Body            | Island  |
| <b>cg06730718</b>  | -0.212 | 0 | -0.036 | 0.619 | 16 | <i>PAPD5</i>         | TSS1500         | N_Shore |
| <b>cg17125699</b>  | -0.222 | 0 | -0.027 | 0.629 | 17 | <i>WSCDI</i>         | S_Shore         | S_Shore |
| <b>cg18478319</b>  | -0.228 | 0 | -0.026 | 0.652 | 13 | <i>SLC15A1</i>       | TSS200          | S_Shore |
| <b>cg093367367</b> | -0.233 | 0 | 0.028  | 0.654 | 12 | <i>RPL6</i>          | TSS200          | S_Shore |
| <b>cg11154384</b>  | -0.237 | 0 | 0.026  | 0.654 | 15 | <i>C15orf61</i>      | Body            | S_Shore |
| <b>cg21722639</b>  | 0.216  | 0 | 0.023  | 0.672 | 11 | <i>TOLLIP</i>        | Body            | S_Shore |
| <b>cg16622920</b>  | -0.228 | 0 | -0.023 | 0.683 | 6  | <i>HCG16</i>         | Island          | Island  |
| <b>cg16287252</b>  | -0.229 | 0 | -0.023 | 0.704 | 12 | <i>GLTID1</i>        | Body            | Island  |
| <b>cg11346837</b>  | -0.227 | 0 | 0.022  | 0.713 | 3  | <i>RPL1-649A16.1</i> |                 |         |
| <b>cg20983032</b>  | -0.198 | 0 | -0.018 | 0.737 | 19 | <i>ATF5</i>          | Body            | Island  |
| <b>cg26816426</b>  | 0.217  | 0 | -0.019 | 0.75  | 8  | <i>JPH1</i>          | TSS1500;1stExon | Island  |
| <b>cg05033322</b>  | -0.226 | 0 | 0.018  | 0.772 | 11 | <i>ATM</i>           |                 |         |

|                   |        |       |        |       |    |                      |              |         |
|-------------------|--------|-------|--------|-------|----|----------------------|--------------|---------|
| <b>cg09386054</b> | -0.23  | 0     | 0.014  | 0.813 | 14 | <i>RPLI-1082A3.1</i> |              |         |
| <b>cg20171559</b> | -0.229 | 0     | -0.015 | 0.825 | 7  | <i>HOXA1</i>         | N_Shore      |         |
| <b>cg18448991</b> | -0.227 | 0     | 0.012  | 0.836 | 20 | <i>MIR941-3</i>      | TS2005UTR    | Island  |
| <b>cg15371806</b> | -0.251 | 0     | -0.009 | 0.881 | 6  | <i>KIF25</i>         | TS1500       |         |
| <b>cg18244483</b> | -0.192 | 0     | -0.008 | 0.884 | 4  | <i>LINC02173</i>     |              |         |
| <b>cg11990770</b> | 0.259  | 0     | 0.007  | 0.909 | 10 | <i>CFAP46</i>        |              |         |
| <b>cg21144922</b> | 0.18   | 0     | -0.005 | 0.941 | 1  | <i>C1orf59</i>       | TSS200       |         |
| <b>cg27224718</b> | -0.224 | 0     | -0.004 | 0.942 | 8  | <i>ZFAT</i>          | Body         |         |
| <b>cg15001132</b> | -0.233 | 0     | -0.004 | 0.949 | 13 | <i>NUP11</i>         | 5'UTR        |         |
| <b>cg04233664</b> | -0.213 | 0     | -0.003 | 0.966 | 10 | <i>CTBP2</i>         | Island       |         |
| <b>cg27232494</b> | 0.202  | 0     | -0.002 | 0.978 | 17 | <i>TOMM2</i>         | Body         |         |
| <b>cg12264049</b> | -0.246 | 0     | -0.001 | 0.979 | 4  | <i>MED28</i>         | Body         |         |
| <b>cg06239131</b> | 0.224  | 0     | -0.001 | 0.99  | 1  | <i>LOC115110</i>     | Body         |         |
| <b>cg25404454</b> | 0.194  | 0.001 | 0.133  | 0.002 | 4  | <i>GABL</i>          | Body         |         |
| <b>cg05770947</b> | 0.2    | 0.001 | 0.137  | 0.011 | 12 | <i>SLC2A13</i>       | Body         |         |
| <b>cg09614565</b> | -0.201 | 0.001 | -0.132 | 0.023 | 3  | <i>IL17RD</i>        | TSS200       |         |
| <b>cg07629844</b> | -0.199 | 0.001 | -0.089 | 0.091 | 1  | <i>CAPN2</i>         | TSS200;Body  |         |
| <b>cg03296761</b> | -0.188 | 0.001 | 0.076  | 0.186 | 22 | <i>MTPE18.00</i>     | Body         | S_Shore |
| <b>cg10324701</b> | 0.226  | 0.001 | 0.063  | 0.273 | 12 | <i>RPLI-897M7.1</i>  | TSS1500      | Island  |
| <b>cg10200608</b> | -0.177 | 0.001 | -0.058 | 0.323 | 5  | <i>KIAA0141</i>      |              |         |
| <b>cg07660473</b> | 0.205  | 0.001 | -0.057 | 0.347 | 16 | <i>BEAN</i>          | 5'UTR        |         |
| <b>cg20241375</b> | -0.191 | 0.001 | 0.049  | 0.36  | 4  | <i>ZNF732</i>        | N_Shelf      |         |
| <b>cg10346242</b> | -0.209 | 0.001 | -0.034 | 0.508 | 12 | <i>ARF3</i>          | S_Shore      |         |
| <b>cg07926996</b> | -0.229 | 0.001 | 0.029  | 0.612 | 2  | <i>PREPL</i>         | 1stExon      | N_Shore |
| <b>cg08111661</b> | -0.192 | 0.001 | 0.026  | 0.613 | 12 | <i>CACNA1C</i>       | Body         | N_Shore |
| <b>cg21868063</b> | -0.194 | 0.001 | 0.022  | 0.701 | 17 | <i>MGAT5B</i>        | Body;1stExon | S_Shelf |
| <b>cg01165752</b> | 0.208  | 0.001 | -0.019 | 0.733 | 16 | <i>HMGGN2P4I</i>     |              |         |
| <b>cg26408861</b> | 0.169  | 0.001 | 0.014  | 0.795 | 1  | <i>LHX4</i>          | Body         |         |
| <b>cg14597726</b> | 0.208  | 0.001 | -0.01  | 0.865 | 13 | <i>LINC00358</i>     |              |         |

|                    |        |       |        |         |    |             |              |         |
|--------------------|--------|-------|--------|---------|----|-------------|--------------|---------|
| <b>cg18694780</b>  | -0.188 | 0.002 | -0.123 | 0.019   | 2  | CXCR7       | TSS1500      | S_Shore |
| <b>cg22979546</b>  | 0.184  | 0.002 | 0.091  | 0.132   | 15 | HERC2       | Body         |         |
| <b>cg06365057</b>  | -0.216 | 0.002 | -0.074 | 0.164   | 10 | C10orf72    | TSS200       | Island  |
| <b>cg16980245</b>  | 0.193  | 0.002 | -0.06  | 0.219   | 15 | SNORD115-42 | TSS200       |         |
| <b>cg09884451</b>  | -0.184 | 0.002 | 0.033  | 0.563   | 4  | ZFYVE28     | Body         | Island  |
| <b>cg19805217</b>  | 0.18   | 0.003 | -0.09  | 0.112   | 10 | RPL428G2.I  | Body         |         |
| <b>cg23121394</b>  | -0.156 | 0.003 | -0.081 | 0.197   | 6  | C6orf123    | Body         | Island  |
| <b>cg22027725</b>  | 0.17   | 0.003 | 0.055  | 0.241   | 11 | SLC37A2     |              |         |
| <b>cg25989745</b>  | 0.202  | 0.003 | 0.058  | 0.32    | 9  | TYRPI       | TSS200       |         |
| <b>cg21042248</b>  | -0.188 | 0.003 | 0.016  | 0.782   | 19 | MGCC2752    | Body         | N_Shore |
| <b>cg27424226</b>  | 0.179  | 0.004 | -0.062 | 0.281   | 22 | HIF0        | 1stExon;5UTR | Island  |
| <b>cg26310551</b>  | -0.191 | 0.004 | 0.03   | 0.613   | 14 | LTB4R2      | Body         | Island  |
| <b>cg26647291</b>  | 0.143  | 0.004 | 0.015  | 0.799   | 11 | ESRA        | Body         | N_Shelf |
| <b>cg23844910</b>  | 0.193  | 0.005 | 0.042  | 0.442   | 1  | RPL90C4.I   |              |         |
| <b>cg02532113</b>  | 0.17   | 0.006 | 0.119  | 0.041   | 6  | RP5-99IC6.2 |              |         |
| <b>cg187333820</b> | 0.19   | 0.007 | -0.069 | 0.227   | 17 | PSMD12      |              |         |
| <b>cg15096549</b>  | 0.172  | 0.007 | 0.054  | 0.29    | 11 | RPL680E19.I | TSS200       | Island  |
| <b>cg01679206</b>  | -0.154 | 0.017 | 0.031  | 0.613   | 7  | WBSCR27     | Body         | N_Shelf |
| <b>cg14563196</b>  | -0.149 | 0.024 | -0.009 | 0.88    | 1  | GBP4        | 1stExon;5UTR |         |
| <b>cg02458483</b>  | -0.127 | 0.031 | -0.053 | 0.377   | 1  | KIAA1522    | TSS1500      | N_Shore |
| <b>cg13181604</b>  | -0.126 | 0.046 | 0.002  | 0.971   | 14 | NEDD8GMPR2  | Body;        | N_Shore |
| <b>cg00141391</b>  | 0.126  | 0.021 | 8      |         |    |             |              |         |
| <b>cg00526274</b>  | 0.189  | 0.001 | 5      | CTNNAI  |    | Body        |              |         |
| <b>cg01199509</b>  | -0.218 | 0     | 1      | SRGAP2C |    | Body        |              |         |
| <b>cg01329939</b>  | 0.181  | 0.004 | 12     | ANO2    |    | Body        |              |         |
| <b>cg01492536</b>  | -0.279 | 0     | 17     |         |    |             |              |         |
| <b>cg02086971</b>  | -0.218 | 0     | 16     | NSMCE1  |    | Body        |              |         |
| <b>cg03080605</b>  | 0.208  | 0     | 1      | LAPTM4A |    | TSS1500     |              |         |
| <b>cg03220054</b>  | 0.176  | 0     | 2      |         |    | S_Shore     |              |         |

|            |        |       |    |                       |
|------------|--------|-------|----|-----------------------|
| cg03335248 | -0.208 | 0.001 | 2  |                       |
| cg03808748 | 0.208  | 0     | 3  |                       |
| cg04021692 | -0.212 | 0     | 9  | <i>KIF12</i>          |
| cg04214626 | -0.207 | 0     | 11 |                       |
| cg04349509 | -0.249 | 0     | 1  |                       |
| cg04445379 | 0.224  | 0     | 5  |                       |
| cg04531165 | 0.211  | 0.001 | 14 | <i>EML5</i>           |
| cg04725937 | 0.251  | 0     | 2  | <i>ACTG2</i>          |
| cg04742865 | 0.201  | 0     | 18 |                       |
| cg04830702 | 0.235  | 0     | 17 | <i>AKAP1</i>          |
| cg04852236 | 0.19   | 0.001 | 2  | <i>ILIR1</i>          |
| cg05001024 | 0.189  | 0.001 | 4  | <i>ABCA11P,ZNF721</i> |
| cg05195455 | 0.155  | 0.005 | 12 | <i>CPSF6</i>          |
| cg06005684 | 0.236  | 0     | 1  |                       |
| cg06082013 | -0.222 | 0     | 18 | <i>TCF4</i>           |
| cg06198596 | -0.259 | 0     | 17 | <i>SPECCI</i>         |
| cg06330158 | -0.212 | 0     | 14 | <i>GPHN</i>           |
| cg06591620 | -0.23  | 0     | 3  | <i>ZNF148</i>         |
| cg07068547 | -0.177 | 0.003 | 16 | <i>TFAP4</i>          |
| cg07236381 | -0.225 | 0     | 5  | <i>AFF4</i>           |
| cg07250429 | 0.242  | 0     | 15 | <i>RORA</i>           |
| cg07741172 | 0.186  | 0     | 21 | <i>TSPEAR-AS2</i>     |
| cg09378610 | 0.213  | 0     | 15 |                       |
| cg09704765 | 0.226  | 0     | 8  | <i>NCALD</i>          |
| cg09728232 | 0.245  | 0     | 9  |                       |
| cg10289292 | 0.169  | 0.001 | 15 | N_Shore               |
| cg10597549 | 0.259  | 0     | 1  | <i>CDK18</i>          |
| cg10729726 | 0.098  | 0.035 | 1  | <i>CACNAIS</i>        |
| cg10771019 | 0.167  | 0.006 | 16 | <i>GSEI</i>           |
|            |        |       |    | 5'UTR                 |
|            |        |       |    | Island                |
|            |        |       |    | N_Shore               |
|            |        |       |    | S_Shore               |
|            |        |       |    | N_Shore               |
|            |        |       |    | N_Shore               |
|            |        |       |    | S_Shore               |
|            |        |       |    | Body                  |
|            |        |       |    | 1stExon;5'UTR         |
|            |        |       |    | Island                |
|            |        |       |    | Body                  |
|            |        |       |    | Body                  |
|            |        |       |    | TSS200                |
|            |        |       |    | TSS1500               |
|            |        |       |    | TSS200                |
|            |        |       |    | TSS1500               |
|            |        |       |    | N_Shore               |
|            |        |       |    | N_Shore               |
|            |        |       |    | S_Shore               |
|            |        |       |    | N_Shore               |
|            |        |       |    | Body                  |
|            |        |       |    | Body                  |
|            |        |       |    | TSS200                |
|            |        |       |    | 5'UTR                 |

|            |        |       |    |                     |               |         |
|------------|--------|-------|----|---------------------|---------------|---------|
| cg10852829 | -0.219 | 0.001 | 7  | <i>CCDC126</i>      | 5'UTR         | S_Shore |
| cg11177277 | -0.172 | 0.003 | 4  | <i>PALLD</i>        | 5'UTR         | S_Shelf |
| cg11270792 | -0.245 | 0     | 1  |                     |               |         |
| cg11805806 | -0.203 | 0     | 12 |                     |               |         |
| cg12022883 | -0.217 | 0     | 1  | 7                   | <i>BMPER</i>  | Body    |
| cg12026805 | -0.206 | 0     | 1  |                     |               |         |
| cg12305405 | 0.232  | 0     | 7  | <i>LAT2</i>         | 3'UTR         |         |
| cg12777182 | 0.212  | 0.002 | 6  |                     |               |         |
| cg12952987 | 0.162  | 0.004 | 4  | <i>SORCS2</i>       | Body          |         |
| cg13201279 | -0.283 | 0     | 1  | <i>KCNK2</i>        | 5'UTR;1stExon |         |
| cg13225210 | -0.129 | 0.024 | 1  | <i>TMEM39B</i>      | Body          |         |
| cg13371260 | -0.215 | 0     | 1  | <i>BCAN</i>         | 1stExon       |         |
| cg14614346 | -0.204 | 0     | 4  | <i>FAM198B</i>      | Body          |         |
| cg14744604 | 0.214  | 0.001 | 14 | <i>ITPK1</i>        | Body          |         |
| cg14811849 | -0.232 | 0     | 8  |                     |               |         |
| cg14980188 | -0.205 | 0.002 | 17 | <i>NARF</i>         | 5'UTR         |         |
| cg15241587 | -0.191 | 0     | 20 | <i>LINC01522</i>    | Body          |         |
| cg15303182 | 0.217  | 0     | 17 | <i>ZBTB4;ZBTB4</i>  | Body          |         |
| cg16464301 | 0.185  | 0.002 | 12 | <i>LOC101927653</i> | Body          |         |
| cg16473632 | -0.238 | 0     | 17 | <i>SDK2</i>         | Body          |         |
| cg16556211 | 0.237  | 0     | 4  |                     |               |         |
| cg16673168 | -0.229 | 0     | 11 | <i>PAFAHIB2</i>     | TSS1500       | N_Shore |
| cg18074323 | 0.226  | 0     | 16 | <i>EDC4</i>         | Body          | N_Shelf |
| cg18749178 | -0.197 | 0.001 | 1  |                     |               |         |
| cg19198400 | -0.23  | 0     | 5  | <i>TSLP</i>         | TSS200        | N_Shelf |
| cg19292908 | 0.176  | 0.004 | 22 | <i>PRAME</i>        | 5'UTR         | N_Shore |
| cg19358359 | -0.215 | 0     | 17 | <i>MPP2</i>         | TSS1500       | S_Shore |
| cg19389227 | -0.122 | 0.035 | 13 |                     |               |         |
| cg20079855 | 0.216  | 0     | 3  |                     |               |         |

|            |        |       |    |
|------------|--------|-------|----|
| cg20422386 | -0.198 | 0.002 | 1  |
| cg20595382 | -0.191 | 0     | 8  |
| cg20603632 | 0.218  | 0     | 12 |
| cg20996735 | -0.207 | 0     | 6  |
| cg21812071 | -0.23  | 0     | 12 |
| cg22842768 | -0.276 | 0     | 1  |
| cg23976120 | 0.222  | 0     | 2  |
| cg24409590 | -0.209 | 0     | 16 |
| cg24869879 | -0.228 | 0     | 2  |
| cg25279605 | 0.235  | 0     | 2  |
| cg26604499 | -0.219 | 0     | 16 |
| cg26906383 | 0.187  | 0.001 | 2  |
| cg27575609 | -0.23  | 0     | 1  |

Supplement Table S8 (A): Association of DNA methylation with neighboring gene expression (n=55)

| coefficient | Pvalue   | CpGs       | Genes         |
|-------------|----------|------------|---------------|
| 1           | 0        | cg19987540 | <i>AKR1E2</i> |
| 0.996115    | 5.14E-11 | cg25121621 | <i>COPRS</i>  |
| 1.340203    | 1.48E-09 | cg25121621 | <i>PAGRI</i>  |
| 0.785081    | 7.66E-09 | cg25121621 | <i>GDPD3</i>  |
| 0.5177      | 1.16E-08 | cg25121621 | <i>TBX6</i>   |
| 0.650241    | 1.85E-08 | cg25121621 | <i>LTN1</i>   |
| 0.626171    | 2.66E-08 | cg25121621 | <i>HIRIP3</i> |
| 0.882073    | 4.30E-08 | cg25121621 | <i>ASCC2</i>  |
| 0.493743    | 2.54E-07 | cg25121621 | <i>TRIM31</i> |
| 0.538803    | 6.39E-07 | cg14080518 | <i>ATP5A1</i> |
| 0.641589    | 1.71E-06 | cg25121621 | <i>TRIM40</i> |
| 0.583802    | 1.82E-06 | cg25121621 | <i>DOC2A</i>  |
| 0.337716    | 5.21E-06 | cg25121621 | <i>SLC7A1</i> |

|          |          |            |               |
|----------|----------|------------|---------------|
| -0.50334 | 5.88E-06 | cg20250341 | <i>BRI3BP</i> |
| 0.578815 | 6.13E-06 | cg25121621 | <i>CDIPT</i>  |
| 0.785116 | 1.09E-05 | cg19288752 | <i>CELA1</i>  |
| 0.439368 | 1.68E-05 | cg25121621 | <i>TMTC1</i>  |
| -0.57209 | 1.95E-05 | cg14080518 | <i>PAIP1</i>  |
| 0.538247 | 2.49E-05 | cg25121621 | <i>SVIL</i>   |
| 1.272328 | 6.43E-05 | cg16781287 | <i>CEP192</i> |
| 0.438529 | 7.32E-05 | cg19288752 | <i>FAM21A</i> |
| 0.602809 | 8.70E-05 | cg25121621 | <i>MTUS2</i>  |
| 0.815957 | 0.000143 | cg01098234 | <i>ARRDC1</i> |
| 0.242793 | 0.000178 | cg02776315 | <i>AGRN</i>   |
| -0.33121 | 0.000199 | cg25121621 | <i>TAOK2</i>  |
| -0.5935  | 0.000207 | cg25121621 | <i>DCTN6</i>  |
| 0.917735 | 0.000211 | cg25121621 | <i>FKBP14</i> |
| -0.64462 | 0.000226 | cg14080518 | <i>UBRI</i>   |
| 0.605009 | 0.000229 | cg25121621 | <i>CORO1A</i> |
| -0.62517 | 0.00026  | cg14080518 | <i>STK4</i>   |
| 0.887041 | 0.000294 | cg01098234 | <i>TUBB4B</i> |
| 0.42375  | 0.000301 | cg19288752 | <i>MBD2</i>   |
| 528.6448 | 0.000383 | cg20250341 | <i>AACS</i>   |
| 0.403133 | 0.000451 | cg19288752 | <i>SLC448</i> |
| 0.443992 | 0.000484 | cg25121621 | <i>RPP21</i>  |
| -0.28898 | 0.000579 | cg13331559 | <i>EXTL3</i>  |
| -0.5668  | 0.000682 | cg20250341 | <i>SNX4</i>   |
| -0.45488 | 0.00074  | cg10855395 | <i>COPZ2</i>  |
| 0.89677  | 0.000782 | cg01098234 | <i>RAB33B</i> |
| 0.997896 | 0.00091  | cg16781287 | <i>GPRC5D</i> |
| 0.869628 | 0.00094  | cg01098234 | <i>BRAF</i>   |
| 1.602771 | 0.000943 | cg16781287 | <i>FAM9C</i>  |
| 0.793746 | 0.001149 | cg19288752 | <i>FRMD6</i>  |
| 0.717724 | 0.001269 | cg25121621 | <i>UTP6</i>   |

|          |          |            |               |
|----------|----------|------------|---------------|
| 0.630309 | 0.001381 | cg25121621 | <i>NEFH</i>   |
| -0.5252  | 0.001418 | cg14080518 | <i>CRIP3</i>  |
| -0.83913 | 0.001524 | cg16781287 | <i>TASPI</i>  |
| 0.42902  | 0.00155  | cg20250341 | <i>RNF139</i> |
| -0.30703 | 0.001578 | cg14080518 | <i>ERMAP</i>  |
| -0.55492 | 0.001868 | cg13139542 | <i>SPCS3</i>  |
| 0.427514 | 0.002089 | cg19288752 | <i>MAGED1</i> |
| -0.66027 | 0.002174 | cg14080518 | <i>GTPBP2</i> |
| 0.391773 | 0.002292 | cg14080518 | <i>TTCI7</i>  |
| -0.73045 | 0.002297 | cg13139542 | <i>PRR7</i>   |
| 0.65202  | 0.002335 | cg16781287 | <i>BEND7</i>  |
| -0.30084 | 0.002373 | cg02776315 | <i>ABC47</i>  |
| 0.183425 | 0.002587 | cg01098234 | <i>ANAPC2</i> |
| 0.537924 | 0.002664 | cg25121621 | <i>SUZ12</i>  |
| 1.247242 | 0.002742 | cg01098234 | <i>NAA15</i>  |
| 0.413378 | 0.00277  | cg25121621 | <i>MTURN</i>  |
| -0.56374 | 0.002887 | cg20250341 | <i>DHX37</i>  |
| 0.679635 | 0.002959 | cg25121621 | <i>KLHL14</i> |
| 0.487107 | 0.002982 | cg01098234 | <i>EHMT1</i>  |
| -0.40538 | 0.003152 | cg13331559 | <i>APOBR</i>  |
| 0.401101 | 0.00324  | cg04214710 | <i>IGF2BP</i> |
| 0.295691 | 0.003483 | cg14093886 | <i>KIF24</i>  |
| 0.751987 | 0.003498 | cg12938020 | <i>SYDE2</i>  |
| 0.268249 | 0.003659 | cg17725477 | <i>HEBPI</i>  |
| -0.49154 | 0.003685 | cg13331559 | <i>BLMH</i>   |
| 0.852727 | 0.003747 | cg01098234 | <i>RNF208</i> |
| 0.364633 | 0.003801 | cg14080518 | <i>SLC2A1</i> |
| -0.34452 | 0.004048 | cg19987540 | <i>PFNI</i>   |
| 0.998641 | 0.004708 | cg16781287 | <i>SEPHSI</i> |
| 0.882772 | 0.00475  | cg01098234 | <i>HARS</i>   |
| 0.340392 | 0.004848 | cg19288752 | <i>SCN8A</i>  |

|          |          |            |               |
|----------|----------|------------|---------------|
| -1.24097 | 0.005144 | cg16781287 | <i>CCDC3</i>  |
| 0.345648 | 0.005293 | cg19288752 | <i>DMLXL2</i> |
| 0.380788 | 0.005533 | cg18073883 | <i>SNDI</i>   |
| -0.1295  | 0.005664 | cg13425962 | <i>ALPK2</i>  |
| -0.4264  | 0.005721 | cg19987540 | <i>CYTL1</i>  |
| 0.428863 | 0.005754 | cg19288752 | <i>RRP9</i>   |
| -0.33256 | 0.006106 | cg20250341 | <i>STT3A</i>  |
| -0.44478 | 0.006165 | cg25165501 | <i>TRIM46</i> |
| 0.53543  | 0.006591 | cg01098234 | <i>RAB19</i>  |
| 0.357756 | 0.007255 | cg02776315 | <i>SOX8</i>   |
| 0.209231 | 0.007265 | cg19288752 | <i>CLDND2</i> |
| -0.33711 | 0.00731  | cg13331559 | <i>EFCAB5</i> |
| -0.42895 | 0.007343 | cg14080518 | <i>SCUBE1</i> |
| -0.47048 | 0.007352 | cg10855395 | <i>TBKBP1</i> |
| 0.347298 | 0.007894 | cg02776315 | <i>METRN</i>  |
| -0.19127 | 0.008537 | cg14080518 | <i>POLRIC</i> |
| -0.63711 | 0.008584 | cg16781287 | <i>NACCI</i>  |
| -0.60162 | 0.008749 | cg20250341 | <i>NDUFB9</i> |
| -0.67467 | 0.009725 | cg19987540 | <i>CHRNE</i>  |
| 0.514161 | 0.009915 | cg02776315 | <i>RAD52</i>  |
| -0.20839 | 0.00997  | cg13425962 | <i>CESIP1</i> |
| -0.31282 | 0.010098 | cg08991599 | <i>RSRC1</i>  |
| 0.57813  | 0.010116 | cg26453588 | <i>PPMIL</i>  |
| 0.572835 | 0.010313 | cg20318748 | <i>NDRG2</i>  |
| -0.64087 | 0.010511 | cg20250341 | <i>HDDC2</i>  |
| 0.25589  | 0.010696 | cg14789960 | <i>AKAP6</i>  |
| 0.047156 | 0.011362 | cg10475970 | <i>ANAPCI</i> |
| 0.254495 | 0.011385 | cg19288752 | <i>POLI</i>   |
| 0.385937 | 0.011681 | cg15909600 | <i>AURKB</i>  |
| 0.552847 | 0.012115 | cg01098234 | <i>TPRN</i>   |
| 0.477949 | 0.012362 | cg02776315 | <i>TMEM18</i> |

|          |          |            |               |
|----------|----------|------------|---------------|
| -0.5421  | 0.012484 | cg19987540 | <i>CSMD1</i>  |
| 0.336494 | 0.012486 | cg01098234 | <i>DPH7</i>   |
| -0.00025 | 0.012491 | cg00067274 | <i>LMF2</i>   |
| 0.530026 | 0.012613 | cg14789960 | <i>EPCI</i>   |
| 0.599867 | 0.013038 | cg01098234 | <i>NDUFCl</i> |
| -0.89414 | 0.013386 | cg16781287 | <i>RAD23A</i> |
| 0.497856 | 0.013421 | cg01098234 | <i>LRRC26</i> |
| 0.223545 | 0.013463 | cg25121621 | <i>TRM26</i>  |
| 0.420948 | 0.013578 | cg02776315 | <i>DGKQ</i>   |
| 0.79402  | 0.013647 | cg01098234 | <i>DND1</i>   |
| 0.737128 | 0.014377 | cg22647738 | <i>FANCA</i>  |
| 0.334207 | 0.015483 | cg01098234 | <i>EXD3</i>   |
| 0.393301 | 0.015623 | cg25121621 | <i>CABP7</i>  |
| -0.38712 | 0.016093 | cg19987540 | <i>ANKS3</i>  |
| 0.576546 | 0.016292 | cg14080518 | <i>TFF3</i>   |
| -0.38324 | 0.016891 | cg10855395 | <i>IPP</i>    |
| 0.432617 | 0.018096 | cg04432599 | <i>MMPII</i>  |
| 0.498346 | 0.018959 | cg26453588 | <i>PEA15</i>  |
| -0.00024 | 0.019777 | cg00067274 | <i>ADM2</i>   |
| -0.59227 | 0.020477 | cg10855395 | <i>CD3E</i>   |
| 0.458692 | 0.020494 | cg16781287 | <i>STX10</i>  |
| -0.29961 | 0.020659 | cg19987540 | <i>NAGPA</i>  |
| -0.65401 | 0.021202 | cg25693132 | <i>COG7</i>   |
| 0.727259 | 0.021258 | cg14789960 | <i>RFPL2</i>  |
| 0.079302 | 0.021465 | cg03488284 | <i>USP19</i>  |
| 0.447974 | 0.021581 | cg20318748 | <i>ZNF219</i> |
| -0.53372 | 0.021684 | cg18073883 | <i>MCM2</i>   |
| 0.254412 | 0.021934 | cg00800038 | <i>NINJ2</i>  |
| 0.309977 | 0.021946 | cg15909600 | <i>TRMT44</i> |
| 0.564316 | 0.022872 | cg18073883 | <i>GOLG4L</i> |
| -0.31266 | 0.023042 | cg19987540 | <i>RB4K</i>   |

|          |          |            |               |
|----------|----------|------------|---------------|
| -0.45076 | 0.023151 | cg19987540 | <i>UBALDI</i> |
| -0.52309 | 0.023389 | cg14080518 | <i>STK17A</i> |
| -0.26807 | 0.023407 | cg00800038 | <i>RHOT2</i>  |
| 0.407399 | 0.023756 | cg14789960 | <i>TAP2</i>   |
| 0.389338 | 0.024784 | cg04432599 | <i>TCERB3</i> |
| 0.237727 | 0.024804 | cg02776315 | <i>FGF22</i>  |
| -0.35807 | 0.025946 | cg02730843 | <i>GPCPDI</i> |
| -0.48064 | 0.026195 | cg14080518 | <i>BMSI</i>   |
| 0.446589 | 0.026554 | cg20318748 | <i>SLC7A4</i> |
| -0.39689 | 0.026804 | cg14093886 | <i>SCAND1</i> |
| 0.221929 | 0.027024 | cg02776315 | <i>GET4</i>   |
| 0.428555 | 0.027637 | cg19288752 | <i>GALNT6</i> |
| -0.22292 | 0.027647 | cg00800038 | <i>VPS53</i>  |
| 0.097624 | 0.027845 | cg13425962 | <i>RDH5</i>   |
| 0.479274 | 0.027869 | cg26453588 | <i>SLAMF6</i> |
| -0.38288 | 0.02787  | cg19987540 | <i>KCN46</i>  |
| 0.229501 | 0.027941 | cg02776315 | <i>TTLL10</i> |
| 0.331949 | 0.027972 | cg18073883 | <i>UROS</i>   |
| -0.5773  | 0.028276 | cg18073883 | <i>ADAM12</i> |
| -0.16179 | 0.028383 | cg13331559 | <i>NPIPB8</i> |
| 0.387407 | 0.028662 | cg00800038 | <i>LRRK2</i>  |
| -0.18441 | 0.028735 | cg13331559 | <i>ZCWPW2</i> |
| -0.11931 | 0.028826 | cg10475970 | <i>DGAT1</i>  |
| 0.59678  | 0.029015 | cg12938020 | <i>SH2D6</i>  |
| -0.78222 | 0.029929 | cg25693132 | <i>NAPB</i>   |
| 0.193826 | 0.030099 | cg19288752 | <i>BIN2</i>   |
| -0.25688 | 0.030803 | cg00800038 | <i>EXOC3</i>  |
| -0.66686 | 0.030823 | cg25165501 | <i>CLK2</i>   |
| 0.302514 | 0.030945 | cg19288752 | <i>CTUI</i>   |
| 0.438057 | 0.031029 | cg02776315 | <i>NXN</i>    |
| -0.60374 | 0.031495 | cg25693132 | <i>DCTN5</i>  |

|          |          |            |        |
|----------|----------|------------|--------|
| 0.484591 | 0.031706 | cg20318748 | ZNF43I |
| 0.771171 | 0.032635 | cg13139542 | LMAN2  |
| 0.634944 | 0.032789 | cg18073883 | FANKI  |
| -0.19642 | 0.03293  | cg0892999  | BMP6   |
| 0.315769 | 0.033176 | cg04432599 | NRID2  |
| 0.362926 | 0.033236 | cg18073883 | ARPC5L |
| -0.24915 | 0.033622 | cg19987540 | GALNT8 |
| -0.43003 | 0.033804 | cg25165501 | THBS3  |
| 0.436408 | 0.034581 | cg26453588 | KPN44  |
| 0.295863 | 0.034992 | cg02776315 | TYMS   |
| 0.370741 | 0.035296 | cg04432599 | FUC4I  |
| -0.45322 | 0.035595 | cg19987540 | STK32B |
| -0.21071 | 0.035794 | cg14080518 | TOMM34 |
| 0.191872 | 0.037001 | cg14093886 | MMP28  |
| 0.556817 | 0.037249 | cg26453588 | BAZ2B  |
| 0.711634 | 0.038235 | cg16781287 | CALLR  |
| -0.38714 | 0.038448 | cg19987540 | PLD2   |
| 0.263068 | 0.038683 | cg04214710 | IRF2   |
| -0.27658 | 0.038754 | cg10855395 | PRKCE  |
| -0.18926 | 0.038915 | cg13331559 | LINGO2 |
| -0.38876 | 0.039009 | cg14080518 | BIK    |
| -0.43759 | 0.03921  | cg20250341 | UBC    |
| 0.274812 | 0.040803 | cg02776315 | JMD8   |
| 0.258628 | 0.040827 | cg14080518 | MAOB   |
| -0.16603 | 0.041301 | cg19558503 | ING5   |
| 0.488836 | 0.041377 | cg04432599 | ZNF726 |
| 0.292591 | 0.043332 | cg04432599 | ID3    |
| 0.000144 | 0.043898 | cg00067274 | KCNC3  |
| -1.22358 | 0.044569 | cg25165501 | ASHIL  |
| 0.254268 | 0.044898 | cg15909600 | TUB    |
| -0.14895 | 0.045202 | cg03921529 | MAP2KI |

|          |          |            |               |
|----------|----------|------------|---------------|
| -0.31274 | 0.045203 | cg02730843 | <i>LONP1</i>  |
| -0.52293 | 0.045223 | cg20250341 | <i>RC3H2</i>  |
| -0.30468 | 0.045359 | cg10855395 | <i>CKM</i>    |
| 0.42769  | 0.045372 | cg19288752 | <i>TFCP2</i>  |
| 0.214434 | 0.045972 | cg02776315 | <i>POLR2E</i> |
| 0.318333 | 0.046357 | cg04432599 | <i>RPL11</i>  |
| -0.25251 | 0.047957 | cg19987540 | <i>DPP9</i>   |
| 0.304856 | 0.048018 | cg01098234 | <i>NELFB</i>  |
| -0.21861 | 0.048196 | cg01098234 | <i>WDR55</i>  |
| 0.638551 | 0.048626 | cg12938020 | <i>ZNF592</i> |
| -0.10228 | 0.048834 | cg19558503 | <i>BOK</i>    |
| -0.13858 | 0.0489   | cg19558503 | <i>STK25</i>  |
| -0.23964 | 0.048916 | cg07452560 | <i>HERC1</i>  |
| 0.280873 | 0.049226 | cg18073883 | <i>PODXL2</i> |

Supplement Table S8 (B): Association of DNAm in females with neighboring gene expression (n=85)

| coefficient | P-value  | CpGs       | Gene            |
|-------------|----------|------------|-----------------|
| 1           | 0        | cg22708914 | <i>ALDH2</i>    |
| -1.84314    | 3.01E-26 | cg04720635 | <i>CCDC7</i>    |
| -0.92871    | 5.38E-10 | cg04720635 | <i>TP53INP2</i> |
| -0.68515    | 2.16E-09 | cg04720635 | <i>MAK16</i>    |
| -1.36396    | 3.74E-09 | cg04720635 | <i>AQP3</i>     |
| -0.40136    | 3.79E-08 | cg04720635 | <i>N4BP2L2</i>  |
| -0.52683    | 2.73E-07 | cg04720635 | <i>SYNGAP1</i>  |
| -0.49397    | 5.44E-07 | cg04720635 | <i>ANKRD27</i>  |
| -0.72536    | 7.25E-07 | cg04720635 | <i>TMEM54</i>   |
| 0.840336    | 9.75E-07 | cg04720635 | <i>NCOA6</i>    |
| -1.34463    | 1.60E-06 | cg04720635 | <i>RP9</i>      |
| -0.65131    | 3.54E-06 | cg02838492 | <i>PI4K2A</i>   |
| -0.42676    | 4.16E-06 | cg04720635 | <i>RFFL</i>     |
| -0.50344    | 5.66E-06 | cg04720635 | <i>TDRD12</i>   |

|          |          |            |                 |
|----------|----------|------------|-----------------|
| 0.587489 | 5.95E-06 | cg04720635 | <i>CEP89</i>    |
| -0.56815 | 6.98E-06 | cg04720635 | <i>SMU1</i>     |
| -0.39016 | 8.00E-06 | cg04720635 | <i>TARS</i>     |
| -0.74814 | 1.28E-05 | cg04720635 | <i>GALNT1</i>   |
| -1.18491 | 1.32E-05 | cg02838492 | <i>UBTD1</i>    |
| -0.50754 | 1.88E-05 | cg04720635 | <i>MAPILC3A</i> |
| 0.390379 | 2.61E-05 | cg06636625 | <i>ABCF2</i>    |
| -0.73341 | 3.17E-05 | cg26580576 | <i>DTX3</i>     |
| -1.17144 | 4.50E-05 | cg26580576 | <i>REST</i>     |
| 0.471511 | 6.23E-05 | cg01193064 | <i>TR42A</i>    |
| 0.325603 | 6.43E-05 | cg04720635 | <i>SYN3</i>     |
| -0.73195 | 7.03E-05 | cg24739326 | <i>CDK5RI</i>   |
| -0.6377  | 9.52E-05 | cg26580576 | <i>ARRHGAP9</i> |
| -0.27891 | 0.000105 | cg04720635 | <i>B4GALT1</i>  |
| -0.59596 | 0.000168 | cg04720635 | <i>RGS9BP</i>   |
| -0.4995  | 0.000184 | cg04720635 | <i>B3GALT4</i>  |
| -0.98188 | 0.000188 | cg26580576 | <i>KATNB1</i>   |
| -1.42817 | 0.000214 | cg26580576 | <i>TUBD1</i>    |
| 0.387642 | 0.000222 | cg16622920 | <i>HOMER3</i>   |
| -0.56075 | 0.000226 | cg02838492 | <i>IGFIR</i>    |
| -0.71616 | 0.000247 | cg02838492 | <i>GJC3</i>     |
| -0.44391 | 0.000258 | cg09890200 | <i>PGRMC1</i>   |
| -0.90366 | 0.00034  | cg26580576 | <i>HEATR6</i>   |
| 0.499198 | 0.000388 | cg16622920 | <i>HAUS6</i>    |
| -0.83463 | 0.000405 | cg04115418 | <i>C1orf159</i> |
| -0.6294  | 0.000425 | cg04720635 | <i>HPCA</i>     |
| -0.40185 | 0.000509 | cg04720635 | <i>TMEM132E</i> |
| -0.81834 | 0.000511 | cg09890200 | <i>CCDC93</i>   |
| -1.10276 | 0.00053  | cg18694780 | <i>NUTM2D</i>   |
| 0.214764 | 0.000533 | cg04115418 | <i>ACAP3</i>    |
| -1.19829 | 0.00067  | cg26580576 | <i>NA430</i>    |

|          |          |            |                 |
|----------|----------|------------|-----------------|
| -0.35857 | 0.0007   | cg09890200 | <i>SLC25A43</i> |
| -2.32443 | 0.000743 | cg26580576 | <i>ZNF17</i>    |
| -0.36431 | 0.00076  | cg04720635 | <i>NUDT19</i>   |
| -0.29356 | 0.000765 | cg04720635 | <i>HIPK3</i>    |
| -0.22082 | 0.00081  | cg10777851 | <i>DGKQ</i>     |
| -0.86713 | 0.000843 | cg02838492 | <i>NIPAL2</i>   |
| -0.76008 | 0.001028 | cg06988995 | <i>TMEM126A</i> |
| 0.344271 | 0.001087 | cg01193064 | <i>RAB36</i>    |
| 0.497102 | 0.001109 | cg01193064 | <i>PSMB11</i>   |
| 0.47927  | 0.001175 | cg01193064 | <i>BCL2L2</i>   |
| -0.29947 | 0.001209 | cg04720635 | <i>CCT6B</i>    |
| 0.524536 | 0.001219 | cg16622920 | <i>ESCO1</i>    |
| -1.46571 | 0.001224 | cg26580576 | <i>IGFBP7</i>   |
| 0.357738 | 0.001232 | cg19807836 | <i>CAB39L</i>   |
| -0.57216 | 0.001248 | cg26580576 | <i>R3HDM2</i>   |
| -0.66003 | 0.001273 | cg26580576 | <i>DENND6A</i>  |
| 0.442483 | 0.00133  | cg20730619 | <i>GLIPRIL2</i> |
| 0.484364 | 0.001412 | cg16622920 | <i>SLC25A1</i>  |
| 0.507496 | 0.001453 | cg01193064 | <i>OTUD1</i>    |
| -0.64229 | 0.001456 | cg26580576 | <i>SLMAP</i>    |
| 0.750972 | 0.001457 | cg12527440 | <i>ERAL1</i>    |
| 0.521893 | 0.001645 | cg20730619 | <i>PTPN9</i>    |
| 1.062825 | 0.001757 | cg20171559 | <i>NEDD4</i>    |
| -0.37826 | 0.001844 | cg22979546 | <i>SLC43A3</i>  |
| 0.432398 | 0.001878 | cg01193064 | <i>SLC25A37</i> |
| 0.532884 | 0.001954 | cg14291650 | <i>MYLK3</i>    |
| -0.31981 | 0.00199  | cg11846905 | <i>PTCD3</i>    |
| -0.52043 | 0.00225  | cg26580576 | <i>MBD6</i>     |
| -1.70586 | 0.002321 | cg26580576 | <i>VMPI</i>     |
| -0.29847 | 0.002378 | cg10777851 | <i>CLPTM1L</i>  |
| -0.54449 | 0.00244  | cg22824651 | <i>IL17C</i>    |

|          |          |            |                |
|----------|----------|------------|----------------|
| -1.11884 | 0.002509 | cg06513695 | <i>ATF5</i>    |
| 1.559744 | 0.002608 | cg02532113 | <i>UQCRESI</i> |
| -1.03303 | 0.002614 | cg20171559 | <i>CCDC106</i> |
| 0.279936 | 0.002645 | cg01193064 | <i>KLHL29</i>  |
| 0.164094 | 0.002679 | cg04080041 | <i>PDXDC2P</i> |
| -1.24443 | 0.00274  | cg02838492 | <i>UNC50</i>   |
| -0.44512 | 0.002848 | cg24736380 | <i>FASN</i>    |
| 0.308826 | 0.002929 | cg01193064 | <i>TCEA3</i>   |
| -0.47778 | 0.00293  | cg22824651 | <i>PABPN1L</i> |
| -0.38477 | 0.002956 | cg22824651 | <i>NAA35</i>   |
| 0.438542 | 0.002959 | cg16622920 | <i>SNRPDI</i>  |
| -0.65678 | 0.003099 | cg26580576 | <i>DDIT3</i>   |
| 0.339495 | 0.003119 | cg20730619 | <i>TBC1D4</i>  |
| -0.49274 | 0.003204 | cg04720635 | <i>RP9P</i>    |
| -0.31834 | 0.003246 | cg11846905 | <i>C9orf64</i> |
| -0.24168 | 0.003342 | cg10777851 | <i>MED16</i>   |
| -0.60305 | 0.003388 | cg06513695 | <i>ATP9A</i>   |
| -0.6217  | 0.003442 | cg06513695 | <i>BRDI</i>    |
| 0.489472 | 0.003583 | cg14159342 | <i>SERP2</i>   |
| -0.88264 | 0.003615 | cg26580576 | <i>KIF5A</i>   |
| -0.29281 | 0.003706 | cg04720635 | <i>SOD1</i>    |
| -0.41132 | 0.003728 | cg23796713 | <i>ZUFSP</i>   |
| -0.3268  | 0.003748 | cg02838492 | <i>STK3</i>    |
| 0.656275 | 0.00376  | cg20730619 | <i>TMC8</i>    |
| -0.42671 | 0.003772 | cg06513695 | <i>HDC</i>     |
| 0.450003 | 0.003813 | cg18244483 | <i>NBPF20</i>  |
| -0.38308 | 0.003843 | cg22824651 | <i>MRPL46</i>  |
| 0.853802 | 0.003888 | cg20730619 | <i>UCHL3</i>   |
| -0.73198 | 0.004092 | cg06513695 | <i>TRABD</i>   |
| 0.328563 | 0.004385 | cg14291650 | <i>SLC19A1</i> |
| -0.27819 | 0.004539 | cg24736380 | <i>GNAQ</i>    |

|          |          |            |                 |
|----------|----------|------------|-----------------|
| -0.3281  | 0.004655 | cg22979546 | <i>HESX1</i>    |
| -0.63358 | 0.004909 | cg06513695 | <i>BCDIN3D</i>  |
| 0.596475 | 0.00494  | cg16622920 | <i>SUGP1</i>    |
| 0.519597 | 0.005093 | cg01193064 | <i>HERC2P2</i>  |
| 0.312492 | 0.005229 | cg14291650 | <i>SLC38A2</i>  |
| 0.42554  | 0.005231 | cg09890200 | <i>PEBPI</i>    |
| 0.286408 | 0.005348 | cg14291650 | <i>TMIE</i>     |
| 0.271596 | 0.005396 | cg19807836 | <i>RPS11</i>    |
| 0.874766 | 0.005586 | cg11586330 | <i>MSANTD4</i>  |
| -0.34482 | 0.005678 | cg11846905 | <i>ARHGAP24</i> |
| 0.779407 | 0.005798 | cg02532113 | <i>PRKDI</i>    |
| 0.500254 | 0.005901 | cg16622920 | <i>CXADR</i>    |
| -0.34291 | 0.005972 | cg06365057 | <i>RNF14</i>    |
| 0.193811 | 0.006071 | cg04080041 | <i>FADD</i>     |
| -1.74059 | 0.006124 | cg26580576 | <i>ZNF548</i>   |
| -0.35474 | 0.006241 | cg17339484 | <i>AIF1</i>     |
| -0.26228 | 0.006512 | cg24739326 | <i>GTF2E2</i>   |
| -0.21227 | 0.006598 | cg10777851 | <i>KLHL17</i>   |
| -1.05141 | 0.006651 | cg26580576 | <i>GAPT</i>     |
| -0.15791 | 0.006657 | cg10777851 | <i>SLC26A1</i>  |
| -0.417   | 0.006828 | cg24739326 | <i>GARS</i>     |
| 0.354519 | 0.006921 | cg16622920 | <i>TMEM161A</i> |
| -0.3704  | 0.007079 | cg22824651 | <i>SNCG</i>     |
| -0.34678 | 0.007099 | cg02838492 | <i>STK24</i>    |
| -0.65541 | 0.007165 | cg04115418 | <i>GNPTG</i>    |
| -1.01026 | 0.007177 | cg26580576 | <i>TSPAN31</i>  |
| 0.435034 | 0.007227 | cg04720635 | <i>CSTF3</i>    |
| -0.37978 | 0.007279 | cg18694780 | <i>ATADI</i>    |
| -0.21775 | 0.007311 | cg24739326 | <i>LBH</i>      |
| 0.55388  | 0.007314 | cg14291650 | <i>UQCRRH</i>   |
| 0.443712 | 0.007405 | cg01193064 | <i>MMP14</i>    |

|           |          |            |                 |
|-----------|----------|------------|-----------------|
| -0.222834 | 0.007466 | cg04720635 | <i>LTBPI</i>    |
| 0.426858  | 0.007768 | cg21330703 | <i>RCBTBI</i>   |
| 0.346618  | 0.008035 | cg01193064 | <i>PLKI</i>     |
| 0.567631  | 0.008237 | cg19807836 | <i>IFRD2</i>    |
| 0.230177  | 0.008309 | cg19807836 | <i>ADCY7</i>    |
| -0.32496  | 0.008372 | cg10527525 | <i>TIFA</i>     |
| -0.98879  | 0.008403 | cg26580576 | <i>PTRH2</i>    |
| -0.50138  | 0.008747 | cg04720635 | <i>YARS</i>     |
| 0.262436  | 0.008779 | cg20730619 | <i>PARMI</i>    |
| -0.78379  | 0.008962 | cg24736380 | <i>CD36</i>     |
| 0.351979  | 0.009015 | cg20730619 | <i>ANXAI</i>    |
| 0.25268   | 0.009051 | cg22979546 | <i>AASDH</i>    |
| 0.136669  | 0.00911  | cg16287252 | <i>CD248</i>    |
| -0.23592  | 0.009138 | cg11846905 | <i>KIF27</i>    |
| 0.286993  | 0.009251 | cg16622920 | <i>DDX49</i>    |
| 0.926577  | 0.009323 | cg20730619 | <i>YWHAG</i>    |
| 0.294573  | 0.009556 | cg01193064 | <i>NDUFABI</i>  |
| 0.270142  | 0.009596 | cg15761799 | <i>MULL</i>     |
| 0.284098  | 0.009649 | cg14159342 | <i>MYO1G</i>    |
| 0.386604  | 0.00967  | cg00740870 | <i>ERCC4</i>    |
| -0.78523  | 0.009706 | cg06513695 | <i>C3orf18</i>  |
| 0.296552  | 0.009882 | cg16622920 | <i>SLC24A3</i>  |
| 0.354824  | 0.009925 | cg16622920 | <i>ARL5B</i>    |
| -0.41919  | 0.009992 | cg22979546 | <i>APPLI</i>    |
| 0.515561  | 0.009997 | cg20730619 | <i>TKI</i>      |
| -0.23875  | 0.010015 | cg11846905 | <i>ST3GAL5</i>  |
| -0.40974  | 0.010069 | cg22979546 | <i>PRIMI</i>    |
| 0.388256  | 0.010585 | cg18393722 | <i>C15orf54</i> |
| 0.255224  | 0.010737 | cg15001132 | <i>ACOT7</i>    |
| 0.849561  | 0.010923 | cg02532113 | <i>INO80E</i>   |
| 0.882336  | 0.010977 | cg02532113 | <i>MEP1B</i>    |

|          |          |            |                 |
|----------|----------|------------|-----------------|
| 0.49741  | 0.011148 | cg06589109 | <i>ACOT7</i>    |
| -0.3992  | 0.011219 | cg24739326 | <i>TM9SF4</i>   |
| -0.43074 | 0.011441 | cg06513695 | <i>HYAL2</i>    |
| -0.76754 | 0.011551 | cg04720635 | <i>ZBTB9</i>    |
| -0.84437 | 0.01174  | cg18694780 | <i>GASI</i>     |
| 0.106386 | 0.011782 | cg04080041 | <i>RUFY2</i>    |
| -0.16269 | 0.012005 | cg10777851 | <i>TMED11P</i>  |
| -1.05891 | 0.012135 | cg22824651 | <i>ZCCHC6</i>   |
| 0.558831 | 0.012209 | cg20730619 | <i>SNX33</i>    |
| 0.080169 | 0.012228 | cg23844910 | <i>DNAJC5</i>   |
| 2.036127 | 0.012293 | cg26580576 | <i>ZNF543</i>   |
| -0.20701 | 0.012656 | cg07629844 | <i>CIB2</i>     |
| -0.29832 | 0.012752 | cg24739326 | <i>GOLG48H</i>  |
| -0.48265 | 0.01323  | cg22824651 | <i>EIF2AK3</i>  |
| 0.000145 | 0.013346 | cg05530448 | <i>KIF13B</i>   |
| 0.397468 | 0.013361 | cg01193064 | <i>RPS2P32</i>  |
| -0.35522 | 0.01337  | cg10527525 | <i>NAA50</i>    |
| 0.507878 | 0.013482 | cg20730619 | <i>COMMD6</i>   |
| -0.35376 | 0.013506 | cg22824651 | <i>PIEZ01</i>   |
| -0.19946 | 0.013591 | cg11586330 | <i>AASDHPP7</i> |
| 0.316756 | 0.013825 | cg19807836 | <i>CYB561D2</i> |
| -0.25488 | 0.013958 | cg22979546 | <i>RDH16</i>    |
| 1.162678 | 0.014149 | cg25404454 | <i>STMN3</i>    |
| 0.282004 | 0.014359 | cg19807836 | <i>POLE2</i>    |
| 0.284202 | 0.014402 | cg16622920 | <i>MBI</i>      |
| 0.207257 | 0.014481 | cg14159342 | <i>PDXK</i>     |
| -0.35555 | 0.015142 | cg09890200 | <i>SPAG17</i>   |
| -0.21177 | 0.015546 | cg04720635 | <i>RPS18</i>    |
| 0.357776 | 0.01566  | cg04080041 | <i>GMCL1</i>    |
| 0.231827 | 0.015675 | cg24739326 | <i>KATNAL1</i>  |
| 0.528471 | 0.015908 | cg11970192 | <i>DUS4L</i>    |

|          |          |            |                 |
|----------|----------|------------|-----------------|
| 0.473624 | 0.015927 | cg01193064 | <i>CCDC126</i>  |
| -0.40131 | 0.01611  | cg26580576 | <i>CLTC</i>     |
| -0.50761 | 0.016725 | cg04720635 | <i>DNAJAI</i>   |
| 0.211879 | 0.017003 | cg14291650 | <i>C18orf32</i> |
| -0.37462 | 0.017316 | cg06988995 | <i>TMSB10</i>   |
| -0.47355 | 0.017695 | cg26580576 | <i>RPS6KB1</i>  |
| 0.243977 | 0.018166 | cg01193064 | <i>CEBPE</i>    |
| -0.54173 | 0.018314 | cg15096549 | <i>GTF3C3</i>   |
| 0.244578 | 0.018432 | cg16622920 | <i>SYT17</i>    |
| -0.72355 | 0.018504 | cg07823273 | <i>TUBBP5</i>   |
| -0.42304 | 0.01873  | cg02838492 | <i>MARVELD1</i> |
| -0.66386 | 0.018852 | cg18694780 | <i>EML5</i>     |
| 0.429423 | 0.018974 | cg11970192 | <i>RIC8B</i>    |
| 0.355851 | 0.019306 | cg12527440 | <i>JAM2</i>     |
| -0.63529 | 0.01966  | cg18844144 | <i>ZFYVE26</i>  |
| 0.430239 | 0.01983  | cg15371806 | <i>TCP10L</i>   |
| 0.42571  | 0.020194 | cg17125699 | <i>SYNPO2</i>   |
| 0.244179 | 0.020501 | cg14714391 | <i>CENPQ</i>    |
| -0.41325 | 0.020707 | cg24736380 | <i>GNAA14</i>   |
| -0.27218 | 0.021039 | cg11846905 | <i>FRMD3</i>    |
| 0.067357 | 0.021085 | cg04080041 | <i>AARS</i>     |
| -0.36601 | 0.02135  | cg06988995 | <i>KIAA0513</i> |
| 0.144738 | 0.021364 | cg16287252 | <i>KPNA2</i>    |
| -0.36341 | 0.02168  | cg22979546 | <i>PLLP</i>     |
| -0.21095 | 0.02172  | cg10527525 | <i>ATP6V1A</i>  |
| 0.331229 | 0.022103 | cg12527440 | <i>PLAA</i>     |
| -0.39757 | 0.022127 | cg22824651 | <i>CDTI</i>     |
| -0.32309 | 0.022162 | cg25989745 | <i>ANKDD1A</i>  |
| 0.503301 | 0.022531 | cg06513695 | <i>MAPKAPK3</i> |
| -0.26218 | 0.022626 | cg06365057 | <i>GRK7</i>     |
| -0.31824 | 0.022791 | cg24736380 | <i>RFNG</i>     |

|          |          |            |                |
|----------|----------|------------|----------------|
| -0.48466 | 0.023118 | cg04720635 | <i>AQP7</i>    |
| 0.556316 | 0.023135 | cg24739326 | <i>TLLL9</i>   |
| 0.097188 | 0.023432 | cg04080041 | <i>ANXA4</i>   |
| -0.32046 | 0.023822 | cg18694780 | <i>GPPI</i>    |
| 0.309236 | 0.023873 | cg14291650 | <i>CDPFI</i>   |
| 0.583916 | 0.024018 | cg20730619 | <i>GLIPRI</i>  |
| -0.37544 | 0.024153 | cg24736380 | <i>RASGRF2</i> |
| -0.34104 | 0.024263 | cg10527525 | <i>CKAP2L</i>  |
| -0.20731 | 0.024281 | cg10527525 | <i>PPMIJ</i>   |
| 0.297208 | 0.024402 | cg20730619 | <i>S10Z</i>    |
| -0.47992 | 0.025638 | cg22979546 | <i>ARHGEF3</i> |
| -0.27157 | 0.025704 | cg04466022 | <i>ABCB7</i>   |
| 0.054705 | 0.025749 | cg23844910 | <i>SPIN4</i>   |
| -0.30899 | 0.025774 | cg22824651 | <i>GALNS</i>   |
| -0.2054  | 0.026081 | cg24736380 | <i>DCXR</i>    |
| 0.278054 | 0.026191 | cg00740870 | <i>TCEANC</i>  |
| 0.459454 | 0.02707  | cg01193064 | <i>IGF2BP3</i> |
| 0.763397 | 0.027459 | cg17339484 | <i>ELP4</i>    |
| 0.181952 | 0.027482 | cg16622920 | <i>KCNH8</i>   |
| -0.23177 | 0.027639 | cg06365057 | <i>ARAP3</i>   |
| 0.275103 | 0.027736 | cg14159342 | <i>KLHL28</i>  |
| 0.318215 | 0.028031 | cg00740870 | <i>OFDI</i>    |
| 0.2985   | 0.028234 | cg14291650 | <i>DYM</i>     |
| 0.515631 | 0.028356 | cg06589109 | <i>FAM64A</i>  |
| -0.62757 | 0.028442 | cg06513695 | <i>KLHDC1</i>  |
| 0.131312 | 0.028974 | cg06730718 | <i>ACADSB</i>  |
| -0.50837 | 0.029047 | cg02838492 | <i>TSPAN5</i>  |
| -0.41087 | 0.029084 | cg09890200 | <i>TAOK3</i>   |
| 0.226585 | 0.02913  | cg14291650 | <i>HARBII</i>  |
| 1.134213 | 0.029582 | cg02532113 | <i>IFITM4P</i> |
| 0.605944 | 0.029618 | cg22979546 | <i>VAPB</i>    |

|          |          |            |                 |
|----------|----------|------------|-----------------|
| 0.11545  | 0.029721 | cg04080041 | <i>ERH</i>      |
| -0.24855 | 0.029733 | cg24739326 | <i>SEC14L2</i>  |
| -0.4458  | 0.029763 | cg06513695 | <i>CACNA2D2</i> |
| 0.3558   | 0.029835 | cg14291650 | <i>F2</i>       |
| -0.17705 | 0.030132 | cg10777851 | <i>IDH1</i>     |
| 0.133393 | 0.030451 | cg16287252 | <i>TMEM248</i>  |
| 0.66018  | 0.030784 | cg17339484 | <i>PISD</i>     |
| -0.33286 | 0.031262 | cg22329021 | <i>MRPL54</i>   |
| 0.248693 | 0.031427 | cg16825643 | <i>RNF219</i>   |
| 0.372488 | 0.031516 | cg19807836 | <i>HEATR3</i>   |
| 0.622309 | 0.031651 | cg04115418 | <i>PUSL1</i>    |
| -0.19055 | 0.032105 | cg07629844 | <i>FUBPI</i>    |
| -0.29996 | 0.032403 | cg11846905 | <i>C42</i>      |
| 0.483288 | 0.032738 | cg15371806 | <i>FER1L4</i>   |
| 0.343301 | 0.032914 | cg12527440 | <i>PDSSI</i>    |
| 0.222466 | 0.032919 | cg01193064 | <i>MSRB2</i>    |
| -0.1293  | 0.032966 | cg04720635 | <i>BRC42</i>    |
| -0.21429 | 0.033323 | cg04720635 | <i>CCR4</i>     |
| 0.301528 | 0.033563 | cg20730619 | <i>KRRI</i>     |
| -0.18065 | 0.033692 | cg10777851 | <i>AURKAIP1</i> |
| 0.174985 | 0.033845 | cg11990770 | <i>TMEM40</i>   |
| 0.132406 | 0.033999 | cg14291650 | <i>C16orf87</i> |
| -0.54628 | 0.034012 | cg06513695 | <i>NCKAP5L</i>  |
| 0.088573 | 0.034018 | cg23844910 | <i>TLN2</i>     |
| -0.18379 | 0.034299 | cg07629844 | <i>JMY</i>      |
| -0.25089 | 0.034503 | cg22979546 | <i>CPNE2</i>    |
| -0.33433 | 0.034506 | cg22824651 | <i>TMTC3</i>    |
| 0.309315 | 0.034636 | cg16622920 | <i>MAP3K15</i>  |
| -0.61869 | 0.034637 | cg18694780 | <i>GBP3</i>     |
| 0.367129 | 0.03533  | cg19807836 | <i>HVAL1</i>    |
| 0.428049 | 0.035466 | cg20730619 | <i>MRPL19</i>   |

|          |          |            |                 |
|----------|----------|------------|-----------------|
| 0.64903  | 0.035714 | cg20730619 | <i>TTLL5</i>    |
| -0.64208 | 0.03603  | cg26647291 | <i>PIGU</i>     |
| 0.257782 | 0.036266 | cg04115418 | <i>PSMF1</i>    |
| -0.32239 | 0.036387 | cg25989745 | <i>CDC42EP2</i> |
| 0.248115 | 0.036505 | cg00740870 | <i>ESF1</i>     |
| -0.63924 | 0.036878 | cg24736380 | <i>ASPSCR1</i>  |
| 0.310499 | 0.036992 | cg01193064 | <i>PPPIR3E</i>  |
| -0.41863 | 0.037003 | cg06513695 | <i>SIGLEC16</i> |
| 0.272192 | 0.037044 | cg18844144 | <i>FAM194I</i>  |
| 0.182417 | 0.037271 | cg14291650 | <i>NSUN4</i>    |
| 0.179698 | 0.037551 | cg20983032 | <i>ADAMTS1</i>  |
| 0.204681 | 0.037617 | cg16287252 | <i>RINI</i>     |
| -0.43731 | 0.037659 | cg16622920 | <i>SMGI</i>     |
| -0.57993 | 0.03775  | cg11990770 | <i>ZNF563</i>   |
| -0.15316 | 0.037823 | cg10777851 | <i>GTPBP4</i>   |
| -0.3919  | 0.03795  | cg22979546 | <i>SERPINGI</i> |
| -0.09677 | 0.038003 | cg15001132 | <i>ALOX12P2</i> |
| 0.330104 | 0.038189 | cg17125699 | <i>C4orf3</i>   |
| -0.31301 | 0.038307 | cg24739326 | <i>PDRG1</i>    |
| -0.22763 | 0.038468 | cg16622920 | <i>PLIN2</i>    |
| -0.27749 | 0.038721 | cg09890200 | <i>DDX6</i>     |
| 0.397485 | 0.038899 | cg20730619 | <i>C17orf99</i> |
| -0.38125 | 0.039205 | cg04017131 | <i>ZNF703</i>   |
| 0.163569 | 0.039313 | cg11990770 | <i>APOLD1</i>   |
| -0.18756 | 0.03943  | cg04017131 | <i>ELFN2</i>    |
| -0.31338 | 0.039651 | cg11990770 | <i>MKRN2</i>    |
| 0.257323 | 0.040243 | cg12527440 | <i>CDK8</i>     |
| -0.04838 | 0.040667 | cg04017131 | <i>ACTR5</i>    |
| 0.22413  | 0.04124  | cg04720635 | <i>LIG3</i>     |
| -0.22538 | 0.041313 | cg22979546 | <i>RTN4RL2</i>  |
| 0.66399  | 0.041416 | cg25404454 | <i>KHDRBS2</i>  |

|          |          |            |                 |
|----------|----------|------------|-----------------|
| -0.28947 | 0.041685 | cg11990770 | <i>PSMG2</i>    |
| -0.26993 | 0.042036 | cg02122376 | <i>ANKRD16</i>  |
| 0.169541 | 0.04225  | cg23844910 | <i>WDR74</i>    |
| 0.258433 | 0.042287 | cg14291650 | <i>FAAH</i>     |
| 0.22371  | 0.042408 | cg22979546 | <i>BAZ2A</i>    |
| 0.155575 | 0.042809 | cg15761799 | <i>ACSM1</i>    |
| 0.215838 | 0.043236 | cg14159342 | <i>TMEM42</i>   |
| -0.3948  | 0.043269 | cg15096549 | <i>HECW2</i>    |
| -0.16838 | 0.043416 | cg16622920 | <i>SH2D4A</i>   |
| -0.2305  | 0.043676 | cg10777851 | <i>SBNO2</i>    |
| -0.12924 | 0.043964 | cg19807836 | <i>ALG12</i>    |
| -0.37991 | 0.044097 | cg10777851 | <i>NOC2L</i>    |
| -0.17697 | 0.044195 | cg10527525 | <i>C4orf32</i>  |
| -0.43414 | 0.044216 | cg11990770 | <i>ARHgap44</i> |
| 0.319814 | 0.044277 | cg16622920 | <i>DGCR2</i>    |
| -0.21387 | 0.044428 | cg24739326 | <i>SF3A1</i>    |
| -0.24885 | 0.044611 | cg18244483 | <i>RHPN1</i>    |
| -0.25582 | 0.04472  | cg22824651 | <i>CBFA2T3</i>  |
| 0.248456 | 0.044733 | cg04080041 | <i>EXOSC6</i>   |
| 0.130623 | 0.044908 | cg04017131 | <i>FBXO10</i>   |
| -0.39399 | 0.04535  | cg15761799 | <i>UBXN10</i>   |
| 0.333617 | 0.046207 | cg14291650 | <i>TTC38</i>    |
| -0.29081 | 0.046928 | cg25989745 | <i>EHBPII</i>   |
| -0.21767 | 0.046981 | cg24739326 | <i>IPO8</i>     |
| -0.52642 | 0.047215 | cg26580576 | <i>DCTN2</i>    |
| 0.116341 | 0.047747 | cg07629844 | <i>ACSBG1</i>   |
| -0.39334 | 0.047986 | cg02122376 | <i>TRIM22</i>   |
| 0.222503 | 0.048405 | cg14159342 | <i>IGSF23</i>   |
| 1.356835 | 0.048449 | cg02532113 | <i>ZFP57</i>    |
| -0.15664 | 0.048789 | cg10777851 | <i>GRIN3B</i>   |
| -0.16528 | 0.048829 | cg10527525 | <i>DTX1</i>     |

|          |          |            |               |
|----------|----------|------------|---------------|
| -0.9938  | 0.049796 | cg11990770 | <i>MANSC1</i> |
| 0.320251 | 0.049835 | cg02054358 | <i>PYGB</i>   |

Supplement Table S9 (A): Statistically significant GO terms and its biological processes from pathway enrichment analysis in each pathway for males, for the identified CpGs.

| GO term    | Biological Processes  | N#  | Raw p value |
|------------|---|-----|-------------|
| GO:0045116 | protein neddylation   | 16  | 0.002       |
| GO:0033622 | integrin activation   | 21  | 0.004       |
| GO:0045956 | positive regulation of calcium ion-dependent exocytosis                                 | 19  | 0.004       |
| GO:1905078 | positive regulation of interleukin-17 secretion   | 2   | 0.004       |
| GO:0008049 | male courtship behavior   | 1   | 0.004       |
| GO:0042407 | cristae formation   | 31  | 0.005       |
| GO:0006393 | termination of mitochondrial transcription  | 2   | 0.006       |
| GO:1904235 | regulation of substrate-dependent cell migration, cell attachment to substrate          | 1   | 0.006       |
| GO:1904237 | positive regulation of substrate-dependent cell migration, cell attachment to substrate | 1   | 0.006       |
| GO:0002636 | positive regulation of germinal center formation  | 3   | 0.007       |
| GO:1902631 | negative regulation of membrane hyperpolarization                                       | 1   | 0.007       |
| GO:0015828 | tyrosine transport  | 1   | 0.008       |
| GO:0007007 | inner mitochondrial membrane organization   | 41  | 0.008       |
| GO:2001202 | negative regulation of transforming growth factor-beta secretion                        | 2   | 0.008       |
| GO:0031296 | B cell costimulation  | 3   | 0.009       |
| GO:0006887 | exocytosis  | 892 | 0.009       |
| GO:0099093 | calcium export from the mitochondrion   | 2   | 0.011       |
| GO:1902630 | regulation of membrane hyperpolarization  | 3   | 0.011       |
| GO:2001201 | regulation of transforming growth factor-beta secretion                                 | 3   | 0.012       |
| GO:0006726 | eye pigment biosynthetic process  | 3   | 0.012       |
| GO:0042441 | eye pigment metabolic process   | 3   | 0.012       |
| GO:0043324 | pigment metabolic process involved in developmental pigmentation                        | 3   | 0.012       |
| GO:0043474 | pigment metabolic process involved in pigmentation                                      | 3   | 0.012       |

|            |   |      |       |
|------------|---|------|-------|
| GO:2000435 | negative regulation of protein neddylation  | 3    | 0.012 |
| GO:0055085 | transmembrane transport   | 1565 | 0.012 |
| GO:0021935 | cerebellar granule cell precursor tangential migration  | 2    | 0.012 |
| GO:0045055 | regulated exocytosis  | 785  | 0.012 |
| GO:0051562 | negative regulation of mitochondrial calcium ion concentration                                      | 4    | 0.013 |
| GO:0060743 | epithelial cell maturation involved in prostate gland development                                   | 3    | 0.013 |
| GO:1905407 | regulation of creatine transmembrane transporter activity   | 2    | 0.013 |
| GO:1905408 | negative regulation of creatine transmembrane transporter activity                                  | 2    | 0.013 |
| GO:0046903 | secretion   | 1639 | 0.014 |
| GO:1905076 | regulation of interleukin-17 secretion  | 5    | 0.014 |
| GO:0051048 | negative regulation of secretion  | 235  | 0.014 |
| GO:0006931 | substrate-dependent cell migration, cell attachment to substrate                                    | 4    | 0.015 |
| GO:2000434 | regulation of protein neddyylation  | 4    | 0.015 |
| GO:1904381 | Golgi apparatus mannose trimming  | 3    | 0.015 |
| GO:0071470 | cellular response to osmotic stress   | 40   | 0.015 |
| GO:0010701 | positive regulation of norepinephrine secretion   | 4    | 0.017 |
| GO:0023016 | signal transduction by trans-phosphorylation  | 3    | 0.017 |
| GO:0021934 | hindbrain tangential cell migration   | 3    | 0.018 |
| GO:0007619 | courtship behavior  | 3    | 0.018 |
| GO:0038165 | oncostatin-M-mediated signaling pathway   | 4    | 0.018 |
| GO:0038044 | transforming growth factor-beta secretion   | 5    | 0.018 |
| GO:1900069 | regulation of cellular hyperosmotic salinity response   | 4    | 0.018 |
| GO:1901000 | regulation of response to salt stress   | 4    | 0.018 |
| GO:2001268 | negative regulation of cysteine-type endopeptidase activity involved in apoptotic signaling pathway | 6    | 0.018 |
| GO:0017158 | regulation of calcium ion-dependent exocytosis  | 43   | 0.020 |
| GO:0035987 | endodermal cell differentiation   | 45   | 0.020 |
| GO:0071526 | semaphorin-plexin signaling pathway   | 40   | 0.022 |
| GO:0072615 | interleukin-17 secretion  | 7    | 0.022 |
| GO:0036438 | maintenance of lens transparency  | 4    | 0.022 |

|            |   |     |       |
|------------|---|-----|-------|
| GO:0007341 | penetration of zona pellucida   | 8   | 0.022 |
| GO:0038146 | chemokine (C-X-C motif) ligand 12 signalling pathway                                      | 4   | 0.023 |
| GO:2000649 | regulation of sodium ion transmembrane transporter activity                               | 51  | 0.023 |
| GO:1903532 | positive regulation of secretion by cell  | 398 | 0.023 |
| GO:2000671 | regulation of motor neuron apoptotic process  | 5   | 0.024 |
| GO:0043615 | astrocyte cell migration  | 7   | 0.024 |
| GO:0001706 | endoderm formation  | 50  | 0.024 |
| GO:0007161 | calcium-independent cell-matrix adhesion  | 4   | 0.025 |
| GO:1903307 | positive regulation of regulated secretory pathway  | 52  | 0.025 |
| GO:0006689 | ganglioside catabolic process   | 6   | 0.025 |
| GO:0090188 | negative regulation of pancreatic juice secretion   | 5   | 0.026 |
| GO:2000697 | negative regulation of epithelial cell differentiation involved in kidney development     | 5   | 0.027 |
| GO:0050433 | regulation of catecholamine secretion   | 62  | 0.028 |
| GO:0090186 | regulation of pancreatic juice secretion  | 6   | 0.028 |
| GO:0036089 | cleavage furrow formation   | 7   | 0.029 |
| GO:0046888 | negative regulation of hormone secretion  | 63  | 0.029 |
| GO:0071475 | cellular hyperosmotic salinity response   | 7   | 0.030 |
| GO:1900454 | positive regulation of long-term synaptic depression                                      | 6   | 0.030 |
| GO:0051047 | positive regulation of secretion  | 423 | 0.030 |
| GO:0050432 | catecholamine secretion   | 64  | 0.030 |
| GO:0007605 | sensory perception of sound   | 143 | 0.031 |
| GO:1902305 | regulation of sodium ion transmembrane transport  | 61  | 0.033 |
| GO:0097049 | motor neuron apoptotic process  | 7   | 0.034 |
| GO:0050707 | regulation of cytokine secretion  | 204 | 0.035 |
| GO:0008360 | regulation of cell shape  | 150 | 0.035 |
| GO:0048069 | eye pigmentation  | 8   | 0.035 |
| GO:0060155 | platelet dense granule organization   | 8   | 0.035 |
| GO:0060526 | prostate glandular acinus morphogenesis   | 6   | 0.036 |
| GO:0060527 | prostate epithelial cord arborization involved in prostate glandular acinus morphogenesis | 6   | 0.036 |

|            |  |      |       |
|------------|--|------|-------|
| GO:0060179 | male mating behavior   | 8    | 0.036 |
| GO:1901166 | neural crest cell migration involved in autonomic nervous system development | 6    | 0.037 |
| GO:1903305 | regulation of regulated secretory pathway                                    | 158  | 0.037 |
| GO:0021957 | corticospinal tract morphogenesis  | 7    | 0.038 |
| GO:1990542 | mitochondrial transmembrane transport  | 88   | 0.038 |
| GO:0032413 | negative regulation of ion transmembrane transporter activity                | 76   | 0.039 |
| GO:0002634 | regulation of germinal center formation                                      | 9    | 0.040 |
| GO:0032940 | secretion by cell  | 1509 | 0.041 |
| GO:0042340 | keratan sulfate catabolic process  | 12   | 0.041 |
| GO:0017156 | calcium-ion regulated exocytosis   | 65   | 0.041 |
| GO:0071476 | cellular hypotonic response  | 8    | 0.042 |
| GO:0060159 | regulation of dopamine receptor signaling pathway                            | 11   | 0.043 |
| GO:1901660 | calcium ion export   | 11   | 0.043 |
| GO:0015849 | organic acid transport   | 330  | 0.043 |
| GO:0051937 | catecholamine transport  | 77   | 0.044 |
| GO:0001867 | complement activation, lectin pathway  | 13   | 0.044 |
| GO:0050954 | sensory perception of mechanical stimulus                                    | 162  | 0.044 |
| GO:0106049 | regulation of cellular response to osmotic stress                            | 10   | 0.045 |
| GO:0060992 | response to fungicide  | 11   | 0.045 |
| GO:0007270 | neuron-neuron synaptic transmission  | 8    | 0.045 |
| GO:0015801 | aromatic amino acid transport  | 10   | 0.046 |
| GO:0018026 | peptidyl-lysine monomethylation  | 10   | 0.046 |
| GO:0042538 | hyperosmotic salinity response   | 12   | 0.046 |
| GO:0046479 | glycosphingolipid catabolic process  | 14   | 0.048 |
| GO:0030150 | protein import into mitochondrial matrix                                     | 17   | 0.048 |
| GO:0140352 | export from cell   | 1553 | 0.049 |
| GO:0099527 | postsynapse to nucleus signaling pathway                                     | 9    | 0.049 |
| GO:0030157 | pancreatic juice secretion   | 12   | 0.050 |
| GO:1903531 | negative regulation of secretion by cell                                     | 209  | 0.050 |

Note: #N: Number of genes involved in the respective pathways

Supplement Table S9 (B): Statistically significant GO terms and its biological processes from pathway enrichment analysis in each pathway for females, for the identified CpGs.

| GO term    | Biological Processes  | N <sup>#</sup> | Raw p value |
|------------|---|----------------|-------------|
| GO:0014834 | skeletal muscle satellite cell maintenance involved in skeletal muscle regeneration       | 4              | 0.001       |
| GO:0035264 | multicellular organism growth   | 146            | 0.001       |
| GO:0001678 | cellular glucose homeostasis  | 151            | 0.002       |
| GO:0089718 | amino acid import across plasma membrane  | 23             | 0.002       |
| GO:0071499 | cellular response to laminar fluid shear stress   | 8              | 0.002       |
| GO:0035902 | response to immobilization stress   | 27             | 0.003       |
| GO:0043090 | amino acid import   | 26             | 0.003       |
| GO:1904491 | protein localization to ciliary transition zone   | 8              | 0.003       |
| GO:0060563 | neuroepithelial cell differentiation  | 53             | 0.003       |
| GO:0046324 | regulation of glucose import  | 60             | 0.003       |
| GO:0001542 | ovulation from ovarian follicle   | 9              | 0.003       |
| GO:1990668 | vesicle fusion with endoplasmic reticulum-Golgi intermediate compartment (ERGIC) membrane | 6              | 0.003       |
| GO:0046466 | membrane lipid catabolic process  | 34             | 0.004       |
| GO:0046323 | glucose import  | 68             | 0.005       |
| GO:2000785 | regulation of autophagosome assembly  | 35             | 0.005       |
| GO:0070914 | UV-damage excision repair   | 13             | 0.005       |
| GO:0042491 | inner ear auditory receptor cell differentiation  | 32             | 0.006       |
| GO:1904425 | negative regulation of GTP binding  | 2              | 0.006       |
| GO:0009650 | UV protection   | 13             | 0.007       |
| GO:0010827 | regulation of glucose transmembrane transport   | 78             | 0.007       |
| GO:0046326 | positive regulation of glucose import   | 38             | 0.008       |
| GO:0033388 | putrescine biosynthetic process from arginine   | 1              | 0.008       |
| GO:0033389 | putrescine biosynthetic process from arginine, using agmatinase                           | 1              | 0.008       |
| GO:0007292 | female gamete generation  | 133            | 0.008       |

|            |   |     |       |
|------------|---|-----|-------|
| GO:0044088 | regulation of vacuole organization                                      | 42  | 0.008 |
| GO:0098712 | L-glutamate import across plasma membrane                               | 13  | 0.008 |
| GO:0045779 | negative regulation of bone resorption                                  | 13  | 0.009 |
| GO:0019377 | glycolipid catabolic process  | 16  | 0.009 |
| GO:0006004 | fucose metabolic process  | 16  | 0.009 |
| GO:0120222 | regulation of blastocyst development                                    | 1   | 0.009 |
| GO:1904073 | regulation of trophectodermal cell proliferation                        | 1   | 0.009 |
| GO:1904075 | positive regulation of trophectodermal cell proliferation               | 1   | 0.009 |
| GO:0042668 | auditory receptor cell fate determination                               | 1   | 0.010 |
| GO:0045609 | positive regulation of inner ear auditory receptor cell differentiation | 1   | 0.010 |
| GO:0045633 | positive regulation of mechanoreceptor differentiation                  | 1   | 0.010 |
| GO:2000982 | positive regulation of inner ear receptor cell differentiation          | 1   | 0.010 |
| GO:0002065 | columnar/cuboidal epithelial cell differentiation                       | 112 | 0.010 |
| GO:0051938 | L-glutamate import  | 14  | 0.010 |
| GO:0010828 | positive regulation of glucose transmembrane transport                  | 44  | 0.011 |
| GO:0035315 | hair cell differentiation   | 40  | 0.011 |
| GO:0032812 | positive regulation of epinephrine secretion                            | 2   | 0.011 |
| GO:0050435 | amyloid-beta metabolic process  | 47  | 0.011 |
| GO:0033342 | negative regulation of collagen binding                                 | 1   | 0.012 |
| GO:0016052 | carbohydrate catabolic process  | 196 | 0.012 |
| GO:1901255 | nucleotide-excision repair involved in interstrand cross-link repair    | 2   | 0.012 |
| GO:0051691 | cellular oligosaccharide metabolic process                              | 2   | 0.012 |
| GO:0051692 | cellular oligosaccharide catabolic process                              | 2   | 0.012 |
| GO:0046851 | negative regulation of bone remodeling                                  | 15  | 0.012 |
| GO:0034616 | response to laminar fluid shear stress                                  | 15  | 0.012 |
| GO:0010560 | positive regulation of glycoprotein biosynthetic process                | 20  | 0.013 |
| GO:0002537 | nitric oxide production involved in inflammatory response               | 2   | 0.013 |
| GO:0006112 | energy reserve metabolic process  | 86  | 0.013 |
| GO:1903435 | positive regulation of constitutive secretory pathway                   | 1   | 0.014 |

|            |   |     |       |
|------------|---|-----|-------|
| GO:0002542 | Factor XII activation   | 2   | 0.014 |
| GO:0008643 | carbohydrate transport  | 148 | 0.014 |
| GO:0030728 | ovulation   | 20  | 0.014 |
| GO:0033140 | negative regulation of peptidyl-serine phosphorylation of STAT protein    | 2   | 0.015 |
| GO:0060766 | negative regulation of androgen receptor signaling pathway                | 15  | 0.015 |
| GO:0001505 | regulation of neurotransmitter levels                                     | 353 | 0.015 |
| GO:0042593 | glucose homeostasis   | 237 | 0.015 |
| GO:0034063 | stress granule assembly   | 19  | 0.015 |
| GO:0033500 | carbohydrate homeostasis  | 238 | 0.015 |
| GO:0030316 | osteoclast differentiation  | 97  | 0.016 |
| GO:0071333 | cellular response to glucose stimulus                                     | 132 | 0.016 |
| GO:0034755 | iron ion transmembrane transport  | 20  | 0.016 |
| GO:0045167 | asymmetric protein localization involved in cell fate determination       | 1   | 0.016 |
| GO:0002038 | positive regulation of L-glutamate import across plasma membrane          | 2   | 0.016 |
| GO:1903428 | positive regulation of reactive oxygen species biosynthetic process       | 54  | 0.017 |
| GO:0071331 | cellular response to hexose stimulus                                      | 134 | 0.017 |
| GO:0006293 | nucleotide-excision repair, preincision complex stabilization             | 20  | 0.017 |
| GO:0006295 | nucleotide-excision repair, DNA incision, 3'-to lesion                    | 135 | 0.017 |
| GO:0071326 | cellular response to monosaccharide stimulus                              | 20  | 0.017 |
| GO:0006525 | arginine metabolic process  | 20  | 0.017 |
| GO:1902631 | negative regulation of membrane hyperpolarization                         | 1   | 0.017 |
| GO:1903020 | positive regulation of glycoprotein metabolic process                     | 24  | 0.018 |
| GO:0001834 | trophoblast cell proliferation  | 2   | 0.018 |
| GO:0039502 | suppression by virus of host type I interferon-mediated signaling pathway | 1   | 0.018 |
| GO:0039503 | suppression by virus of host innate immune response                       | 1   | 0.018 |
| GO:0039514 | suppression by virus of host JAK-STAT cascade                             | 1   | 0.018 |
| GO:0039562 | suppression by virus of host STAT activity                                | 1   | 0.018 |
| GO:0039563 | suppression by virus of host STAT1 activity                               | 1   | 0.018 |
| GO:0039564 | suppression by virus of host STAT2 activity                               | 1   | 0.018 |

|            |   |     |       |
|------------|---|-----|-------|
| GO:0044414 | suppression of host defenses by symbiont  | 1   | 0.018 |
| GO:0052029 | suppression by symbiont of host signal transduction pathway                         | 1   | 0.018 |
| GO:0052031 | modulation by symbiont of host defense response                                     | 1   | 0.018 |
| GO:0052167 | modulation by symbiont of host innate immune response                               | 1   | 0.018 |
| GO:0052170 | suppression by symbiont of host innate immune response                              | 1   | 0.018 |
| GO:0052553 | modulation by symbiont of host immune response                                      | 1   | 0.018 |
| GO:0052562 | suppression by symbiont of host immune response                                     | 1   | 0.018 |
| GO:0052572 | response to host immune response  | 1   | 0.018 |
| GO:0075109 | modulation by symbiont of host receptor-mediated signal transduction                | 1   | 0.018 |
| GO:0075111 | suppression by symbiont of host receptor-mediated signal transduction               | 1   | 0.018 |
| GO:0075112 | modulation by symbiont of host transmembrane receptor-mediated signal transduction  | 1   | 0.018 |
| GO:0075114 | suppression by symbiont of host transmembrane receptor-mediated signal transduction | 1   | 0.018 |
| GO:0075528 | modulation by virus of host immune response   | 1   | 0.018 |
| GO:0043316 | cytotoxic T cell degranulation  | 3   | 0.018 |
| GO:0010506 | regulation of autophagy   | 325 | 0.018 |
| GO:0044026 | DNA hypermethylation  | 2   | 0.019 |
| GO:1902475 | L-alpha-amino acid transmembrane transport  | 53  | 0.019 |
| GO:0060370 | susceptibility to T cell mediated cytotoxicity                                      | 2   | 0.019 |
| GO:0071498 | cellular response to fluid shear stress   | 21  | 0.019 |
| GO:0002018 | remin-angiotensin regulation of aldosterone production                              | 4   | 0.019 |
| GO:0097055 | agmatine biosynthetic process   | 2   | 0.019 |
| GO:0032625 | interleukin-21 production   | 1   | 0.020 |
| GO:0072619 | interleukin-21 secretion  | 1   | 0.020 |
| GO:1902913 | positive regulation of neuroepithelial cell differentiation                         | 2   | 0.020 |
| GO:0040032 | post-embryonic body morphogenesis   | 1   | 0.020 |
| GO:0071409 | cellular response to cycloheximide  | 3   | 0.020 |
| GO:0045670 | regulation of osteoclast differentiation  | 64  | 0.020 |
| GO:0006091 | generation of precursor metabolites and energy                                      | 517 | 0.020 |
| GO:0042667 | auditory receptor cell fate specification   | 2   | 0.020 |

|            |  |     |       |
|------------|--|-----|-------|
| GO:0033341 | regulation of collagen binding   | 2   | 0.020 |
| GO:0071467 | cellular response to pH  | 23  | 0.020 |
| GO:0071322 | cellular response to carbohydrate stimulus                                   | 143 | 0.021 |
| GO:0097532 | stress response to acid chemical   | 3   | 0.021 |
| GO:0097533 | cellular stress response to acid chemical                                    | 3   | 0.021 |
| GO:1904659 | glucose transmembrane transport  | 108 | 0.021 |
| GO:0070911 | global genome nucleotide-excision repair                                     | 25  | 0.021 |
| GO:0051919 | positive regulation of fibrinolysis  | 4   | 0.021 |
| GO:1903433 | regulation of constitutive secretory pathway                                 | 2   | 0.022 |
| GO:0034104 | negative regulation of tissue remodeling                                     | 20  | 0.022 |
| GO:0002254 | kinin cascade  | 3   | 0.022 |
| GO:0002353 | plasma kallikrein-kinin cascade  | 3   | 0.022 |
| GO:0060283 | negative regulation of oocyte development                                    | 4   | 0.023 |
| GO:1905880 | negative regulation of oogenesis   | 4   | 0.023 |
| GO:0045821 | positive regulation of glycolytic process                                    | 23  | 0.023 |
| GO:0008645 | hexose transmembrane transport   | 112 | 0.023 |
| GO:0045671 | negative regulation of osteoclast differentiation                            | 27  | 0.023 |
| GO:0014036 | neural crest cell fate specification   | 2   | 0.024 |
| GO:0001582 | detection of chemical stimulus involved in sensory perception of sweet taste | 2   | 0.024 |
| GO:0002541 | activation of plasma proteins involved in acute inflammatory response        | 3   | 0.025 |
| GO:0015749 | monosaccharide transmembrane transport                                       | 114 | 0.025 |
| GO:0009441 | glycolate metabolic process  | 3   | 0.025 |
| GO:0048791 | calcium ion-regulated exocytosis of neurotransmitter                         | 21  | 0.025 |
| GO:0015813 | L-glutamate transmembrane transport  | 23  | 0.025 |
| GO:0014737 | positive regulation of muscle atrophy  | 2   | 0.025 |
| GO:0098968 | neurotransmitter receptor transport postsynaptic membrane to endosome        | 2   | 0.026 |
| GO:0061789 | dense core granule priming   | 3   | 0.026 |
| GO:0060113 | inner ear receptor cell differentiation                                      | 56  | 0.026 |
| GO:0006096 | glycolytic process   | 112 | 0.026 |

|             |   |      |       |
|-------------|---|------|-------|
| GO:0034219  | carbohydrate transmembrane transport  | 116  | 0.026 |
| GO:0001544  | initiation of primordial ovarian follicle growth                              | 2    | 0.027 |
| GO:0046903  | secretion   | 1639 | 0.027 |
| GO:0006757  | ATP generation from ADP   | 113  | 0.027 |
| GO:1990145  | maintenance of translational fidelity   | 2    | 0.027 |
| GO:0061819  | telomeric DNA-containing double minutes formation                             | 3    | 0.027 |
| GO:1905764  | regulation of protection from non-homologous end joining at telomere          | 3    | 0.027 |
| GO:0000710  | negative regulation of protection from non-homologous end joining at telomere | 3    | 0.027 |
| GO:0043153  | meiotic mismatch repair   | 3    | 0.027 |
| GO:0009605  | entrainment of circadian clock by photoperiod response to external stimulus   | 21   | 0.027 |
| GO:0061470  | T follicular helper cell differentiation                                      | 2669 | 0.028 |
| GO:00066914 | autophagy   | 4    | 0.028 |
| GO:0061919  | process utilizing autophagic mechanism  | 492  | 0.028 |
| GO:1904431  | positive regulation of t-circle formation                                     | 4    | 0.029 |
| GO:1902630  | regulation of membrane hyperpolarization                                      | 3    | 0.029 |
| GO:0002761  | regulation of myeloid leukocyte differentiation                               | 117  | 0.029 |
| GO:1903409  | reactive oxygen species biosynthetic process                                  | 119  | 0.029 |
| GO:0008594  | photoreceptor cell morphogenesis  | 3    | 0.030 |
| GO:0071386  | cellular response to corticosterone stimulus                                  | 3    | 0.030 |
| GO:0044501  | modulation of signal transduction in other organism                           | 2    | 0.030 |
| GO:0052027  | modulation by symbiont of host signal transduction pathway                    | 2    | 0.030 |
| GO:1904891  | positive regulation of excitatory synapse assembly                            | 3    | 0.031 |
| GO:0046898  | response to cycloheximide   | 4    | 0.031 |
| GO:0042698  | ovulation cycle   | 69   | 0.031 |
| GO:1905384  | regulation of protein localization to presynapse                              | 2    | 0.031 |
| GO:1905386  | positive regulation of protein localization to presynapse                     | 2    | 0.031 |
| GO:0050729  | positive regulation of inflammatory response                                  | 152  | 0.032 |
| GO:0046834  | lipid phosphorylation   | 64   | 0.032 |

|            |   |      |       |
|------------|---|------|-------|
| GO:1903861 | positive regulation of dendrite extension                                       | 22   | 0.032 |
| GO:0039506 | modulation by virus of host molecular function                                  | 2    | 0.032 |
| GO:0039507 | suppression by virus of host molecular function                                 | 2    | 0.032 |
| GO:0052055 | modulation by symbiont of host molecular function                               | 2    | 0.032 |
| GO:0052056 | negative regulation by symbiont of host molecular function                      | 2    | 0.032 |
| GO:1990834 | response to odorant   | 4    | 0.032 |
| GO:0010157 | response to chlorate  | 2    | 0.033 |
| GO:0006826 | iron ion transport  | 75   | 0.033 |
| GO:0070253 | somatostatin secretion  | 4    | 0.033 |
| GO:0050727 | regulation of inflammatory response   | 368  | 0.033 |
| GO:0042490 | mechanoreceptor differentiation   | 61   | 0.033 |
| GO:0015807 | L-amino acid transport  | 67   | 0.033 |
| GO:0031347 | regulation of defense response  | 685  | 0.034 |
| GO:0046031 | ADP metabolic process   | 121  | 0.034 |
| GO:0032849 | positive regulation of cellular pH reduction                                    | 4    | 0.034 |
| GO:0005975 | carbohydrate metabolic process  | 610  | 0.034 |
| GO:0000720 | pyrimidine dimer repair by nucleotide-excision repair                           | 4    | 0.035 |
| GO:0035166 | post-embryonic hemopoiesis  | 3    | 0.035 |
| GO:0010508 | positive regulation of autophagy  | 119  | 0.035 |
| GO:0009648 | photoperiodism  | 25   | 0.035 |
| GO:1905460 | negative regulation of vascular associated smooth muscle cell apoptotic process | 7    | 0.035 |
| GO:0032940 | secretion by cell   | 1509 | 0.036 |
| GO:2000828 | regulation of parathyroid hormone secretion                                     | 2    | 0.036 |
| GO:0060765 | regulation of androgen receptor signaling pathway                               | 26   | 0.036 |
| GO:0009743 | response to carbohydrate  | 229  | 0.036 |
| GO:1903859 | regulation of dendrite extension  | 24   | 0.037 |
| GO:0006836 | neurotransmitter transport  | 268  | 0.037 |
| GO:0098706 | iron ion import across cell outer membrane                                      | 3    | 0.037 |
| GO:1990785 | response to water-immersion restraint stress                                    | 4    | 0.037 |

|            |   |     |       |
|------------|---|-----|-------|
| GO:2001025 | positive regulation of response to drug                                 | 33  | 0.037 |
| GO:0033137 | negative regulation of peptidyl-serine phosphorylation                  | 27  | 0.038 |
| GO:0006517 | protein deglycosylation   | 29  | 0.038 |
| GO:1903530 | regulation of secretion by cell   | 749 | 0.038 |
| GO:0015800 | acidic amino acid transport   | 66  | 0.039 |
| GO:0071787 | endoplasmic reticulum tubular network formation                         | 4   | 0.039 |
| GO:1901300 | positive regulation of hydrogen peroxide-mediated programmed cell death | 5   | 0.039 |
| GO:0046942 | carboxylic acid transport   | 328 | 0.039 |
| GO:1990809 | endoplasmic reticulum tubular network membrane organization             | 4   | 0.039 |
| GO:0006526 | arginine biosynthetic process   | 5   | 0.039 |
| GO:0097638 | L-arginine import across plasma membrane                                | 4   | 0.039 |
| GO:0006110 | regulation of glycolytic process  | 77  | 0.039 |
| GO:0048147 | negative regulation of fibroblast proliferation                         | 30  | 0.040 |
| GO:0006165 | nucleoside diphosphate phosphorylation                                  | 131 | 0.040 |
| GO:0030683 | mitigation of host immune response by virus                             | 3   | 0.040 |
| GO:0010260 | animal organ senescence   | 3   | 0.041 |
| GO:0009649 | entrainment of circadian clock  | 27  | 0.041 |
| GO:0015849 | organic acid transport  | 330 | 0.041 |
| GO:0034644 | cellular response to UV   | 81  | 0.041 |
| GO:0070093 | negative regulation of glucagon secretion                               | 5   | 0.041 |
| GO:0060066 | oviduct development   | 3   | 0.042 |
| GO:0044821 | meiotic telomere tethering at nuclear periphery                         | 5   | 0.042 |
| GO:0070197 | meiotic attachment of telomere to nuclear envelope                      | 5   | 0.042 |
| GO:0097240 | chromosome attachment to the nuclear envelope                           | 5   | 0.042 |
| GO:0046939 | nucleotide phosphorylation  | 133 | 0.042 |
| GO:1904505 | regulation of telomere maintenance in response to DNA damage            | 4   | 0.043 |
| GO:1904506 | negative regulation of telomere maintenance in response to DNA damage   | 4   | 0.043 |
| GO:0005977 | glycogen metabolic process  | 73  | 0.043 |
| GO:0006073 | cellular glucan metabolic process                                       | 74  | 0.043 |

|            |   |      |       |
|------------|---|------|-------|
| GO:0044042 | glucan metabolic process  | 74   | 0.043 |
| GO:0002860 | positive regulation of natural killer cell mediated cytotoxicity directed against tumor cell target | 6    | 0.043 |
| GO:0014034 | neural crest cell fate commitment   | 4    | 0.043 |
| GO:0021747 | cochlear nucleus development  | 3    | 0.044 |
| GO:0006855 | drug transmembrane transport  | 76   | 0.044 |
| GO:0014707 | branchiomeric skeletal muscle development   | 3    | 0.044 |
| GO:0021817 | nucleokinesis involved in cell motility in cerebral cortex radial glia guided migration             | 3    | 0.044 |
| GO:0048866 | stem cell fate specification  | 4    | 0.045 |
| GO:0014045 | establishment of endothelial blood-brain barrier  | 4    | 0.045 |
| GO:0022009 | central nervous system vasculogenesis   | 4    | 0.045 |
| GO:0043578 | nuclear matrix organization   | 3    | 0.045 |
| GO:0090292 | nuclear matrix anchoring at nuclear membrane  | 3    | 0.045 |
| GO:0008295 | spermidine biosynthetic process   | 4    | 0.046 |
| GO:0070777 | D-aspartate transport   | 4    | 0.046 |
| GO:0070779 | D-aspartate import across plasma membrane   | 4    | 0.046 |
| GO:0048477 | oogenesis   | 85   | 0.046 |
| GO:0031646 | positive regulation of nervous system process   | 63   | 0.046 |
| GO:0045341 | MHC class I biosynthetic process  | 5    | 0.046 |
| GO:0045343 | regulation of MHC class I biosynthetic process  | 5    | 0.046 |
| GO:0045345 | positive regulation of MHC class I biosynthetic process   | 5    | 0.046 |
| GO:0002036 | regulation of L-glutamate import across plasma membrane   | 5    | 0.046 |
| GO:0051954 | positive regulation of amine transport  | 35   | 0.046 |
| GO:0140352 | export from cell  | 1553 | 0.047 |
| GO:0006296 | nucleotide-excision repair, DNA incision, 5'-to lesion  | 36   | 0.047 |
| GO:0042733 | embryonic digit morphogenesis   | 61   | 0.047 |
| GO:0009135 | purine nucleoside diphosphate metabolic process   | 133  | 0.047 |
| GO:0009179 | purine ribonucleoside diphosphate metabolic process   | 133  | 0.047 |
| GO:0031133 | regulation of axon diameter   | 5    | 0.047 |
| GO:0006880 | intracellular sequestering of iron ion  | 5    | 0.047 |

|            |  |     |       |
|------------|--|-----|-------|
| GO:0014735 | regulation of muscle atrophy   | 4   | 0.047 |
| GO:0045054 | constitutive secretory pathway   | 4   | 0.047 |
| GO:1902116 | negative regulation of organelle assembly  | 36  | 0.048 |
| GO:0033572 | transferrin transport  | 36  | 0.048 |
| GO:0009744 | response to sucrose  | 6   | 0.049 |
| GO:0034285 | response to disaccharide   | 6   | 0.049 |
| GO:0002420 | natural killer cell mediated cytotoxicity directed against tumor cell target               | 8   | 0.049 |
| GO:0002858 | regulation of natural killer cell mediated cytotoxicity directed against tumor cell target | 8   | 0.049 |
| GO:1901162 | primary amino compound biosynthetic process  | 5   | 0.049 |
| GO:0015711 | organic anion transport  | 491 | 0.049 |
| GO:0009185 | ribonucleoside diphosphate metabolic process   | 135 | 0.049 |
| GO:0099011 | neuronal dense core vesicle exocytosis   | 6   | 0.049 |
| GO:0099525 | presynaptic dense core vesicle exocytosis  | 6   | 0.049 |
| GO:0006643 | membrane lipid metabolic process   | 203 | 0.049 |
| GO:0001958 | endochondral ossification  | 27  | 0.050 |
| GO:0036075 | replacement ossification   | 27  | 0.050 |
| GO:0035931 | mineralocorticoid secretion  | 6   | 0.050 |
| GO:0035932 | aldosterone secretion  | 6   | 0.050 |
| GO:2000855 | regulation of mineralocorticoid secretion  | 6   | 0.050 |
| GO:2000858 | regulation of aldosterone secretion  | 6   | 0.050 |
| GO:0097577 | sequestering of iron ion   | 6   | 0.050 |
| GO:0010559 | regulation of glycoprotein biosynthetic process  | 40  | 0.050 |

Note: #N: Number of genes involved in the respective pathways

Supplement Table S10(A): Association of DNAm in newborn with pre-adolescent Ast\_Rh at 405 CpGs that are sex specific. Males are the reference group.

| CpGs | IOWBC interaction | IOWBC RAW | IOWBC fdr | ALSPAC Interaction | ALSPAC main | ALSPAC RAW | CpG Island    |
|------|-------------------|-----------|-----------|--------------------|-------------|------------|---------------|
|      | Estimate          | Pvalue    |           | Estimates          | estimate    | Pvalue     | Gene location |

| <b>cg24818434</b> | -2.55 | 6E-06 | 0.0007 | -0.35 | 0.09  | 0.6476 | 1  | <i>SLC25A44</i> | 5UTR         |
|-------------------|-------|-------|--------|-------|-------|--------|----|-----------------|--------------|
| cg09095892        | -1.32 | 1E-05 | 0.0007 | 0.81  | -0.64 | 0.0357 | 10 |                 | Island       |
| cg08617683        | -1.94 | 1E-05 | 0.0007 | 0.73  | -0.18 | 0.0642 | 12 | <i>FBRSL1</i>   | Body         |
| cg05000348        | -2.44 | 9E-06 | 0.0007 | 0.86  | -0.18 | 0.3167 | 11 | <i>CDK2AP2</i>  | TSS1500      |
| <b>cg01538301</b> | 3.79  | 1E-05 | 0.0007 | 0.23  | -0.83 | 0.8014 | 14 |                 | Island       |
| cg04206337        | -2.46 | 3E-05 | 0.0008 | 0.84  | -0.05 | 0.2912 | 1  | <i>SNORA16A</i> | Body         |
| <b>cg21349849</b> | 2.91  | 2E-05 | 0.0008 | 0.40  | -0.29 | 0.3993 | 8  | <i>STK3</i>     | N_Shore      |
| <b>cg05396987</b> | -2.29 | 3E-05 | 0.0008 | -0.41 | 0.33  | 0.5156 | 4  | <i>TMEM155</i>  | 1stExon      |
| <b>cg21476203</b> | 2.64  | 2E-05 | 0.0008 | 0.27  | -0.18 | 0.6335 | 8  | <i>SCRIB</i>    | S_Shore      |
| <b>cg06791670</b> | -2.14 | 3E-05 | 0.0008 | -0.14 | 0.32  | 0.8508 | 19 | <i>HAUS5</i>    | Body         |
| cg27635422        | -2.47 | 3E-05 | 0.0008 | 0.05  | 0.01  | 0.9375 | 6  | <i>TAPBP</i>    | 3UTR         |
| cg27635422        | -2.47 | 3E-05 | 0.0008 | 0.05  | 0.01  | 0.9375 | 6  | <i>TAPBP</i>    | 3UTR         |
| cg00980784        | -3.17 | 3E-05 | 0.0008 | 0.03  | 0.05  | 0.9683 | 17 | <i>ABI3, GN</i> | TSS200       |
| cgunit            | -2.77 | 3E-05 | 0.0008 |       |       |        |    |                 |              |
| cg12292402        | -1.91 | 4E-05 | 0.0008 | 1.75  | -0.47 | 0.0221 | 13 | <i>HSPHI</i>    | TSS1500      |
| cg26615794        | 2.94  | 4E-05 | 0.0008 | 0.74  | 0.00  | 0.3316 | 1  | <i>RGS16</i>    | S_Shelf      |
| <b>cg22081558</b> | -2.48 | 4E-05 | 0.0008 | -0.13 | 0.20  | 0.8484 | 11 |                 | Island       |
| <b>cg04019843</b> | 3.16  | 4E-05 | 0.0009 | 1.31  | -0.06 | 0.1190 | 1  | <i>RPS6KCI</i>  |              |
| cg15421520        | 2.88  | 5E-05 | 0.0009 | -0.66 | 0.88  | 0.5206 | 14 | <i>C14orf18</i> | 1stExon;5UTR |
| <b>cg03740167</b> | -2.43 | 6E-05 | 0.0009 | -0.46 | 0.70  | 0.4706 | 10 |                 | Island       |
| <b>cg00315816</b> | 2.45  | 6E-05 | 0.0009 | 0.37  | -0.61 | 0.6006 | 7  | <i>PRKAG2</i>   | 5UTR;Body    |
| cg00823229        | -2.05 | 7E-05 | 0.0010 | 0.47  | -0.06 | 0.5187 | 12 | <i>PFKM</i>     | 1stExon      |
| cg17618092        | -2.12 | 8E-05 | 0.0010 | 0.35  | -0.08 | 0.6191 | 11 | <i>RBM14</i>    | Island       |
| <b>cg19874450</b> | -2.70 | 8E-05 | 0.0010 | -0.23 | 0.01  | 0.6729 | 17 | <i>GGNBP2</i>   | 1stExon;5UTR |
| <b>cg23973524</b> | 3.19  | 1E-04 | 0.0011 | 0.80  | -0.70 | 0.2431 | 19 | <i>CRTCL</i>    | Body;Body    |
| <b>cg18787783</b> | 3.90  | 1E-04 | 0.0011 | 1.49  | -0.01 | 0.1753 | 12 | <i>MMP19</i>    | TSS1500      |
| cg15943437        | -1.88 | 1E-04 | 0.0011 | 0.08  | 0.43  | 0.8936 | 11 | <i>MRPL21</i>   | N_Shore      |
| cg21834204        | -2.82 | 1E-04 | 0.0012 | 1.44  | -0.50 | 0.0952 | 12 | <i>MTERFD3</i>  | S_Shore      |
| cg14591123        | -2.21 | 1E-04 | 0.0012 | 0.74  | -1.07 | 0.2914 | 3  | <i>VILL</i>     | Island       |

|                   |       |       |        |       |       |        |    |                 |             |         |
|-------------------|-------|-------|--------|-------|-------|--------|----|-----------------|-------------|---------|
| <b>cg13539395</b> | -3.25 | 1E-04 | 0.0012 | -0.45 | 0.44  | 0.3265 | 19 | <i>CFD</i>      | TSS200      | N_Shore |
| <b>cg12661452</b> | -1.97 | 1E-04 | 0.0012 | 0.62  | 0.05  | 0.4560 | 12 | <i>AACS</i>     | 1stExon     | Island  |
| <b>cg20852846</b> | -2.14 | 1E-04 | 0.0012 | -0.49 | -0.11 | 0.4819 | 19 | <i>ZFR2</i>     | Body        | Island  |
| <b>cg16073958</b> | 1.38  | 1E-04 | 0.0012 | 0.30  | -0.63 | 0.5138 | 8  |                 |             |         |
| <b>cg17081157</b> | -2.05 | 1E-04 | 0.0012 | 0.32  | -0.25 | 0.6544 | 6  | <i>SESN1</i>    | TSS1500     | Island  |
| <b>cg14101302</b> | -1.93 | 1E-04 | 0.0012 | 0.41  | -0.34 | 0.5671 | 6  | <i>RIMSI</i>    | TSS200      | S_Shore |
| <b>cg16013246</b> | -2.27 | 1E-04 | 0.0012 | 0.14  | -0.43 | 0.7946 | 1  | <i>SNHG3-RC</i> | Body        |         |
| <b>cg20630567</b> | -1.86 | 1E-04 | 0.0012 | -0.04 | 0.42  | 0.9560 | 2  | <i>CCDC115</i>  | 5UTR        | Island  |
| <b>cg20736492</b> | -1.53 | 2E-04 | 0.0013 | 0.38  | -0.30 | 0.3158 | 12 |                 |             |         |
| <b>cg09888026</b> | -3.36 | 2E-04 | 0.0013 | -0.90 | 0.36  | 0.3690 | 17 | <i>TMEM105</i>  | 5UTR        |         |
| <b>cg15847685</b> | -3.04 | 2E-04 | 0.0013 | -0.88 | -0.23 | 0.3214 | 4  |                 |             |         |
| <b>cg07965714</b> | -1.74 | 2E-04 | 0.0013 | 0.86  | -0.63 | 0.3736 | 9  | <i>XPA</i>      | TSS200      | S_Shore |
| <b>cg19367136</b> | -1.70 | 2E-04 | 0.0014 | 0.21  | 0.43  | 0.7014 | 1  | <i>FUC1A1</i>   | TSS1500     | S_Shore |
| <b>cg18478353</b> | 3.05  | 2E-04 | 0.0014 | 1.18  | -0.66 | 0.2627 | 21 | <i>SLC37A1</i>  | Body        | N_Shelf |
| <b>cg19954739</b> | -1.87 | 2E-04 | 0.0015 | 0.11  | -0.19 | 0.8645 | 9  | <i>ZMYND19</i>  | TSS1500     | Island  |
| <b>cg13213118</b> | -1.98 | 3E-04 | 0.0017 | 0.80  | 0.29  | 0.2798 | 12 |                 |             |         |
| <b>cg04575467</b> | -2.30 | 3E-04 | 0.0017 | 0.41  | 0.10  | 0.5561 | 8  |                 |             |         |
| <b>cg14099990</b> | -1.77 | 3E-04 | 0.0018 | 0.35  | 0.11  | 0.5299 | 13 | <i>NBEA</i>     | Body        | Island  |
| <b>cg02461806</b> | -2.07 | 3E-04 | 0.0018 | 0.33  | -0.51 | 0.6794 | 17 | <i>ZZEF1</i>    | TSS200      |         |
| <b>cg21656600</b> | -1.79 | 3E-04 | 0.0018 | 0.16  | -0.02 | 0.7860 | 12 | <i>PPP1CC</i>   | TSS1500     | Island  |
| <b>cg01540571</b> | -1.81 | 3E-04 | 0.0018 | 0.09  | 0.16  | 0.8970 | 1  | <i>AGMAT</i>    | Body        | Island  |
| <b>cg24343755</b> | -1.67 | 3E-04 | 0.0020 | -0.21 | 0.20  | 0.7177 | 10 | <i>PDSSI</i>    | Body        | Island  |
| <b>cg10179363</b> | 3.16  | 4E-04 | 0.0020 | 0.48  | -0.17 | 0.4991 | 15 | <i>ANPEP</i>    | 5UTR        |         |
| <b>cg07642705</b> | -1.62 | 3E-04 | 0.0020 | -0.09 | 0.11  | 0.8741 | 16 | <i>SNHG9_R</i>  | TSS200      | Island  |
| <b>cg05440435</b> | -1.82 | 4E-04 | 0.0020 | -0.15 | 0.36  | 0.7806 | 16 | <i>C47</i>      | TSS200;Body | Island  |
| <b>cg13420923</b> | -1.91 | 4E-04 | 0.0020 | 0.02  | 0.16  | 0.9688 | 10 | <i>DCLRE1A</i>  | TSS1500     | Island  |
| <b>cg23683674</b> | -2.18 | 4E-04 | 0.0020 | -0.51 | 0.33  | 0.4030 | 11 | <i>ARHGEF17</i> | 1stExon     | Island  |
| <b>cg14724918</b> | -1.75 | 4E-04 | 0.0021 | -0.15 | 0.61  | 0.8324 | 5  | <i>SEC24A</i>   | TSS1500     | Island  |
| <b>cg07538364</b> | 1.86  | 4E-04 | 0.0022 | 0.51  | -0.33 | 0.2858 | 8  | <i>SLC7A2</i>   | Body        |         |

|                   |       |       |        |       |       |        |    |                            |
|-------------------|-------|-------|--------|-------|-------|--------|----|----------------------------|
| <b>cg25279644</b> | -1.91 | 5E-04 | 0.0024 | -0.10 | -0.11 | 0.8629 | 4  | Island                     |
| cg13696436        | 1.95  | 5E-04 | 0.0025 | -0.53 | 0.64  | 0.2316 | 10 | <i>EBF3</i><br>Body        |
| <b>cg02998992</b> | -2.48 | 5E-04 | 0.0025 | -0.35 | 0.22  | 0.5639 | 17 | <i>B9DI</i><br>Body        |
| <b>cg22192692</b> | -2.07 | 5E-04 | 0.0025 | -0.36 | 0.31  | 0.5161 | 20 | <i>SNRPB</i><br>TSS1500    |
| cg22377767        | 1.32  | 5E-04 | 0.0025 | -0.51 | 0.42  | 0.6223 | 7  | <i>ZKSC4N5</i><br>TSS200   |
| cg24820996        | -1.91 | 5E-04 | 0.0025 | 0.28  | -0.34 | 0.6411 | 19 | <i>UNC13A</i><br>Body      |
| <b>cg1322248</b>  | -2.36 | 6E-04 | 0.0026 | -0.32 | 0.06  | 0.6053 | 15 | <i>PSTPIP1</i><br>Body     |
| cg18948488        | -2.51 | 6E-04 | 0.0026 | 0.88  | -0.17 | 0.2343 | 10 | <i>FLJ41350</i><br>Body    |
| <b>cg10579012</b> | -1.04 | 6E-04 | 0.0027 | -1.03 | 0.45  | 0.0091 | 1  | S_Shore                    |
| <b>cg26054167</b> | 2.35  | 6E-04 | 0.0027 | 1.43  | -1.01 | 0.2003 | 20 | <i>COL20A1</i><br>Body     |
| <b>cg24496614</b> | -2.41 | 6E-04 | 0.0027 | -0.76 | 0.38  | 0.3163 | 11 | <i>FTHI</i><br>TSS1500     |
| cg02419873        | -2.89 | 6E-04 | 0.0027 | 0.34  | -0.50 | 0.6466 | 16 | <i>SNX29PL</i><br>S_Shore  |
| cg0652657         | -1.66 | 6E-04 | 0.0027 | 0.26  | -0.11 | 0.6575 | 10 | <i>EBF3</i><br>Body        |
| cg22041190        | -1.93 | 6E-04 | 0.0027 | 0.15  | 0.02  | 0.8164 | 11 | <i>PKNOX2</i><br>S_Shore   |
| cg21857959        | -1.85 | 6E-04 | 0.0027 | 0.54  | -0.30 | 0.4424 | 3  | <i>MCF2L2</i><br>Island    |
| <b>cg00707741</b> | 2.22  | 7E-04 | 0.0028 | 0.24  | -0.63 | 0.7568 | 2  | <i>FARP2</i><br>TSS1500    |
| <b>cg16360777</b> | 1.30  | 7E-04 | 0.0029 | 0.43  | 0.04  | 0.5041 | 4  | <i>AMBN</i><br>Body        |
| cg16000406        | 3.21  | 7E-04 | 0.0029 | -0.43 | 0.58  | 0.6205 | 19 | <i>FUT5</i><br>Body        |
| cg27241576        | 2.37  | 7E-04 | 0.0029 | -0.26 | 0.61  | 0.7113 | 16 | <i>CMP</i><br>Body         |
| cg00500229        | -1.72 | 8E-04 | 0.0030 | 1.25  | -0.02 | 0.0263 | 1  | Island                     |
| <b>cg11661809</b> | -1.78 | 8E-04 | 0.0030 | -0.05 | 0.03  | 0.9384 | 22 | <i>PI4KA_S</i><br>Island   |
| cg03694279        | -2.44 | 8E-04 | 0.0032 | 1.17  | -0.96 | 0.1327 | 10 | <i>RHPN1</i><br>S_Shore    |
| <b>cg04410091</b> | 2.43  | 9E-04 | 0.0034 | 1.22  | -0.28 | 0.1022 | 8  | <i>DCAF8</i><br>Island     |
| cg02457683        | -1.54 | 9E-04 | 0.0034 | 1.21  | -0.39 | 0.3382 | 1  | <i>TNFSF13B</i><br>Body    |
| cg09158314        | -2.19 | 9E-04 | 0.0034 | 0.81  | -0.49 | 0.4320 | 13 | <i>MGC42105</i><br>TSS1500 |
| cg23502772        | -1.70 | 9E-04 | 0.0034 | 0.08  | 0.03  | 0.8710 | 5  | <i>CC2D2A</i><br>Island    |
| cg01015662        | 1.24  | 9E-04 | 0.0035 | -0.09 | 0.03  | 0.8666 | 1  | <i>PPT1</i><br>N_Shore     |
| cg16359663        | 2.41  | 1E-03 | 0.0035 | -0.09 | 0.08  | 0.8836 | 4  | <i>ERCCI</i><br>Body       |
| <b>cg16629408</b> | 2.07  | 1E-03 | 0.0035 | 0.16  | -0.06 | 0.7190 | 19 | N_Shelf                    |

|                   |       |       |        |       |       |        |    |                 |         |         |
|-------------------|-------|-------|--------|-------|-------|--------|----|-----------------|---------|---------|
| <b>cg06412092</b> | -1.62 | 1E-03 | 0.0036 | 0.40  | -0.12 | 0.6891 | 5  | <i>MER3</i>     | Body    | Island  |
| <b>cg19653117</b> | -2.07 | 1E-03 | 0.0036 | 0.75  | 0.19  | 0.2796 | 2  | <i>YIPF4</i>    | TSS200  | N_Shore |
| <b>cg19142181</b> | 0.34  | 1E-03 | 0.0037 | 0.14  | -0.09 | 0.4893 | 20 | <i>SLC17A9</i>  | Body    | Island  |
| <b>cg23023263</b> | -1.64 | 1E-03 | 0.0037 | 0.14  | 0.01  | 0.8221 | 3  | <i>ULK4</i>     | TSS1500 | S_Shore |
| <b>cg18733433</b> | 1.73  | 1E-03 | 0.0039 | -0.20 | -0.16 | 0.5809 | 3  | <i>MORCI</i>    | TSS200  | Island  |
| <b>cg26348902</b> | -1.66 | 1E-03 | 0.0039 | 0.33  | -0.07 | 0.5726 | 4  |                 |         | Island  |
| <b>cg05990720</b> | -1.83 | 1E-03 | 0.0040 | -0.53 | 0.23  | 0.3935 | 9  | <i>C9orf72</i>  | 5UTR    | N_Shore |
| <b>cg22279519</b> | 1.77  | 1E-03 | 0.0041 | -1.18 | 0.71  | 0.2154 | 12 | <i>NCOR2</i>    | Body    | S_Shelf |
| <b>cg20176285</b> | -1.05 | 1E-03 | 0.0041 | -1.24 | 0.03  | 0.3831 | 2  | <i>REEPI</i>    | Body    | Island  |
| <b>cg15081402</b> | -2.14 | 1E-03 | 0.0041 | 0.33  | -0.07 | 0.6260 | 3  | <i>PRICKLE2</i> |         | S_Shelf |
| <b>cg00763510</b> | 1.46  | 1E-03 | 0.0045 | -0.26 | -0.21 | 0.6620 | 14 |                 |         |         |
| <b>cg24601716</b> | -2.11 | 2E-03 | 0.0047 | 0.46  | -0.36 | 0.5286 | 13 | <i>PDX1</i>     | Body    | Island  |
| <b>cg25739003</b> | -1.81 | 2E-03 | 0.0047 | -0.52 | 0.24  | 0.4676 | 11 | <i>EEF1G</i>    | Body    | Island  |
| <b>cg24198840</b> | 1.92  | 2E-03 | 0.0047 | 0.22  | -0.02 | 0.6612 | 2  | <i>NEU2</i>     | 1stExon |         |
| <b>cg05800641</b> | -0.89 | 2E-03 | 0.0051 | 0.12  | 0.00  | 0.7277 | 22 | <i>CACNA1I</i>  | Body    |         |
| <b>cg07292251</b> | 1.32  | 2E-03 | 0.0051 | -0.09 | 0.54  | 0.8589 | 5  | <i>F12</i>      | 3UTR    | N_Shore |
| <b>cg01798661</b> | 2.63  | 2E-03 | 0.0051 | -0.33 | -0.20 | 0.6475 | 13 | <i>NEK5</i>     | TSS1500 | S_Shore |
| <b>cg07555102</b> | 2.19  | 2E-03 | 0.0051 | 0.09  | 0.11  | 0.8742 | 1  |                 |         | N_Shelf |
| <b>cg09396181</b> | -2.18 | 2E-03 | 0.0052 | 0.00  | -0.22 | 0.9939 | 3  | <i>WNT7A</i>    | TSS1500 | Island  |
| <b>cg01461299</b> | -1.94 | 2E-03 | 0.0052 | 0.37  | 0.10  | 0.5490 | 19 | <i>MCOLN1</i>   | TSS1500 | N_Shore |
| <b>cg03177034</b> | 1.74  | 2E-03 | 0.0056 | -0.42 | 0.03  | 0.6362 | 2  | <i>STK39</i>    | Body    |         |
| <b>cg12967050</b> | -0.68 | 2E-03 | 0.0056 | -0.28 | 0.19  | 0.6745 | 19 | <i>TMEM149</i>  | 1stExon | S_Shore |
| <b>cg14240353</b> | -1.55 | 2E-03 | 0.0057 | -0.23 | 0.36  | 0.6457 | 12 | <i>IGF1</i>     | Body    |         |
| <b>cg07873926</b> | 0.96  | 2E-03 | 0.0058 | 0.43  | -0.21 | 0.3579 | 18 |                 |         | Island  |
| <b>cg26349362</b> | -1.71 | 2E-03 | 0.0058 | 0.02  | -0.07 | 0.9767 | 12 | <i>CAPS2</i>    | 1stExon | Island  |
| <b>cg15832329</b> | 1.29  | 2E-03 | 0.0058 | -0.32 | -0.18 | 0.6128 | 2  | <i>FARP2</i>    | 5UTR    | S_Shore |
| <b>cg08643007</b> | -1.30 | 2E-03 | 0.0058 | -0.87 | 0.66  | 0.3640 | 2  | <i>ATF2</i>     | 1stExon | Island  |
| <b>cg04107037</b> | -1.61 | 2E-03 | 0.0058 | 0.38  | -0.07 | 0.4925 | 4  | <i>ATOH1</i>    | 1stExon | Island  |
| <b>cg06216103</b> | 0.96  | 3E-03 | 0.0060 | 0.83  | -0.92 | 0.1871 | 12 | <i>GALNT9</i>   | Body    | Island  |

|                   |       |       |        |       |       |        |    |                 |              |         |
|-------------------|-------|-------|--------|-------|-------|--------|----|-----------------|--------------|---------|
| <b>cg09776718</b> | -1.17 | 2E-03 | 0.0060 | -0.27 | 0.14  | 0.5018 | 19 | <i>PLEKHFI</i>  | Body         | Island  |
| <b>cg19374731</b> | 1.75  | 3E-03 | 0.0061 | 0.16  | 0.02  | 0.7627 | 1  | <i>MORNI</i>    | Body         | S_Shelf |
| <b>cg01662869</b> | 3.09  | 3E-03 | 0.0062 | 0.21  | -0.35 | 0.6378 | 16 | <i>MGRNI</i>    | Body         | Island  |
| <b>cg01604539</b> | -1.43 | 3E-03 | 0.0062 | -0.06 | 0.19  | 0.9118 | 16 | <i>TRADD</i>    | Body         | Island  |
| <b>cg20491695</b> | -1.91 | 3E-03 | 0.0062 | -0.49 | 0.29  | 0.4233 | 11 |                 |              |         |
| <b>cg10692870</b> | -1.73 | 3E-03 | 0.0064 | 0.06  | -0.07 | 0.9218 | 2  | <i>FNI</i>      | Body         | Island  |
| <b>cg05104811</b> | 1.88  | 3E-03 | 0.0064 | -0.17 | 0.49  | 0.8198 | 6  | <i>PACRG</i>    | Body         | S_Shore |
| <b>cg26904787</b> | -1.60 | 3E-03 | 0.0067 | 0.38  | -0.18 | 0.5808 | 10 | <i>RTKN2</i>    | 1stExon;5UTR | Island  |
| <b>cg05232576</b> | 1.56  | 3E-03 | 0.0068 | -1.48 | 0.75  | 0.0978 | 20 | <i>CPXMI</i>    | Body         | N_Shelf |
| <b>cg24151841</b> | 1.27  | 3E-03 | 0.0069 | 0.23  | -0.10 | 0.7114 | 2  | <i>SPATS2L</i>  | Body         |         |
| <b>cg00169776</b> | 1.10  | 3E-03 | 0.0069 | 0.20  | 0.11  | 0.5648 | 1  | <i>LINC0098</i> |              |         |
| <b>cg25266327</b> | 0.94  | 3E-03 | 0.0069 | 0.02  | -0.25 | 0.9536 | 19 | <i>KLF2</i>     | 5UTR;1stExon | Island  |
| <b>cg23197881</b> | -1.50 | 3E-03 | 0.0071 | 0.19  | 0.00  | 0.8213 | 12 | <i>RAB3IP</i>   | 5UTR         | Island  |
| <b>cg20200460</b> | 1.36  | 3E-03 | 0.0074 | 0.45  | -0.23 | 0.3340 | 10 |                 |              |         |
| <b>cg00374554</b> | 1.63  | 4E-03 | 0.0076 | -0.25 | -0.11 | 0.6766 | 5  | <i>LINC0102</i> |              |         |
| <b>cg18786125</b> | -1.64 | 4E-03 | 0.0076 | -0.35 | 0.87  | 0.5816 | 1  | <i>MEGF6</i>    | TSS1500      | Island  |
| <b>cg27435903</b> | 2.38  | 4E-03 | 0.0077 | 1.31  | -0.16 | 0.0902 | 17 | <i>GSDMB</i>    | Body         |         |
| <b>cg25090315</b> | 1.96  | 4E-03 | 0.0079 | -0.86 | 0.38  | 0.1373 | 14 | <i>GPR68</i>    | 5UTR         | S_Shelf |
| <b>cg03468115</b> | 2.41  | 4E-03 | 0.0079 | 0.57  | -0.27 | 0.4600 | 10 |                 |              |         |
| <b>cg09543792</b> | -1.36 | 4E-03 | 0.0079 | -0.57 | 0.55  | 0.5681 | 17 | <i>SLC16A13</i> | TSS200       | Island  |
| <b>cg15365426</b> | 1.16  | 4E-03 | 0.0079 | 0.12  | 0.25  | 0.8471 | 2  |                 |              |         |
| <b>cg17821664</b> | 2.59  | 4E-03 | 0.0079 | 0.87  | 0.04  | 0.3330 | 15 | <i>OSTBETA</i>  | 1stExon;5UTR |         |
| <b>cg17724054</b> | -1.67 | 4E-03 | 0.0080 | 1.98  | -0.94 | 0.0480 | 5  | <i>RPS23</i>    | TSS200       | S_Shore |
| <b>cg06824318</b> | -0.90 | 4E-03 | 0.0083 | 0.31  | 0.14  | 0.5266 | 1  |                 |              | N_Shore |
| <b>cg05029148</b> | -1.02 | 4E-03 | 0.0085 | 0.06  | 0.03  | 0.8934 | 8  |                 |              | S_Shore |
| <b>cg06861115</b> | -2.16 | 4E-03 | 0.0086 | 1.06  | -0.75 | 0.1106 | 15 |                 |              | N_Shelf |
| <b>cg15651099</b> | -1.55 | 5E-03 | 0.0089 | 0.46  | -0.23 | 0.4886 | 1  | <i>KIRREL</i>   | Body         | Island  |
| <b>cg15847604</b> | 1.86  | 5E-03 | 0.0091 | 0.96  | -0.62 | 0.1349 | 12 | <i>ETV6</i>     | Body         |         |
| <b>cg04839616</b> | 1.77  | 5E-03 | 0.0093 | -0.13 | 0.46  | 0.8517 | 16 |                 |              |         |

|                   |       |       |        |       |       |        |    |                 |         |
|-------------------|-------|-------|--------|-------|-------|--------|----|-----------------|---------|
| <b>cg10410121</b> | 1.71  | 5E-03 | 0.0097 | 1.01  | -0.22 | 0.0865 | 7  |                 |         |
| <b>cg26406994</b> | -1.19 | 5E-03 | 0.0097 | 0.73  | -0.03 | 0.2207 | 4  | <i>RAP1GDS1</i> | Body    |
| <b>cg17490648</b> | 1.68  | 5E-03 | 0.0097 | -0.19 | -0.27 | 0.8439 | 8  | <i>PXMP3</i>    | TSS1500 |
| <b>cg06852255</b> | -1.59 | 5E-03 | 0.0097 | 0.03  | 0.10  | 0.9684 | 6  | <i>PSMB9</i>    | Island  |
| <b>cg22588936</b> | 1.55  | 5E-03 | 0.0097 | 0.61  | -0.57 | 0.1376 | 9  | <i>LCN10</i>    | Body    |
| <b>cg27479400</b> | -1.30 | 5E-03 | 0.0098 | 0.56  | -0.06 | 0.3318 | 22 | <i>SREBF2</i>   | Island  |
| <b>cg02725872</b> | 0.83  | 5E-03 | 0.0102 | 0.18  | -0.14 | 0.7291 | 8  |                 |         |
| <b>cg01870679</b> | 1.70  | 6E-03 | 0.0103 | -0.34 | -0.12 | 0.5784 | 19 | <i>ZNF506</i>   | 3UTR    |
| <b>cg01692279</b> | -1.41 | 6E-03 | 0.0106 | 0.34  | -0.67 | 0.7224 | 7  |                 |         |
| <b>cg08995424</b> | -1.42 | 6E-03 | 0.0109 | 0.57  | -0.02 | 0.3411 | 12 | <i>ATP5G2</i>   | N_Shore |
| <b>cg01426818</b> | -1.58 | 6E-03 | 0.0109 | -0.28 | 0.04  | 0.6732 | 17 | <i>CBX4</i>     | Island  |
| <b>cg23283875</b> | -1.36 | 6E-03 | 0.0111 | -1.11 | 0.75  | 0.1211 | 7  | <i>C7orf63</i>  | 1stExon |
| <b>cg09791665</b> | -1.16 | 6E-03 | 0.0112 | -0.43 | 0.07  | 0.5191 | 19 | <i>ZNF441</i>   | Island  |
| <b>cg02015280</b> | -1.21 | 6E-03 | 0.0112 | 0.03  | -0.10 | 0.9656 | 7  | <i>AGBL3</i>    | TSS200  |
| <b>cg15101985</b> | 2.07  | 6E-03 | 0.0113 | 1.46  | -0.34 | 0.0756 | 10 | <i>PCDH21</i>   | Body    |
| <b>cg16010178</b> | -1.52 | 6E-03 | 0.0113 | 0.64  | -0.46 | 0.2938 | 17 | <i>EPN3</i>     | N_Shelf |
| <b>cg22993878</b> | 2.33  | 6E-03 | 0.0113 | 0.61  | -0.24 | 0.4067 | 2  | <i>MYEOV2</i>   | S_Shore |
| <b>cg11160820</b> | -1.46 | 7E-03 | 0.0117 | -0.24 | 0.23  | 0.8272 | 1  | <i>CD58</i>     | TSS1500 |
| <b>cg00812799</b> | 1.56  | 7E-03 | 0.0122 | -0.52 | -0.18 | 0.4107 | 13 | <i>IL17D</i>    | Island  |
| <b>cg13963729</b> | -1.58 | 7E-03 | 0.0125 | -0.81 | 0.54  | 0.2808 | 19 | <i>4RJD3A</i>   | Island  |
| <b>cg24517858</b> | -1.11 | 7E-03 | 0.0129 | 1.55  | -0.85 | 0.1085 | 1  | <i>REN</i>      | Body    |
| <b>cg21634993</b> | 1.34  | 8E-03 | 0.0133 | -0.73 | -0.11 | 0.2715 | 4  | <i>MGST2</i>    | Island  |
| <b>cg02430497</b> | -1.44 | 8E-03 | 0.0136 | 0.34  | -0.02 | 0.6095 | 10 | <i>GTPBP4</i>   | Island  |
| <b>cg00131618</b> | -1.06 | 8E-03 | 0.0137 | 0.63  | -0.29 | 0.4148 | 5  | <i>C5orf42</i>  | Island  |
| <b>cg17508018</b> | -1.08 | 8E-03 | 0.0142 | 0.90  | -0.11 | 0.2862 | 19 | <i>PLD3</i>     | Island  |
| <b>cg19862616</b> | 0.65  | 9E-03 | 0.0144 | 0.29  | 0.02  | 0.5066 | 7  | <i>NCRNA001</i> | Island  |
| <b>cg00755287</b> | -1.98 | 9E-03 | 0.0145 | 0.13  | 0.06  | 0.8641 | 17 | <i>KRTAP9-3</i> | TSS1500 |
| <b>cg26417188</b> | 1.63  | 9E-03 | 0.0149 | 0.46  | -0.39 | 0.3950 | 1  | <i>KLF17</i>    | TSS1500 |
| <b>cg22085702</b> | -1.56 | 9E-03 | 0.0150 | -0.29 | 0.92  | 0.6500 | 11 | <i>CALCA</i>    | N_Shore |

|                   |       |       |        |       |       |        |    |                |              |
|-------------------|-------|-------|--------|-------|-------|--------|----|----------------|--------------|
| <b>cg22364465</b> | 1.99  | 9E-03 | 0.0152 | 1.07  | -0.44 | 0.1672 | 1  | <i>PLXN42</i>  | Body         |
| <b>cg13659360</b> | 1.27  | 9E-03 | 0.0152 | 0.62  | -0.04 | 0.2657 | 11 | <i>TECT4</i>   | Body         |
| <b>cg02948476</b> | -1.15 | 9E-03 | 0.0152 | 0.14  | 0.11  | 0.8673 | 14 | <i>GSC</i>     | Body         |
| <b>cg00152175</b> | -0.93 | 1E-02 | 0.0156 | 0.93  | -0.09 | 0.2495 | 16 | <i>AMFR</i>    | TSS1500      |
| <b>cg01499522</b> | -1.34 | 1E-02 | 0.0157 | 0.26  | 0.19  | 0.6387 | 7  | <i>MLXIP1</i>  | Body         |
| <b>cg05564836</b> | 1.28  | 1E-02 | 0.0157 | -0.20 | 0.41  | 0.6534 | 15 | <i>OCA2</i>    | Body         |
| <b>cg04871364</b> | -1.27 | 1E-02 | 0.0158 | -0.10 | 0.02  | 0.8265 | 1  | <i>ESPN</i>    | Body         |
| <b>cg02266878</b> | -1.02 | 1E-02 | 0.0161 | -0.89 | 0.60  | 0.0450 | 16 | <i>MSLN1</i>   | Body         |
| <b>cg06102330</b> | -1.42 | 1E-02 | 0.0161 | 1.41  | -0.08 | 0.0850 | 8  | <i>MSC</i>     | TSS1500      |
| <b>cg07614018</b> | -1.53 | 1E-02 | 0.0164 | -1.12 | 0.48  | 0.3621 | 19 | <i>CRTCL</i>   | Body         |
| <b>cg12348202</b> | 1.06  | 1E-02 | 0.0168 | 0.05  | -0.24 | 0.9125 | 7  | <i>PTPRN2</i>  | TSS1500      |
| <b>cg03821689</b> | 1.43  | 1E-02 | 0.0170 | 1.18  | -0.13 | 0.0280 | 11 | <i>FXYD6</i>   | TSS1500      |
| <b>cg14967868</b> | 1.12  | 1E-02 | 0.0172 | -0.22 | -0.49 | 0.9051 | 4  | <i>SPATA4</i>  | 1stExon;5UTR |
| <b>cg06902665</b> | -1.65 | 1E-02 | 0.0177 | 1.42  | -1.06 | 0.1078 | 19 | <i>ONECUT3</i> | Body         |
| <b>cg13590117</b> | 1.38  | 1E-02 | 0.0177 | 0.43  | -0.02 | 0.3923 | 9  | <i>OLFM1</i>   | N_Shore      |
| <b>cg10920378</b> | -2.02 | 1E-02 | 0.0177 | 0.59  | -0.68 | 0.4640 | 4  | <i>RBM46</i>   | TSS1500      |
| <b>cg20728639</b> | -1.08 | 1E-02 | 0.0178 | 0.66  | -0.05 | 0.3502 | 11 | <i>ABTB2</i>   | TSS1500      |
| <b>cg14442841</b> | -0.98 | 1E-02 | 0.0180 | -0.43 | 0.46  | 0.3551 | 6  | <i>MBOAT1</i>  | Body         |
| <b>cg08990264</b> | -1.29 | 1E-02 | 0.0191 | 0.21  | 0.02  | 0.6738 | 8  |                |              |
| <b>cg02712036</b> | -0.69 | 1E-02 | 0.0191 | -0.29 | 0.27  | 0.5843 | 15 | <i>RAB27A</i>  | 5UTR         |
| <b>cg24478630</b> | -1.04 | 1E-02 | 0.0196 | 0.68  | -0.42 | 0.1757 | 2  | <i>MOGS</i>    | TSS200       |
| <b>cg01687864</b> | -1.46 | 1E-02 | 0.0200 | 0.26  | 0.04  | 0.6349 | 7  | <i>ING3</i>    | Body;Body    |
| <b>cg14736210</b> | -1.28 | 1E-02 | 0.0208 | -0.44 | 0.59  | 0.3312 | 20 | <i>KCNBI</i>   | 1stExon      |
| <b>cg16358034</b> | 1.10  | 1E-02 | 0.0219 | -0.50 | -0.05 | 0.2770 | 5  | <i>SNX18</i>   | Island       |
| <b>cg15584606</b> | 1.62  | 2E-02 | 0.0221 | 0.38  | -0.66 | 0.6314 | 10 | <i>GATA3</i>   | Island       |
| <b>cg02691091</b> | 2.03  | 2E-02 | 0.0225 | 0.33  | -0.39 | 0.6447 | 17 | <i>SP2</i>     | Body         |
| <b>cg22755534</b> | 0.66  | 2E-02 | 0.0226 | 0.15  | -0.22 | 0.7840 | 11 |                |              |
| <b>cg05346295</b> | 0.98  | 2E-02 | 0.0234 | 0.85  | -0.34 | 0.3404 | 19 | <i>NUP62</i>   | Body         |
| <b>cg21197594</b> | -1.44 | 2E-02 | 0.0244 | 1.83  | -0.97 | 0.0387 | 9  | <i>EHMT1</i>   | Body         |

|                   |       |       |        |       |       |        |    |                 |
|-------------------|-------|-------|--------|-------|-------|--------|----|-----------------|
| <b>cg06759374</b> | -1.00 | 2E-02 | 0.0244 | 0.03  | 0.68  | 0.9576 | 3  | Island          |
| <b>cg12271966</b> | -0.98 | 2E-02 | 0.0247 | 0.66  | 0.06  | 0.4578 | 22 | <i>PATZI</i>    |
| <b>cg06486582</b> | 1.46  | 2E-02 | 0.0250 | -0.16 | 0.09  | 0.8209 | 5  | TSS1500         |
| <b>cg18481137</b> | -1.00 | 2E-02 | 0.0282 | 0.53  | -0.10 | 0.5271 | 3  | <i>FOXPI</i>    |
| <b>cg18232125</b> | -1.58 | 2E-02 | 0.0282 | -0.14 | -0.02 | 0.8211 | 5  | 5UTR;5UTR       |
| <b>cg24708694</b> | 1.25  | 2E-02 | 0.0293 | -0.04 | 0.34  | 0.9272 | 4  | Island          |
| <b>cg20383390</b> | -0.98 | 2E-02 | 0.0297 | -0.56 | 0.44  | 0.2895 | 1  | <i>MANIA2</i>   |
| <b>cg16526287</b> | 1.01  | 2E-02 | 0.0297 | 0.05  | -0.56 | 0.9389 | 6  | <i>DTNBP1</i>   |
| <b>cg07750914</b> | -1.37 | 2E-02 | 0.0298 | 0.14  | -0.05 | 0.9283 | 2  | <i>PAPOLG</i>   |
| <b>cg07580479</b> | 0.99  | 2E-02 | 0.0305 | -0.11 | 0.00  | 0.9042 | 6  | <i>FOXO3</i>    |
| <b>cg00925953</b> | -1.35 | 2E-02 | 0.0307 | 0.31  | -0.24 | 0.6172 | 1  | <i>TASIR2</i>   |
| <b>cg07475890</b> | -0.98 | 2E-02 | 0.0307 | -0.13 | -0.10 | 0.8535 | 11 | <i>PPP1R14B</i> |
| <b>cg01754267</b> | 0.87  | 2E-02 | 0.0311 | 0.38  | 0.19  | 0.6253 | 12 | <i>NDUFA4L2</i> |
| <b>cg27230396</b> | 1.02  | 2E-02 | 0.0312 | 0.56  | -0.05 | 0.3829 | 4  | <i>SHROOM3</i>  |
| <b>cg00385142</b> | 1.53  | 2E-02 | 0.0318 | 0.11  | -0.65 | 0.8759 | 3  | <i>CLDND1</i>   |
| <b>cg05098096</b> | 1.12  | 2E-02 | 0.0319 | 0.31  | -0.56 | 0.5215 | 16 | <i>ARL6IP1</i>  |
| <b>cg08258650</b> | -1.02 | 2E-02 | 0.0323 | 0.81  | -0.25 | 0.1284 | 11 | <i>SLC1A2</i>   |
| <b>cg11694433</b> | -0.97 | 2E-02 | 0.0328 | 0.24  | -0.08 | 0.6887 | 15 | <i>USP3</i>     |
| <b>cg23619399</b> | 0.99  | 3E-02 | 0.0334 | -0.06 | 0.19  | 0.9244 | 13 | TSS200          |
| <b>cg10200408</b> | -1.22 | 3E-02 | 0.0336 | -0.21 | 0.57  | 0.7977 | 12 | <i>ASB8</i>     |
| <b>cg20477591</b> | 1.15  | 3E-02 | 0.0350 | 0.15  | -0.42 | 0.7929 | 5  | <i>PIK3R1</i>   |
| <b>cg24976131</b> | 1.60  | 3E-02 | 0.0355 | -0.41 | 0.23  | 0.5752 | 17 | <i>NAGS</i>     |
| <b>cg05441854</b> | 0.49  | 3E-02 | 0.0359 | -1.21 | 0.65  | 0.1484 | 16 | <i>KIAA0182</i> |
| <b>cg01266916</b> | -0.99 | 3E-02 | 0.0368 | 0.54  | -0.68 | 0.4712 | 20 | <i>MMP9</i>     |
| <b>cg04436634</b> | 1.45  | 3E-02 | 0.0369 | 0.97  | -0.30 | 0.3039 | 1  | <i>OR10Z1</i>   |
| <b>cg02374944</b> | 1.61  | 3E-02 | 0.0369 | 0.53  | 0.35  | 0.3988 | 15 | <i>MAN2A2</i>   |
| <b>cg20232060</b> | -1.13 | 3E-02 | 0.0374 | -1.49 | 0.43  | 0.2027 | 3  | <i>RNF7</i>     |
| <b>cg16332065</b> | -0.88 | 3E-02 | 0.0390 | 0.62  | 0.20  | 0.2593 | 4  | <i>GABRG1</i>   |
| <b>cg11817533</b> | 1.31  | 3E-02 | 0.0395 | -0.09 | 0.05  | 0.8482 | 6  | TSS200          |
|                   |       |       |        |       |       |        |    | S_Shore         |

|                   |       |       |        |       |                 |              |    |                 |         |         |
|-------------------|-------|-------|--------|-------|-----------------|--------------|----|-----------------|---------|---------|
| <b>cg26146287</b> | -1.32 | 3E-02 | 0.0397 | -1.06 | 0.39            | 0.1542       | 5  | <i>CARTPT</i>   | TSS1500 | N_Shore |
| <b>cg05951364</b> | 1.42  | 3E-02 | 0.0403 | 0.64  | -0.21           | 0.2326       | 8  | <i>DLGAP2</i>   | 5UTR    | S_Shelf |
| <b>cg13664588</b> | -2.00 | 3E-02 | 0.0413 | -0.12 | 0.00            | 0.8891       | 17 | <i>SNORD1A</i>  | TSS1500 |         |
| <b>cg00017461</b> | -0.86 | 3E-02 | 0.0417 | -0.22 | -0.18           | 0.8572       | 22 | <i>OSM</i>      | TSS1500 |         |
| <b>cg00003722</b> | 1.33  | 3E-02 | 0.0427 | 0.22  | -0.36           | 0.8219       | 10 |                 |         |         |
| <b>cg17596905</b> | -1.01 | 4E-02 | 0.0445 | 0.68  | -0.51           | 0.4598       | 3  | <i>CCDC50</i>   | 5UTR    | Island  |
| <b>cg11021321</b> | 0.86  | 4E-02 | 0.0452 | 0.14  | 0.17            | 0.8006       | 20 | <i>GNAS</i>     | Body    | S_Shelf |
| <b>cg26756083</b> | -1.06 | 4E-02 | 0.0452 | 0.25  | 0.71            | 0.8239       | 8  | <i>MMP16</i>    | 5UTR    | N_Shore |
| <b>cg19738404</b> | -1.21 | 4E-02 | 0.0460 | -0.30 | 0.30            | 0.6539       | 2  | <i>BIN1</i>     |         | S_Shore |
| <b>cg03533979</b> | -0.85 | 4E-02 | 0.0481 | 0.17  | 0.06            | 0.6458       | 22 | <i>CERK</i>     | Body    | Island  |
| <b>cg05876918</b> | -1.10 | 4E-02 | 0.0492 | 0.91  | -0.38           | 0.2242       | 12 | <i>PIP4K2C</i>  | 1stExo  | Island  |
| <b>cg00770837</b> | 1.70  | 1E-03 | 0.0035 |       |                 |              | 2  | <i>RGPD5</i>    | TSS1500 | S_Shore |
| <b>cg00893493</b> | -1.52 | 4E-03 | 0.0085 |       |                 |              | 1  | <i>MCOLN3</i>   | 5UTR    | N_Shore |
| <b>cg00971789</b> | 1.02  | 6E-03 | 0.0113 |       |                 |              | 17 | <i>ARSG</i>     | Body    |         |
| <b>cg01120423</b> | 1.71  | 2E-03 | 0.0051 |       |                 |              | 16 | <i>KIAA0430</i> | Body    |         |
| <b>cg01325599</b> | -2.36 | 1E-02 | 0.0208 | 3     |                 |              |    |                 |         |         |
| <b>cg01341327</b> | 1.87  | 9E-04 | 0.0033 | 2     | <i>CNOT11</i>   | Body         |    |                 |         |         |
| <b>cg01558754</b> | -2.12 | 1E-02 | 0.0204 | 6     | <i>KCNQ5</i>    | Body         |    |                 |         |         |
| <b>cg01578625</b> | -2.22 | 3E-03 | 0.0063 |       |                 |              | 11 | <i>CD44</i>     | Body    |         |
| <b>cg01786959</b> | -1.87 | 2E-04 | 0.0014 | 1     | <i>NPPA-ASI</i> | Body         |    |                 |         |         |
| <b>cg02300001</b> | 2.34  | 4E-05 | 0.0008 | 16    |                 |              |    |                 |         |         |
| <b>cg02496392</b> | 1.32  | 4E-03 | 0.0077 | 1     | <i>AHDCL</i>    | 5UTR         |    |                 |         |         |
| <b>cg02665414</b> | 1.44  | 2E-02 | 0.0280 | 11    |                 |              |    |                 |         |         |
| <b>cg02683869</b> | -1.70 | 9E-03 | 0.0153 | 12    |                 |              |    |                 |         |         |
| <b>cg02901886</b> | 2.74  | 6E-04 | 0.0027 | 14    | <i>RAD51B</i>   | Body;Body    |    |                 |         |         |
| <b>cg03035177</b> | -2.21 | 2E-04 | 0.0014 | 3     | <i>DGKG</i>     | 1stExon      |    |                 |         |         |
| <b>cg03123201</b> | -2.45 | 4E-04 | 0.0020 | 5     | <i>IRXI</i>     | Body         |    |                 |         |         |
| <b>cg03490138</b> | -1.80 | 4E-03 | 0.0081 | 12    | <i>CD27</i>     | Body;TSS1500 |    |                 |         |         |
| <b>cg03493480</b> | 3.30  | 1E-04 | 0.0011 | 8     |                 |              |    |                 |         |         |

|                   |       |       |        |    |                |         |
|-------------------|-------|-------|--------|----|----------------|---------|
| <i>cg03501936</i> | 1.42  | 7E-03 | 0.0125 | 5  | <i>CDH2R</i>   | Body    |
| <i>cg03618886</i> | 1.45  | 4E-02 | 0.0497 | 3  | <i>GOLG44</i>  | TSS1500 |
| <i>cg03809583</i> | 1.79  | 2E-03 | 0.0056 | 12 |                | N_Shore |
| <i>cg03898146</i> | -1.28 | 1E-02 | 0.0168 | 20 |                |         |
| <i>cg03920147</i> | 1.42  | 2E-02 | 0.0235 | 1  |                |         |
| <i>cg04091518</i> | -2.93 | 9E-05 | 0.0011 | 9  |                |         |
| <i>cg04188137</i> | -1.06 | 4E-02 | 0.0494 | 11 | <i>CLMP</i>    | Body    |
| <i>cg04335891</i> | -1.67 | 2E-03 | 0.0052 | 20 | <i>CDH4</i>    | Body    |
| <i>cg04390191</i> | -1.90 | 3E-03 | 0.0069 | 2  | <i>SPL10</i>   | TSS200  |
| <i>cg04397316</i> | -1.64 | 2E-03 | 0.0051 | 6  | <i>TAB2</i>    | Body    |
| <i>cg04453170</i> | -1.53 | 2E-02 | 0.0227 | 4  |                | S_Shore |
| <i>cg05308867</i> | 2.02  | 5E-05 | 0.0009 | 2  |                |         |
| <i>cg05356782</i> | 1.91  | 2E-03 | 0.0056 | 11 | <i>PACSI</i>   | Body    |
| <i>cg05501127</i> | 2.24  | 3E-03 | 0.0061 | 1  | <i>WASF2</i>   | 3UTR    |
| <i>cg05538745</i> | -2.05 | 5E-05 | 0.0009 | 14 | <i>PRKCH</i>   | 1stExon |
| <i>cg05753257</i> | 1.56  | 1E-03 | 0.0044 | 12 |                | Island  |
| <i>cg05789318</i> | 1.93  | 6E-03 | 0.0113 | 5  |                | S_Shore |
| <i>cg06034584</i> | -1.46 | 6E-03 | 0.0112 | 9  | <i>TOPORS4</i> | Body    |
| <i>cg06311780</i> | -1.85 | 2E-03 | 0.0056 | 18 |                | N_Shore |
| <i>cg06670685</i> | 1.07  | 9E-03 | 0.0152 | 9  | <i>NUP214</i>  | Body    |
| <i>cg06703980</i> | 1.93  | 2E-03 | 0.0051 | 3  | <i>CHCHD6</i>  | Body    |
| <i>cg06771173</i> | 1.89  | 9E-05 | 0.0011 | 1  | <i>ZSWIM5</i>  | Body    |
| <i>cg06949394</i> | -2.59 | 2E-05 | 0.0008 | 10 | <i>MKX</i>     | 5UTR    |
| <i>cg07194517</i> | -2.88 | 2E-05 | 0.0008 | 9  |                | Island  |
| <i>cg07201235</i> | 1.90  | 9E-05 | 0.0011 | 1  | <i>SPOCD1</i>  | Body    |
| <i>cg07300949</i> | 1.06  | 3E-03 | 0.0065 | 14 | <i>SLC8A3</i>  | 5UTR    |
| <i>cg08172212</i> | 1.51  | 1E-03 | 0.0035 | 2  | <i>SPHKAP</i>  | Body    |
| <i>cg08504214</i> | -1.57 | 4E-02 | 0.0452 | 19 | <i>SBNO2</i>   | TSS1500 |
| <i>cg08533932</i> | -1.10 | 9E-05 | 0.0011 | 8  | <i>PDGFRL</i>  | TSS200  |
|                   |       |       |        |    |                | N_Shore |

|                         |       |       |        |    |                 |         |
|-------------------------|-------|-------|--------|----|-----------------|---------|
| <code>cg08626295</code> | 1.83  | 3E-03 | 0.0061 | 22 | <i>RANGAPI</i>  | 3'UTR   |
| <code>cg08653158</code> | 1.90  | 1E-03 | 0.0041 | 11 |                 |         |
| <code>cg08890816</code> | -2.36 | 3E-05 | 0.0008 | 4  | <i>PAPSSI</i>   | TSS1500 |
| <code>cg09171201</code> | 1.09  | 4E-02 | 0.0481 | 5  |                 | Island  |
| <code>cg09314901</code> | -1.73 | 9E-03 | 0.0146 | 10 |                 |         |
| <code>cg09584604</code> | -1.47 | 4E-04 | 0.0021 | 4  | <i>COX18</i>    | TSS1500 |
| <code>cg09762585</code> | 1.58  | 3E-02 | 0.0337 | 1  |                 | S_Shore |
| <code>cg09953309</code> | 1.84  | 2E-03 | 0.0058 | 7  | <i>LINC0052</i> | N_Shore |
| <code>cg10060082</code> | 2.60  | 5E-04 | 0.0023 | 14 | <i>VTIIB</i>    | Body    |
| <code>cg10105621</code> | 2.47  | 2E-03 | 0.0047 | 11 | <i>CELF1</i>    | 3'UTR   |
| <code>cg10247069</code> | 1.75  | 3E-03 | 0.0075 | 1  |                 |         |
| <code>cg10428526</code> | -2.53 | 3E-04 | 0.0017 | 9  | <i>RABEPK</i>   | TSS1500 |
| <code>cg10518693</code> | -0.92 | 4E-02 | 0.0466 | 14 | <i>EXOC5_A</i>  | Island  |
| <code>cg10604470</code> | -0.58 | 2E-02 | 0.0237 | 18 | <i>RNF125</i>   | 1stExon |
| <code>cg10761100</code> | -2.30 | 4E-03 | 0.0078 | 17 | <i>SLC39A11</i> | TSS200  |
| <code>cg10769180</code> | -1.26 | 1E-02 | 0.0168 | 3  |                 | N_Shore |
| <code>cg10903440</code> | -1.75 | 3E-03 | 0.0066 | 13 |                 |         |
| <code>cg11081247</code> | -2.17 | 2E-03 | 0.0051 | 1  | <i>STPG1</i>    | N_Shore |
| <code>cg11121987</code> | -1.42 | 1E-03 | 0.0044 | 11 | <i>OPCM1</i>    | Body    |
| <code>cg11125823</code> | 2.72  | 7E-05 | 0.0010 | 16 | <i>4RHGAPI7</i> | Body    |
| <code>cg11170610</code> | -2.35 | 6E-05 | 0.0009 | 1  |                 | Island  |
| <code>cg11327392</code> | 1.06  | 3E-02 | 0.0356 | 3  |                 |         |
| <code>cg11328665</code> | -1.58 | 2E-02 | 0.0239 | 17 | <i>9-Sep</i>    | TSS1500 |
| <code>cg11502583</code> | -2.27 | 5E-05 | 0.0009 | 3  | <i>U2SURP</i>   | N_Shore |
| <code>cg11516862</code> | 1.61  | 7E-03 | 0.0119 | 12 | <i>ANAPC7</i>   | Body    |
| <code>cg11590775</code> | 1.43  | 2E-02 | 0.0266 | 16 | <i>RPS15A</i>   | TSS1500 |
| <code>cg11713268</code> | -2.35 | 8E-03 | 0.0130 | 13 | <i>TBC1D4</i>   | S_Shore |
| <code>cg11784870</code> | -3.04 | 2E-04 | 0.0013 | 22 | <i>SYN3</i>     | Body    |
| <code>cg11904216</code> | 3.09  | 4E-07 | 0.0002 | 16 | <i>C16orf46</i> | 5'UTR   |

|                   |       |       |        |    |               |         |
|-------------------|-------|-------|--------|----|---------------|---------|
| <i>cg11916384</i> | -2.40 | 1E-04 | 0.0012 | 7  |               |         |
| <i>cg12016449</i> | 1.74  | 1E-02 | 0.0180 | 20 | <i>PREXI</i>  | Body    |
| <i>cg12224382</i> | -1.31 | 4E-03 | 0.0084 | 1  | <i>GJA8</i>   | TSS200  |
| <i>cg12736742</i> | 1.58  | 2E-03 | 0.0056 | 13 |               |         |
| <i>cg12872535</i> | 1.80  | 1E-02 | 0.0173 | 1  |               |         |
| <i>cg13098169</i> | 1.35  | 4E-03 | 0.0081 | 6  | <i>USP45</i>  | 5UTR    |
| <i>cg13155790</i> | -1.58 | 8E-03 | 0.0130 | 15 |               | N_Shelf |
| <i>cg13255969</i> | -1.38 | 3E-03 | 0.0069 | 9  |               |         |
| <i>cg13942631</i> | -2.30 | 2E-03 | 0.0052 | 10 |               |         |
| <i>cg13973074</i> | -2.00 | 6E-03 | 0.0111 | 1  |               |         |
| <i>cg13986784</i> | -2.57 | 2E-03 | 0.0052 | 3  |               |         |
| <i>cg14181092</i> | -1.54 | 5E-03 | 0.0102 | 5  | <i>PPIC</i>   | Body    |
| <i>cg14278029</i> | -1.35 | 5E-04 | 0.0025 | 1  | <i>NFLA</i>   | Island  |
| <i>cg14293818</i> | -1.89 | 9E-05 | 0.0011 | 7  | <i>DNAJC2</i> | N_Shore |
| <i>cg14336545</i> | -1.76 | 1E-03 | 0.0042 | 13 | <i>ATP8A2</i> | S_Shore |
| <i>cg14714087</i> | -2.01 | 2E-03 | 0.0051 | 19 |               | ExonBnd |
| <i>cg14767360</i> | -2.56 | 3E-04 | 0.0017 | 18 | <i>DYM</i>    | Island  |
| <i>cg14794991</i> | -2.14 | 3E-03 | 0.0075 | 10 | <i>GRID1</i>  | Body    |
| <i>cg15051432</i> | -1.00 | 2E-02 | 0.0291 | 3  |               |         |
| <i>cg15260373</i> | -1.31 | 4E-02 | 0.0487 | 21 |               |         |
| <i>cg15418976</i> | 1.90  | 4E-04 | 0.0020 | 11 | <i>PTPRU</i>  | Body    |
| <i>cg15469038</i> | -2.05 | 4E-04 | 0.0020 | 17 |               | N_Shore |
| <i>cg15556088</i> | 0.86  | 3E-02 | 0.0386 | 18 | <i>TCF4</i>   | Body    |
| <i>cg15705918</i> | 2.11  | 2E-04 | 0.0015 | 22 | <i>MIEFL</i>  | 5UTR    |
| <i>cg15887809</i> | -2.18 | 6E-04 | 0.0026 | 6  | <i>ARID1B</i> | Body    |
| <i>cg15979711</i> | 1.42  | 2E-02 | 0.0314 | 15 |               |         |
| <i>cg16181199</i> | 1.26  | 3E-02 | 0.0432 | 7  | <i>ESYT2</i>  | Body    |
| <i>cg16181878</i> | 1.19  | 2E-02 | 0.0297 | 12 |               | N_Shore |
| <i>cg16253805</i> | -1.70 | 2E-02 | 0.0229 | 16 |               |         |

|                         |       |       |        |    |                 |         |         |
|-------------------------|-------|-------|--------|----|-----------------|---------|---------|
| <code>cg16404609</code> | 2.12  | 3E-03 | 0.0068 | 1  | <i>KPN46</i>    | Body    |         |
| <code>cg16423486</code> | -2.17 | 2E-04 | 0.0013 | 2  |                 |         | N_Shore |
| <code>cg16809249</code> | -0.92 | 3E-03 | 0.0071 | 14 |                 |         | S_Shelf |
| <code>cg16947819</code> | 2.75  | 4E-04 | 0.0022 | 10 | <i>KIA41462</i> | Body    |         |
| <code>cg17364708</code> | 1.65  | 2E-03 | 0.0047 | 17 | <i>UBE2O</i>    | Body    |         |
| <code>cg17698505</code> | -2.33 | 1E-04 | 0.0012 | 22 | <i>EWSR1, R</i> | TSS1500 | S_Shore |
| <code>cg17775336</code> | 1.99  | 2E-04 | 0.0014 | 8  | <i>GRHL2</i>    | Body    |         |
| <code>cg17853121</code> | -1.91 | 7E-04 | 0.0027 | 2  | <i>CENPO</i>    | TSS200  | Island  |
| <code>cg17939602</code> | -2.13 | 4E-03 | 0.0076 | 5  |                 |         |         |
| <code>cg18019618</code> | -2.10 | 1E-03 | 0.0042 | 5  | <i>ARHGEF28</i> | 5UTR    |         |
| <code>cg18104668</code> | -1.19 | 1E-03 | 0.0039 | 5  | <i>RGMB</i>     | TSS1500 |         |
| <code>cg18622049</code> | -1.61 | 4E-03 | 0.0085 | 1  | <i>RABGAP1L</i> | Body    |         |
| <code>cg19382123</code> | 4.39  | 2E-04 | 0.0014 | 4  | <i>LINC0098</i> | TSS1500 |         |
| <code>cg19427589</code> | -3.40 | 6E-03 | 0.0106 | 17 | <i>PLEKHM1</i>  | Body    |         |
| <code>cg19545865</code> | 1.02  | 9E-03 | 0.0152 | 16 |                 |         |         |
| <code>cg19635805</code> | -1.90 | 1E-06 | 0.0003 | 10 | <i>LRRK2D</i>   | 5UTR    |         |
| <code>cg19637744</code> | 1.82  | 9E-03 | 0.0146 | 1  | <i>OBSCN</i>    | Body    |         |
| <code>cg19825503</code> | 1.26  | 1E-02 | 0.0196 | 2  | <i>EHBPI</i>    | Body    |         |
| <code>cg19958721</code> | -1.31 | 1E-03 | 0.0039 | 2  | <i>ARHGAP15</i> | Body    |         |
| <code>cg19994575</code> | 2.38  | 6E-04 | 0.0027 | 3  | <i>FAM19A4</i>  | Body    |         |
| <code>cg20040976</code> | -1.48 | 2E-03 | 0.0047 | 15 |                 |         |         |
| <code>cg20397901</code> | 2.43  | 1E-05 | 0.0007 | 10 |                 |         |         |
| <code>cg20728881</code> | -2.34 | 4E-04 | 0.0020 | 10 | <i>ARID5B</i>   | TSS1500 |         |
| <code>cg20756051</code> | 2.08  | 6E-03 | 0.0113 | 3  | <i>LNPL</i>     | Body    |         |
| <code>cg20866256</code> | 2.83  | 5E-05 | 0.0009 | 12 |                 |         | N_Shore |
| <code>cg20951352</code> | 2.36  | 6E-04 | 0.0025 | 2  |                 |         |         |
| <code>cg21055045</code> | -3.01 | 2E-03 | 0.0056 | 2  | <i>TTC7A</i>    | Body    |         |
| <code>cg21202847</code> | -2.03 | 5E-03 | 0.0093 | 1  | <i>E2F2</i>     | TSS1500 | Island  |
| <code>cg21353284</code> | -1.83 | 1E-03 | 0.0037 | 1  | <i>GJB3</i>     | 5UTR    | S_Shore |

|            |       |       |        |    |                 |         |         |
|------------|-------|-------|--------|----|-----------------|---------|---------|
| cg21433170 | -3.14 | 1E-02 | 0.0180 | 11 | <i>IFITM1</i>   | TSS1500 | S_Shore |
| cg21459672 | -3.39 | 1E-03 | 0.0035 | 13 | <i>DCUNID2</i>  | Body    |         |
| cg21548114 | -2.24 | 4E-04 | 0.0020 | 11 | <i>GDPD5</i>    | Body    |         |
| cg21568193 | -1.80 | 2E-03 | 0.0048 | 1  | <i>SLC9C2</i>   | Body    |         |
| cg22471376 | -1.76 | 2E-02 | 0.0266 | 15 | <i>ISG20</i>    | 5UTR    |         |
| cg22874664 | -1.51 | 3E-02 | 0.0343 | 20 |                 |         |         |
| cg23033164 | 1.89  | 2E-03 | 0.0059 | 12 |                 |         |         |
| cg23059673 | 1.65  | 6E-03 | 0.0111 | 19 |                 |         |         |
| cg23128484 | 2.11  | 3E-03 | 0.0063 | 2  |                 |         |         |
| cg23263679 | 1.63  | 2E-03 | 0.0056 | 19 | <i>DNAAF3</i>   | Body    | N_Shore |
| cg23293998 | -2.07 | 2E-03 | 0.0047 | 1  | <i>CACNA1E</i>  | Body    |         |
| cg23339014 | -2.89 | 3E-04 | 0.0017 | 14 | <i>PRKCH</i>    | Body    |         |
| cg23653514 | 1.55  | 1E-03 | 0.0037 | 12 | <i>MR2CI</i>    | Body    |         |
| cg24061073 | -1.83 | 6E-04 | 0.0026 | 1  | <i>CASP9</i>    | TSS1500 |         |
| cg24736834 | 0.83  | 3E-02 | 0.0430 | 15 | <i>PDE8A</i>    | TSS200  | Island  |
| cg24785373 | 1.27  | 1E-02 | 0.0178 | 2  |                 |         |         |
| cg25042436 | -1.99 | 4E-03 | 0.0079 | 11 | <i>ZC3H12C</i>  | Body    |         |
| cg25095420 | 2.72  | 1E-03 | 0.0041 | 22 | <i>NEFH</i>     | Body    | S_Shelf |
| cg25114671 | 2.58  | 2E-03 | 0.0059 | 16 | <i>SMPD3</i>    | 5UTR    |         |
| cg25434113 | -1.80 | 4E-02 | 0.0481 | 13 | <i>C1QTNF9</i>  | TSS1500 | Island  |
| cg25503398 | -2.95 | 4E-06 | 0.0006 | 3  | <i>BBX</i>      | 1stExon | N_Shore |
| cg25587451 | 2.44  | 2E-04 | 0.0013 | 19 | <i>ALCAM</i>    | TSS200  | N_Shore |
| cg25665603 | -1.77 | 7E-04 | 0.0027 |    |                 |         |         |
| cg25985183 | -1.82 | 1E-02 | 0.0191 | 10 |                 |         |         |
| cg26466155 | 1.79  | 2E-03 | 0.0052 | 1  | <i>KIF26B</i>   | Body    |         |
| cg27127276 | 1.44  | 2E-03 | 0.0056 | 10 |                 |         |         |
| cg27575100 | -3.46 | 6E-05 | 0.0009 | 11 | <i>LGR4</i>     | Body    |         |
| cg27647719 | -1.52 | 2E-02 | 0.0248 | 6  | <i>LOC10192</i> | Body    |         |

Supplement Table S10 (B): Association of DNAm in newborn with pre-adolescent Ast\_Rh at 70 CpGs that are sex nonspecific. Males are the reference group.

| CpGs              | IOWBC<br>Estimates | IOWBC<br>Raw<br>Pvalue | IOWBC<br>fdr<br>Pvalue | Alspac<br>Estimate | AlSPAC<br>pvalue | CHR | Gene            | Gene<br>Location | CpG<br>Island |
|-------------------|--------------------|------------------------|------------------------|--------------------|------------------|-----|-----------------|------------------|---------------|
| <b>cg16616362</b> | 0.88               | 0.0000                 | 0.0003                 | 0.14               | 0.5021           | 21  | <i>C21orf81</i> | TSS1500          | S_Shore       |
| <b>cg09397375</b> | -0.61              | 0.0002                 | 0.0030                 | -0.16              | 0.7800           | 1   | <i>ZNF672</i>   | TSS1500          | Island        |
| cg11864592        | 1.17               | 0.0006                 | 0.0053                 | -0.02              | 0.9504           | 15  | <i>GOLG46L4</i> |                  |               |
| cg10189362        | 1.29               | 0.0010                 | 0.0055                 | -0.18              | 0.4304           | 2   | <i>STEAP3</i>   | Body             | Island        |
| cg13999210        | -1.23              | 0.0009                 | 0.0055                 | 0.32               | 0.5323           | 4   | <i>NPY2R</i>    |                  |               |
| cg19766820        | -0.76              | 0.0010                 | 0.0055                 | 0.10               | 0.7274           | 5   |                 | N_Shore          |               |
| cg00815214        | -0.55              | 0.0010                 | 0.0055                 | 0.06               | 0.8073           | 21  |                 | Island           |               |
| cg04946910        | 0.92               | 0.0010                 | 0.0055                 | 0.06               | 0.8270           | 16  | <i>ORIFI</i>    | Island           |               |
| cg13793782        | -0.68              | 0.0014                 | 0.0063                 | 0.22               | 0.2755           | 9   | <i>RALGDS</i>   | Body             | N_Shore       |
| cg21100167        | 0.81               | 0.0013                 | 0.0063                 | -0.13              | 0.6735           | 21  | <i>PCBP3</i>    | Body;Body        | S_Shore       |
| <b>cg13627491</b> | 0.57               | 0.0032                 | 0.0126                 | 0.18               | 0.6581           | 9   | <i>LPPRI</i>    | 5'UTR            | Island        |
| <b>cg20977448</b> | -0.56              | 0.0036                 | 0.0126                 | -0.10              | 0.8464           | 5   | <i>GRPEL2</i>   | Body             | S_Shore       |
| cg10890016        | 0.58               | 0.0041                 | 0.0131                 | -0.23              | 0.4355           | 7   | <i>UNC844</i>   | Body             | N_Shore       |
| cg17574471        | 0.54               | 0.0046                 | 0.0131                 | -0.15              | 0.5065           | 4   | <i>LETM1</i>    | Body             |               |
| cg14062152        | -0.89              | 0.0048                 | 0.0131                 | 0.23               | 0.5913           | 10  | <i>TMEM26</i>   | Body             | N_Shore       |
| cg18845692        | -0.72              | 0.0056                 | 0.0136                 | 0.40               | 0.2064           | 14  | <i>FLRT2</i>    | TSS1500          | N_Shore       |
| <b>cg26806713</b> | 0.52               | 0.0061                 | 0.0145                 | 0.31               | 0.2330           | 6   |                 | N_Shore          |               |
| <b>cg08976554</b> | 0.81               | 0.0071                 | 0.0164                 | 0.19               | 0.4951           | 12  | <i>NCOR2</i>    | Body             | N_Shelf       |
| <b>cg14399790</b> | -0.51              | 0.0074                 | 0.0167                 | -0.01              | 0.9740           | 8   |                 | N_Shore          |               |
| <b>cg13675319</b> | 0.81               | 0.0081                 | 0.0178                 | 0.22               | 0.3255           | 9   |                 | Island           |               |
| <b>cg02982198</b> | 0.56               | 0.0092                 | 0.0178                 | 0.29               | 0.5596           | 10  | <i>ANKRD26</i>  | Body             | N_Shore       |
| cg27357049        | 0.64               | 0.0095                 | 0.0178                 | -0.10              | 0.7104           | 15  | <i>MIR548H4</i> | Body             | N_Shore       |
| cg27357049        | 0.64               | 0.0095                 | 0.0178                 | -0.10              | 0.7104           | 15  | <i>MIR548H4</i> | Body             | N_Shore       |
| cg00105306        | 0.95               | 0.0094                 | 0.0178                 | -0.07              | 0.8357           | 15  | <i>WDR73</i>    | Body             | N_Shelf       |

|                   |       |        |        |       |        |    |                 |         |         |
|-------------------|-------|--------|--------|-------|--------|----|-----------------|---------|---------|
| <b>cg14273401</b> | -0.27 | 0.0084 | 0.0178 | -0.01 | 0.9837 | 6  | <i>TRIM31</i>   | 3'UTR   | N_Shore |
| <b>cg20241375</b> | -0.79 | 0.0125 | 0.0217 | -0.25 | 0.5185 | 4  |                 |         | N_Shelf |
| <b>cg23112563</b> | -0.46 | 0.0135 | 0.0229 | 0.05  | 0.8036 | 7  | <i>LOC64200</i> | TSS200  | Island  |
| <b>cg07455685</b> | -0.64 | 0.0152 | 0.0249 | 0.27  | 0.3089 | 19 | <i>PVR</i>      | Body    | Island  |
| <b>cg21103269</b> | 0.55  | 0.0163 | 0.0263 | 0.60  | 0.0585 | 6  |                 |         |         |
| <b>cg02724025</b> | 0.47  | 0.0176 | 0.0273 | 0.14  | 0.5980 | 16 | <i>CDH11</i>    | Body    | Island  |
| <b>cg16654216</b> | 0.64  | 0.0191 | 0.0291 | -0.26 | 0.4185 | 2  | <i>SATB2</i>    |         |         |
| <b>cg13185308</b> | -0.81 | 0.0200 | 0.0300 | 0.26  | 0.6392 | 11 | <i>ABCC8</i>    | TSS1500 | S_Shore |
| <b>cg01395217</b> | -0.81 | 0.0214 | 0.0316 | -0.35 | 0.3267 | 1  | <i>SEC22B</i>   | Body    | S_Shelf |
| <b>cg19248893</b> | 0.86  | 0.0261 | 0.0367 | 0.58  | 0.0651 | 1  | <i>DNAJC11</i>  | Body    |         |
| <b>cg12372414</b> | -0.57 | 0.0381 | 0.0499 | -0.42 | 0.1838 | 3  | <i>KY</i>       | 3'UTR   |         |
| <b>cg24366127</b> | -0.51 | 0.0379 | 0.0499 | 0.35  | 0.2315 | 3  | <i>BOC</i>      | Body    |         |
| <b>cg17133224</b> | 0.50  | 0.0382 | 0.0499 | -0.38 | 0.2438 | 20 | <i>WFDC9</i>    | 3'UTR   |         |
| <b>cg16556156</b> | -2.17 | 0.0000 | 0.0001 |       |        | 16 | <i>CLEC1A</i>   | Body    | S_Shore |
| <b>cg03106024</b> | -1.03 | 0.0000 | 0.0003 |       |        | 11 |                 |         |         |
| <b>cg04078283</b> | -1.36 | 0.0000 | 0.0007 |       |        | 4  | <i>HTT</i>      | Body    |         |
| <b>cg26933978</b> | 1.88  | 0.0000 | 0.0007 |       |        | 8  | <i>HTRA4, P</i> | TSS1500 | N_Shore |
| <b>cg04580455</b> | 0.70  | 0.0002 | 0.0023 |       |        | 6  |                 |         |         |
| <b>cg02017733</b> | -1.31 | 0.0003 | 0.0034 |       |        | 22 | <i>PISD, MI</i> | Body    |         |
| <b>cg04672034</b> | -1.04 | 0.0004 | 0.0037 |       |        | 20 | <i>PTPNI</i>    | 5'UTR   |         |
| <b>cg03892671</b> | 0.69  | 0.0009 | 0.0055 |       |        | 4  | <i>PPA2</i>     | Body    |         |
| <b>cg08227938</b> | -1.10 | 0.0009 | 0.0055 |       |        | 17 | <i>DBF4B</i>    | Body    |         |
| <b>cg14970957</b> | 1.09  | 0.0014 | 0.0063 |       |        | 9  | <i>RUSC2</i>    | TSS1500 |         |
| <b>cg02160496</b> | 0.82  | 0.0033 | 0.0126 |       |        | 1  | <i>LOC14937</i> | Body    |         |
| <b>cg06117032</b> | -0.72 | 0.0036 | 0.0126 |       |        | 5  | <i>LOC10050</i> | TSS200  | S_Shore |
| <b>cg10639871</b> | -1.02 | 0.0032 | 0.0126 |       |        | 10 |                 |         |         |
| <b>cg19337057</b> | -1.18 | 0.0035 | 0.0126 |       |        | 20 | <i>CEP250</i>   | Body    |         |
| <b>cg00718959</b> | 0.75  | 0.0046 | 0.0131 |       |        | 5  |                 |         |         |
| <b>cg01479032</b> | -1.29 | 0.0045 | 0.0131 |       |        | 1  |                 |         |         |

|            |       |        |        |    |                 |         |
|------------|-------|--------|--------|----|-----------------|---------|
| cg12220491 | 0.93  | 0.0044 | 0.0131 | 15 | ZNF106          | Body    |
| cg19098799 | -0.92 | 0.0046 | 0.0131 | 2  |                 |         |
| cg02571397 | -0.83 | 0.0053 | 0.0131 | 11 |                 | S_Shelf |
| cg11609995 | -0.88 | 0.0052 | 0.0131 | 2  | <i>IL18RI</i>   | 5'UTR   |
| cg26165441 | -0.79 | 0.0052 | 0.0131 | 4  | <i>PIGG</i>     | Body    |
| cg14760788 | 0.63  | 0.0090 | 0.0178 | 22 | <i>EFCAB6-A</i> | Body    |
| cg21519785 | 0.76  | 0.0090 | 0.0178 | 13 | <i>SACS</i>     | TSS1500 |
| cg22638066 | -0.69 | 0.0090 | 0.0178 | 6  | <i>SGKI</i>     | Body    |
| cg10398502 | -1.10 | 0.0107 | 0.0192 | 13 | <i>LINC0038</i> | TSS1500 |
| cg10408324 | -1.00 | 0.0106 | 0.0192 | 21 |                 |         |
| cg13601382 | 0.80  | 0.0113 | 0.0200 | 4  |                 |         |
| cg26281383 | -0.42 | 0.0144 | 0.0240 | 2  |                 |         |
| cg02174096 | -0.86 | 0.0168 | 0.0266 | 16 | <i>LINC0030</i> | Body    |
| cg02856340 | 0.44  | 0.0217 | 0.0316 | 1  | <i>ZBTB40</i>   | 5'UTR   |
| cg04698728 | -0.90 | 0.0251 | 0.0359 | 8  |                 |         |
| cg01160497 | 0.91  | 0.0307 | 0.0425 | 11 | <i>LMO1</i>     | Body    |
| cg21005828 | -0.63 | 0.0351 | 0.0478 | 22 |                 |         |

Supplement Table S11 (A): Association of DNAm in males with neighboring gene expression (n=55)

coefficient Pvalue CpGs Gene

|          |          |            |               |
|----------|----------|------------|---------------|
| 0.916875 | 4.30E-07 | cg01662869 | <i>DPYSL4</i> |
| 0.827036 | 6.55E-07 | cg01662869 | <i>QRFP</i>   |
| -1.80075 | 8.53E-07 | cg19248893 | <i>RGS6</i>   |
| 1.045963 | 1.56E-06 | cg01662869 | <i>JADE2</i>  |
| 1.924089 | 2.18E-06 | cg01662869 | <i>JAM3</i>   |
| -0.81809 | 3.53E-06 | cg05990720 | <i>GNBI</i>   |
| -1.14956 | 7.47E-06 | cg19248893 | <i>BCL7B</i>  |
| -0.63891 | 9.09E-06 | cg19248893 | <i>ARMC7</i>  |

|          |          |            |               |
|----------|----------|------------|---------------|
| 0.878885 | 1.31E-05 | cg01662869 | <i>LAMC3</i>  |
| -1.47691 | 1.35E-05 | cg02266878 | <i>TLE2</i>   |
| 0.818827 | 2.82E-05 | cg14273401 | <i>NME8</i>   |
| -0.631   | 3.67E-05 | cg19248893 | <i>KLF9</i>   |
| -0.49871 | 0.000158 | cg05990720 | <i>HIC1</i>   |
| -0.47902 | 0.000175 | cg02266878 | <i>SGTA</i>   |
| 1.494738 | 0.000233 | cg01662869 | <i>IGSF9B</i> |
| 0.800258 | 0.000306 | cg27230396 | <i>ABHD8</i>  |
| -0.40952 | 0.000345 | cg05990720 | <i>ATP8B3</i> |
| 1.619155 | 0.000349 | cg14273401 | <i>MEN1</i>   |
| -1.04492 | 0.000437 | cg02266878 | <i>THOPI</i>  |
| 0.777331 | 0.000445 | cg14273401 | <i>RMDN2</i>  |
| 0.710671 | 0.000517 | cg11661809 | <i>METTL4</i> |
| -0.90581 | 0.000517 | cg27230396 | <i>MED9</i>   |
| 0.822986 | 0.000534 | cg01662869 | <i>EXOC4</i>  |
| -0.48546 | 0.000566 | cg19248893 | <i>FCHSD2</i> |
| 0.954409 | 0.000604 | cg27230396 | <i>CNTLN</i>  |
| 1.852549 | 0.000666 | cg11661809 | <i>CLUH</i>   |
| -0.16162 | 0.000792 | cg26146287 | <i>AKRIE2</i> |
| -0.44096 | 0.000797 | cg04019843 | <i>SEC22B</i> |
| 1.09255  | 0.000807 | cg14273401 | <i>CASC3</i>  |
| -0.36014 | 0.000927 | cg21322248 | <i>LZTS2</i>  |
| -0.47291 | 0.001029 | cg19248893 | <i>SMC5</i>   |
| -0.72681 | 0.001109 | cg19248893 | <i>MRPS7</i>  |
| -1.41225 | 0.001155 | cg01538301 | <i>MUS8I</i>  |
| 0.943836 | 0.001202 | cg11661809 | <i>BRATI</i>  |
| -1.11397 | 0.001211 | cg02982198 | <i>TUTI</i>   |
| -1.09334 | 0.001242 | cg27230396 | <i>MED28</i>  |
| -0.71297 | 0.00129  | cg19248893 | <i>EXOC6B</i> |
| -0.25449 | 0.001297 | cg05990720 | <i>GABRD</i>  |
| 0.84544  | 0.001342 | cg12967050 | <i>RASAL3</i> |

|          |          |            |                |
|----------|----------|------------|----------------|
| -0.44503 | 0.00141  | cg02266878 | <i>HTT</i>     |
| 1.082943 | 0.001546 | cg20232060 | <i>CESIPI</i>  |
| -0.70906 | 0.001597 | cg13963729 | <i>SAMD8</i>   |
| -0.49925 | 0.001684 | cg05951364 | <i>JMDIC</i>   |
| -0.47547 | 0.002058 | cg04019843 | <i>GYPB</i>    |
| -0.48668 | 0.002154 | cg02266878 | <i>NOP14</i>   |
| 0.629126 | 0.002195 | cg01662869 | <i>LRGUK</i>   |
| -0.24427 | 0.002196 | cg16629408 | <i>FNTB</i>    |
| 0.632839 | 0.002411 | cg14273401 | <i>THR4</i>    |
| 1.13781  | 0.002498 | cg05396987 | <i>SPTAI</i>   |
| 1.497453 | 0.0025   | cg12967050 | <i>TMEM27</i>  |
| 1.244615 | 0.002659 | cg25266327 | <i>CITED2</i>  |
| -0.23246 | 0.002674 | cg05990720 | <i>CASKIN</i>  |
| -0.50168 | 0.002684 | cg12967050 | <i>RBMII</i>   |
| 0.517246 | 0.002733 | cg01662869 | <i>TBC1D14</i> |
| 1.678386 | 0.002773 | cg11661809 | <i>CHST12</i>  |
| 0.997468 | 0.002802 | cg20477591 | <i>TG</i>      |
| 0.468938 | 0.002951 | cg01662869 | <i>GLBIL3</i>  |
| -1.01751 | 0.002954 | cg23973524 | <i>DTX3</i>    |
| -0.27214 | 0.003055 | cg05990720 | <i>NPW</i>     |
| -0.79804 | 0.003161 | cg27230396 | <i>NR2F6</i>   |
| -0.5486  | 0.003224 | cg02266878 | <i>CARDII</i>  |
| 0.841411 | 0.003582 | cg20232060 | <i>TMEM86B</i> |
| -0.33408 | 0.003754 | cg04019843 | <i>PDE4DIP</i> |
| 0.152495 | 0.003829 | cg11160820 | <i>PCDH1</i>   |
| 0.48695  | 0.003924 | cg22192692 | <i>FAMI27A</i> |
| -1.0216  | 0.00403  | cg00315816 | <i>FBXL16</i>  |
| 0.572832 | 0.004281 | cg20232060 | <i>TESPA1</i>  |
| 0.49941  | 0.004323 | cg14273401 | <i>OXSRI</i>   |
| 0.529218 | 0.004429 | cg14273401 | <i>SHB</i>     |
| 1.313691 | 0.004615 | cg02691091 | <i>C20orf1</i> |

|          |          |            |                |
|----------|----------|------------|----------------|
| 0.683974 | 0.004662 | cg14273401 | <i>EPHA10</i>  |
| -0.33952 | 0.004685 | cg02266878 | <i>CSMD1</i>   |
| -0.39979 | 0.004788 | cg05990720 | <i>NDUFS6</i>  |
| 0.428407 | 0.004813 | cg22192692 | <i>INPP5A</i>  |
| -0.74014 | 0.004827 | cg27230396 | <i>SLC27A1</i> |
| 0.44378  | 0.004832 | cg22192692 | <i>TG</i>      |
| 0.304036 | 0.004857 | cg03468115 | <i>INO80E</i>  |
| 1.067266 | 0.00492  | cg19738404 | <i>PTK6</i>    |
| 0.568628 | 0.004932 | cg03468115 | <i>RPP2I</i>   |
| -0.28982 | 0.005009 | cg04019843 | <i>NBPF20</i>  |
| -0.42611 | 0.005033 | cg05951364 | <i>CCT6P1</i>  |
| -0.5341  | 0.00523  | cg02266878 | <i>PTPRA</i>   |
| -0.35257 | 0.00527  | cg05951364 | <i>ARL2</i>    |
| 0.51873  | 0.005412 | cg01662869 | <i>FAMI27A</i> |
| 0.857096 | 0.00543  | cg12967050 | <i>CYP4F22</i> |
| 0.808963 | 0.005787 | cg20477591 | <i>MCPH1</i>   |
| 0.594884 | 0.006029 | cg03468115 | <i>UBL3</i>    |
| -0.18189 | 0.006055 | cg05990720 | <i>LSP1</i>    |
| 0.342058 | 0.006379 | cg05951364 | <i>ADAMTS6</i> |
| -1.20768 | 0.006392 | cg27230396 | <i>LAP3</i>    |
| 0.457482 | 0.006521 | cg01662869 | <i>FIBCD1</i>  |
| -0.24    | 0.006615 | cg16629408 | <i>CHURC1</i>  |
| 0.53727  | 0.006728 | cg01426818 | <i>PIP5K1B</i> |
| -0.18514 | 0.006783 | cg05990720 | <i>PGP</i>     |
| 0.81459  | 0.00707  | cg03468115 | <i>TMTCI</i>   |
| -0.70461 | 0.007081 | cg0315816  | <i>TNFRSF1</i> |
| 0.940001 | 0.007088 | cg20477591 | <i>PTMS</i>    |
| -0.56879 | 0.007156 | cg00315816 | <i>PNPLA2</i>  |
| -0.427   | 0.007239 | cg04019843 | <i>NBPF9</i>   |
| 0.674981 | 0.007287 | cg11661809 | <i>TMC2</i>    |
| -0.70206 | 0.00732  | cg13539395 | <i>GPR153</i>  |

|          |          |            |                |
|----------|----------|------------|----------------|
| 0.452796 | 0.007363 | cg03468115 | <i>C19orf1</i> |
| 914.0104 | 0.007559 | cg22081558 | <i>AAGAB</i>   |
| 0.390845 | 0.007696 | cg03468115 | <i>COPRS</i>   |
| 1.796971 | 0.007757 | cg20232060 | <i>RSL24D1</i> |
| -0.5013  | 0.007902 | cg02266878 | <i>GNA15</i>   |
| 0.592209 | 0.008155 | cg14273401 | <i>ERBB2</i>   |
| 0.829912 | 0.008166 | cg19874450 | <i>MAP3K2</i>  |
| -0.67031 | 0.008225 | cg01538301 | <i>EDA2R</i>   |
| -0.97457 | 0.008235 | cg21322248 | <i>KAZALDI</i> |
| 0.604316 | 0.008288 | cg14273401 | <i>CARD10</i>  |
| 0.895658 | 0.008484 | cg14442841 | <i>ADARB2</i>  |
| -0.33326 | 0.008563 | cg05990720 | <i>KLF16</i>   |
| -0.23909 | 0.008596 | cg05990720 | <i>TRAF7</i>   |
| -0.48844 | 0.008779 | cg02266878 | <i>PRSS30P</i> |
| 0.453102 | 0.008932 | cg11661809 | <i>PGP</i>     |
| 0.755833 | 0.009066 | cg11661809 | <i>MIR940</i>  |
| 0.646959 | 0.00913  | cg11661809 | <i>TRPM5</i>   |
| 0.638253 | 0.009173 | cg11661809 | <i>MYLK4</i>   |
| 1.465945 | 0.009284 | cg01662869 | <i>STK32C</i>  |
| -0.50146 | 0.009312 | cg10410121 | <i>MRPL9</i>   |
| -2.2322  | 0.009417 | cg18787783 | <i>GRIN3B</i>  |
| -0.30927 | 0.009835 | cg27435903 | <i>ACTRIB</i>  |
| 0.527638 | 0.009952 | cg01662869 | <i>GLB1L2</i>  |
| -0.2717  | 0.010023 | cg21322248 | <i>TECPR2</i>  |
| -0.33398 | 0.010024 | cg02266878 | <i>SMCHD1</i>  |
| -0.60384 | 0.010048 | cg02266878 | <i>DDRGKL</i>  |
| -0.54279 | 0.010198 | cg27230396 | <i>PGLS</i>    |
| 0.477404 | 0.010219 | cg14273401 | <i>EPDRI</i>   |
| 0.489023 | 0.01044  | cg01662869 | <i>MOSPD1</i>  |
| -0.42491 | 0.010503 | cg05951364 | <i>FRMD8</i>   |
| 1.072044 | 0.010551 | cg22192692 | <i>TXNDCI5</i> |

|          |          |            |                |
|----------|----------|------------|----------------|
| 0.282792 | 0.01079  | cg14273401 | <i>RPGR</i>    |
| -1.30837 | 0.010814 | cg22081558 | <i>RTTN</i>    |
| -0.81153 | 0.010822 | cg09791665 | <i>GPR179</i>  |
| 0.918757 | 0.010837 | cg24818434 | <i>CERS4</i>   |
| -0.22332 | 0.010966 | cg05990720 | <i>SYNGR3</i>  |
| -0.56661 | 0.011023 | cg27230396 | <i>MRPL34</i>  |
| -0.51295 | 0.011038 | cg05951364 | <i>TRIP4</i>   |
| 0.707645 | 0.011071 | cg06791670 | <i>EXOC3L2</i> |
| 0.748489 | 0.011104 | cg09543792 | <i>GATC</i>    |
| 1.082027 | 0.011237 | cg22192692 | <i>FAM127C</i> |
| 0.443105 | 0.011638 | cg22192692 | <i>DDX46</i>   |
| 1.194002 | 0.011676 | cg09543792 | <i>TRIAP1</i>  |
| -0.60216 | 0.011888 | cg05098096 | <i>EPS8L2</i>  |
| 0.903851 | 0.011897 | cg01395217 | <i>TACO1</i>   |
| -0.61102 | 0.012104 | cg05951364 | <i>CDC45</i>   |
| -0.39125 | 0.012118 | cg13539395 | <i>PHF13</i>   |
| 0.45426  | 0.012189 | cg19248893 | <i>JPX</i>     |
| -1.24426 | 0.012298 | cg13963729 | <i>TBCA</i>    |
| 0.691221 | 0.012318 | cg24343755 | <i>ARID2</i>   |
| -1.0212  | 0.012419 | cg13963729 | <i>SDADI</i>   |
| -0.63454 | 0.012599 | cg20491695 | <i>PRKY</i>    |
| 0.414925 | 0.012634 | cg13675319 | <i>SDF2</i>    |
| 0.570204 | 0.012743 | cg03468115 | <i>FKBP14</i>  |
| 0.553652 | 0.01281  | cg01662869 | <i>SMM10</i>   |
| -0.2827  | 0.012896 | cg05990720 | <i>CTSD</i>    |
| -1.347   | 0.012987 | cg02982198 | <i>UCKLI</i>   |
| -0.2511  | 0.013074 | cg00315816 | <i>RPLP2</i>   |
| -0.4807  | 0.013106 | cg04019843 | <i>EPPKI</i>   |
| 1.697077 | 0.013192 | cg21476203 | <i>PLXDC2</i>  |
| 0.851012 | 0.013263 | cg20477591 | <i>RRP8</i>    |
| -0.52387 | 0.013448 | cg02266878 | <i>EMILIN2</i> |

|          |          |             |                |
|----------|----------|-------------|----------------|
| 0.426049 | 0.013512 | cg03468115  | <i>KLHL14</i>  |
| 0.44001  | 0.013547 | cg00169776  | <i>PPRCI</i>   |
| -0.23101 | 0.01355  | cg05990720  | <i>SPSB3</i>   |
| 0.759456 | 0.013613 | cg05440435  | <i>MRPS17</i>  |
| 0.725944 | 0.013616 | cg274335903 | <i>COX5B</i>   |
| 0.538644 | 0.013696 | cg09543792  | <i>GRIK4</i>   |
| -0.27694 | 0.013736 | cg00315816  | <i>NARFL</i>   |
| -0.45043 | 0.013777 | cg00315816  | <i>SLC12A7</i> |
| 1.093944 | 0.013799 | cg01395217  | <i>HARIB</i>   |
| 0.659123 | 0.013804 | cg25266327  | <i>PTGDS</i>   |
| 0.235956 | 0.014209 | cg10179363  | <i>GPPILL</i>  |
| -0.43889 | 0.014337 | cg02266878  | <i>MYLK4</i>   |
| 0.336036 | 0.014616 | cg03468115  | <i>CORO1A</i>  |
| -0.40175 | 0.014834 | cg02266878  | <i>SLC39A3</i> |
| 0.304    | 0.014989 | cg03468115  | <i>TBX6</i>    |
| -0.56826 | 0.015132 | cg02266878  | <i>GNG7</i>    |
| 0.438001 | 0.015171 | cg01426818  | <i>TSPAN15</i> |
| 0.000262 | 0.015331 | cg00003722  | <i>CCNH</i>    |
| 0.305861 | 0.015424 | cg01426818  | <i>NCOA2</i>   |
| 1.355311 | 0.015589 | cg01395217  | <i>SERPINB</i> |
| 0.529508 | 0.016062 | cg13675319  | <i>OTOF</i>    |
| 0.720181 | 0.016119 | cg19862616  | <i>CEP164</i>  |
| 0.889357 | 0.016296 | cg13659360  | <i>MRPL40</i>  |
| 0.407787 | 0.016789 | cg14273401  | <i>TBC1D1</i>  |
| -0.55679 | 0.016835 | cg00315816  | <i>NXN</i>     |
| -0.31242 | 0.016852 | cg00707741  | <i>TIE1</i>    |
| 0.739673 | 0.016913 | cg14442841  | <i>PRPF8</i>   |
| -0.3839  | 0.017005 | cg00315816  | <i>TMED11P</i> |
| 0.667976 | 0.017572 | cg09543792  | <i>TAF2</i>    |
| 0.619871 | 0.017744 | cg14442841  | <i>SLC35E2</i> |
| -0.81184 | 0.017792 | cg00315816  | <i>SUN1</i>    |

|          |          |            |                |
|----------|----------|------------|----------------|
| -0.95372 | 0.017905 | cg13963729 | <i>GSAP</i>    |
| 0.527185 | 0.017992 | cg09543792 | <i>NANOS1</i>  |
| -1.25458 | 0.01813  | cg27230396 | <i>FAM84I</i>  |
| -0.69025 | 0.018167 | cg27230396 | <i>CECR5</i>   |
| -0.61047 | 0.018262 | cg13963729 | <i>CAPN5</i>   |
| 1.331242 | 0.018278 | cg20232060 | <i>FBXO34</i>  |
| 0.506395 | 0.018279 | cg03468115 | <i>DCTN6</i>   |
| 1.166207 | 0.018292 | cg09543792 | <i>DSCC1</i>   |
| -0.33057 | 0.018368 | cg04019843 | <i>SH3RF2</i>  |
| 0.350908 | 0.018569 | cg03468115 | <i>MTUS2</i>   |
| -1.32028 | 0.018718 | cg02982198 | <i>PTK6</i>    |
| 0.248229 | 0.018755 | cg0169776  | <i>LDB1</i>    |
| 0.285528 | 0.018874 | cg20491695 | <i>DEFA4</i>   |
| -0.4989  | 0.019099 | cg05951364 | <i>BATF2</i>   |
| 0.368192 | 0.019308 | cg02724025 | <i>TMEM30B</i> |
| 0.737372 | 0.019373 | cg11661809 | <i>PANK4</i>   |
| -0.43217 | 0.019576 | cg13675319 | <i>GPATCH3</i> |
| 1.221838 | 0.0199   | cg02691091 | <i>CAMP</i>    |
| -1.23788 | 0.019914 | cg01395217 | <i>FTH1</i>    |
| -0.42068 | 0.020162 | cg10410121 | <i>CGN</i>     |
| -0.84011 | 0.020191 | cg12967050 | <i>HACLI</i>   |
| -0.30398 | 0.020375 | cg19248893 | <i>UNC5B</i>   |
| 0.753671 | 0.020457 | cg01426818 | <i>FOXPI</i>   |
| -0.43544 | 0.020565 | cg00707741 | <i>GCK</i>     |
| -0.30189 | 0.020716 | cg02266878 | <i>CLDN9</i>   |
| -0.56294 | 0.021049 | cg05951364 | <i>TM7SF2</i>  |
| -0.33744 | 0.021074 | cg00315816 | <i>MFSD7</i>   |
| -1.25789 | 0.021179 | cg12967050 | <i>BMX</i>     |
| 1.112547 | 0.021295 | cg11661809 | <i>TMPRSS9</i> |
| 0.276217 | 0.021342 | cg03468115 | <i>MTURN</i>   |
| -0.30127 | 0.021465 | cg00315816 | <i>LMFI</i>    |

|          |          |            |                |
|----------|----------|------------|----------------|
| 0.448635 | 0.021623 | cg27435903 | <i>RGMB</i>    |
| -0.60559 | 0.022082 | cg02266878 | <i>TTYH3</i>   |
| 0.514821 | 0.022118 | cg12967050 | <i>CC2D2A</i>  |
| 0.540944 | 0.022183 | cg18232125 | <i>PDCD2L</i>  |
| 0.420639 | 0.022412 | cg25279644 | <i>TMEM185</i> |
| 0.247024 | 0.022664 | cg22192692 | <i>PCBD2</i>   |
| 0.275855 | 0.023214 | cg03468115 | <i>LRRC37B</i> |
| 0.728372 | 0.023253 | cg01426818 | <i>B3GAT2</i>  |
| 0.58071  | 0.02332  | cg03468115 | <i>PRKD1</i>   |
| -0.59747 | 0.023343 | cg02266878 | <i>PRSS22</i>  |
| -0.36329 | 0.023427 | cg10579012 | <i>AK3</i>     |
| -0.49297 | 0.023548 | cg02266878 | <i>ITFG2</i>   |
| -0.81681 | 0.024409 | cg07555102 | <i>RSFI</i>    |
| -0.31872 | 0.024465 | cg09396181 | <i>NDUFA10</i> |
| -0.46978 | 0.024515 | cg02266878 | <i>PAQR4</i>   |
| -0.67381 | 0.024601 | cg23973524 | <i>CDK4</i>    |
| 0.213325 | 0.024754 | cg22192692 | <i>ACAD8</i>   |
| -0.32247 | 0.024812 | cg22364465 | <i>R3HDM2</i>  |
| 0.385618 | 0.024817 | cg21476203 | <i>AKAP10</i>  |
| -0.27396 | 0.024861 | cg24151841 | <i>RBMI</i>    |
| 0.479016 | 0.025094 | cg00169776 | <i>NOLCI</i>   |
| 0.791425 | 0.025179 | cg19248893 | <i>FZD9</i>    |
| 0.60237  | 0.025241 | cg19738404 | <i>FAM161A</i> |
| 0.311622 | 0.025364 | cg00315816 | <i>RAB40C</i>  |
| 0.637911 | 0.02549  | cg07538364 | <i>UBE2E2</i>  |
| 0.860927 | 0.025585 | cg17821664 | <i>ATP9A</i>   |
| 1.524991 | 0.026233 | cg05440435 | <i>GNAOI</i>   |
| 0.723389 | 0.026485 | cg19374731 | <i>TIGD7</i>   |
| 1.149834 | 0.026518 | cg25266327 | <i>SLC4A9</i>  |
| 0.461499 | 0.026644 | cg19738404 | <i>AR</i>      |
| 0.552245 | 0.026671 | cg21322248 | <i>ANKRD9</i>  |

|          |          |            |                |
|----------|----------|------------|----------------|
| -0.70669 | 0.0267   | cg00707741 | <i>TMEM63B</i> |
| -0.96034 | 0.026712 | cg22588936 | <i>FBXL8</i>   |
| 0.35095  | 0.026792 | cg14724918 | <i>EXOC2</i>   |
| 0.441938 | 0.0268   | cg11661809 | <i>CASKIN1</i> |
| 0.564571 | 0.026925 | cg12967050 | <i>NPIP45</i>  |
| -1.13603 | 0.026935 | cg02982198 | <i>TM2D1</i>   |
| -0.91601 | 0.027092 | cg22588936 | <i>OPHNI</i>   |
| 0.684316 | 0.027116 | cg20232060 | <i>LPCAT2</i>  |
| -0.48855 | 0.027447 | cg00315816 | <i>TMEM18</i>  |
| 1.571906 | 0.027568 | cg19142181 | <i>ASB8</i>    |
| 0.397792 | 0.027685 | cg24151841 | <i>PGLYRP2</i> |
| -0.34275 | 0.027883 | cg22364465 | <i>DNAH12</i>  |
| 0.320524 | 0.028088 | cg22192692 | <i>GLB1L3</i>  |
| -1.0727  | 0.028111 | cg22081558 | <i>MAP2K6</i>  |
| 0.651756 | 0.028354 | cg11661809 | <i>MLST8</i>   |
| 0.154699 | 0.028407 | cg07642705 | <i>SPRY3</i>   |
| 1.243103 | 0.028474 | cg20232060 | <i>NLRP2</i>   |
| -0.37053 | 0.028786 | cg03740167 | <i>ADAMTS7</i> |
| 0.533515 | 0.028803 | cg11661809 | <i>OAZ1</i>    |
| -0.25838 | 0.028862 | cg02712036 | <i>IMMP1L</i>  |
| -0.54936 | 0.028867 | cg22081558 | <i>MCMDC2</i>  |
| 0.520855 | 0.028884 | cg05396987 | <i>SNX9</i>    |
| 0.349712 | 0.028898 | cg01604539 | <i>PACSI1</i>  |
| -0.59897 | 0.02897  | cg13539395 | <i>MCPHI</i>   |
| 0.694685 | 0.028986 | cg14273401 | <i>PNMT</i>    |
| 0.164956 | 0.029134 | cg26054167 | <i>COPZ2</i>   |
| -1.03614 | 0.029307 | cg01538301 | <i>EIF1AD</i>  |
| -0.65649 | 0.029468 | cg13539395 | <i>MRPL51</i>  |
| -0.48544 | 0.029577 | cg23973524 | <i>RPS6KB1</i> |
| -0.26803 | 0.029898 | cg05990720 | <i>HAUS3</i>   |
| 0.685783 | 0.029999 | cg14240353 | <i>GNG7</i>    |

|          |          |            |                |
|----------|----------|------------|----------------|
| 1.25322  | 0.030145 | cg08643007 | <i>EEPDI</i>   |
| 0.232124 | 0.030325 | cg10179363 | <i>CBXI</i>    |
| -0.28642 | 0.030329 | cg05990720 | <i>MSRB1</i>   |
| 0.751503 | 0.03034  | cg03468115 | <i>MPPED2</i>  |
| -1.04051 | 0.030727 | cg00385142 | <i>CNPY4</i>   |
| 0.747709 | 0.030793 | cg22192692 | <i>FAM78A</i>  |
| 0.823609 | 0.030831 | cg01538301 | <i>CNIH2</i>   |
| 0.229152 | 0.031039 | cg10179363 | <i>SMAD7</i>   |
| 0.38846  | 0.031085 | cg14273401 | <i>MTFI</i>    |
| -2.3819  | 0.031178 | cg03821689 | <i>NRM</i>     |
| -0.37801 | 0.031224 | cg02266878 | <i>FAM193A</i> |
| -0.42173 | 0.032203 | cg00315816 | <i>CEND1</i>   |
| 1.078219 | 0.03223  | cg20977448 | <i>SSB</i>     |
| 0.618513 | 0.032558 | cg19374731 | <i>RPS7</i>    |
| -0.18966 | 0.032799 | cg16629408 | <i>NLN</i>     |
| -0.95831 | 0.033028 | cg23973524 | <i>RNF11</i>   |
| 0.559089 | 0.033052 | cg20477591 | <i>PMS2CL</i>  |
| -0.59327 | 0.033132 | cg01395217 | <i>TCFL5</i>   |
| -0.60405 | 0.033418 | cg02982198 | <i>SNAPCI</i>  |
| -0.65339 | 0.033545 | cg00707741 | <i>TFF3</i>    |
| 0.662712 | 0.033606 | cg11661809 | <i>TSRI</i>    |
| -0.29208 | 0.033638 | cg18787783 | <i>ABR</i>     |
| -0.36264 | 0.033681 | cg02712036 | <i>SLC5A2</i>  |
| 1.399547 | 0.033894 | cg12967050 | <i>KAZN</i>    |
| -0.07612 | 0.033902 | cg11160820 | <i>AGK</i>     |
| 0.538616 | 0.033968 | cg14273401 | <i>PGAP3</i>   |
| -0.57579 | 0.034015 | cg16073958 | <i>ANKRD29</i> |
| 0.46021  | 0.034116 | cg19374731 | <i>CEP104</i>  |
| 0.799391 | 0.034322 | cg20477591 | <i>PRKCQ</i>   |
| 0.577944 | 0.034343 | cg11661809 | <i>TSSC4</i>   |
| -0.16926 | 0.034685 | cg16629408 | <i>RASSF3</i>  |

|          |          |            |                |
|----------|----------|------------|----------------|
| -0.7171  | 0.034922 | cg15847604 | <i>KRT8I</i>   |
| 0.624624 | 0.034989 | cg05440435 | <i>BLOC1S1</i> |
| 0.701347 | 0.035109 | cg20232060 | <i>MTIF2</i>   |
| 0.649857 | 0.035158 | cg11661809 | <i>CCNF</i>    |
| -0.75447 | 0.035324 | cg13963729 | <i>COMTD1</i>  |
| -0.31588 | 0.035548 | cg19248893 | <i>TMEM104</i> |
| -0.39835 | 0.035811 | cg02266878 | <i>OXT</i>     |
| -0.49308 | 0.036055 | cg02266878 | <i>RIPK1</i>   |
| -0.37586 | 0.036101 | cg05951364 | <i>TRAPPCL</i> |
| -0.43916 | 0.036407 | cg13539395 | <i>DNAJC11</i> |
| 0.371742 | 0.036963 | cg12967050 | <i>EPS8</i>    |
| 0.772264 | 0.037085 | cg14273401 | <i>ELFN2</i>   |
| -1.18386 | 0.037336 | cg09791665 | <i>APOL6</i>   |
| -0.554   | 0.037357 | cg21322248 | <i>CINP</i>    |
| -0.88229 | 0.037458 | cg15847685 | <i>UBLCP1</i>  |
| -0.39482 | 0.037585 | cg02266878 | <i>KCTD5</i>   |
| 0.599604 | 0.037601 | cg01426818 | <i>TEX261</i>  |
| -1.17465 | 0.037604 | cg13963729 | <i>ISL2</i>    |
| 0.671445 | 0.037858 | cg11661809 | <i>GNG7</i>    |
| 0.85893  | 0.038324 | cg14240353 | <i>THOP1</i>   |
| 0.217516 | 0.038875 | cg24343755 | <i>NFE2LI</i>  |
| 0.248076 | 0.03907  | cg24343755 | <i>LRRC3</i>   |
| 0.34544  | 0.039072 | cg14273401 | <i>SH3BP1</i>  |
| -0.52446 | 0.039218 | cg23973524 | <i>TUBD1</i>   |
| 1.330471 | 0.039502 | cg0385142  | <i>CQO3</i>    |
| 0.444833 | 0.039517 | cg09791665 | <i>RNF38</i>   |
| 0.663577 | 0.039606 | cg03468115 | <i>TRIM31</i>  |
| -0.52082 | 0.039629 | cg23973524 | <i>HEATR6</i>  |
| -0.78218 | 0.039722 | cg03740167 | <i>ANXA3</i>   |
| 0.728746 | 0.039801 | cg09543792 | <i>TECTA</i>   |
| -0.43213 | 0.039843 | cg00315816 | <i>TRIP13</i>  |

|          |          |            |                |
|----------|----------|------------|----------------|
| -0.45046 | 0.040247 | cg20491695 | <i>LAG3</i>    |
| -0.5346  | 0.040417 | cg20491695 | <i>RNF144A</i> |
| -0.71525 | 0.040757 | cg05440435 | <i>ORMDL2</i>  |
| -0.33777 | 0.041836 | cg05951364 | <i>HELZ</i>    |
| -0.7923  | 0.042265 | cg25266327 | <i>LCN10</i>   |
| -0.62326 | 0.04231  | cg22081558 | <i>CD226</i>   |
| -0.40879 | 0.042708 | cg02712036 | <i>CAPN14</i>  |
| 0.437655 | 0.042903 | cg19738404 | <i>COMMD1</i>  |
| -0.70672 | 0.042967 | cg02266878 | <i>FLYWCHI</i> |
| -0.38558 | 0.043056 | cg07555102 | <i>AQP11</i>   |
| -0.39428 | 0.043087 | cg0315816  | <i>IDUA</i>    |
| -0.34345 | 0.043298 | cg09888026 | <i>ALG6</i>    |
| -0.91828 | 0.043312 | cg19874450 | <i>ETSI</i>    |
| 0.51665  | 0.043633 | cg22192692 | <i>TBPL1</i>   |
| 0.360252 | 0.04417  | cg14442841 | <i>MAFK</i>    |
| 0.488877 | 0.044242 | cg14240353 | <i>MYLK4</i>   |
| -0.35152 | 0.044259 | cg09396181 | <i>RGS7</i>    |
| 0.346271 | 0.044294 | cg14273401 | <i>NRID1</i>   |
| 0.379147 | 0.044361 | cg12372414 | <i>FKBP8</i>   |
| 0.201452 | 0.044609 | cg03468115 | <i>GDPD3</i>   |
| 0.738691 | 0.044972 | cg02982198 | <i>KHDRBS2</i> |
| -0.77933 | 0.044978 | cg13963729 | <i>MAGT1</i>   |
| 0.166783 | 0.045229 | cg18232125 | <i>IFNGR2</i>  |
| -0.43553 | 0.045275 | cg10410121 | <i>SNX27</i>   |
| 0.494864 | 0.045308 | cg14442841 | <i>BRSK2</i>   |
| -0.24078 | 0.045705 | cg14273401 | <i>GRB7</i>    |
| 0.489728 | 0.045768 | cg00315816 | <i>CCDC78</i>  |
| 0.625124 | 0.045909 | cg11661809 | <i>HAU33</i>   |
| -1.35544 | 0.045914 | cg01538301 | <i>KPN42</i>   |
| 0.325657 | 0.046245 | cg02998992 | <i>HSP49</i>   |
| 0.175626 | 0.046355 | cg10179363 | <i>COPZ2</i>   |

|           |          |            |                |
|-----------|----------|------------|----------------|
| 0.305394  | 0.046406 | cg14273401 | <i>ANKRD54</i> |
| 1.174632  | 0.046621 | cg20176285 | <i>LYVE1</i>   |
| -0.24608  | 0.046669 | cg05990720 | <i>TSRI</i>    |
| -0.38683  | 0.046863 | cg05990720 | <i>SKI</i>     |
| 0.406408  | 0.046879 | cg07538364 | <i>RPS2P32</i> |
| 0.757276  | 0.047992 | cg00315816 | <i>PDDCI</i>   |
| 0.786197  | 0.048379 | cg05440435 | <i>MSX2PI</i>  |
| -0.353117 | 0.048538 | cg15847685 | <i>EBF1</i>    |
| -0.29449  | 0.048552 | cg15584606 | <i>ABR</i>     |
| -0.35707  | 0.04864  | cg00315816 | <i>SBNO2</i>   |
| 0.657886  | 0.048678 | cg20852846 | <i>ANKRD6</i>  |
| -0.44947  | 0.048837 | cg13675319 | <i>TBC1D19</i> |
| 0.172925  | 0.049405 | cg02724025 | <i>PSMC5</i>   |
| 0.761859  | 0.049517 | cg11661809 | <i>LSM7</i>    |
| 0.227197  | 0.049624 | cg18478353 | <i>ANKRD26</i> |
| 0.289648  | 0.04998  | cg26054167 | <i>PNPO</i>    |

Supplement Table S11 (B): Association of DNAm in females with neighboring gene expression (n=85)

| coefficient | Pvalue   | CpGs       | Gene          |
|-------------|----------|------------|---------------|
| 0.933795    | 1.72E-11 | cg01662869 | <i>JADE2</i>  |
| 0.828278    | 2.99E-10 | cg01662869 | <i>DPYSL4</i> |
| 0.556397    | 8.41E-08 | cg01662869 | <i>MOSPD1</i> |
| 0.613822    | 1.66E-07 | cg01662869 | <i>GLB1L2</i> |
| 0.684088    | 1.67E-07 | cg01662869 | <i>LAMC3</i>  |
| 0.867954    | 1.78E-07 | cg09543792 | <i>NANOS1</i> |
| 0.659914    | 2.23E-07 | cg01662869 | <i>QRFP</i>   |
| -0.92084    | 3.42E-07 | cg18478353 | <i>4RNTL2</i> |
| -1.15058    | 4.31E-07 | cg02266878 | <i>THOP1</i>  |
| 1.169448    | 7.08E-07 | cg01662869 | <i>IGSF9B</i> |
| 1.382506    | 1.06E-06 | cg01662869 | <i>JAM3</i>   |
| 0.860626    | 2.33E-06 | cg09543792 | <i>TAF2</i>   |

|          |          |            |                |
|----------|----------|------------|----------------|
| -1.1085  | 3.64E-06 | cg18478353 | <i>GPN2</i>    |
| 1.433978 | 3.67E-06 | cg01662869 | <i>STK32C</i>  |
| 0.901585 | 3.72E-06 | cg09543792 | <i>GATC</i>    |
| -0.83808 | 4.42E-06 | cg19248893 | <i>BCL7B</i>   |
| -0.79322 | 5.77E-06 | cg02266878 | <i>PTPRA</i>   |
| 1.30047  | 6.10E-06 | cg12967050 | <i>RASAL3</i>  |
| -1.21233 | 6.32E-06 | cg19248893 | <i>RGS6</i>    |
| 0.806838 | 6.71E-06 | cg14273401 | <i>CARD10</i>  |
| 2.561337 | 7.64E-06 | cg12967050 | <i>KAZN</i>    |
| -0.62546 | 8.82E-06 | cg04019843 | <i>GYPB</i>    |
| -0.70195 | 1.02E-05 | cg05990720 | <i>SKI</i>     |
| -0.80897 | 1.07E-05 | cg19248893 | <i>SFXN5</i>   |
| 1.023046 | 1.18E-05 | cg12967050 | <i>NPIP45</i>  |
| 0.848806 | 1.26E-05 | cg09543792 | <i>TECTA</i>   |
| -0.82428 | 1.36E-05 | cg19248893 | <i>BAZIB</i>   |
| 0.931676 | 1.38E-05 | cg09543792 | <i>DSCC1</i>   |
| -1.03002 | 1.41E-05 | cg18478353 | <i>SLC9A1</i>  |
| 0.634557 | 1.48E-05 | cg09543792 | <i>GRIK4</i>   |
| -0.74619 | 2.36E-05 | cg18478353 | <i>MAPRE3</i>  |
| -1.38492 | 2.61E-05 | cg02266878 | <i>TLE2</i>    |
| 0.674314 | 2.91E-05 | cg01662869 | <i>TG</i>      |
| 0.910733 | 3.30E-05 | cg12967050 | <i>MEIS3P1</i> |
| 0.925519 | 3.87E-05 | cg09543792 | <i>CABP1</i>   |
| -0.25581 | 3.88E-05 | cg13539395 | <i>AGPAT5</i>  |
| 0.752606 | 3.89E-05 | cg12967050 | <i>SH3BP5</i>  |
| -0.78295 | 4.64E-05 | cg02266878 | <i>MYLK4</i>   |
| -0.73025 | 5.52E-05 | cg18478353 | <i>PIPOX</i>   |
| -0.87476 | 5.70E-05 | cg02266878 | <i>KCTD5</i>   |
| 0.702191 | 6.43E-05 | cg01662869 | <i>EXOC4</i>   |
| 1.243577 | 7.07E-05 | cg14273401 | <i>TRIOBP</i>  |
| -0.52545 | 7.13E-05 | cg03740167 | <i>ADAMTS7</i> |

|          |          |            |                |
|----------|----------|------------|----------------|
| -0.23275 | 7.98E-05 | cg05990720 | <i>SCAMP4</i>  |
| 0.608641 | 0.0001   | cg09543792 | <i>CQ5</i>     |
| -0.90795 | 0.000101 | cg19248893 | <i>TSIX</i>    |
| 0.298292 | 0.000103 | cg19248893 | <i>NUP85</i>   |
| 0.871695 | 0.000106 | cg11661809 | <i>BRATI</i>   |
| 1.247531 | 0.000107 | cg14273401 | <i>HLCS</i>    |
| 0.910255 | 0.000117 | cg01395217 | <i>FADSI</i>   |
| -0.70083 | 0.000117 | cg18478353 | <i>HOXA3</i>   |
| 0.456164 | 0.00012  | cg13539395 | <i>ACOT7</i>   |
| 0.852893 | 0.000125 | cg21103269 | <i>PNRCI</i>   |
| -0.64067 | 0.000133 | cg02266878 | <i>HTT</i>     |
| 0.462665 | 0.00014  | cg01662869 | <i>GLB1L3</i>  |
| -0.814   | 0.000141 | cg02266878 | <i>EMILIN2</i> |
| 0.336581 | 0.000141 | cg2192692  | <i>AKR1BI</i>  |
| 0.603816 | 0.00015  | cg01662869 | <i>FAMI27A</i> |
| 0.853473 | 0.00015  | cg14273401 | <i>THR4</i>    |
| -0.35671 | 0.000156 | cg19248893 | <i>ARMC7</i>   |
| -0.72745 | 0.000193 | cg02266878 | <i>RIPK1</i>   |
| 1.077572 | 0.000198 | cg02374944 | <i>ARL10</i>   |
| 0.764746 | 0.0002   | cg14273401 | <i>EPHA10</i>  |
| 0.671462 | 0.000208 | cg19862616 | <i>COL27A1</i> |
| 1.208781 | 0.000211 | cg09543792 | <i>TRIAPI</i>  |
| 0.64508  | 0.000216 | cg09543792 | <i>RALB</i>    |
| 0.745947 | 0.00022  | cg14273401 | <i>RMDN2</i>   |
| 0.461875 | 0.000224 | cg07873926 | <i>NRBPI</i>   |
| -0.52506 | 0.000235 | cg02266878 | <i>SLC39A3</i> |
| -0.73347 | 0.000237 | cg02266878 | <i>NOP14</i>   |
| 1.649648 | 0.000284 | cg14273401 | <i>MEN1</i>    |
| -0.57048 | 0.00029  | cg18478353 | <i>GPATCH3</i> |
| 0.645035 | 0.000291 | cg09543792 | <i>EIF3A</i>   |
| 0.465566 | 0.000292 | cg14273401 | <i>SNIP1</i>   |

|          |          |            |                |
|----------|----------|------------|----------------|
| -0.4626  | 0.000301 | cg04019843 | <i>SEC22B</i>  |
| 0.533005 | 0.000322 | cg09543792 | <i>SRSF9</i>   |
| 0.562213 | 0.000344 | cg17821664 | <i>ALG12</i>   |
| -0.53076 | 0.000369 | cg19248893 | <i>KCTD2</i>   |
| 1.031218 | 0.000372 | cg14273401 | <i>PNMT</i>    |
| -0.4031  | 0.000381 | cg14273401 | <i>LGALSI</i>  |
| -0.65898 | 0.000392 | cg02266878 | <i>PRSS30P</i> |
| -0.38558 | 0.000396 | cg19248893 | <i>TMEM104</i> |
| 0.821664 | 0.000402 | cg12967050 | <i>ANKRD28</i> |
| 0.726829 | 0.000429 | cg09543792 | <i>RNF10</i>   |
| -0.66184 | 0.000436 | cg19248893 | <i>CDR2L</i>   |
| 0.820457 | 0.000465 | cg23683674 | <i>MCURI</i>   |
| -0.69654 | 0.000478 | cg13659360 | <i>SNRPDI</i>  |
| 1.324977 | 0.000495 | cg14273401 | <i>GNL2</i>    |
| 0.689536 | 0.000498 | cg12967050 | <i>CA5BPI</i>  |
| -0.65677 | 0.000502 | cg02266878 | <i>FKBP4</i>   |
| -0.81895 | 0.000505 | cg20477591 | <i>LAG3</i>    |
| 0.549877 | 0.000524 | cg14273401 | <i>OXSRI</i>   |
| 0.779375 | 0.000533 | cg14273401 | <i>NME8</i>    |
| 0.396474 | 0.000549 | cg01662869 | <i>BNIP3</i>   |
| -0.47663 | 0.000562 | cg05990720 | <i>GNBI</i>    |
| 0.428093 | 0.000574 | cg01395217 | <i>DAGLA</i>   |
| -1.22895 | 0.000582 | cg09776718 | <i>COMMD3</i>  |
| -0.67294 | 0.000642 | cg02266878 | <i>GNA15</i>   |
| 0.915412 | 0.000696 | cg01395217 | <i>FTSJ3</i>   |
| -0.45498 | 0.0007   | cg19248893 | <i>KLF9</i>    |
| -0.57563 | 0.000772 | cg14273401 | <i>GRB7</i>    |
| 0.472908 | 0.000787 | cg19862616 | <i>P4FAHIB</i> |
| -0.91883 | 0.000867 | cg18478353 | <i>ESCO2</i>   |
| 0.364562 | 0.000905 | cg07873926 | <i>EPHX2</i>   |
| 0.400155 | 0.000931 | cg20241375 | <i>ACAD9</i>   |

|          |          |            |                |
|----------|----------|------------|----------------|
| 0.87238  | 0.00096  | cg19142181 | <i>SIAHI</i>   |
| 0.421222 | 0.001023 | cg01662869 | <i>SMM10</i>   |
| 1.211253 | 0.001054 | cg11661809 | <i>ATP6V0C</i> |
| -1.1161  | 0.001062 | cg20477591 | <i>CHD4</i>    |
| 0.575566 | 0.001069 | cg02266878 | <i>NQO2</i>    |
| 0.865072 | 0.001072 | cg01395217 | <i>HARIB</i>   |
| 1.00295  | 0.001169 | cg21103269 | <i>POLR3G</i>  |
| -0.90661 | 0.001178 | cg08976554 | <i>MEX3A</i>   |
| 0.665429 | 0.001223 | cg14273401 | <i>NRID1</i>   |
| 1.172479 | 0.001224 | cg14273401 | <i>LSMI</i>    |
| -0.70102 | 0.001238 | cg13659360 | <i>UBR4</i>    |
| -1.56977 | 0.001257 | cg22588936 | <i>E2F4</i>    |
| -0.53757 | 0.001303 | cg19248893 | <i>TBL2</i>    |
| 1.258372 | 0.00136  | cg19142181 | <i>RNF114</i>  |
| -0.27018 | 0.001483 | cg06791670 | <i>ALOX5</i>   |
| -0.35696 | 0.001501 | cg04019843 | <i>SH3RF2</i>  |
| -0.51798 | 0.001526 | cg12967050 | <i>BTD</i>     |
| 0.727815 | 0.001589 | cg01395217 | <i>MYRF</i>    |
| -0.27264 | 0.0016   | cg05990720 | <i>MORNI</i>   |
| 0.36686  | 0.001616 | cg07873926 | <i>MOB3B</i>   |
| -0.78684 | 0.001619 | cg06216103 | <i>LUM</i>     |
| -0.80587 | 0.001628 | cg02266878 | <i>DDRGKI</i>  |
| 0.760826 | 0.001652 | cg19142181 | <i>LRRC59</i>  |
| 1.022889 | 0.001711 | cg14273401 | <i>GSDMA</i>   |
| 0.925602 | 0.001748 | cg14273401 | <i>BAG4</i>    |
| 0.773689 | 0.001782 | cg02266878 | <i>OR342</i>   |
| 1.079656 | 0.001815 | cg11661809 | <i>SKI</i>     |
| 1.131115 | 0.001816 | cg11661809 | <i>CLUH</i>    |
| -0.66002 | 0.001923 | cg20200460 | <i>UBASH3B</i> |
| 0.742505 | 0.001975 | cg19862616 | <i>HRK</i>     |
| -1.23158 | 0.001976 | cg02982198 | <i>PTK6</i>    |

|          |          |            |                |
|----------|----------|------------|----------------|
| 1.003832 | 0.00201  | cg21103269 | <i>UBE2J1</i>  |
| 0.397452 | 0.002061 | cg01395217 | <i>RAB3LI</i>  |
| -0.20315 | 0.002089 | cg05990720 | <i>CASKIN1</i> |
| 0.661792 | 0.002118 | cg05990720 | <i>NUBP2</i>   |
| 0.240723 | 0.002128 | cg19874450 | <i>ADAM12</i>  |
| -0.41791 | 0.002167 | cg19248893 | <i>EXOC6B</i>  |
| -0.70847 | 0.002226 | cg18478353 | <i>PRSSI6</i>  |
| 0.478653 | 0.002327 | cg14273401 | <i>SH3BP1</i>  |
| -0.3454  | 0.002538 | cg19248893 | <i>FCHSD2</i>  |
| 0.547037 | 0.002639 | cg12967050 | <i>EFHD2</i>   |
| 0.441938 | 0.002707 | cg13627491 | <i>MED6</i>    |
| -1.85397 | 0.002762 | cg22588936 | <i>PTPRC4P</i> |
| 0.961635 | 0.002818 | cg13539395 | <i>FAM220A</i> |
| 1.057247 | 0.002819 | cg22588936 | <i>C8orf46</i> |
| 0.738126 | 0.002826 | cg14273401 | <i>DNALII</i>  |
| 0.544385 | 0.002832 | cg01395217 | <i>TACO1</i>   |
| 0.629631 | 0.00286  | cg12967050 | <i>CYP4F22</i> |
| -0.59227 | 0.002871 | cg19248893 | <i>TSHZ1</i>   |
| 0.418905 | 0.002949 | cg05396987 | <i>CDIB</i>    |
| 0.531016 | 0.002986 | cg21103269 | <i>MC1R</i>    |
| 0.554522 | 0.002998 | cg19142181 | <i>SLC9A8</i>  |
| 1.471632 | 0.003008 | cg19142181 | <i>PFKM</i>    |
| 1.281381 | 0.003042 | cg26806713 | <i>PHLDA3</i>  |
| -0.61922 | 0.003076 | cg22588936 | <i>RPS6KB2</i> |
| 0.268298 | 0.003146 | cg07873926 | <i>LGR4</i>    |
| 0.867522 | 0.003242 | cg20232060 | <i>FBXO34</i>  |
| -0.40461 | 0.00332  | cg18478353 | <i>MED21</i>   |
| 0.285188 | 0.003393 | cg05440435 | <i>AMFR</i>    |
| 0.920107 | 0.003393 | cg23683674 | <i>NANOS3</i>  |
| 0.462949 | 0.003437 | cg10579012 | <i>AKAP3</i>   |
| 1.279882 | 0.003475 | cg23683674 | <i>OFDI</i>    |

|          |          |            |                |
|----------|----------|------------|----------------|
| 0.906914 | 0.003528 | cg01662869 | <i>TXNDC15</i> |
| -0.45627 | 0.003547 | cg04019843 | <i>NBPF9</i>   |
| 0.686131 | 0.003611 | cg19738404 | <i>TUTI</i>    |
| 0.329141 | 0.003654 | cg22081558 | <i>ACY3</i>    |
| 0.699556 | 0.003696 | cg13664588 | <i>GTDCl</i>   |
| -0.34484 | 0.003784 | cg05990720 | <i>HCl</i>     |
| -0.65506 | 0.003807 | cg13539395 | <i>ALKBH7</i>  |
| 1.102307 | 0.003925 | cg01395217 | <i>FADS2</i>   |
| 0.360724 | 0.003959 | cg01395217 | <i>PTPRG</i>   |
| -0.29444 | 0.004038 | cg05990720 | <i>DPHI</i>    |
| 0.467382 | 0.004086 | cg09543792 | <i>MAD2L1</i>  |
| -0.37907 | 0.004088 | cg04019843 | <i>NBPF20</i>  |
| 0.935978 | 0.004202 | cg21103269 | <i>GBP6</i>    |
| -0.49353 | 0.004203 | cg22588936 | <i>PLEKHG4</i> |
| -0.3131  | 0.004207 | cg02266878 | <i>SGTA</i>    |
| 0.31795  | 0.004313 | cg26417188 | <i>IRF2BPL</i> |
| 0.367992 | 0.004331 | cg11661809 | <i>ABCA17P</i> |
| 0.681151 | 0.004339 | cg23683674 | <i>NFIB</i>    |
| 0.391421 | 0.004443 | cg01426818 | <i>PHLPP2</i>  |
| 0.752863 | 0.004453 | cg00315816 | <i>GLOD4</i>   |
| 0.952842 | 0.004498 | cg19142181 | <i>PLXNBI</i>  |
| -0.55547 | 0.004581 | cg22588936 | <i>SMAD3</i>   |
| 0.779026 | 0.004596 | cg11661809 | <i>MYTIL</i>   |
| 0.567278 | 0.004669 | cg01395217 | <i>CCDC47</i>  |
| 0.41099  | 0.004695 | cg19248893 | <i>CHCl</i>    |
| -0.55157 | 0.004775 | cg20200460 | <i>B3GNT4</i>  |
| -0.505   | 0.004842 | cg02266878 | <i>OXT</i>     |
| 1.062986 | 0.004862 | cg19142181 | <i>CCDC51</i>  |
| 0.963836 | 0.004868 | cg01426818 | <i>RUFY3</i>   |
| 0.659539 | 0.004903 | cg01395217 | <i>TANC2</i>   |
| 0.428655 | 0.004929 | cg01662869 | <i>FAM784</i>  |

|          |          |            |                |
|----------|----------|------------|----------------|
| 0.773338 | 0.004942 | cg19142181 | <i>ELACI</i>   |
| -0.3984  | 0.004976 | cg04019843 | <i>GPAAI</i>   |
| 0.620773 | 0.005008 | cg00315816 | <i>TRIP13</i>  |
| -0.40538 | 0.005043 | cg19248893 | <i>PPP4R2</i>  |
| 1.512198 | 0.005175 | cg05440435 | <i>DYNLL2</i>  |
| 0.605028 | 0.005223 | cg01395217 | <i>CCDC6</i>   |
| -0.36529 | 0.005378 | cg18478353 | <i>CCDC25</i>  |
| 0.251542 | 0.005414 | cg26417188 | <i>ATP7A</i>   |
| -0.84016 | 0.005548 | cg20477591 | <i>NCAPD2</i>  |
| -0.47724 | 0.005702 | cg20477591 | <i>UBE2QL1</i> |
| 0.363449 | 0.005787 | cg14273401 | <i>ANKRD54</i> |
| 0.264605 | 0.005966 | cg27435903 | <i>RAP2A</i>   |
| -0.68021 | 0.006052 | cg15584606 | <i>ACAP3</i>   |
| -0.90311 | 0.006201 | cg02982198 | <i>TUT1</i>    |
| 0.286058 | 0.006312 | cg05990720 | <i>RAB26</i>   |
| 0.873446 | 0.006463 | cg14273401 | <i>NOL12</i>   |
| 0.394597 | 0.006556 | cg09543792 | <i>GRK5</i>    |
| -0.71541 | 0.006575 | cg20477591 | <i>GAPDH</i>   |
| -1.06002 | 0.006604 | cg20200460 | <i>TSN</i>     |
| 0.562877 | 0.006608 | cg14273401 | <i>EPDRI</i>   |
| -0.78223 | 0.006612 | cg02266878 | <i>TSSCI</i>   |
| 0.390489 | 0.00668  | cg01395217 | <i>FADS3</i>   |
| -0.29554 | 0.006861 | cg19248893 | <i>SMC5</i>    |
| 0.499616 | 0.007034 | cg01395217 | <i>PSMC5</i>   |
| 0.344656 | 0.007187 | cg13664588 | <i>FAM83H</i>  |
| -0.77103 | 0.007224 | cg20477591 | <i>TNFSF9</i>  |
| 0.304845 | 0.007271 | cg13627491 | <i>KCNMB4</i>  |
| 0.59953  | 0.007357 | cg14273401 | <i>MSLI</i>    |
| 0.358817 | 0.007358 | cg19738404 | <i>MT42</i>    |
| -0.30065 | 0.007453 | cg12372414 | <i>ROCK1</i>   |
| 0.510832 | 0.007551 | cg01395217 | <i>RORA</i>    |

|           |          |            |                |
|-----------|----------|------------|----------------|
| -0.23971  | 0.00756  | cg05098096 | <i>TTLL10</i>  |
| -0.4617   | 0.007613 | cg24496614 | <i>GLI4</i>    |
| 1.065227  | 0.007649 | cg09543792 | <i>EMBP1</i>   |
| 0.893084  | 0.007653 | cg21103269 | <i>PM20D2</i>  |
| 0.219824  | 0.007681 | cg24151841 | <i>AKAP8L</i>  |
| -0.69449  | 0.007768 | cg20477591 | <i>BMP2</i>    |
| 0.489759  | 0.007872 | cg11661809 | <i>MORNI</i>   |
| -0.927752 | 0.008171 | cg02691091 | <i>DLX4</i>    |
| 0.42244   | 0.008232 | cg17821664 | <i>SOS2</i>    |
| -0.28981  | 0.00834  | cg13539395 | <i>ACER1</i>   |
| 0.607249  | 0.008376 | cg23683674 | <i>RANBP9</i>  |
| -0.60214  | 0.008771 | cg20477591 | <i>NOL9</i>    |
| 0.40756   | 0.008831 | cg11021321 | <i>ARPC5L</i>  |
| -0.47463  | 0.008914 | cg02266878 | <i>CARD11</i>  |
| -0.69467  | 0.00897  | cg20477591 | <i>DCHS1</i>   |
| 573.7044  | 0.009081 | cg22081558 | <i>AAGAB</i>   |
| 0.788674  | 0.009082 | cg19374731 | <i>SIGLEC1</i> |
| 0.727753  | 0.009164 | cg14273401 | <i>CASC3</i>   |
| 0.706663  | 0.009214 | cg01426818 | <i>FOXPI</i>   |
| 0.000232  | 0.009302 | cg00003722 | <i>RMI1</i>    |
| -0.81093  | 0.009308 | cg06216103 | <i>GPR68</i>   |
| 0.383342  | 0.009358 | cg01395217 | <i>PRKCH</i>   |
| -0.42531  | 0.009447 | cg02266878 | <i>FAMI93A</i> |
| 1.211913  | 0.009514 | cg01538301 | <i>SLC24A1</i> |
| -0.59238  | 0.009523 | cg15584606 | <i>SLC12A7</i> |
| 0.460126  | 0.009532 | cg19862616 | <i>CD2</i>     |
| -0.48717  | 0.009544 | cg02266878 | <i>EBF4</i>    |
| 0.782505  | 0.009582 | cg11661809 | <i>LSM7</i>    |
| 0.642343  | 0.009608 | cg12967050 | <i>HSPA13</i>  |
| 1.065503  | 0.009609 | cg05440435 | <i>GNAO1</i>   |
| 0.977256  | 0.009628 | cg05440435 | <i>IKZF4</i>   |

|          |          |            |                |
|----------|----------|------------|----------------|
| -0.92652 | 0.009676 | cg21322248 | <i>ERP44</i>   |
| 0.213812 | 0.009705 | cg07873926 | <i>TMEM222</i> |
| 1.360989 | 0.009831 | cg01395217 | <i>LIMD2</i>   |
| 0.426892 | 0.009854 | cg01426818 | <i>PIP5K1B</i> |
| -0.69571 | 0.009876 | cg03821689 | <i>BCL7C</i>   |
| 0.92108  | 0.009926 | cg12967050 | <i>CTRC</i>    |
| 0.328705 | 0.010213 | cg26417188 | <i>FBXL3</i>   |
| 0.495353 | 0.010278 | cg19738404 | <i>C3orf14</i> |
| 0.320003 | 0.01049  | cg10579012 | <i>AJAPI</i>   |
| 0.528826 | 0.010714 | cg21476203 | <i>DGCR6L</i>  |
| 0.763138 | 0.010854 | cg05440435 | <i>MMP19</i>   |
| 0.46138  | 0.010938 | cg07538364 | <i>ARMC3</i>   |
| 0.971858 | 0.011007 | cg13659360 | <i>B9D1</i>    |
| 0.681868 | 0.011184 | cg01662869 | <i>FAM127C</i> |
| -0.32693 | 0.011188 | cg19248893 | <i>UNC5B</i>   |
| -0.31142 | 0.011273 | cg07555102 | <i>AQP11</i>   |
| -0.57434 | 0.011329 | cg22588936 | <i>SUCLG2</i>  |
| 0.250419 | 0.011589 | cg13627491 | <i>MAP3K9</i>  |
| -0.27306 | 0.011713 | cg04019843 | <i>PDE4DIP</i> |
| 0.464968 | 0.01175  | cg26417188 | <i>COX7B</i>   |
| -0.53903 | 0.011789 | cg02982198 | <i>ROMI</i>    |
| 0.540746 | 0.011947 | cg21103269 | <i>LRRC8B</i>  |
| 0.168573 | 0.012021 | cg19862616 | <i>AKNA</i>    |
| 0.344715 | 0.012045 | cg02266878 | <i>PITRMI</i>  |
| -1.04228 | 0.012097 | cg22588936 | <i>CABP4</i>   |
| 0.392649 | 0.012178 | cg19738404 | <i>PSMC5</i>   |
| 0.590725 | 0.012229 | cg19248893 | <i>RELT</i>    |
| 0.476069 | 0.012289 | cg04871364 | <i>COPG2</i>   |
| 0.79815  | 0.012349 | cg25739003 | <i>MAP2K4</i>  |
| -0.4436  | 0.012349 | cg20477591 | <i>DNHDI</i>   |
| 0.242995 | 0.012382 | cg18478353 | <i>SFN</i>     |

|           |          |            |                |
|-----------|----------|------------|----------------|
| 0.587444  | 0.012409 | cg23683674 | <i>ERCC4</i>   |
| -0.64131  | 0.012682 | cg18478353 | <i>OST4</i>    |
| -0.52451  | 0.01286  | cg04019843 | <i>SHARPIN</i> |
| -0.63418  | 0.012973 | cg0017461  | <i>MAP2K2</i>  |
| 0.672351  | 0.013139 | cg02374944 | <i>ATF2</i>    |
| -0.79192  | 0.013287 | cg09776718 | <i>LL22NC0</i> |
| -0.5865   | 0.013733 | cg20200460 | <i>PKIB</i>    |
| -0.9669   | 0.013823 | cg02691091 | <i>C7orf57</i> |
| 1.11326   | 0.013927 | cg12967050 | <i>EAF1</i>    |
| -0.36083  | 0.013999 | cg13675319 | <i>OTOF</i>    |
| -0.69142  | 0.01413  | cg20477591 | <i>TPPI</i>    |
| -0.3891   | 0.01436  | cg13659360 | <i>E2F8</i>    |
| -0.1711   | 0.014402 | cg11160820 | <i>SSBPI</i>   |
| -0.39319  | 0.014541 | cg09888026 | <i>ALG6</i>    |
| -0.19866  | 0.014725 | cg08643007 | <i>AGO1</i>    |
| 0.551306  | 0.014781 | cg05396987 | <i>GALNT5</i>  |
| 0.684691  | 0.014854 | cg00315816 | <i>POLR2L</i>  |
| 0.899116  | 0.015023 | cg19142181 | <i>B4GALT5</i> |
| -0.8463   | 0.015077 | cg20200460 | <i>TMEM155</i> |
| -0.49872  | 0.01508  | cg00385142 | <i>LNPI</i>    |
| 0.210571  | 0.015122 | cg22755534 | <i>ACE</i>     |
| 0.324081  | 0.015314 | cg26417188 | <i>RSFI</i>    |
| 0.304597  | 0.015528 | cg17821664 | <i>NCKAP5L</i> |
| -0.424448 | 0.015601 | cg02266878 | <i>NCLN</i>    |
| -0.76508  | 0.015614 | cg18478353 | <i>HOXA4</i>   |
| 0.275674  | 0.015857 | cg12967050 | <i>CYP4F3</i>  |
| 0.116396  | 0.015883 | cg26417188 | <i>SYCE1L</i>  |
| 0.555058  | 0.016001 | cg14273401 | <i>PSMD3</i>   |
| -0.22762  | 0.016135 | cg07555102 | <i>SYCE1L</i>  |
| 0.83084   | 0.016225 | cg01662869 | <i>JAKMIP3</i> |
| -0.56024  | 0.016246 | cg08976554 | <i>SLC25A4</i> |

|          |          |            |                |
|----------|----------|------------|----------------|
| 1.079897 | 0.016395 | cg12967050 | <i>NOTCH3</i>  |
| 0.732385 | 0.016524 | cg00315816 | <i>JMJD8</i>   |
| 0.540718 | 0.016572 | cg01395217 | <i>FEN1</i>    |
| -0.54751 | 0.016755 | cg02266878 | <i>PRSS33</i>  |
| -0.31241 | 0.016988 | cg05990720 | <i>MYTIL</i>   |
| -0.98259 | 0.017005 | cg20176285 | <i>KR11</i>    |
| 0.36622  | 0.017173 | cg19738404 | <i>ROMI</i>    |
| -0.21304 | 0.017187 | cg05990720 | <i>SPSB3</i>   |
| 0.448935 | 0.017223 | cg00385142 | <i>HHIPL1</i>  |
| 0.313695 | 0.017316 | cg19248893 | <i>SLC29A3</i> |
| -0.797   | 0.01741  | cg05440435 | <i>MAP3K1</i>  |
| 0.529936 | 0.017422 | cg20176285 | <i>ATG4D</i>   |
| 0.99129  | 0.017531 | cg23683674 | <i>COX10</i>   |
| 0.296421 | 0.017544 | cg18478353 | <i>HOXA10</i>  |
| -1.08335 | 0.017616 | cg02691091 | <i>C20orf1</i> |
| -0.24978 | 0.01785  | cg05990720 | <i>STK35</i>   |
| 0.613656 | 0.017971 | cg02374944 | <i>NOP16</i>   |
| 0.481676 | 0.017994 | cg15365426 | <i>NAA38</i>   |
| -0.33236 | 0.018023 | cg05990720 | <i>GMDS</i>    |
| -0.61144 | 0.018215 | cg19142181 | <i>SPATA20</i> |
| 0.44438  | 0.018616 | cg21103269 | <i>PTEN</i>    |
| 0.28569  | 0.018683 | cg13963729 | <i>TIMP2</i>   |
| -0.30218 | 0.018813 | cg22081558 | <i>ALDH3B1</i> |
| -0.51696 | 0.018951 | cg20477591 | <i>C3</i>      |
| -0.43591 | 0.019158 | cg13659360 | <i>KCNH8</i>   |
| -0.75123 | 0.019169 | cg13539395 | <i>GTF2F1</i>  |
| 0.248204 | 0.019469 | cg07873926 | <i>C9orf72</i> |
| 0.390532 | 0.019579 | cg12967050 | <i>CC2D2A</i>  |
| -0.44749 | 0.019613 | cg05990720 | <i>DOTIL</i>   |
| -0.75107 | 0.019615 | cg06216103 | <i>FURIN</i>   |
| 0.374455 | 0.019747 | cg19862616 | <i>PCSK7</i>   |

|          |          |            |                |
|----------|----------|------------|----------------|
| -0.79355 | 0.019904 | cg20477591 | <i>FBXO39</i>  |
| -0.33474 | 0.020055 | cg11661809 | <i>RNF4</i>    |
| 0.50069  | 0.020095 | cg14273401 | <i>LETM2</i>   |
| -0.60719 | 0.020117 | cg09776718 | <i>BMSIP20</i> |
| 0.633527 | 0.020461 | cg12967050 | <i>DDX1</i>    |
| 0.775566 | 0.020503 | cg19142181 | <i>SHS45</i>   |
| -0.59327 | 0.02055  | cg20477591 | <i>TRIP10</i>  |
| 0.264935 | 0.020609 | cg19374731 | <i>SDK1</i>    |
| -1.0376  | 0.020699 | cg22588936 | <i>FBXL8</i>   |
| 0.488806 | 0.020738 | cg20176285 | <i>TMEDI</i>   |
| -0.39209 | 0.020742 | cg13659360 | <i>NAV2</i>    |
| -1.06913 | 0.020824 | cg16073958 | <i>HPIP3</i>   |
| 0.383414 | 0.020894 | cg18478353 | <i>HOXA7</i>   |
| 0.410918 | 0.020932 | cg21103269 | <i>LRRC8C</i>  |
| 0.342808 | 0.020971 | cg12372414 | <i>UPF1</i>    |
| 0.537857 | 0.020978 | cg22588936 | <i>KCTD19</i>  |
| 0.516425 | 0.020983 | cg00315816 | <i>TALDO1</i>  |
| 0.496734 | 0.021159 | cg07538364 | <i>DCTN5</i>   |
| -0.46385 | 0.021177 | cg13539395 | <i>MRPL51</i>  |
| 1.388839 | 0.021191 | cg23683674 | <i>CD83</i>    |
| -0.58837 | 0.021279 | cg20383390 | <i>FXYD6</i>   |
| -0.41254 | 0.021282 | cg13659360 | <i>SUGPI</i>   |
| -0.70076 | 0.021402 | cg24496614 | <i>RHPNI</i>   |
| 1.314702 | 0.021589 | cg22588936 | <i>RRSI</i>    |
| 0.39205  | 0.021591 | cg05951364 | <i>HELZ</i>    |
| 0.594872 | 0.021599 | cg05951364 | <i>PPPIR36</i> |
| -0.50166 | 0.021604 | cg19142181 | <i>CABP5</i>   |
| 0.338426 | 0.021761 | cg00385142 | <i>AGFG2</i>   |
| 0.510747 | 0.021834 | cg05440435 | <i>ERBB3</i>   |
| -0.4983  | 0.022028 | cg13659360 | <i>PLIN2</i>   |
| 0.482103 | 0.022188 | cg17821664 | <i>CACNA2D</i> |

|          |          |            |                |
|----------|----------|------------|----------------|
| -0.28115 | 0.022198 | cg05990720 | <i>MSRB1</i>   |
| -0.56112 | 0.022202 | cg02982198 | <i>B3GNT2</i>  |
| 0.748511 | 0.0223   | cg13539395 | <i>LY86</i>    |
| 0.349034 | 0.022339 | cg04871364 | <i>PIK3R4</i>  |
| 0.430525 | 0.022415 | cg00315816 | <i>TMEM18</i>  |
| 0.323685 | 0.022493 | cg01426818 | <i>NAGK</i>    |
| 0.300388 | 0.022555 | cg00385142 | <i>C7orf43</i> |
| -0.2998  | 0.022704 | cg21103269 | <i>SPATA2L</i> |
| -0.68318 | 0.022726 | cg09776718 | <i>C1Q4</i>    |
| 0.587193 | 0.022938 | cg13664588 | <i>GSDMD</i>   |
| 0.631215 | 0.023123 | cg00315816 | <i>DGKQ</i>    |
| 0.563595 | 0.023169 | cg19142181 | <i>UQCRC1</i>  |
| -0.53031 | 0.023258 | cg02266878 | <i>GNG7</i>    |
| 0.437388 | 0.023267 | cg11661809 | <i>KCNQ1</i>   |
| 0.314907 | 0.023403 | cg26417188 | <i>MAGT1</i>   |
| -0.68303 | 0.023473 | cg02266878 | <i>FLYWCH1</i> |
| 0.490145 | 0.023611 | cg19142181 | <i>PCSK1N</i>  |
| 0.611066 | 0.023762 | cg19142181 | <i>FBNI</i>    |
| -1.28343 | 0.023787 | cg07555102 | <i>ATP9B</i>   |
| -0.43132 | 0.023814 | cg13664588 | <i>EPPK1</i>   |
| -0.50275 | 0.023817 | cg02691091 | <i>MSH6</i>    |
| 0.467666 | 0.02385  | cg19142181 | <i>SPATA2</i>  |
| -0.50609 | 0.023933 | cg02266878 | <i>ITFG2</i>   |
| 0.372015 | 0.024057 | cg14273401 | <i>MTFI</i>    |
| 0.338186 | 0.024228 | cg02724025 | <i>EEF1A2</i>  |
| 0.53463  | 0.024239 | cg19142181 | <i>SMAD4</i>   |
| -0.32677 | 0.024306 | cg02724025 | <i>HELZ2</i>   |
| -0.44216 | 0.024356 | cg09543792 | <i>POLQ</i>    |
| 0.505422 | 0.024425 | cg01426818 | <i>PTCD2</i>   |
| -0.38632 | 0.024479 | cg14724918 | <i>HBQ1</i>    |
| -0.78339 | 0.024574 | cg02266878 | <i>LPIN2</i>   |

|          |          |            |                |
|----------|----------|------------|----------------|
| -0.56072 | 0.024689 | cg20477591 | <i>THAP3</i>   |
| -0.42086 | 0.024879 | cg02691091 | <i>ABCA13</i>  |
| 0.203463 | 0.024897 | cg16616362 | <i>ABCC6</i>   |
| -0.40309 | 0.024926 | cg07555102 | <i>TMEM60</i>  |
| 0.404513 | 0.025204 | cg10579012 | <i>SPATA6L</i> |
| 0.592243 | 0.025959 | cg00017461 | <i>RHOG</i>    |
| 0.569656 | 0.026513 | cg19142181 | <i>LIG1</i>    |
| 0.273495 | 0.026574 | cg18786125 | <i>ABHD17B</i> |
| 0.244289 | 0.026575 | cg19738404 | <i>PPDPF</i>   |
| 0.229383 | 0.026626 | cg09791665 | <i>AGO4</i>    |
| 0.347825 | 0.026664 | cg07538364 | <i>MSRB2</i>   |
| 0.408761 | 0.026786 | cg19738404 | <i>FAMI61A</i> |
| 0.616247 | 0.026933 | cg13539395 | <i>GAPDH</i>   |
| 0.68206  | 0.026945 | cg19862616 | <i>IGSF3</i>   |
| 0.510594 | 0.027054 | cg19142181 | <i>RBM3</i>    |
| 0.429472 | 0.027136 | cg11661809 | <i>MYLK4</i>   |
| -0.48011 | 0.027331 | cg02982198 | <i>INTS5</i>   |
| 0.386894 | 0.027401 | cg19374731 | <i>DFFB</i>    |
| -0.28168 | 0.027568 | cg20477591 | <i>GRID2IP</i> |
| -0.50623 | 0.02763  | cg15584606 | <i>FGFRLI</i>  |
| 0.360182 | 0.027662 | cg14273401 | <i>SHB</i>     |
| -0.17348 | 0.027695 | cg05990720 | <i>ATP8B3</i>  |
| -0.44554 | 0.027739 | cg20383390 | <i>TNFSF8</i>  |
| -0.36175 | 0.027756 | cg21103269 | <i>LYSMD3</i>  |
| -0.29202 | 0.027765 | cg18478353 | <i>STK38L</i>  |
| -0.66157 | 0.02787  | cg02982198 | <i>TTC9C</i>   |
| -0.42159 | 0.028039 | cg20477591 | <i>MRPL51</i>  |
| 0.422334 | 0.028071 | cg19142181 | <i>FRYL</i>    |
| -0.31248 | 0.028141 | cg05990720 | <i>RPA1</i>    |
| 0.395359 | 0.028169 | cg19862616 | <i>DSCAMLI</i> |
| 0.404772 | 0.028341 | cg11661809 | <i>EBF4</i>    |

|          |          |            |                |
|----------|----------|------------|----------------|
| 0.315969 | 0.028396 | cg05951364 | NEATI          |
| 0.291912 | 0.028503 | cg10579012 | <i>ALOX15</i>  |
| -0.64842 | 0.028771 | cg22588936 | <i>DOC2GP</i>  |
| 1.328639 | 0.028938 | cg05440435 | <i>EPX</i>     |
| 0.520188 | 0.028957 | cg20176285 | <i>PINX1</i>   |
| 0.286946 | 0.029343 | cg07538364 | <i>PALB2</i>   |
| 0.273242 | 0.029367 | cg27435903 | <i>FANCC</i>   |
| 0.336178 | 0.029702 | cg07538364 | <i>RPS2P32</i> |
| 0.517487 | 0.029834 | cg11661809 | <i>SRR</i>     |
| 0.888891 | 0.029902 | cg18478353 | <i>CAD</i>     |
| 0.704681 | 0.029921 | cg05440435 | <i>NEDD4</i>   |
| -0.40845 | 0.03     | cg02982198 | <i>MTA2</i>    |
| 0.646493 | 0.030046 | cg11661809 | <i>GMDS</i>    |
| -0.98823 | 0.030157 | cg02691091 | <i>KPTN</i>    |
| -0.3604  | 0.030172 | cg19248893 | <i>FAMI68A</i> |
| 0.338452 | 0.030271 | cg05396987 | <i>RNF145</i>  |
| 0.392028 | 0.030294 | cg00315816 | <i>STUB1</i>   |
| 0.345043 | 0.030404 | cg20477591 | <i>TAPBPL</i>  |
| 0.254928 | 0.030549 | cg00315816 | <i>TMED11P</i> |
| 0.343327 | 0.030709 | cg19374731 | <i>ATRN</i>    |
| -0.31426 | 0.031277 | cg09776718 | <i>C1QB</i>    |
| -0.52448 | 0.031506 | cg13590117 | <i>ARL6IP1</i> |
| 0.328683 | 0.031534 | cg21103269 | <i>FANCA</i>   |
| 0.582561 | 0.031649 | cg05951364 | <i>DSEL</i>    |
| -0.34373 | 0.031658 | cg07538364 | <i>PLKI</i>    |
| 0.405924 | 0.031798 | cg00017461 | <i>PIP5K1C</i> |
| 0.000262 | 0.031876 | cg00003722 | <i>COL24AI</i> |
| 0.547244 | 0.031894 | cg19142181 | <i>PIM2</i>    |
| -0.28639 | 0.032071 | cg02712036 | <i>ASXL1</i>   |
| 0.449303 | 0.032302 | cg21103269 | <i>HERC3</i>   |
| 0.56804  | 0.032426 | cg19142181 | <i>SUV39HI</i> |

|          |          |            |                |
|----------|----------|------------|----------------|
| -0.50492 | 0.032726 | cg02691091 | <i>PKDIL1</i>  |
| -0.41652 | 0.033055 | cg20477591 | <i>LPAR5</i>   |
| 0.400834 | 0.033256 | cg11661809 | <i>TSSC4</i>   |
| 0.387138 | 0.033312 | cg18478353 | <i>HOXA5</i>   |
| 0.505539 | 0.033404 | cg03468115 | <i>FKBP14</i>  |
| 0.549721 | 0.033525 | cg27435903 | <i>TSPYL5</i>  |
| -0.49947 | 0.033769 | cg24818434 | <i>KANK3</i>   |
| 0.313741 | 0.033785 | cg19374731 | <i>LRPAP1</i>  |
| -0.79669 | 0.033993 | cg02691091 | <i>SLC48A1</i> |
| 0.226192 | 0.034185 | cg01426818 | <i>MAP3K9</i>  |
| -0.67949 | 0.034285 | cg10410121 | <i>PSMB4</i>   |
| 0.470954 | 0.034343 | cg13627491 | <i>NADSYN1</i> |
| -0.47837 | 0.034491 | cg20477591 | <i>ARFIP2</i>  |
| -0.88484 | 0.034575 | cg20630567 | <i>FLII</i>    |
| -0.21488 | 0.034622 | cg05098096 | <i>PSMFI</i>   |
| -0.41608 | 0.034676 | cg20630567 | <i>ACAD9</i>   |
| -0.35217 | 0.034718 | cg20477591 | <i>MRPL17</i>  |
| 0.316136 | 0.034743 | cg19738404 | <i>COMMD1</i>  |
| -0.47061 | 0.0352   | cg09397375 | <i>SUPT3H</i>  |
| -0.36944 | 0.03577  | cg19374731 | <i>MEGF6</i>   |
| 0.262454 | 0.035861 | cg14724918 | <i>DECR2</i>   |
| -0.17597 | 0.035919 | cg10200408 | <i>ABCA17P</i> |
| 0.371606 | 0.036176 | cg11661809 | <i>TMC2</i>    |
| 0.722527 | 0.036322 | cg15847604 | <i>SFMBT1</i>  |
| -0.35729 | 0.036375 | cg07873926 | <i>CCDC34</i>  |
| 0.58406  | 0.036447 | cg05440435 | <i>NAT14</i>   |
| 0.675705 | 0.036601 | cg14273401 | <i>ELFN2</i>   |
| -0.21377 | 0.036657 | cg05990720 | <i>NTHL1</i>   |
| 0.349279 | 0.036853 | cg19738404 | <i>IPO11</i>   |
| 0.124977 | 0.036918 | cg05990720 | <i>POLN</i>    |
| 0.412857 | 0.037059 | cg25739003 | <i>ELOF1</i>   |

|          |          |            |                |
|----------|----------|------------|----------------|
| 0.91686  | 0.037199 | cg15847604 | <i>CC2DIB</i>  |
| 0.294849 | 0.037569 | cg11661809 | <i>CASKIN1</i> |
| 0.15455  | 0.037719 | cg11021321 | <i>SLC12A2</i> |
| 0.527778 | 0.037957 | cg14724918 | <i>IFITM3</i>  |
| 0.442094 | 0.03797  | cg10179363 | <i>PRDX1</i>   |
| 0.345971 | 0.037989 | cg19142181 | <i>SLAIN2</i>  |
| -0.44356 | 0.038097 | cg14273401 | <i>ORMDL3</i>  |
| -0.27238 | 0.038369 | cg21322248 | <i>MOK</i>     |
| -0.7295  | 0.038394 | cg21476203 | <i>PSPCI</i>   |
| 0.630351 | 0.038467 | cg20232060 | <i>LANCL2</i>  |
| 0.235695 | 0.038572 | cg26417188 | <i>RORB</i>    |
| -0.19563 | 0.038688 | cg26146287 | <i>RCL1</i>    |
| -0.3076  | 0.03894  | cg02982198 | <i>PTPRG</i>   |
| -0.21895 | 0.038973 | cg05990720 | <i>HAUS3</i>   |
| 0.510386 | 0.038973 | cg19738404 | <i>TM2DI</i>   |
| -0.23876 | 0.039157 | cg14442841 | <i>TELO2</i>   |
| -0.50789 | 0.039241 | cg07555102 | <i>FAM47E</i>  |
| 0.276039 | 0.039378 | cg19738404 | <i>TEX2</i>    |
| 0.931817 | 0.039403 | cg19142181 | <i>NME6</i>    |
| -0.41006 | 0.039518 | cg13659360 | <i>MAP3K15</i> |
| 0.511165 | 0.03957  | cg00315816 | <i>RHOT2</i>   |
| -0.47515 | 0.039801 | cg23683674 | <i>RLN3</i>    |
| -0.24143 | 0.039881 | cg05990720 | <i>RPL3L</i>   |
| 0.31303  | 0.039885 | cg01395217 | <i>TMEM258</i> |
| 0.454424 | 0.040204 | cg11661809 | <i>MIR940</i>  |
| 0.192036 | 0.04039  | cg19374731 | <i>ADII</i>    |
| -0.45705 | 0.040476 | cg13539395 | <i>L3MBTL4</i> |
| 0.275523 | 0.040675 | cg19248893 | <i>JPX</i>     |
| 0.573055 | 0.040712 | cg21103269 | <i>FOXXN3</i>  |
| 0.177389 | 0.040936 | cg26417188 | <i>PEAK1</i>   |
| 0.312139 | 0.041268 | cg14273401 | <i>TBC1D1</i>  |

|          |          |            |                |
|----------|----------|------------|----------------|
| -0.49406 | 0.041301 | cg18478353 | <i>CCDC34</i>  |
| -0.21957 | 0.041332 | cg05990720 | <i>NDUFS6</i>  |
| -0.74149 | 0.041545 | cg20200460 | <i>DIRC2</i>   |
| 0.173581 | 0.041634 | cg16629408 | <i>RAB15</i>   |
| 0.358901 | 0.041767 | cg19738404 | <i>AR</i>      |
| 0.486212 | 0.042021 | cg23683674 | <i>TCEANC</i>  |
| -0.52955 | 0.042162 | cg02982198 | <i>DDX5</i>    |
| -0.86428 | 0.042694 | cg12967050 | <i>FAM200B</i> |
| 0.491014 | 0.042719 | cg18787783 | <i>CHID1</i>   |
| -0.27658 | 0.04281  | cg05098096 | <i>MED16</i>   |
| -0.39603 | 0.042872 | cg19248893 | <i>ARH1</i>    |
| -0.13891 | 0.042914 | cg11160820 | <i>TBC1D9</i>  |
| 0.78841  | 0.042947 | cg20232060 | <i>KIR3DL2</i> |
| -0.31469 | 0.043166 | cg00315816 | <i>METRN</i>   |
| -1.15559 | 0.043457 | cg20232060 | <i>BRSK1</i>   |
| -0.37308 | 0.04367  | cg00385142 | <i>TM9SF2</i>  |
| -0.18734 | 0.043881 | cg02712036 | <i>MTMR10</i>  |
| -0.16779 | 0.043999 | cg05098096 | <i>ELANE</i>   |
| -0.49814 | 0.044019 | cg21103269 | <i>RNGTT</i>   |
| -0.26019 | 0.044164 | cg12348202 | <i>MACROD2</i> |
| 2.257353 | 0.044254 | cg05440435 | <i>MER3</i>    |
| -0.42819 | 0.044578 | cg12967050 | <i>BST1</i>    |
| -0.2526  | 0.044691 | cg05098096 | <i>SNTG2</i>   |
| -0.36977 | 0.044758 | cg02266878 | <i>CLDN9</i>   |
| -0.21722 | 0.044787 | cg05990720 | <i>KLF16</i>   |
| 0.345218 | 0.044812 | cg11661809 | <i>METTL4</i>  |
| -0.15365 | 0.044812 | cg11160820 | <i>ATP1B3</i>  |
| 0.341714 | 0.044902 | cg20977448 | <i>RANBP17</i> |
| -0.14356 | 0.044973 | cg22081558 | <i>AGRP</i>    |
| 0.293828 | 0.045072 | cg11661809 | <i>SNX8</i>    |
| 0.465994 | 0.04509  | cg19738404 | <i>FTSJ3</i>   |

|          |          |            |                |
|----------|----------|------------|----------------|
| -0.26305 | 0.046154 | cg19248893 | <i>SLC16A5</i> |
| -0.4844  | 0.046313 | cg10179363 | <i>SP2</i>     |
| -0.44044 | 0.046571 | cg02266878 | <i>PAQR4</i>   |
| 0.590703 | 0.046603 | cg01395217 | <i>DIMT1</i>   |
| 1.038057 | 0.046633 | cg09888026 | <i>ITGB3BP</i> |
| -0.67027 | 0.046759 | cg02982198 | <i>BSCL2</i>   |
| 0.445084 | 0.046821 | cg10579012 | <i>CCND2</i>   |
| -0.39192 | 0.046842 | cg0385142  | <i>GAL3ST4</i> |
| 0.716386 | 0.046881 | cg09543792 | <i>EPB4L5</i>  |
| 0.514233 | 0.047202 | cg13539395 | <i>KLHL2I</i>  |
| 0.234445 | 0.047424 | cg01395217 | <i>NFLA</i>    |
| -0.27142 | 0.047548 | cg14442841 | <i>CRIPAK</i>  |
| 0.370539 | 0.048141 | cg11661809 | <i>TRPM5</i>   |
| 0.238998 | 0.048443 | cg19374731 | <i>DOK7</i>    |
| 0.24697  | 0.048747 | cg07538364 | <i>OX4IL</i>   |
| 0.747233 | 0.049029 | cg05440435 | <i>CHCHD2</i>  |
| 0.433705 | 0.049285 | cg23683674 | <i>RFXI</i>    |
| 0.558064 | 0.049806 | cg20232060 | <i>CESIP1</i>  |
| -0.59043 | 0.049939 | cg09776718 | <i>BMLI</i>    |

Supplement Table S12 (A): MethQTLs identified based on association of SNPs with DNAm in males (n=306)

| Dependent  | Parameter   | Estimate | StdErr   | tValue | Prob       |
|------------|-------------|----------|----------|--------|------------|
| cg20383390 | rs10095492  | -0.10734 | 0.050753 | -2.11  | 0.035248   |
| cg24343755 | rs105087201 | 0.328499 | 0.142266 | 2.31   | 0.021614   |
| cg24343755 | rs105087202 | 0.173538 | 0.054484 | 3.19   | 0.001598   |
| cg06216103 | rs107517111 | 0.559468 | 0.088146 | 6.35   | <.00000001 |
| cg06216103 | rs107517112 | 0.220685 | 0.067784 | 3.26   | 0.001259   |
| cg13627491 | rs108198992 | 0.17396  | 0.070011 | 2.48   | 0.013503   |
| cg13627491 | rs108199031 | -0.22148 | 0.088303 | -2.51  | 0.012656   |
| cg04871364 | rs108645481 | -0.26342 | 0.090796 | -2.9   | 0.00399    |

|            |              |          |          |       |          |
|------------|--------------|----------|----------|-------|----------|
| cg06216103 | rs10902512 1 | 0.546382 | 0.091213 | 5.99  | 6E-09    |
| cg06216103 | rs10902512 2 | 0.176893 | 0.069047 | 2.56  | 0.010893 |
| cg24343755 | rs11015236 2 | -0.13888 | 0.060897 | -2.28 | 0.023265 |
| cg24343755 | rs11015249 1 | -0.28527 | 0.073259 | -3.89 | 0.000121 |
| cg24343755 | rs11015249 2 | -0.11335 | 0.052374 | -2.16 | 0.031225 |
| cg15847604 | rs11054443 1 | 0.111962 | 0.046403 | 2.41  | 0.016424 |
| cg15847604 | rs11054443 2 | 0.077741 | 0.033723 | 2.31  | 0.021829 |
| cg19142181 | rs11086147 1 | 1.481875 | 0.240551 | 6.16  | 2E-09    |
| cg19142181 | rs11086147 2 | 1.211184 | 0.200082 | 6.05  | 4E-09    |
| cg19248893 | rs11122115 2 | -0.09099 | 0.030955 | -2.94 | 0.00354  |
| cg06216103 | rs11246996 1 | 0.580753 | 0.177039 | 3.28  | 0.001158 |
| cg06216103 | rs11246996 2 | 0.242206 | 0.067109 | 3.61  | 0.000359 |
| cg06216103 | rs11247000 1 | 0.371331 | 0.14846  | 2.5   | 0.012904 |
| cg06216103 | rs11247000 2 | 0.196931 | 0.067832 | 2.9   | 0.003965 |
| cg20383390 | rs1146297 2  | -0.11337 | 0.050797 | -2.23 | 0.026359 |
| cg20383390 | rs1146298 2  | -0.10802 | 0.050836 | -2.12 | 0.034411 |
| cg26146287 | rs11575893 1 | -0.62074 | 0.150313 | -4.13 | 4.7E-05  |
| cg21322248 | rs11639459 1 | -0.32628 | 0.130124 | -2.51 | 0.012683 |
| cg21322248 | rs11639459 2 | -0.13683 | 0.036325 | -3.77 | 0.000199 |
| cg02724025 | rs11647164 2 | 0.113646 | 0.053106 | 2.14  | 0.033154 |
| cg02998992 | rs11652712 2 | 0.428023 | 0.12835  | 3.33  | 0.000959 |
| cg00707741 | rs11682333 2 | -0.0803  | 0.037783 | -2.13 | 0.034364 |
| cg04871364 | rs12074379 1 | 0.955603 | 0.349143 | 2.74  | 0.006566 |
| cg18786125 | rs12080677 2 | 0.100514 | 0.046039 | 2.18  | 0.029786 |
| cg13627491 | rs12236239 1 | -0.36219 | 0.129323 | -2.8  | 0.005428 |
| cg09396181 | rs12492784 2 | 0.068696 | 0.032835 | 2.09  | 0.037256 |
| cg02724025 | rs12708869 2 | 0.113646 | 0.053106 | 2.14  | 0.033154 |
| cg20383390 | rs12905339 2 | -0.10959 | 0.050825 | -2.16 | 0.031853 |
| cg20383390 | rs1290541 2  | -0.10959 | 0.050825 | -2.16 | 0.031853 |
| cg21322248 | rs12912465 2 | 0.08542  | 0.035152 | 2.43  | 0.015678 |
| cg14736210 | rs13044588 1 | -0.60835 | 0.216397 | -2.81 | 0.005257 |

|            |              |          |          |       |             |
|------------|--------------|----------|----------|-------|-------------|
| cg27230396 | rs13121538 2 | 0.122612 | 0.059802 | 2.05  | 0.041196    |
| cg20383390 | rs1316011 2  | -0.10734 | 0.050753 | -2.11 | 0.035248    |
| cg00707741 | rs13388333 1 | -0.11093 | 0.053411 | -2.08 | 0.038653    |
| cg00707741 | rs13388333 2 | -0.08652 | 0.037597 | -2.3  | 0.022059    |
| cg13627491 | rs1339424 2  | -0.11882 | 0.059916 | -1.98 | 0.048258    |
| cg02724025 | rs1520237 2  | -0.12654 | 0.052876 | -2.39 | 0.017316    |
| cg15847604 | rs1547392 2  | 0.074214 | 0.033508 | 2.21  | 0.027517    |
| cg24343755 | rs1564271 1  | -0.34603 | 0.090443 | -3.83 | 0.000158    |
| cg24343755 | rs16927305 2 | -0.1344  | 0.061814 | -2.17 | 0.030462    |
| cg10179363 | rs17239917 2 | 0.072495 | 0.028527 | 2.54  | 0.011543    |
| cg21322248 | rs17465692 1 | 0.1224   | 0.048343 | 2.53  | 0.01185     |
| cg21322248 | rs17465692 2 | 0.080154 | 0.03978  | 2.01  | 0.044798    |
| cg15847604 | rs17745932 2 | -0.12189 | 0.046507 | -2.62 | 0.009209    |
| cg24343755 | rs1780179 1  | -0.2314  | 0.078554 | -2.95 | 0.003471    |
| cg24343755 | rs1780180 1  | -0.23096 | 0.080138 | -2.88 | 0.004233    |
| cg24343755 | rs1780196 1  | 0.444575 | 0.182203 | 2.44  | 0.01526     |
| cg24343755 | rs1780196 2  | 0.317385 | 0.054198 | 5.86  | 1.2E-08     |
| cg18478353 | rs1878069 2  | -0.07696 | 0.029166 | -2.64 | 0.008754    |
| cg19248893 | rs201151 2   | 0.067569 | 0.032711 | 2.07  | 0.039713    |
| cg13627491 | rs2012728 2  | -0.12251 | 0.062103 | -1.97 | 0.049437    |
| cg23683674 | rs2027761 2  | 0.106327 | 0.051225 | 2.08  | 0.038766    |
| cg00707741 | rs2055566 1  | 0.506693 | 0.215877 | 2.35  | 0.019562    |
| cg19142181 | rs2093045 1  | 0.805617 | 0.257458 | 3.13  | 0.001924    |
| cg19142181 | rs2093045 2  | 0.604156 | 0.197963 | 3.05  | 0.002476    |
| cg19248893 | rs2235564 1  | 0.10569  | 0.046646 | 2.27  | 0.02417     |
| cg19248893 | rs2235564 2  | 0.064978 | 0.030063 | 2.16  | 0.03145     |
| cg26146287 | rs2239670 2  | 0.162742 | 0.048614 | 3.35  | 0.000918    |
| cg14273401 | rs2240068 2  | -0.22208 | 0.099837 | -2.22 | 0.026857    |
| cg19142181 | rs2248900 1  | 1.362868 | 0.413597 | 3.3   | 0.0011      |
| cg19142181 | rs2248900 2  | 1.232939 | 0.174187 | 7.08  | <.000000001 |
| cg13627491 | rs2251885 2  | 0.153934 | 0.061332 | 2.51  | 0.0126      |

|            |            |   |          |          |       |             |
|------------|------------|---|----------|----------|-------|-------------|
| cg14736210 | rs237473   | 2 | 0.092034 | 0.045942 | 2     | 0.046037    |
| cg24343755 | rs2448111  | 1 | 0.342416 | 0.167838 | 2.04  | 0.042202    |
| cg24343755 | rs2448111  | 2 | 0.303687 | 0.054346 | 5.59  | 5.1E-08     |
| cg14273401 | rs2523990  | 2 | 0.278927 | 0.103883 | 2.69  | 0.007652    |
| cg15847604 | rs2723830  | 2 | 0.078481 | 0.033544 | 2.34  | 0.019954    |
| cg18786125 | rs2821050  | 2 | 0.083201 | 0.042103 | 1.98  | 0.049044    |
| cg18478353 | rs2839550  | 2 | -0.07684 | 0.034743 | -2.21 | 0.027738    |
| cg18478353 | rs2839557  | 2 | -0.08825 | 0.029685 | -2.97 | 0.003187    |
| cg05951364 | rs2972175  | 2 | -0.07118 | 0.032909 | -2.16 | 0.031323    |
| cg05951364 | rs2972175  | 2 | -0.07123 | 0.034521 | -2.06 | 0.039938    |
| cg13627491 | rs2993805  | 2 | 0.17396  | 0.070011 | 2.48  | 0.013503    |
| cg24343755 | rs3118153  | 1 | 0.34161  | 0.16786  | 2.04  | 0.042712    |
| cg24343755 | rs3118153  | 2 | 0.304538 | 0.054606 | 5.58  | 5.4E-08     |
| cg04871364 | rs34064241 | 1 | 0.953681 | 0.348644 | 2.74  | 0.006598    |
| cg13963729 | rs349311   | 1 | 0.780327 | 0.381801 | 2.04  | 0.041837    |
| cg20977448 | rs352346   | 1 | -0.64128 | 0.070292 | -9.12 | <.000000001 |
| cg20977448 | rs352346   | 2 | -0.30691 | 0.05939  | -5.17 | 4.31E-07    |
| cg20977448 | rs352347   | 1 | -0.64997 | 0.070027 | -9.28 | <.000000001 |
| cg20977448 | rs352347   | 2 | -0.31976 | 0.059166 | -5.4  | 1.32E-07    |
| cg19142181 | rs3729555  | 1 | 1.957778 | 0.226678 | 8.64  | <.000000001 |
| cg19142181 | rs3729555  | 2 | 2.02826  | 0.162029 | 12.52 | <.000000001 |
| cg02724025 | rs3760056  | 2 | 0.113646 | 0.053106 | 2.14  | 0.033154    |
| cg00707741 | rs3771551  | 2 | 0.13163  | 0.04806  | 2.74  | 0.00653     |
| cg00707741 | rs3771583  | 2 | 0.132413 | 0.052639 | 2.52  | 0.012404    |
| cg15847604 | rs3782137  | 1 | 0.109399 | 0.046414 | 2.36  | 0.019059    |
| cg19142181 | rs3810460  | 1 | 2.660948 | 0.181245 | 14.68 | <.000000001 |
| cg19142181 | rs3810460  | 2 | 2.630518 | 0.149955 | 17.54 | <.000000001 |
| cg16360777 | rs3924573  | 1 | -0.21778 | 0.103271 | -2.11 | 0.03578     |
| cg09791665 | rs412816   | 2 | 0.114386 | 0.057729 | 1.98  | 0.048446    |
| cg24343755 | rs4369307  | 1 | 0.331357 | 0.142085 | 2.33  | 0.02035     |
| cg24343755 | rs4369307  | 2 | 0.179586 | 0.053995 | 3.33  | 0.00099     |

|            |             |          |          |       |             |
|------------|-------------|----------|----------|-------|-------------|
| cg21322248 | rs4420499 1 | -0.31635 | 0.119648 | -2.64 | 0.008619    |
| cg21322248 | rs4420499 2 | -0.11935 | 0.038395 | -3.11 | 0.002058    |
| cg09791665 | rs444131 2  | 0.114386 | 0.057729 | 1.98  | 0.048446    |
| cg05951364 | rs4552929 1 | 0.195468 | 0.092009 | 2.12  | 0.034441    |
| cg18786125 | rs4648524 2 | 0.111049 | 0.040435 | 2.75  | 0.006387    |
| cg00707741 | rs4675947 2 | -0.0803  | 0.037783 | -2.13 | 0.034364    |
| cg14736210 | rs4809746 1 | 0.452865 | 0.217917 | 2.08  | 0.038537    |
| cg05951364 | rs4876074 1 | -0.17366 | 0.080462 | -2.16 | 0.031692    |
| cg05951364 | rs4876121 1 | 0.260136 | 0.111736 | 2.33  | 0.020564    |
| cg21322248 | rs4886508 1 | -0.15351 | 0.048167 | -3.19 | 0.001587    |
| cg02724025 | rs4967866 2 | 0.14469  | 0.057556 | 2.51  | 0.012458    |
| cg21322248 | rs5021805 1 | -0.33235 | 0.118815 | -2.8  | 0.005484    |
| cg21322248 | rs5021805 2 | -0.13776 | 0.03652  | -3.77 | 0.000195    |
| cg09396181 | rs6442414 2 | 0.06652  | 0.033417 | 1.99  | 0.047424    |
| cg24343755 | rs6482573 2 | 0.117113 | 0.052817 | 2.22  | 0.027341    |
| cg13627491 | rs649892 2  | 0.139856 | 0.061462 | 2.28  | 0.023575    |
| cg09888026 | rs6565550 1 | -0.17037 | 0.084442 | -2.02 | 0.044514    |
| cg09888026 | rs6565550 2 | -0.07397 | 0.027892 | -2.65 | 0.008419    |
| cg02998992 | rs6587074 2 | 0.327018 | 0.097489 | 3.35  | 0.000896    |
| cg06216103 | rs6598209 1 | 0.482705 | 0.200275 | 2.41  | 0.016539    |
| cg06216103 | rs6598209 2 | 0.160074 | 0.069068 | 2.32  | 0.021136    |
| cg19248893 | rs6659873 1 | 0.093748 | 0.04576  | 2.05  | 0.041356    |
| cg19248893 | rs6659873 2 | 0.069069 | 0.030193 | 2.29  | 0.022851    |
| cg27230396 | rs6849066 2 | 0.122612 | 0.059802 | 2.05  | 0.041196    |
| cg13627491 | rs7037253 2 | 0.188035 | 0.066942 | 2.81  | 0.005294    |
| cg23683674 | rs7125978 2 | 0.106327 | 0.051225 | 2.08  | 0.038766    |
| cg09888026 | rs7223219 2 | -0.08267 | 0.026182 | -3.16 | 0.001751    |
| cg23683674 | rs725103 2  | 0.102796 | 0.041919 | 2.45  | 0.014761    |
| cg18478353 | rs7280392 2 | -0.08986 | 0.029839 | -3.01 | 0.002818    |
| cg06216103 | rs7306456 1 | 0.626219 | 0.088433 | 7.08  | <.000000001 |
| cg06216103 | rs7306456 2 | 0.213995 | 0.066478 | 3.22  | 0.001426    |

| Dependent  | Parameter  | Estimate | Biased | StdErr   | tValue | Prob       |
|------------|------------|----------|--------|----------|--------|------------|
| cg27230396 | rs10013334 | -0.12954 | 1      | 0.057453 | -2.25  | 0.024843   |
| cg13627491 | rs10120384 | -0.72009 | 1      | 0.332668 | -2.16  | 0.031177   |
| cg13627491 | rs10156478 | -0.16551 | 1      | 0.062701 | -2.64  | 0.008715   |
| cg21322248 | rs1022198  | 0.058968 | 1      | 0.029163 | 2.02   | 0.044027   |
| cg02724025 | rs1040271  | -0.20601 | 1      | 0.073517 | -2.8   | 0.005393   |
| cg24343755 | rs10508720 | 0.200818 | 1      | 0.045419 | 4.42   | 1.36E-05   |
| cg02374944 | rs1057105  | 0.578655 | 1      | 0.272534 | 2.12   | 0.034521   |
| cg06216103 | rs10751711 | 0.587038 | 1      | 0.082079 | 7.15   | <.00000001 |
| cg06216103 | rs10751711 | 0.312146 | 1      | 0.066489 | 4.69   | 4E-06      |
| cg22364465 | rs10863698 | 0.121887 | 1      | 0.038832 | 3.14   | 0.001859   |
| cg06216103 | rs10902512 | 0.46887  | 1      | 0.086755 | 5.4    | 1.29E-07   |
| cg06216103 | rs10902512 | 0.197132 | 1      | 0.069822 | 2.82   | 0.005058   |

Supplement Table S12 (B): MethQTLs identified based on association of SNPs with DNAm in females (n=315)

|            |              |          |   |          |       |              |
|------------|--------------|----------|---|----------|-------|--------------|
| cg24343755 | rs11015236 1 | -0.42432 | 1 | 0.215247 | -1.97 | 0.049573     |
| cg24343755 | rs11015249 1 | -0.33466 | 1 | 0.057591 | -5.81 | 1.5E-08      |
| cg24343755 | rs11015249 2 | -0.12583 | 1 | 0.044031 | -2.86 | 0.004552     |
| cg24343755 | rs11015253 1 | -0.42885 | 1 | 0.123559 | -3.47 | 0.000592     |
| cg24343755 | rs11015253 2 | -0.11813 | 1 | 0.045566 | -2.59 | 0.009974     |
| cg24343755 | rs11015262 1 | -0.56143 | 1 | 0.163554 | -3.43 | 0.000678     |
| cg24343755 | rs11015262 2 | -0.14338 | 1 | 0.047777 | -3    | 0.002907     |
| cg23683674 | rs1107038 1  | 0.445586 | 1 | 0.132259 | 3.37  | 0.000849     |
| cg21322248 | rs11072639 2 | -0.13182 | 1 | 0.036563 | -3.61 | 0.000363     |
| cg19142181 | rs11086147 1 | 2.311959 | 1 | 0.24966  | 9.26  | <0.000000001 |
| cg19142181 | rs11086147 2 | 1.58134  | 1 | 0.210926 | 7.5   | <0.00000001  |
| cg19248893 | rs11222115 2 | -0.081   | 1 | 0.029443 | -2.75 | 0.006285     |
| cg06216103 | rs11246996 1 | 0.523004 | 1 | 0.136279 | 3.84  | 0.00015      |
| cg06216103 | rs11246996 2 | 0.197637 | 1 | 0.065322 | 3.03  | 0.002688     |
| cg06216103 | rs11247000 1 | 0.285558 | 1 | 0.128025 | 2.23  | 0.026426     |
| cg06216103 | rs11247000 2 | 0.219937 | 1 | 0.06577  | 3.34  | 0.000926     |
| cg21322248 | rs11639459 1 | -0.23072 | 1 | 0.092726 | -2.49 | 0.013361     |
| cg21322248 | rs11639459 2 | -0.12285 | 1 | 0.028733 | -4.28 | 2.54E-05     |
| cg27230396 | rs11727631 2 | -0.10551 | 1 | 0.047424 | -2.22 | 0.026804     |
| cg27230396 | rs11734394 2 | -0.1093  | 1 | 0.047129 | -2.32 | 0.021032     |
| cg18786125 | rs12080677 2 | 0.108272 | 1 | 0.047918 | 2.26  | 0.024541     |
| cg13659360 | rs12275038 1 | 0.237002 | 1 | 0.1155   | 2.05  | 0.041008     |
| cg18478353 | rs12482752 2 | 0.072625 | 1 | 0.026006 | 2.79  | 0.005552     |
| cg27230396 | rs12501546 2 | -0.13609 | 1 | 0.052645 | -2.59 | 0.010191     |
| cg09396181 | rs12639607 1 | -0.148   | 1 | 0.06699  | -2.21 | 0.027885     |
| cg27230396 | rs12651108 1 | -0.72452 | 1 | 0.281533 | -2.57 | 0.010529     |
| cg02374944 | rs1266479 1  | 0.579019 | 1 | 0.272504 | 2.12  | 0.034388     |
| cg02374944 | rs1266481 1  | 0.579019 | 1 | 0.272504 | 2.12  | 0.034388     |
| cg21322248 | rs12912465 1 | 0.191172 | 1 | 0.060743 | 3.15  | 0.001808     |
| cg00707741 | rs13388333 1 | -0.10112 | 1 | 0.048071 | -2.1  | 0.036211     |
| cg00707741 | rs13388333 2 | -0.07778 | 1 | 0.032991 | -2.36 | 0.01901      |

|            |              |          |   |          |       |            |
|------------|--------------|----------|---|----------|-------|------------|
| cg13627491 | rs1410854 2  | -0.1718  | 1 | 0.062332 | -2.76 | 0.006192   |
| cg02724025 | rs1520237 2  | 0.117897 | 1 | 0.055462 | 2.13  | 0.03431    |
| cg02724025 | rs1532418 1  | -0.2527  | 1 | 0.087254 | -2.9  | 0.004045   |
| cg24343755 | rs1564271 1  | -0.27052 | 1 | 0.084728 | -3.19 | 0.001553   |
| cg22364465 | rs1604364 1  | -0.13016 | 1 | 0.039357 | -3.31 | 0.001052   |
| cg02724025 | rs16968480 1 | -0.17377 | 1 | 0.084762 | -2.05 | 0.041187   |
| cg21322248 | rs16968625 2 | -0.11042 | 1 | 0.043248 | -2.55 | 0.01115    |
| cg27230396 | rs17002091 1 | -0.36235 | 1 | 0.178414 | -2.03 | 0.043109   |
| cg27230396 | rs17002091 2 | -0.13215 | 1 | 0.051887 | -2.55 | 0.011351   |
| cg27230396 | rs17002139 2 | -0.12597 | 1 | 0.054902 | -2.29 | 0.022427   |
| cg09396181 | rs17038710 1 | -0.16599 | 1 | 0.06879  | -2.41 | 0.016401   |
| cg21322248 | rs17465692 1 | 0.132558 | 1 | 0.041377 | 3.2   | 0.001497   |
| cg05951364 | rs17748677 1 | 0.208365 | 1 | 0.077692 | 2.68  | 0.00771    |
| cg24343755 | rs1780196 1  | 0.352862 | 1 | 0.092132 | 3.83  | 0.000155   |
| cg24343755 | rs1780196 2  | 0.296619 | 1 | 0.045263 | 6.55  | <.00000001 |
| cg23683674 | rs2027761 2  | 0.083491 | 1 | 0.041785 | 2     | 0.046574   |
| cg19374731 | rs2055204 1  | 0.139013 | 1 | 0.046452 | 2.99  | 0.002987   |
| cg02724025 | rs2088285 1  | -0.21163 | 1 | 0.078568 | -2.69 | 0.00745    |
| cg19142181 | rs2093045 1  | 1.973028 | 1 | 0.27116  | 7.28  | <.00000001 |
| cg19142181 | rs2093045 2  | 1.309237 | 1 | 0.204292 | 6.41  | <.00000001 |
| cg02724025 | rs2195431 2  | 0.199969 | 1 | 0.0676   | 2.96  | 0.003332   |
| cg13963729 | rs2238577 2  | -0.07973 | 1 | 0.038718 | -2.06 | 0.040308   |
| cg26146287 | rs2239670 2  | 0.085961 | 1 | 0.040694 | 2.11  | 0.035451   |
| cg19142181 | rs2248900 1  | 1.512895 | 1 | 0.398406 | 3.8   | 0.000176   |
| cg19142181 | rs2248900 2  | 1.314265 | 1 | 0.207093 | 6.35  | <.00000001 |
| cg13627491 | rs2252151 1  | 0.151881 | 1 | 0.075983 | 2     | 0.046487   |
| cg02724025 | rs2280396 1  | -0.22419 | 1 | 0.072297 | -3.1  | 0.002105   |
| cg05951364 | rs2301963 1  | 0.092896 | 1 | 0.042037 | 2.21  | 0.02784    |
| cg24343755 | rs2448111 1  | 0.349453 | 1 | 0.098377 | 3.55  | 0.000441   |
| cg24343755 | rs2448111 2  | 0.303419 | 1 | 0.044956 | 6.75  | <.00000001 |
| cg21322248 | rs2469203 2  | 0.06076  | 1 | 0.029199 | 2.08  | 0.038262   |

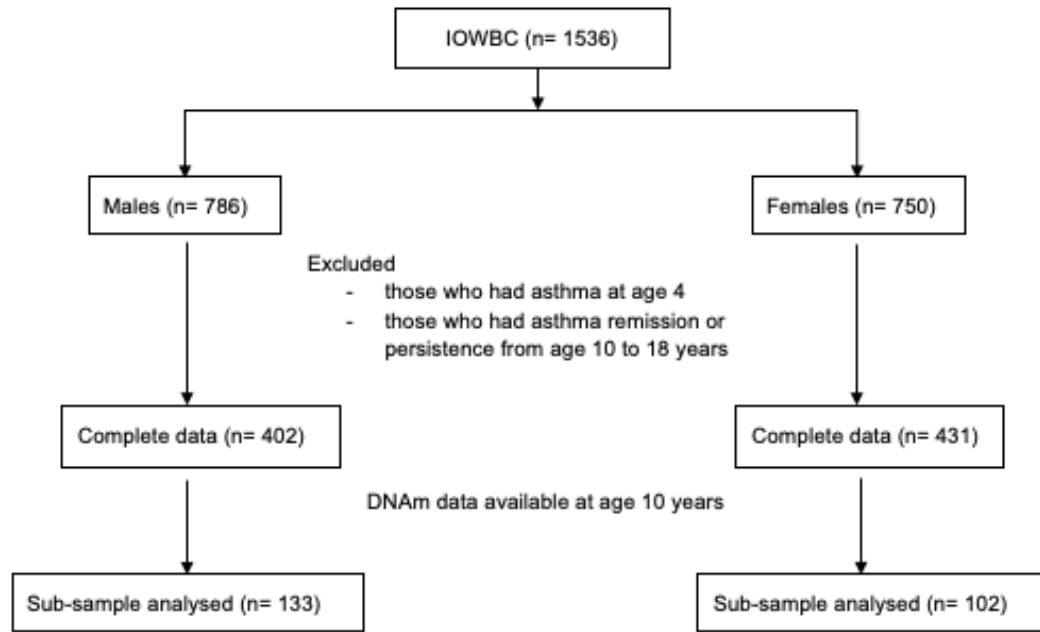
|            |             |          |   |          |       |             |
|------------|-------------|----------|---|----------|-------|-------------|
| cg21322248 | rs2469232 2 | 0.06076  | 1 | 0.029199 | 2.08  | 0.038262    |
| cg22364465 | rs2478816 2 | 0.063383 | 1 | 0.032005 | 1.98  | 0.048532    |
| cg22364465 | rs2498024 2 | 0.068236 | 1 | 0.029257 | 2.33  | 0.020323    |
| cg02724025 | rs28216 1   | -0.21046 | 1 | 0.075088 | -2.8  | 0.005383    |
| cg19374731 | rs2843142 2 | -0.12797 | 1 | 0.039391 | -3.25 | 0.001285    |
| cg19374731 | rs2843146 2 | -0.07298 | 1 | 0.036634 | -1.99 | 0.047234    |
| cg14273401 | rs2844795 2 | 0.230071 | 1 | 0.112662 | 2.04  | 0.041979    |
| cg05951364 | rs2906590 2 | -0.07388 | 1 | 0.035152 | -2.1  | 0.036371    |
| cg13627491 | rs2993808 1 | -0.26857 | 1 | 0.086701 | -3.1  | 0.002128    |
| cg24343755 | rs3118153 1 | 0.343324 | 1 | 0.095124 | 3.61  | 0.000358    |
| cg24343755 | rs3118153 2 | 0.30198  | 1 | 0.045417 | 6.65  | <.000000001 |
| cg13963729 | rs349311 1  | -0.32797 | 1 | 0.166205 | -1.97 | 0.049345    |
| cg13963729 | rs349312 2  | -0.07198 | 1 | 0.035678 | -2.02 | 0.044496    |
| cg02724025 | rs35188 1   | -0.21198 | 1 | 0.079666 | -2.66 | 0.008196    |
| cg02724025 | rs35195 1   | -0.21198 | 1 | 0.079666 | -2.66 | 0.008196    |
| cg20977448 | rs352346 1  | -0.38123 | 1 | 0.066871 | -5.7  | 2.8E-08     |
| cg20977448 | rs352346 2  | -0.12314 | 1 | 0.057403 | -2.15 | 0.032711    |
| cg20977448 | rs352347 1  | -0.38123 | 1 | 0.066871 | -5.7  | 2.8E-08     |
| cg20977448 | rs352347 2  | -0.12314 | 1 | 0.057403 | -2.15 | 0.032711    |
| cg19142181 | rs3729555 1 | 2.273284 | 1 | 0.24666  | 9.22  | <.00000001  |
| cg19142181 | rs3729555 2 | 2.18586  | 1 | 0.179668 | 12.17 | <.00000001  |
| cg27230396 | rs3733242 2 | -0.11429 | 1 | 0.049298 | -2.32 | 0.021081    |
| cg09776718 | rs3745169 1 | -0.74515 | 1 | 0.34351  | -2.17 | 0.030821    |
| cg20383390 | rs3767794 1 | -0.30326 | 1 | 0.146095 | -2.08 | 0.038731    |
| cg19374731 | rs3795272 1 | -0.15803 | 1 | 0.051568 | -3.06 | 0.002371    |
| cg19374731 | rs3795272 2 | -0.10214 | 1 | 0.0364   | -2.81 | 0.005331    |
| cg18478353 | rs380152 1  | 0.113605 | 1 | 0.049667 | 2.29  | 0.022846    |
| cg19142181 | rs3810460 1 | 3.159986 | 1 | 0.182489 | 17.32 | <.00000001  |
| cg19142181 | rs3810460 2 | 2.933449 | 1 | 0.155866 | 18.82 | <.00000001  |
| cg22364465 | rs3811386 2 | 0.06578  | 1 | 0.030218 | 2.18  | 0.030244    |
| cg22364465 | rs3811389 1 | 0.117058 | 1 | 0.039257 | 2.98  | 0.003091    |

|            |              |          |   |          |       |          |
|------------|--------------|----------|---|----------|-------|----------|
| cg04410091 | rs3814772 2  | 0.100256 | 1 | 0.037312 | 2.69  | 0.007597 |
| cg18478353 | rs3390840 1  | 0.111982 | 1 | 0.049705 | 2.25  | 0.024959 |
| cg16360777 | rs33924573 2 | -0.22314 | 1 | 0.055623 | -4.01 | 7.55E-05 |
| cg00707741 | rs4075818 2  | -0.12897 | 1 | 0.034792 | -3.71 | 0.000248 |
| cg24343755 | rs4369307 1  | 0.301343 | 1 | 0.129533 | 2.33  | 0.020639 |
| cg24343755 | rs4369307 2  | 0.200818 | 1 | 0.045419 | 4.42  | 1.36E-05 |
| cg27230396 | rs4380545 2  | -0.11896 | 1 | 0.050666 | -2.35 | 0.019501 |
| cg21322248 | rs4420499 2  | -0.09512 | 1 | 0.029357 | -3.24 | 0.001324 |
| cg09396181 | rs4685039 1  | -0.18642 | 1 | 0.072963 | -2.55 | 0.011095 |
| cg16360777 | rs4694075 1  | 0.196432 | 1 | 0.077264 | 2.54  | 0.011494 |
| cg14736210 | rs4809745 1  | 0.573553 | 1 | 0.188412 | 3.04  | 0.002532 |
| cg14736210 | rs48809746 1 | 0.379276 | 1 | 0.164646 | 2.3   | 0.021903 |
| cg27230396 | rs4859688 1  | 0.221634 | 1 | 0.098691 | 2.25  | 0.025421 |
| cg21322248 | rs4886508 1  | -0.16147 | 1 | 0.039376 | -4.1  | 5.26E-05 |
| cg21322248 | rs4886508 2  | -0.11106 | 1 | 0.033407 | -3.32 | 0.000992 |
| cg13659360 | rs4936580 2  | 0.123813 | 1 | 0.047621 | 2.6   | 0.009766 |
| cg02724025 | rs4967866 1  | 0.20123  | 1 | 0.076194 | 2.64  | 0.008682 |
| cg02724025 | rs4967886 1  | -0.22309 | 1 | 0.077687 | -2.87 | 0.004362 |
| cg21322248 | rs5021805 1  | -0.22968 | 1 | 0.092854 | -2.47 | 0.013908 |
| cg21322248 | rs5021805 2  | -0.11992 | 1 | 0.028772 | -4.17 | 3.99E-05 |
| cg13659360 | rs520805 1   | -0.22351 | 1 | 0.09127  | -2.45 | 0.014881 |
| cg22364465 | rs556625 2   | 0.060218 | 1 | 0.029872 | 2.02  | 0.044671 |
| cg13659360 | rs583842 1   | -0.22351 | 1 | 0.09127  | -2.45 | 0.014881 |
| cg22364465 | rs600031 2   | 0.116912 | 1 | 0.035541 | 3.29  | 0.001118 |
| cg26054167 | rs6010903 2  | 0.107768 | 1 | 0.044397 | 2.43  | 0.015773 |
| cg14736210 | rs6090977 2  | 0.10316  | 1 | 0.049381 | 2.09  | 0.037512 |
| cg13627491 | rs649414 1   | 0.155166 | 1 | 0.07694  | 2.02  | 0.044583 |
| cg05951364 | rs6558511 1  | 0.091816 | 1 | 0.043569 | 2.11  | 0.035883 |
| cg06216103 | rs6598209 2  | 0.246193 | 1 | 0.068577 | 3.59  | 0.000384 |
| cg26417188 | rs6657162 1  | -0.10792 | 1 | 0.052121 | -2.07 | 0.03922  |
| cg22364465 | rs6673084 1  | 0.086443 | 1 | 0.041222 | 2.1   | 0.036799 |

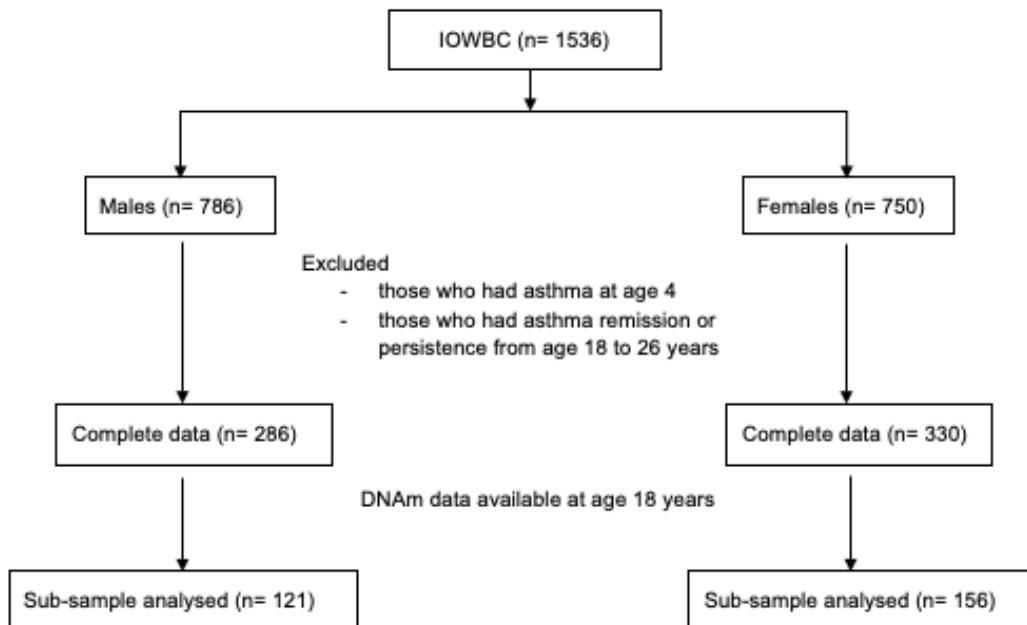
|            |             |           |   |          |       |             |
|------------|-------------|-----------|---|----------|-------|-------------|
| cg22364465 | rs6688878 2 | 0.085682  | 1 | 0.039148 | 2.19  | 0.02936     |
| cg22364465 | rs6697350 1 | -0.12144  | 1 | 0.037714 | -3.22 | 0.001416    |
| cg22364465 | rs681241 2  | 0.076383  | 1 | 0.031475 | 2.43  | 0.0158      |
| cg27230396 | rs6824297 1 | 0.201693  | 1 | 0.073902 | 2.73  | 0.006709    |
| cg05951364 | rs6999089 1 | -0.08986  | 1 | 0.044058 | -2.04 | 0.042236    |
| cg09888026 | rs7223219 1 | -0.1467   | 1 | 0.068435 | -2.14 | 0.032837    |
| cg09888026 | rs7223219 2 | -0.08919  | 1 | 0.023916 | -3.73 | 0.000228    |
| cg23683674 | rs725103 1  | 0.146559  | 1 | 0.070537 | 2.08  | 0.038548    |
| cg23683674 | rs725103 2  | 0.101071  | 1 | 0.035981 | 2.81  | 0.005282    |
| cg06216103 | rs7306456 1 | 0.626346  | 1 | 0.082672 | 7.58  | <.000000001 |
| cg06216103 | rs7306456 2 | 0.313631  | 1 | 0.065364 | 4.8   | 2.49E-06    |
| cg09396181 | rs734176 1  | -0.18864  | 1 | 0.095197 | -1.98 | 0.048406    |
| cg22364465 | rs752016 2  | 0.061189  | 1 | 0.029023 | 2.11  | 0.035807    |
| cg22364465 | rs7540179 1 | 0.078563  | 1 | 0.038575 | 2.04  | 0.042532    |
| cg00707741 | rs764081 1  | 0.131383  | 1 | 0.060002 | 2.19  | 0.02929     |
| cg27230396 | rs7677847 1 | -0.22774  | 1 | 0.1038   | -2.19 | 0.028968    |
| cg27230396 | rs7687284 1 | -0.16087  | 1 | 0.070246 | -2.29 | 0.02268     |
| cg27230396 | rs7687284 2 | -0.11647  | 1 | 0.047962 | -2.43 | 0.015729    |
| cg20977448 | rs783777 1  | -0.33801  | 1 | 0.127469 | -2.65 | 0.008417    |
| cg20977448 | rs783777 2  | -0.16313  | 1 | 0.058494 | -2.79 | 0.005614    |
| cg06216103 | rs7977641 1 | 0.262448  | 1 | 0.132352 | 1.98  | 0.048248    |
| cg06216103 | rs7977641 2 | 0.160083  | 1 | 0.065447 | 2.45  | 0.014997    |
| cg06216103 | rs7977750 2 | 0.164319  | 1 | 0.065654 | 2.5   | 0.012832    |
| cg10179363 | rs8041622 1 | -0.49904  | 1 | 0.202587 | -2.46 | 0.014304    |
| cg09888026 | rs8076437 1 | -0.117007 | 1 | 0.065086 | -2.61 | 0.00941     |
| cg09888026 | rs8076437 2 | -0.08395  | 1 | 0.023746 | -3.54 | 0.000469    |
| cg18478353 | rs8134499 2 | 0.077877  | 1 | 0.026112 | 2.98  | 0.003085    |
| cg10179363 | rs8192297 1 | -0.24078  | 1 | 0.102023 | -2.36 | 0.018886    |
| cg09396181 | rs873853 1  | -0.18556  | 1 | 0.072971 | -2.54 | 0.011475    |
| cg22364465 | rs895241 1  | 0.115949  | 1 | 0.039439 | 2.94  | 0.003528    |
| cg19142181 | rs910934 1  | 1.112032  | 1 | 0.513914 | 2.16  | 0.031235    |

|            |           |   |          |   |          |      |                 |
|------------|-----------|---|----------|---|----------|------|-----------------|
| cg19142181 | rs910934  | 2 | 1.613536 | 1 | 0.206826 | 7.8  | <.00000001      |
| cg02724025 | rs974782  | 1 | -0.22419 | 1 | 0.072297 | -3.1 | 0.002105        |
| cg18478353 | rs9976600 | 1 | 0.06593  | 1 | 0.032379 | 2.04 | 0.042575        |
| cg26054167 | rs6090357 | 2 | 0.218768 | 1 | 0.077774 | 2.81 | <u>0.005221</u> |

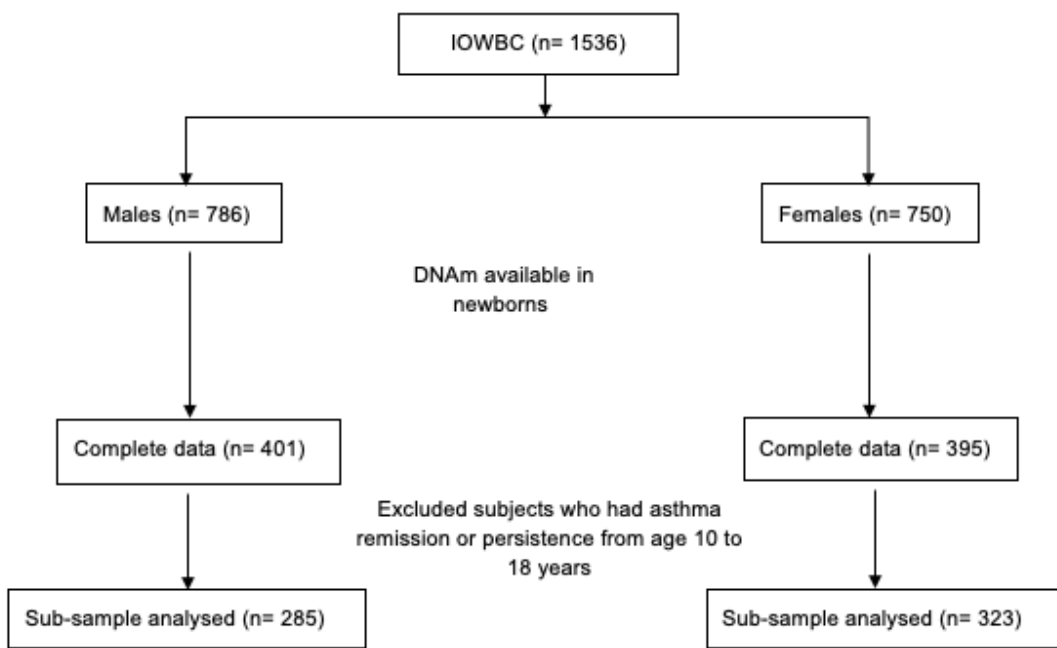
## Figures



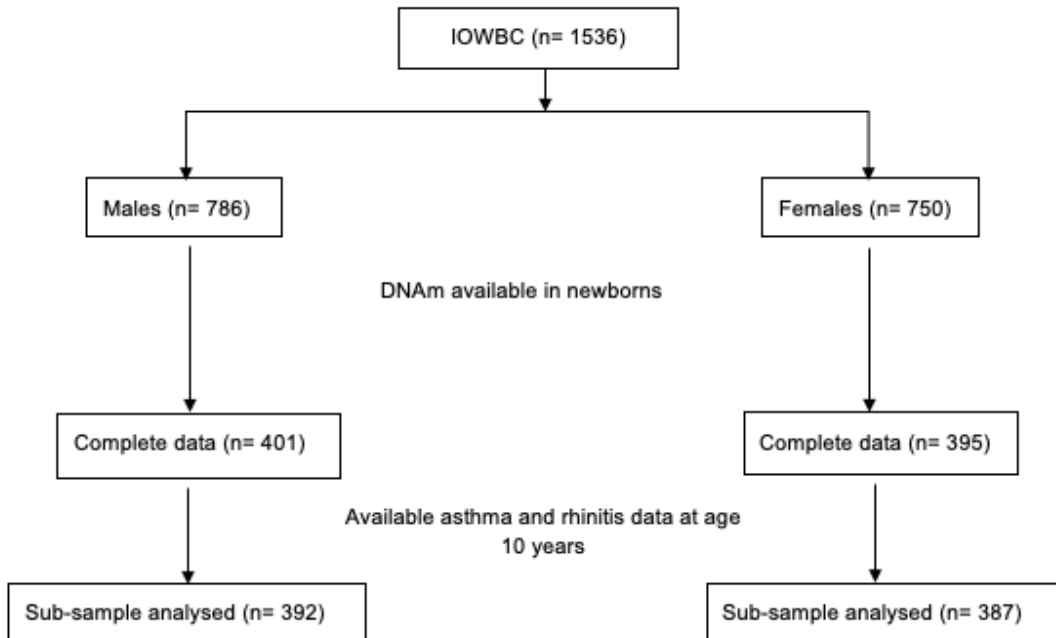
Supplement Figure S3(A): Consort diagram of Asthma acquisition subjects included in Aim 3 for 10-18 period (IOWBC).



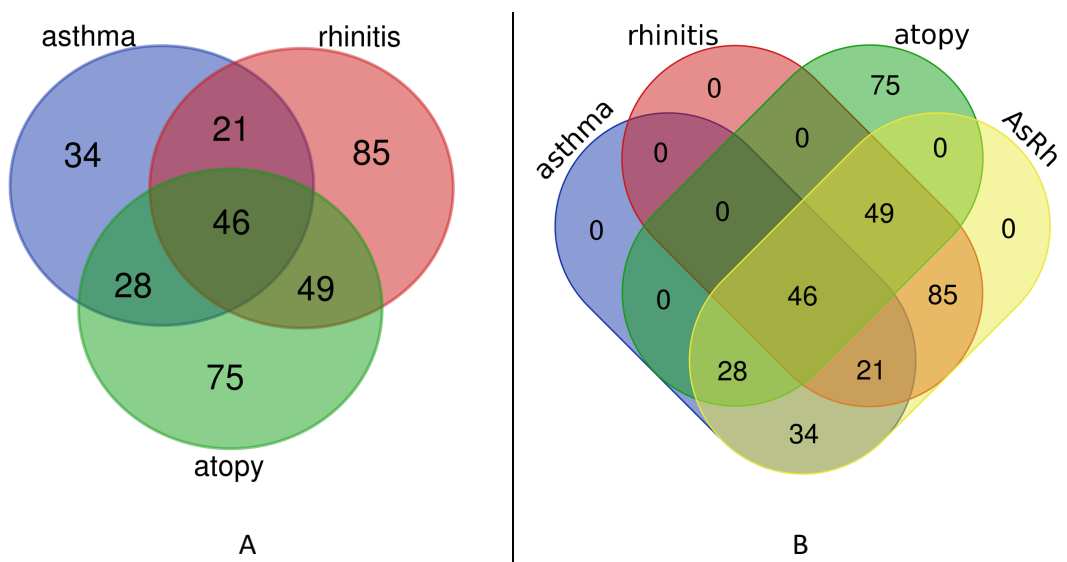
Supplement Figure S3(B): Consort diagram of Asthma acquisition subjects included in Aim 3 for 18-26 period (IOWBC).



Supplement Figure S4: Consort diagram of Asthma acquisition subjects included in Aim 4 for 10-18 period (IOWBC).



Supplement Figure S5: Consort diagram of Asthma and Rhinitis subjects included in Aim 5 at age 10 years (IOWBC).



Supplement Figure S6: Venn diagram representing not all subjects who had asthma or rhinitis also have atopy at age 10 years (IOWBC).

## IRB Approvals

Sunday, October 10, 2021 at 13:06:34 Central Daylight Time

**Subject:** PRO-FY2021-442 - Admin Withdrawal: Not Human Subject Research  
**Date:** Wednesday, June 30, 2021 at 9:06:51 AM Central Daylight Time  
**From:** do-not-reply@cayuse.com  
**To:** Aniruddha Bhadresh Rathod (abratbod), Hongmei Zhang (hzhang6)  
**Attachments:** ATT00001.png

**CAUTION: This email originated from outside of the organization. Do not click links or open attachments unless you recognize the sender and trust the content is safe.**



Institutional Review Board  
Division of Research and Innovation  
Office of Research Compliance  
University of Memphis  
315 Admin Bldg  
Memphis, TN 38152-3370

June 30, 2021

PI Name: Aniruddha Rathod  
Co-Investigators:  
Advisor and/or Co-PI: Hongmei Zhang  
Submission Type: Admin Withdrawal  
Title: DNA Methylation and Asthma acquisition during and post-adolescence, an epigenome-wide longitudinal study  
IRB ID: PRO-FY2021-442

From the information provided on your determination review request for "DNA Methylation and Asthma acquisition during and post-adolescence, an epigenome-wide longitudinal study", the IRB has determined that your activity does not meet the Office of Human Subjects Research Protections definition of human subjects research and 45 CFR part 46 does not apply.

This study does not require IRB approval nor review. Your determination will be administratively withdrawn from Cayuse IRB and you will receive an email similar to this correspondence from irb@memphis.edu. This submission will be archived in Cayuse IRB.

Thanks,

IRB Administrator  
Division of Research and Innovation  
Office of Research Compliance  
315 Administration Building  
Memphis, TN 38152-3370  
P: 901.678.2705

**Sunday, October 10, 2021 at 13:05:48 Central Daylight Time**

**Subject:** PRO-FY2021-443 - Admin Withdrawal: Not Human Subject Research  
**Date:** Wednesday, June 30, 2021 at 9:05:30 AM Central Daylight Time  
**From:** do-not-reply@cayuse.com  
**To:** Aniruddha Bhadresh Rathod (abratbod), Hongmei Zhang (hzhang6)  
**Attachments:** ATT00001.png

**CAUTION: This email originated from outside of the organization. Do not click links or open attachments unless you recognize the sender and trust the content is safe.**



Institutional Review Board  
Division of Research and Innovation  
Office of Research Compliance  
University of Memphis  
315 Admin Bldg  
Memphis, TN 38152-3370

June 30, 2021

PI Name: Aniruddha Rathod  
Co-Investigators:  
Advisor and/or Co-PI: Hongmei Zhang  
Submission Type: Admin Withdrawal  
Title: DNA Methylation at Birth is Associated with Asthma Acquisition from Pre- to Post-Adolescence Mediated by Atopy  
IRB ID: PRO-FY2021-443

From the information provided on your determination review request for "DNA Methylation at Birth is Associated with Asthma Acquisition from Pre- to Post-Adolescence Mediated by Atopy", the IRB has determined that your activity does not meet the Office of Human Subjects Research Protections definition of human subjects research and 45 CFR part 46 does not apply.

This study does not require IRB approval nor review. Your determination will be administratively withdrawn from Cayuse IRB and you will receive an email similar to this correspondence from irb@memphis.edu. This submission will be archived in Cayuse IRB.

Thanks,

IRB Administrator  
Division of Research and Innovation  
Office of Research Compliance  
315 Administration Building  
Memphis, TN 38152-3370

**Sunday, October 10, 2021 at 13:04:14 Central Daylight Time**

**Subject:** PRO-FY2021-480 - Admin Withdrawal: Not Human Subject Research  
**Date:** Wednesday, June 30, 2021 at 9:04:05 AM Central Daylight Time  
**From:** do-not-reply@cayuse.com  
**To:** Aniruddha Bhadresh Rathod (abratbod), Hongmei Zhang (hzhang6)  
**Attachments:** ATT00001.png

**CAUTION: This email originated from outside of the organization. Do not click links or open attachments unless you recognize the sender and trust the content is safe.**



Institutional Review Board  
Division of Research and Innovation  
Office of Research Compliance  
University of Memphis  
315 Admin Bldg  
Memphis, TN 38152-3370

June 30, 2021

PI Name: Aniruddha Rathod  
Co-Investigators:  
Advisor and/or Co-PI: Hongmei Zhang  
Submission Type: Admin Withdrawal  
Title: Sex-specific associations of Preadolescence Asthma and Rhinitis with DNA methylation at birth  
IRB ID: PRO-FY2021-480

From the information provided on your determination review request for "Sex-specific associations of Preadolescence Asthma and Rhinitis with DNA methylation at birth", the IRB has determined that your activity does not meet the Office of Human Subjects Research Protections definition of human subjects research and 45 CFR part 46 does not apply.

This study does not require IRB approval nor review. Your determination will be administratively withdrawn from Cayuse IRB and you will receive an email similar to this correspondence from irb@memphis.edu. This submission will be archived in Cayuse IRB.

Thanks,

IRB Administrator  
Division of Research and Innovation  
Office of Research Compliance  
315 Administration Building  
Memphis, TN 38152-3370  
P: 901.678.2705